Bioinspired template-based control of legged locomotion

Bioinspirierte, template-basierte Kontrolle von Laufbewegungen
Zur Erlangung des Grades eines Doktors der Naturwissenschaften (Dr. rer. nat.)
genehmigte Dissertation von Dr. Ing. Maziar Ahmad Sharbafi aus Rasht, Iran
Tag der Einreichung: 15. May 2017, Tag der Prüfung: 15. August 2017
Darmstadt 2018— D 17

1. Gutachten: Prof. Dr. André Seyfarth
2. Gutachten: Prof. Dr. Robert J. Full, Prof. Dr. Sangbae Kim and Prof. Dr. Jan Peters

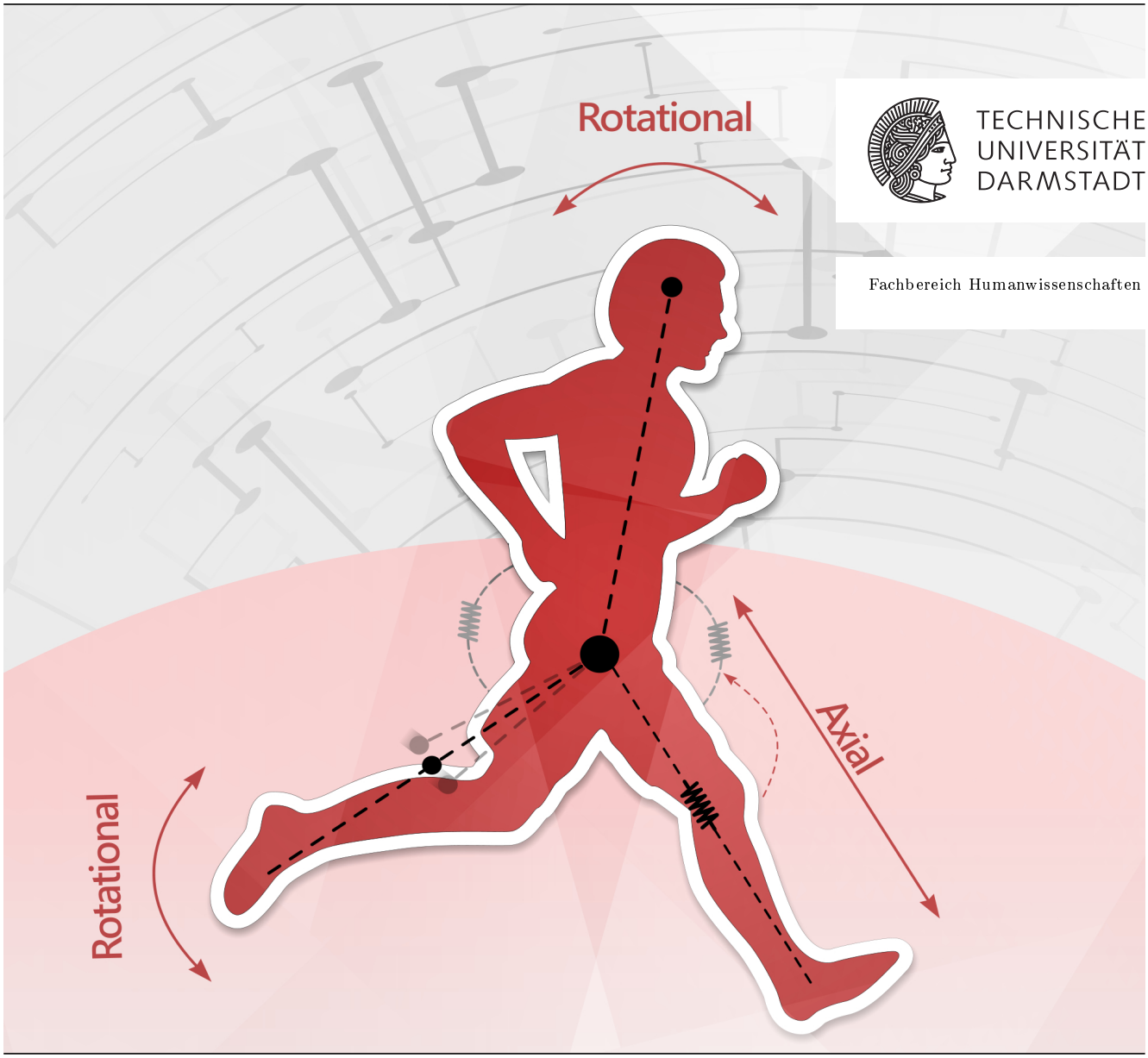

TECHNISCHE UNIVERSITÄT DARMSTADT

Fachbereich Humanwissenschaften

Bioinspired template-based control of legged locomotion
Bioinspirierte, template-basierte Kontrolle von Laufbewegungen

Genehmigte Dissertation von Dr. Ing. Maziar Ahmad Sharbafi aus Rasht, Iran

1. Gutachten: Prof. Dr. André Seyfarth
2. Gutachten: Prof. Dr. Robert J. Full, Prof. Dr. Sangbae Kim and Prof. Dr. Jan Peters

Tag der Einreichung: 15. May 2017
Tag der Prüfung: 15. August 2017

Darmstadt 2018— D 17

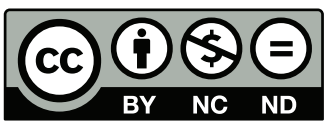

Erklärung zur Dissertation

Hiermit versichere ich, die vorliegende Dissertation ohne Hilfe Dritter nur mit den angegebenen Quellen und Hilfsmitteln angefertigt zu haben. Alle Stellen, die aus Quellen entnommen wurden, sind als solche kenntlich gemacht. Diese Arbeit hat in gleicher oder ähnlicher Form noch keiner Prüfungsbehörde vorgelegen.

Darmstadt, den 15. May 2017

Maziar A. Sharbafi

Zusammenfassung

Der Fähigkeit effizient und robust zu laufen ist eine wichtige Voraussetzung für die Verwendung und Nutzung von Laufrobotern in realen Umgebungen. Hier können Roboter von Tieren lernen, indem die der Lokomotion zugrundeliegenden Prinzipien in die künstlichen Laufsysteme übertragen werden. Jedoch ist die pedale Lokomotion in biologischen Systemen komplex und noch nicht vollständig verstanden. Ein wichtiger Fortschritt ist dabei die Vereinfachung der Lokomotionsdynamik und -kontrolle (im Sinne von Regelung und Steuerung) durch die Einführung einfacher Modelle, welche als template bezeichnet werden. Diese beschreiben die generelle Dynamik des Gangs von Tieren (und auch von Menschen). Eines der bekanntesten Modelle ist das Masse Feder Modell (spring-loaded inverted pendulum, SLIP) welches eine Punktmasse über einer masselosen Feder repräsentiert. Dieses Modell liefert eine gute Beschreibung menschlicher Gangformen wie Gehen, Hüpfen und Rennen. Trotz seinem hohen Abstraktionsgrad hat es die Entwicklung von erfolgreichen Laufmaschinen unterstützt und inspiriert und war ein gezielte Vorlage für Kontrollansätzen in den vergangenen Jahren.

Inspiriert von den Template-Modellen zur Beschreibung von biologischen Laufsystemen und den beispielgebenden Laufrobotern von Marc Raibert, ist es möglich die pedale Lokomotion in Grund- funktion umzusetzen: (i) Standbeinfunktion, (2) Schwungbeinfunktion, und (iii) Balance im Sinne von posturalem Gleichgewicht. Kombinationen dieser drei Grundfunktionen ermöglichen die Erzeugung unterschiedlicher Gangarten mit verschiedenartigen Eigenschaften. Mithilfe der Templatemodelle untersuchen wir, wie die lokomotorischen Grundfunktionen zur Stabilisierung verschiedener Gangarten (Hüpfen, Rennen und Gehen) in verschiedenen Bedingungen (z.B. Geschwindigkeit) beitragen. Wir zeigen, dass diese grundlegenden Analysen der menschlichen Lokomotion mithilfe von konzeptionellen Modellen in die Entwicklung neuer Methoden für das Desing und die Kontrolle von Laufsystemene wie humanoide Roboter und Assistenzsysteme (Exoskelette, Orthesen, und Prothesen) einfließen können.

Diese Promotionsschrift umfasst verschiedene Forschungsfelder: Biomechanik, Robotik und Kontrollansätze (d.h. Regelungs- und Steuerungsansätze). Die Arbeiten umfassen Experimente mit Menschen, Datenanalyse, Modellierung von Laufsystemen und die Umsetzung in Robotern und Exoskeletten. Dabei konnten wir von den Einrichtungen und Experimenten am Lauflabor profitieren. Die Modellierung umfasst zwei Kategorien: konzeptuelle Modelle (Template-basiert, z.B. SLIP) und detaillierte Modelle (mit segmentierten Beinen, Massen und Trägheiten). Mithilfe der BioBiped Roboter Generationen (und den detaillierten MBS Modellen, MBS steht für Multi-Body-System) haben wir die neu entwickelten Design und Kontrollmethoden mit Bezug zum Konzept der lokomotorischen Grundfunktionen entweder im MBS Modell oder direkt am Roboter umgesetzt. Zusätzlich haben wir im Rahmen des BALANCE Projekts (`http://balance-fp7.eu/`) Kontrollansätze auf einem Exoskelett implementiert und deren Wirkungsweise beim menschlichen Gehen demonstriert. Die Ergebnisse dieser Forschung beinhalten neue konzeptuelle Modelle für Laufbewegungen, die Analyse menschlicher Laufbewegungen basierend auf diesen neu entwickelten Modellen im Sinne der Trilogie der lokomotorischen Grundfunktionen, und die Entwicklung von Methoden, um die Modelle in das Design und die Kontrolle von Robotern und Exoskeletten zu übertragen.

Als wichtigsten Beitrag liefert diese Arbeit einen neuen Ansatz für die modulare Kontrolle von Laufbewegungen. Mit diesem Ansatz können Beziehungen zwischen den lokomotorischen Grundfunktionen hergestellt werden, z.B. zwischen Balance und Standfunktion (Nutzung von Stützkräften im Stand für die Abstimmung der Balance-Kontrolle) oder Balance und Schwungbeinfunktion (zweigelenkige Hüftmuskeln können die Schwungbeinkontrolle und die posturale Balance des Oberkörpers unterstützen). Damit

kann das Konzept der modularen Kontrolle basierend auf den lokomotorischen Grundfunktionen mit einem beschränkten Austausch von sensorischen Informationen auf verschiedenen Hardwareplattformen (Laufroboter, Exoskelett) implementiert werden.

Abstract

The ability to perform efficient and robust locomotion is a crucial condition for the more extensive use of legged robots in real world applications. In that respect, robots can learn from animals, if the principles underlying locomotion in biological legged systems can be transferred to their artificial counterparts. However, legged locomotion in biological systems is a complex and not fully understood problem. A great progress to simplify understanding locomotion dynamics and control was made by introducing simple models, coined "templates", able to represent the overall dynamics of animal (including human) gaits. One of the most recognized models is the spring-loaded inverted pendulum (SLIP) which consists of a point mass atop a massless spring. This model provides a good description of human gaits, such as walking, hopping and running. Despite its high level of abstraction, it supported and inspired the development of successful legged robots and was used as explicit targets for control, over the years.

Inspired from template models explaining biological locomotory systems and Raibert's pioneering legged robots, locomotion can be realized by basic subfunctions: (i) stance leg function, (ii) leg swinging and (iii) balancing. Combinations of these three subfunctions can generate different gaits with diverse properties. Using the template models, we investigate how locomotor subfunctions contribute to stabilize different gaits (hopping, running and walking) in different conditions (e.g., speeds). We show that such basic analysis on human locomotion using conceptual models can result in developing new methods in design and control of legged systems like humanoid robots and assistive devices (exoskeletons, orthoses and prostheses).

This thesis comprises research in different disciplines: biomechanics, robotics and control. These disciplines are required to do human experiments and data analysis, modeling of locomotory systems, and implementation on robots and an exoskeleton. We benefited from facilities and experiments performed in the Lauflabor locomotion laboratory. Modeling includes two categories: conceptual (template-based, e.g. SLIP) models and detailed models (with segmented legs, masses/inertias). Using the BioBiped series of robots (and the detailed BioBiped MBS models; MBS stands for Multi-Body-System), we have implemented newly-developed design and control methods related to the concept of locomotor subfunctions on either MBS models or on the robot directly. In addition, with involvement in BALANCE project (`http://balance-fp7.eu/`), we implemented balance-related control approaches on an exoskeleton to demonstrate their performance in human walking. The outcomes of this research includes developing new conceptual models of legged locomotion, analysis of human locomotion based on the newly developed models following the locomotor subfunction trilogy, developing methods to benefit from the models in design and control of robots and exoskeletons. The main contribution of this work is providing a novel approach for modular control of legged locomotion. With this approach we can identify the relation between different locomotor subfunctions e.g., between balance and stance (using stance force for tuning balance control) or balance and swing (two joint hip muscles can support the swing leg control relating it to the upper body posture) and implement the concept of modular control based on locomotor subfunctions with a limited exchange of sensory information on several hardware platforms (legged robots, exoskeleton).

Inhaltsverzeichnis

1 Introduction and Motivation

Legged systems are the preferred biological technology for locomotion on ground. Identifying basic concepts of legged locomotion in nature such as design and control principles supports enhancement in developing more efficient and agile artificial locomotory systems e.g., biped robots. Furthermore, learning such lessons from nature may be very useful in mechanical design and control of assistive devices such as exoskeletons. Therein, findings in biology and robotics can greatly complement each other (Collins et al., 2015). In spite of long historical research on animal (including human) locomotion, many fundamental concepts and advantages of different architectures (body and actuator morphology) are not identified. Understanding these principles may be critical for improving artificial legged systems and especially assistive devices. Nevertheless, significant differences exist between biological and artificial locomotory systems e.g., with respect to the actuation mechanisms and properties. This fact is challenging the transfer of bioinspired approaches to the design and control of legged robots.

We believe that learning from nature means discovering the principles and translating them to artificial legged locomotion considering all constraints and capabilities of machines. This is completely different from copying every details of biological locomotion to the robot. Inspired from muscle mechanics, inserting elasticity in actuator design e.g., SEAs (series elastic actuators) (Pratt and Krupp, 2004) resulted in a great enhancement in efficiency and robustness of actuators employed for legged systems. Recently, principles of body mechanics and control in legged locomotion attracted attention of researchers from different disciplines ranged from biology (Ijspeert, 2008; Duysens et al., 2002; Holmes et al., 2006; Winter, 2009; Koditschek et al., 2004) to control engineering (Westervelt et al., 2007; Raibert, 1986; Alexander, 2003; Chevallereau et al., 2013).

For a better understanding of the fundamental concepts of legged locomotion we follow the principle of simplified model descriptions which is inspired from the "Template & Anchor" concept (Full and Koditschek, 1999). We aim at simplifying the methods (models, concepts and control rules) as much as possible while keeping the basic targeted features. For this, we benefit from two conceptual elements: templates (Full and Koditschek, 1999) and locomotor subfunctions (Seyfarth et al., 2013).

Legged locomotion can be explained by composing three locomotor subfunctions (Seyfarth et al., 2013): **Stance** (axial leg function), (leg) **swing** and **balance**, (Fig. 1). Stance describes the (e.g. elastic) rebounding or resistance of the stance leg (ground contact) to counteract gravity (Blickhan, 1989). Leg swinging is mainly a rotational movement of the swing leg (Blum et al., 2010) combined with an additional axial leg movement for ground clearance. In bipedal legged systems with body center of mass above hip joint (like in humans) results in inverted pendulum like upper body dynamics which is inherently unstable (Winter, 1995). Maintaining balance (Massion, 1994) is therefore considered as the third locomotor subfunction.

In this thesis we explain how locomotor subfunctions can be used to simplify understanding human locomotion for the design and control of robots and assistive devices. In the first chapter we design a human-inspired controller for walking using hybrid zero dynamics, HZD (Westervelt et al., 2007). We show that even without specifically considering locomotor subfunctions, they emerge from resemblance of human joint kinematics. In the following chapters we present different models for describing locomotor subfunctions in human gaits and for novel design and control approaches in robots (Oehlke et al., 2016), (Sharbafi et al., 2014, 2013b, 2016), (Mohammadinejad et al., 2014), (Sharbafi et al., 2017; Sharbafi and Seyfarth, 2017), (Zhao et al., 2017). Splitting legged locomotion into simpler subfunctions has different advantages such as improving our understanding of human gaits, facilitating modular de-

sign and control of artificial legged systems in relation to the underlying locomotor subfunctions. This subfunction based approach for design and control could lead to more functional assistive devices e.g., prostheses or orthoses.

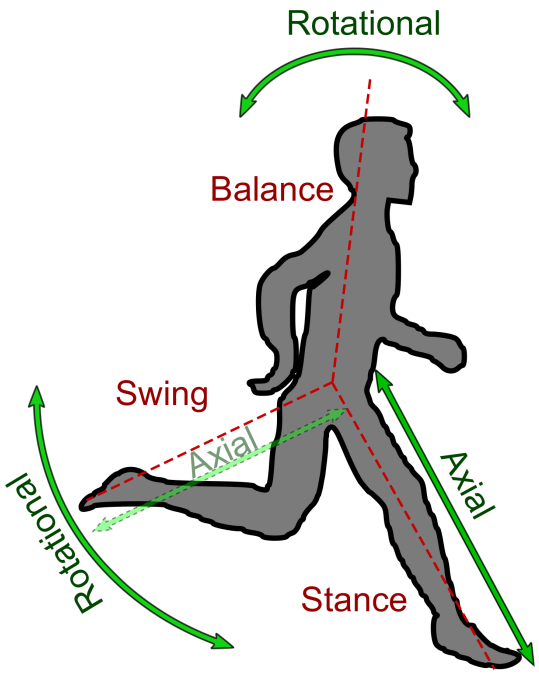

Figure 1: Main locomotion subfunctions; i) axial stance leg function, ii) rotational swing leg function and iii) balance for maintaining posture.

Synchronizing the different subfunctions could require an additional control level. However, we have shown that no extra control layer is required and few sensory interconnections between different subfunction or between body and the subfunctions are sufficient to synchronize them. Such interconnections could be realized by reflex pathways as observed in animal neuromuscular control. In addition, a bioinspired distributed control architecture using a unifying actuation mechanism (like muscles) can support interactions between subfunctions. Human-inspired control based on locomotor subfunctions facilitates interaction between machines and humans. For instance, in human-robot scenario (e.g., in assistive devices), the human motor control system could help coordinate the interaction dynamics between different locomotor subfunctions. This may be achieved by providing the required sensory information of human locomotor subfunctions to the correspondingly represented robot controllers.

To implement the proposed distributed control architecture, we use the template models (Full and Koditschek, 1999) for realization and coordination of the subfunctions (Raibert, 1986; Blickhan, 1989). In our studies we utilize mass-spring and pendulum as oscillators providing basic characteristics of periodic movement. For stance leg we use the SLIP (spring loaded inverted pendulum) model (Blickhan, 1989) which is based on a spring mass oscillator. For leg swinging, our template model stems from a physical pendulum movement developed in (Mohammadinejad et al., 2014). We extend this model to a double pendulum (upper and lower leg) equipped with biarticular thigh muscles. For balancing, the corresponding oscillatory movement is produced by a virtual pendulum (Maus et al., 2010). Table 1 presents an overview of our simplifying approach comprising the locomotor subfunction concept and related template models. In the following, we present an overview of the thesis with brief summaries of each article. The articles are presented in the following ten chapters. The thesis ends with conclusion and outlook.

Table 1: Overview of locomotion subfunctions with basic characteristics and their representation in template models

locomotion subfunction	**objective**	**leg force direction**	**biomechanical template models**
Stance	Interacting with ground	in leg axis	leg spring
Swing	adjust leg orientation during swing phase	perpendicular to and in leg axis	pendulum-like leg with adaptable length + hip spring
Balance	maintaining an upright body orientation	perpendicular to leg axis	hip spring, virtual pendulum

As another object of *simplification principle*, to implement the proposed distributed control architecture, we use the template models (Full and Koditschek, 1999) which are helpful in realization and coordination of the subfunctions (Blickhan, 1989), (Raibert, 1986). In our studies we utilize mass-spring and pendulum as oscillators providing basic characteristics of periodic movement. For stance leg we use the SLIP (spring loaded inverted pendulum) model (Blickhan, 1989)) which is based on spring mass oscillator. For leg swinging, our template model stems from a physical pendulum movement developed in (Mohammadinejad et al., 2014). We extend this model to a double pendulum equipped with biarticular thigh muscles. This oscillatory movement is produced by a virtual pendulum (Maus et al., 2010) as the template model balancing. Table 1 presents an overview of our *simplification principle* including locomotor subfunction concept and their related template models. In the following we present an overview of the thesis through brief summaries of each articles. Then, the articles are presented in ten chapters. Finally, the conclusion and outlook of the thesis are provided.

1.1 Overview

This dissertation contains ten articles presented in separate chapters. Articles I to IX were published as journal papers or presented at conferences. Information on each publisher and the original publication can be found at the chapter's cover page. Article X is submitted to a journal and is currently under review. Each chapter contains a list of the references.
In the following paragraphs the contents of all articles are summarized. The relationships between the different publications are illustrated.

Article I: Mimicking Human Walking with 5-link Model using HZD Controller

In the first chapter we investigate the value of kinematic data for predicting kinetic features of human gait. We employ the HZD controller (Westervelt et al., 2007) to generate stable walking with a 5-link model using human experimental data. In this approach, the virtual leg angle is considered as the coordinator and all joint angles are given as functions of this leg angle. These functions are formulated as virtual constraints which are calculated from human walking data. The controlled model is not only stable, but also robust against model uncertainties while the same controller works for different sets of body parameters. Here, the control goal was mimicking human kinematic behavior with feedback linearization which is the core control rule in HZD. However, we show that virtual pivot point (VPP) concept (Maus et al., 2010) emerges from the simulation results which was not targeted. The VPP as an intersection point of ground reaction forces on the upper body results from human (and animals) kinetic behavior. Therefore, human-like kinetic behavior is also replicated by this controller as an extra achievement. Although this approach was successful to describe human-like walking based on kinematic constraints, it fails in explaining how locomotion is achieved and organized in the human body. This paper presents an engineering-based control approach to mimic human walking features. Even though this method could provide a better understanding in the relation between locomotion kinematics and kinetics, it did not reflect the concept of locomotor subfunctions and does not well represent the way how locomotion control is achieved in humans.

To improve the design and control of legged robots and assistive devices, we need to better understand the control concept used in humans which can be analyzed using locomotor subfunctions. For this, we employ gait templates and develop new models to realize the different locomotor subfunctions and their interconnections. We start with stance as the first locomotor subfunction in Article II. In this chapter a template-based control is implemented on a hopping robot (MARCO-Hopper-II). In the next two chapters, two novel approaches are presented for swing leg modeling and control. In Article V, template-based approaches for stance and swing leg control are applied to control of the BioBiped robot for forward hopping. Articles VI and VII introduce a new template for balancing - the third locomotor subfunction - in running and walking, respectively. Article VIII presents how body morphology regarding the muscle arrangement in the leg can support implementation of template-based control approaches in a bioinspired robot (BioBiped3). Article IX describes the role of different locomotor subfunctions in human walking control at different speeds. Finally, Article X summarizes outcomes of distributing control to the three subfunctions and describes how this method can support assistance in exoskeletons.

Article II: Template-based Hopping Control of a Bio-inspired Segmented Robotic Leg

Vertical hopping can be considered as a primitive dynamic movement within the human locomotion repertoire which addresses axial stance leg subfunction. In this article, the SLIP model (Spring Loaded

Inverted pendulum) (Blickhan, 1989) is used as a template for stance leg control in vertical hopping. The VMC (virtual model control) approach (Pratt et al., 1997) was utilized to emulate a virtual spring between the hip joint and the foot. This controller was implemented on a two-segment hopping robot called MARCO-Hopper-II. The SLIP model was used as a template for human hopping to control the previous MARCO-Hopper comprising a prismatic leg (Kalveram et al., 2012). Extending the concept of SLIP-based control to the robot with a more human-like leg architecture shows its ability to mimic human hopping.

This paper is a first step of investigating the locomotor subfunction control concept using template models. Since the SLIP model can well describe human hopping (and running), with this approach we targeted at two objectives: (i) evaluating the ability of the bioinspired control approach in stabilizing robot hopping and (ii) mimicking human hopping with a segmented leg. Successful implementation on the hardware setup and meeting the objectives demonstrate that such a template based control has a desirable performance when focusing on only one locomotor subfunction. In the next steps, we add other subfunction controllers and study their interactions.

Article III: VBLA, a Swing Leg Control Approach for Humans and Robots

The next locomotor subfunction is leg swinging. We considered two different control approaches for swing leg adjustment: (i) velocity based approach and (ii) template-based control. In this chapter we describe the first approach and the next chapter presents the template- (pendulum-) based swing leg control. Inspired from Raibert's leg adjustment strategy (Raibert, 1986), we have developed the VBLA (Velocity Based Leg Adjustment) method for swing leg control. This method uses the CoM (Center of Mass) velocity vector to determine the desired leg angle. This method was employed to describe human leg adjustment during walking and perturbed hopping and also to generate stable walking, running and hopping using SLIP-based models. These results and also comparisons with two other methods using the same concept of leg adjustment based on CoM speed (Peuker et al., 2012; Raibert, 1986) are described in this article. Therefore, we focus on human swing leg control by analyzing swing leg movements and considering SLIP for stance leg modeling. We show that an isolated swing leg control is working without transferring any sensory information from (or to) other locomotor subfunctions. This approach is later considered in combination with other subfunctions to generate stable gait or predict human locomotion.

Article IV: Reconstruction of Human Swing Leg Motion with Passive Biarticular Muscle Models

In this chapter we present a novel approach for swing leg adjustment. Considering the spring mass system as a template for stance leg, pendulum oscillatory movement was introduced as template model of swing leg. Knuesel et al. introduced the pendulum model for modeling the swing leg movement for running (Knuesel et al., 2005). However, the way of representing the swing leg in the model was closer to forward hopping instead of running. In (Mohammadinejad et al., 2014), we have improved this model to predict swing leg movements in human running and provided a stabilizing method of swing leg adjustment using the SLIP model. However, to make the controlled system asymptotically stable and robust against perturbations, adaptation of pendulum length at apex was suggested. This pendulum model for swing leg movement can be used as a control approach relying on the natural dynamics of a physical system. Additionally, it provides a description of human swing-leg movements and establishes a novel template for swing locomotor subfunction.

In the proposed model, the center of mass dynamics were considered independent of the swing-leg dynamics, which is not realistic. In Article IV, an extension of the pendulum model is developed for

swing leg adjustment in walking. In this approach, a double pendulum is attached to the SLIP model during single support for modeling the swing leg movement. This model is called DPS, standing for Double Pendulum + SLIP. Two biarticular springs are spanning the double pendulum for modeling biarticular thigh muscles (rectus femoris and hamstrings). These springs connect the lower leg (shank) to a virtual upright trunk. It was shown that appropriate adjustment of spring rest lengths not only predicts stable walking, but also mimics human kinematic and kinetic behaviors. In addition, the spring forces are similar to the human biarticular thigh muscle forces.

Article V: Hopping Control for the Musculoskeletal Bipedal Robot BioBiped

In this article, we have employed the stance and swing leg template models to control the BioBiped robot (Radkhah et al., 2011) for forward hopping. The BioBiped series of robots are designed and manufactured in a joined DFG project between the Lauflabor Locomotion Laboratory (sport science) and the SIM group (computer sciences) of TU Darmstadt. In this project, a series of bipedal robots was developed, inspired from human leg musculoskeletal system with a representation of up to 9 muscle groups (Radkhah et al., 2011).

Complementing the robot development, detailed multi-body-system models (MBS model) of the robots were developed (Radkhah, 2014). Using these simulation models, we have investigated the interaction of two different locomotor subfunctions in control of robot hopping. By fixing the trunk to be aligned upright in the hardware set-up using a frame (shown in Fig. 2), we concentrated on stance and swing leg control. For stance leg control, we emulated a virtual spring between the forefoot and hip mimicking SLIP model. The ankle joint is controlled to generate the desired leg force-length relation compensating the energy losses by providing sufficient energy. The knee joint is spanned by passive springs. For the swing leg adjustment, the VBLA was implemented through hip joint actuators. Therefore, modular control of swing and stance phases was examined in interaction with each other. Concentrating on forward hopping allows us to focus one locomotor subfunction for each phase of motion. During swing phase the knee and ankle actuators are used to keep the leg length. This study shows that SLIP-based stance leg control works properly beside swing leg control through VBLA in a real robot model instead of template models. Stable hopping at different speeds and ability to tune the hopping speed with minimal number of parameters were achieved by this control approach. Considering MBS as an anchor model (Full and Koditschek, 1999), here we demonstrate the successful translation from templates to anchors for a real application using BioBiped robot model.

Article VI: Stable Running by Leg Force-modulated Hip Stiffness

In this paper, we introduce a new method for posture control as the third locomotor subfunction. This novel method, called FMCH (force modulated compliant hip), was applied to the TSLIP (Trunk SLIP) model for describing perturbed hopping and running. In order to keep upright trunk posture in human gaits, Maus et al. found that ground reaction forces in different gaits of humans and animals are intersecting in a virtual point above the center of mass, called VPP (virtualt pivot point) (Maus et al., 2010). In our studies, we found a physical representation for this observation: a leg force feedback to modulate hip stiffness (described as FMCH concept). This can be interpreted as a reflex signal in neuromuscular control for hip muscle tuning and is similar to the positive force feedback found in neuromuscular model for axial leg function in bouncing gaits (Geyer et al., 2003).

The FMCH can be considered as a mechanical representation of a neuromuscular model. Here, the properties of the muscle are not modeled. Still required sensory pathways are suggested to adjust hip muscle function to maintain upper body posture. Interestingly, this simple FMCH mechanism is able

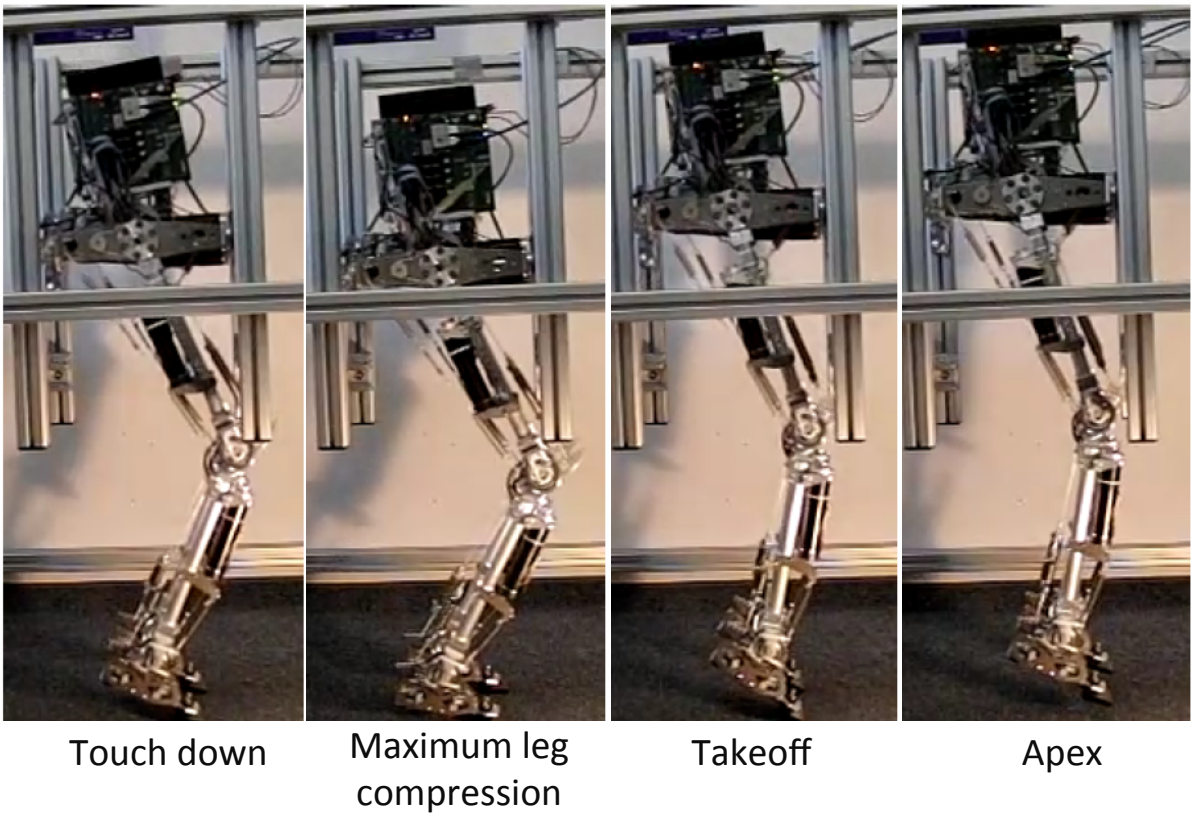

Figure 2: A sample experiment of vertical hopping with BioBiped1 robot. The trunk is constrained by rigid frame to be upright and move only in vertical direction.

to reproduce the VPP as previously described in (Maus et al., 2010). In the model proposed by (Geyer et al., 2003) for repulsive stance leg subfunction (in hopping and running), the positive feedback relies on the force signal of the same muscle. In FMCH, in contrast, the sensory pathway originates from another muscle. This kind of sensory connection can be also considered for coordination between stance and balance subfunctions (knee extensor force tunes hip muscle stiffness for balance). As a result, the leg force tunes the muscle activations required for posture control. In other studies we investigated this approach for walking (Article VII) and extended it to the neuromuscluar level (unpublished work of Sharbafi et al.). In the here presented Article VI, all three locomotor subfunctions are combined to achieve stable movements. We use a leg spring model to describe axial stance leg function, VBLA for swing leg function and virtual pendulum concept implemented through FMCH for balancing.

Article VII: FMCH: a new model for human-like postural control in walking

In this study we use the BTSLIP (bipedal TSLIP) model as the template model to study balance control in walking. Similar to the previous paper (Article VI), spring-mass, VBLA and FMCH are utilized for modeling stance, swing and balance subfunctions. We show that replicating the same VBLA controller for both legs results in stable walking. With the FMCH-related force feedback more human-like hip torques can be obtained in the simulation model compared to (Rummel and Seyfarth, 2010) in which passive hip springs were used for posture control.

With FMCH, the similarity of the model to human posture control can be demonstrated. The ratio between human hip torque and leg force can be approximated by a linear function of the angle between upper body and the virtual leg (line from hip to ankle). This validates the FMCH concept for human

posture control. The evolution of the hip spring parameters (stiffness and rest length) with respect to walking speed is also analyzed in this paper. The role of different locomotor subfunctions at different walking speeds is explained in more detail in Article IX.

Article VIII: A New Biarticular Actuator Design Facilitates Control of Leg Function in BioBiped3

In this paper we focus on the implementation of locomotor subfunction control strategies using biarticular actuators in the new BioBiped3 robot. The main difference of this robot to the previous versions is replacement of passive biarticular muscles with the active ones. With the additional access to the biarticular muscle properties (e.g. rest length) we can support the control of different locomotor subfunctions. We want to show how body morphology and actuation mechanism can support gait and posture control based on the modular architecture of locomotor subfunctions. With that, we do not just demonstrate the advantages of the proposed concept in template models, but also in the control of a robot as an anchor.

Application of the biarticular muscles in stance control is tested by the effect of appropriate adjustment of gastrocnemius (GAS) for synchronizing knee and ankle joints. It is shown that fine tuning of this muscle improves storing and release of elastic energy in a more SLIP-like manner. Therefore, to approach human-like hopping (or running) the GAS muscle can assist the ankle extensor muscle as proposed in Article V.

For swing leg control, we have implemented the double-pendulum SLIP (DPS) model presented in Article IV on the BioBiped MBS model. For that a similar study to Article V was performed while the VBLA is replaced by this pendulum based swing leg control approach. We have shown that appropriate adjustment of biarticular hip muscles just before takeoff is sufficient to provide stable forward hopping. In addition, the gait speed can be tuned by this control parameter. Energy management is achieved through ankle joint control during stance.

Finally, for the posture control, we have investigated the ability of biarticular hip muscles to adjust the ground reaction force direction. It is shown that GRF control can be divided to magnitude and direction control which can be separately performed by monoarticular (knee) and biarticular (thigh) muscles, respectively. Since, control of GRF direction is the key for VPP based balancing, these findings demonstrate that biarticular muscles are more beneficial compared to monoarticular muscles for posture control.

Article IX: How Locomotion Sub-functions Can Control Walking at Different Speeds?

The focus of this article is on explaining human walking at different speeds using locomotor subfunctions. We have selected single support phase, because it includes all subfunctions while leg swinging is absent in double support. We consider different models to characterize the subfunctions with minimum number of parameters. The SLIP model describes stance control by determining stiffness and rest length of the leg spring. Based on human walking data we show that there is a prominent change in these two parameters at middle of single support phase. The angle of attack and angular speed at touchdown characterize leg swinging and the variable hip stiffness (feedback gain) and the hip spring rest angle are utilized to maintain balance.

Evolution of these parameters is dependent on walking speed, especially for fast walking (higher than normal walking speed). This study demonstrates that the modular concept of locomotor subfunction can well describe human motion control and contributions of the different subfunctions at different walking speeds.

This final chapter presents an outlook on how this locomotor subfunction approach can be applied to an assistive device. An appropriate matching between human and exoskeleton controller is important for a successful human-robot interaction. We apply our modular control approach based on human locomotor subfunction to the design and control of an assistive device. The human subject can play the role of a coordinator between different locomotor subfunction controllers if required. For example using ground reaction force signals for posture control supports the interaction between robot and human. We have shown first results of implementing the FMCH on the exoskeleton LOPES II for assisting human walking (Zhao et al., 2017). In all subjects we found a reduction in muscle activation and metabolic cost in assisted walking with FMCH-based control.

1.2 REFERENCES

Alexander, R. M. (2003). *Principles of animal locomotion*. Princeton University Press.

Blickhan, R. (1989). The spring-mass model for running and hopping. *Journal of Biomechanics*, 22(11):1217–1227.

Blum, Y., Lipfert, S., Rummel, J., and eyfarth, A. (2010). Swing leg control in human running. *Bioinspiration and Biomimetics*, 5(2).

Chevallereau, C., Bessonnet, G., Abba, G., and Aoustin, Y. (2013). *Bipedal robots: Modeling, design and walking synthesis*. John Wiley & Sons.

Collins, S. H., Wiggin, M. B., and Sawicki, G. S. (2015). Reducing the energy cost of human walking using an unpowered exoskeleton. *Nature*, 522(7555):212–215.

Duysens, J., Van de Crommert, H. W., Smits-Engelsman, B. C., and Van der Helm, F. C. (2002). A walking robot called human: lessons to be learned from neural control of locomotion. *Journal of biomechanics*, 35(4):447–453.

Full, R. J. and Koditschek, D. (1999). Templates and anchors: Neuromechanical hypotheses of legged locomotion on land. *Journal of Experimental Biology*, 22:3325–3332.

Geyer, H. Seyfarth, A. and Blickhan, R. (2003). Positive force feedback in bouncing gaits? *Proceedings of the Royal Society of London B: Biological Sciences*, 270: 2173–2183.

Holmes, P., Full, R. J., Koditschek, D., and Guckenheimer, J. (2006). The dynamics of legged locomotion: Models, analyses, and challenges. *Siam Review*, 48(2):207–304.

Hurst, J. (2008). *The Role and Implementation of Compliance in Legged Locomotion*. PhD thesis, Robotics Institute, Carnegie Mellon University.

Ijspeert, A. J. (2008). Central pattern generators for locomotion control in animals and robots: a review. *Neural networks*, 21(4):642–653.

Kalveram, K. T., Haeufle, D. F. B., Seyfarth, A., and Grimmer, S. (2012). Energy management that generates terrain following versus apex-preserving hopping in man and machine. *Biological Cybernetics*, 106(1):1–13.

Knuesel, H., Geyer, H., and Seyfarth, A. (2005). Influence of swing leg movement on running stability. *Human Movement Science*, 24:532–543.

Koditschek, D. E., Full, R. J., and Buehler, M. (2004). Mechanical aspects of legged locomotion control. *Arthropod structure & development*, 33(3):251–272.

Massion, J. (1994). Postural control system. *Current opinion in neurobiology*, 4(6):877–887.

Maus, H. M., Lipfert, S., Gross, M., Rummel, J., and Seyfarth, A. (2010). Upright human gait did not provide a major mechanical challenge for our ancestors. *Nature Communications*, 1(6):1–6.

Mohammadinejad, A., Sharbafi, M. A., and Seyfarth, A. (2014). Slip with swing leg augmentation as a model for running. In *Intelligent Robots and Systems, IEEE/RSJ International Conference on*, pages 2543–2549.

Oehlke, J., Sharbafi, M. A., Beckerle, P., and Seyfarth, A. (2016). Template-based hopping control of a bio-inspired segmented robotic leg. In *Biomedical Robotics and Biomechatronics, IEEE International Conference on*, pages 35–40.

Peuker, F., Maufroy, C., and Seyfarth, A. (2012). Leg adjustment strategies for stable running in three dimensions. *Bioinspiration and Biomimetics*, 7(3).

Pratt, J. E. and Krupp, B. T. (2004). Series elastic actuators for legged robots. In *Defense and Security*, pages 135–144. International Society for Optics and Photonics.

Pratt, J., Dilworth, P., and Pratt, G. (1997). Virtual model control of a bipedal walking robot. In *Robotics and Automation, 1997. Proceedings., 1997 IEEE International Conference on*, volume 1, pages 193–198. IEEE.

Radkhah, K. (2014). *Advancing musculoskeletal robot design for dynamic and energy-efficient bipedal locomotion*. PhD thesis, Technische Universität.

Radkhah, K., Maufroy, C., Maus, M., Scholz, D., Seyfarth, A., and Von Stryk, O. (2011). Concept and design of the biobiped1 robot for human-like walking and running. *International Journal of Humanoid Robotics*, 8(03):439–458.

Raibert, M. H. (1986). *Legged Robots that Balance*. MIT Press, Cambridge MA.

Rummel, J. and Seyfarth, A. (2010). Passive stabilization of the trunk in walking. In *International Conference on Simulation, Modeling and Programming for Autonomous Robots*, Darmstadt, Germany.

Seyfarth, A., Grimmer, S., Maus, M., Häufle, D., Peuker, F., and Kalveram, K.-T. (2013). Biomechanical and neuromechanical concepts for legged locomotion. *Routledge Handbook of Motor Control and Motor Learning*, pages 90–112.

Sharbafi, M. A., , Radkhah, K., von Stryk, O., and Seyfarth, A. (2014). Hopping control for the musculoskeletal bipedal robot: Biobiped. In *Intelligent Robots and Systems, IEEE/RSJ International Conference on*, pages 4868–4875.

Sharbafi, M. A., Maufroy, C., Ahmadabadi, M. N., Yazdanpanah, M. J., and Seyfarth, A. (2013). Robust hopping based on virtual pendulum posture control. *Bioinspiration & biomimetics*, 8(3):036002.

Sharbafi, M. A., Mohammadinejad, A., Rode, C., and Seyfarth, A. (2017). Reconstruction of human swing leg motion with passive biarticular muscle models. *Human Movement Science*, 52:96–107.

Sharbafi, M. A., Rode, C., Kurowski, S., Scholz, D., Möckel, R., Radkhah, K., Zhao, G., Rashty, A. M., von Stryk, O., and Seyfarth, A. (2016). A new biarticular actuator design facilitates control of leg function in biobiped3. *Bioinspiration & Biomimetics*, 11(4):046003.

Sharbafi, M. A. and Seyfarth, A. (2017). How locomotion sub-functions can control walking at different speeds? *Journal of Biomechanics*.

Westervelt, E. R., Grizzle, J. W., Chevallereau, C., Choi, J. H., and Morris, B. (2007). *Feedback Control of Dynamic Bipedal Robot Locomotion*. Taylor & Francis, CRC Press.

Winter, D. (1995). Human balance and posture control during standing and walking. *Gait & posture*, 3(4):193–214.

Winter, D. A. (2009). *Biomechanics and motor control of human movement*. John Wiley & Sons.

Zhao, G., Sharbafi, M., Vlutters, M., van Asseldonk, E., and Seyfarth, A. (2017). Template model inspired leg force feedback based control can assist human walking. In *IEEE-RAS-EMBS International Conference on Rehabilitation Robotics*.

2 Article I: Mimicking human walking with 5-link model using HZD controller

Authors:

Maziar Ahmad Sharbafi and André Seyfarth

Technische Universität Darmstadt

64289 Darmstadt, Germany

Published as a paper at the

2015 IEEE/RSJ International Conference on Robotics and Automation (ICRA)

ABSTRACT

Walking with 5-link model has been achieved by HZD (Hybrid Zero Dynamics) controller based on virtual constraints. These holonomic constraints are obtained by optimizing a set of virtual relations (e.g., Beziér polynomial) between system states which mostly do not have physical interpretations. In this paper, the virtual constraints are designed using human walking experiment data. Inspiring from human locomotion, different polynomials are extracted to mimic human joint angles patterns during walking. The virtual leg angle is the increasing variable which synchronize the joints angles and defines the virtual constraints. Simulation results show that stable locomotion with leg and upper-body behavior similar to human experiment data is achieved for a wide range of speeds and body configuration parameters. VPP (Virtual Pivot Point) concept, a significant balancing feature found in human/animal locomotion, is investigated for different gait speeds as a performance index to compare the kinetic behavior of the simulated and human walking. Hence, we present human-like posture control as an outcome of motion control achieved by HZD with human inspired virtual constraints.

2.1 INTRODUCTION

Bipedal walking has been extensively investigated by researchers in the recent decades. Diverse control approaches were developed, from biologically inspired (e.g., CPG controllers Ijspeert (2008); Owaki et al. (2011)) and conceptual model based approach (e.g., SLIP model Geyer et al. (2003); Seyfarth et al. (2002)) to engineering methods (e.g., ZMP VukobratoviÂt'c and Stepanenko (1972) or HZD Westervelt et al. (2007)). Most of the popular methods are focusing on one, either human locomotion or robot control technique. Applying the conceptual models as templates for control may be a useful approach to fill the gap between human experiments and robot control Full and Koditschek (1999). For this, abstraction is the key feature in simplifying the human locomotion problem, finding a solution and extending the simple control to the complex model, namely "template and anchor" Full and Koditschek (1999). Finding virtual pendulum concept in human/animal locomotion and utilizing it for postural control can be considered as another approach in extracting locomotion rules from nature and applying them to the machines Maus et al. (2010). The control rule resulted from this study is producing hip torque in order to redirect the ground reaction forces to a predefined Virtual Pivot Point (VPP). However, all control disciplines of human locomotion might not be as straight forward as this one. Therefore, we select a well established control method with sufficiently flexible degrees of freedom, design it based on human experiment data and investigate existence of VPP.

Hybrid Zero Dynamics (HZD), employing feedback linearization as a powerful nonlinear control approach, is founded on defining some relations between the system states, namely virtual constraints Westervelt et al. (2007). These relations are defined as holonomic constraints on robot's configuration which are mostly computed mathematically, based on optimization approaches Morris and Grizzle (2009); Poulakakis and Grizzle (2009); Sreenath et al. (2010). In Ames (2012a), Ames presented a linear spring-mass-damper system characterized by human experimental data, called "canonical human walking functions", to generate virtual constraints of the leg movement, based on hip position. In other studies (e.g., Jiang et al. (2012), Powel et al. (2012), Ames (2012b)) similar constraints, were considered for copying human kinematic behavior in a model and/or a robot even without upper body.

In this paper, we utilize data from human walking experiments to extract internal relations between joints' angles and stance leg orientation which hold the configuration harmonized during the gaits. It is shown that with such virtual constraints, mimicking human kinematic and kinetic walking behaviors is achievable. In our previous studies, the relation between VPP and HZD was investigated by conceptual models for hopping and running Sharbafi et al. (2013, 2012). Here, a five link model with a rigid upper body and two segmented legs is used to implement a human-inspired HZD controller for walking (See

Fig. 1). With the presented controller, VPP exists for all speed and its contribution in motion speed is also analyzed. Postural stability is one of significant achievements of this paper which was not addressed in the previous studies with similar HZD contoller Ames (2012a); Jiang et al. (2012), Powel et al. (2012),Ames (2012b). In addition, we show that the proposed controller is also robust against body parameters' variations which shows that control rules are fixed even for different structures (e.g, distribution of mass and inertia). In summary, the results show three significant outcomes: 1) The human inspired HZD controller can stabilize the walking at different speeds. 2) The kinematics (gait trajectories like joint angles) are similar to those obtained in human experiments 3) VPP exists which can be interpreted as an index for similarity to human walking kinetics.

2.2 METHODS

2.2.1 Simulation model

A 5-link model[1] is defined with five rigid segments, four active joints and one passive contact with the ground as shown in Fig. 1. This model is widely used for different robots like Mabel Sreenath et al. (2010) and Rabbit Grizzle and Westervelt (2008). In our simulations, the model parameters are set to match the characteristics of a human with 70.9 kg weight and 1.73 m height (see Table 1) which are the average values computed from the experiment subjects' body characteristics Lipfert. (2010). Walking dynamics (gait cycle) has two phases: *swing phase (single support)* and *stance phase (double support)*. In single support, one leg (stance leg) is in contact with the ground when the other leg (swing leg) moves forward to complete the step. Based on the angles (q_i, $i = 1..5$) shown in Fig. 1, single support walking dynamics are defined using Lagrange equation on the angle vector $q = [q_1..q_5]^T$ as

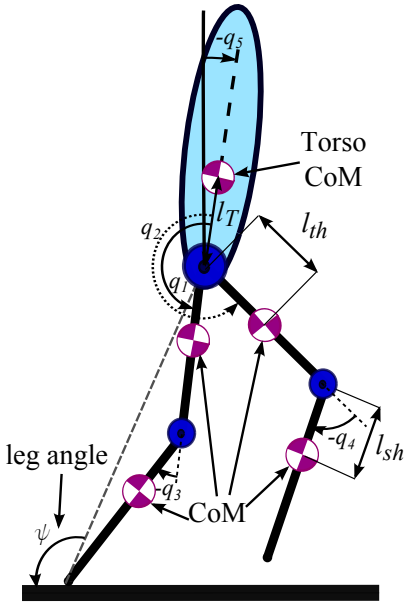

Figure 1: The schematic of 5-link model.

$$D(q)\ddot{q} + C(q,\dot{q})\dot{q} + G(q) = Bu \tag{1}$$

in which D and C are the inertia and the Coriolis matrices, respectively. G is the gravity vector and B is a constant matrix that maps the joints' torques vector u to the generalized forces.

$$\dot{x} = \begin{bmatrix} \dot{q} \\ D^{-1}[-C\dot{q} - G] \end{bmatrix} + \begin{bmatrix} 0 \\ D^{-1}B \end{bmatrix} u = f(x) + g(x)u. \tag{2}$$

At the end of the swing phase, when the moving leg hits the ground (instant of touchdown) an impact occurs (instantaneous double support). With inelastic impact, the velocity of the contact leg end becomes zero instantaneously and the system initiates in a new continuous phase. Without impulsive actuation,

[1] The simulation model is a modified version of 5-link model presented in `http://web.eecs.umich.edu/~grizzle/westervelt_thesis/code/`

Table 1: 5-link model parameters with average weight and height from human experiments. The segments parameters are computed based on ratios in Winter (2005).

Name	Parameter	value	unit
M_T	Torso mass	47.9	
M_{th}	Thigh mass	7.1	kg
M_{sh}	Shank mass	4.4	
L_T	Torso length	0.81	
L_{th}	Thigh length	0.46	m
L_{sh}	Shank length	0.46	
l_T	Hip to torso CoM distance	0.3	
l_{th}	Hip to thigh CoM distance	0.2	m
l_{sh}	Knee to shank CoM distance	0.27	
I_T	Torso inertia	7.9	
I_{th}	Thigh inertia	1.3	kgm^2
I_{sh}	Shank inertia	0.7	
g	Gravitational acceleration	9.81	m/s^2
μ	Static friction coefficient	0.6	–

integrating the system dynamic equation[2] over the impact duration results in $x^+ = \Delta(x^-)$, when superscript signs $^-$ and $^+$ describe the variables exactly before and after impact, respectively. Considering S as the manifold of double support configurations, the hybrid model will be

$$\Sigma = \begin{cases} \dot{x} = f(x) + g(x)u & x^- \notin S \\ x^+ = \Delta(x^-) & x^- \in S \end{cases} \tag{3}$$

2.2.2 Control approach

HZD controller:

Hybrid zero dynamics (HZD) analysis and HZD controller based on virtual constraints were developed in Westervelt et al. (2003) and Grizzle et al. (2001). HZD controller is selected in this paper for its outstanding stability analysis background and successful applications to different robots Grizzle et al. (2009), Grizzle et al. (2008), Morris and Grizzle (2009) and Poulakakis and Grizzle (2009). In HZD, holonomic constraints on the robot's configuration which are asymptotically achieved through the feedback control action are defined as virtual constraints by $y = h(q)$ Shih et al. (2007). In other words, virtual constraints' concept presents the ability to reproduce a desired kinematic behavior of a mechanical construction, via designing the controller instead of using the physical mechanism Westervelt et al. (2007). The control torque is determined via feedback linearization to regulate the output (y) to zero which should prepare a stable attractive manifold, namely "hybrid zero dynamics manifold". Since its stability cannot be evaluated in the stage of designing the output, some free parameters are considered in output definition to be used later to stabilize this manifold. The output only depends on the angles

[2] At impact, to consider the external force at the end of the second leg, Eq. (2) is written with two more degrees of freedom (e.g., adding the second foot position to the generalized coordinate). For more details, see Westervelt et al. (2007).

$(h(x) = h(q))$ and from the second order system (2), the system relative degree is 2 and the following controller results in the input-output linearization.

$$u(x) = (L_g L_f h(x))^{-1}(\overbrace{-K_D\dot{y} - K_P y}^{v} - L_f^2 h(x)) \tag{4}$$

$L_f h(x) := \frac{\partial h}{\partial x} f$ is the Lie derivative of h along f and repeating this operator on $L_f h(x)$ along g and f, results in $L_g L_f h(x)$ and $L_f^2 h(x)$, respectively. We assume $L_g L_f h$ is invertible. Putting (4) in (2) results in $\ddot{y} = v$, a linear differential equation between the new input v and the output y which converges exponentially to zero employing a traditional *PD* controller. Thus, the input-output stability is gained; but the internal stability depends on the stability of the internal dynamics. On the zero dynamics manifold $Z := \{x|\ h(q) = L_f h(q) = 0\}$, the internal dynamics are simplified to the zero dynamics. The stability of the zero dynamics is investigated using Poincaré map analysis (see Westervelt et al. (2007) for more details).

Virtual Constraint from human experiment:

In order to define the virtual constraints, the outputs (of dimension 4) should be determined as functions of the angles and a monotonically increasing variable $\theta(q)$. Similar to Westervelt et al. (2003), we select the first four angles $[q_1\ ..\ q_4]$ and also $\theta(q) := \psi$, the leg angle shown in Fig. 1, for output definition.

$$y = \begin{bmatrix} y_1 \\ y_2 \\ y_3 \\ y_4 \end{bmatrix} := \begin{bmatrix} q_1 \\ q_2 \\ q_3 \\ q_4 \end{bmatrix} - \begin{bmatrix} h_1(\psi) \\ h_2(\psi) \\ h_3(\psi) \\ h_4(\psi) \end{bmatrix} \tag{5}$$

where $h_i(\psi)$ is a function of the leg angle (for $i \in [1,2,3,4]$). In Westervelt et al. (2003), it is shown that with these output definition, virtual constraints can be found to simplify zero dynamics computations. The only remained step in designing the HZD controller is defining the desired evolution of the angles with appropriate functions $h_1(\psi)$ to $h_4(\psi)$. We extract these functions from experimental data by fitting a 5 degrees polynomial of the leg angle to each joint angle q_i. It means that, we employ walking data to define the virtual constraints between the joint angles and the leg angle. This is the main difference of this paper with the previous studies which can reproduce the human walking patterns in a closed loop manner.

2.2.3 Experimental data

The data was collected in walking experiments on a treadmill (type ADAL-WR, Hef Tecmachine, Andrezieux Boutheon, France) at different speeds. Motion capture data (Qualisys, Gothenburg, Sweden) from 11 markers and ground reaction force data (12 piezo-electric force transducers within the treadmill) were collected. Twenty one subjects (11 female, 10 male) were asked to walk at different percentages of their preferred transition speed (PTS)[3]. The treadmill speed which equals the average velocity during strides was employed as the walking speed. The subjects were between 22 to 28 years old with $1.73 \pm 0.09m$ height and $70.9 \pm 11.7kg$ weight.

[3] PTS is the preferred speed for transition between running and walking which is typically about $1.9 - 2.1\ m/s$ for humans Lipfert. (2010) .

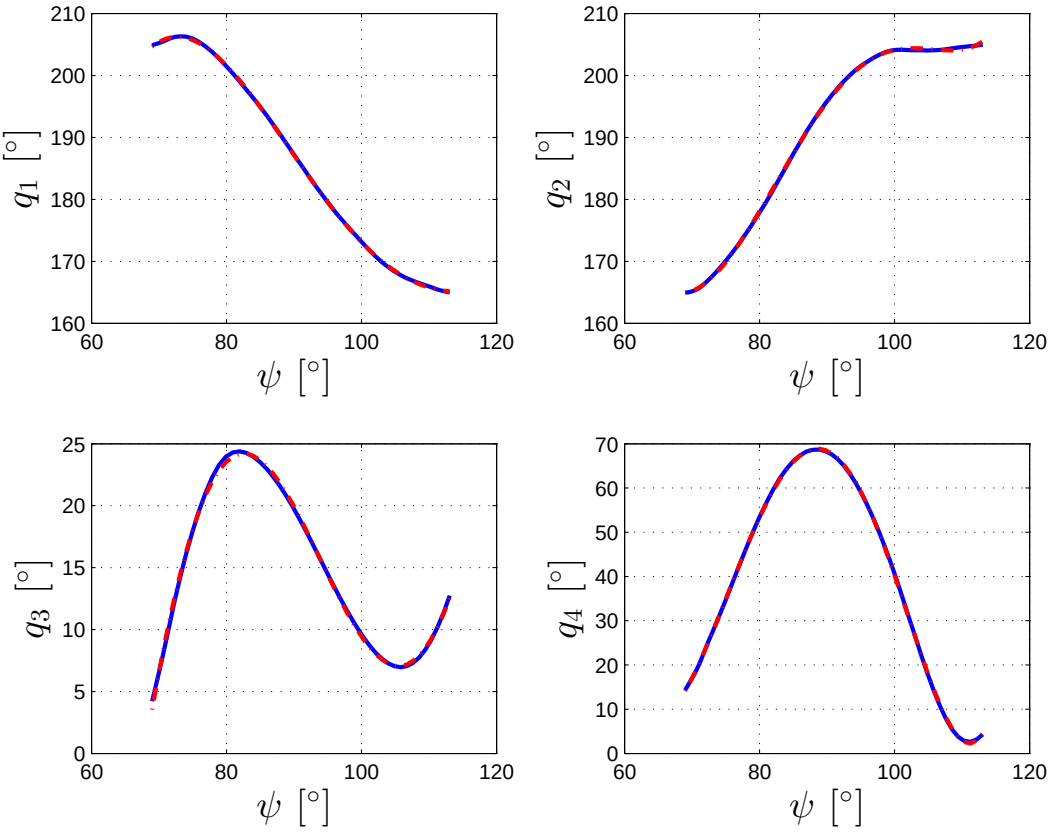

Figure 2: The relation between the joint angles and the leg angle during one step. The blue line is the angles of the human experiment and the red dashed line is the 5 degree polynomial fitted to the data.

2.2.4 Finding VPP location

VPP (virtual pivot point) is a point where the ground reaction forces intersect in the coordinate system centered at CoM and with the body orientation as the vertical axis. This property, observed in human/animal locomotion Maus et al. (2010), may be considered as a target for control or an index to evaluate the similarity of the control strategy to that of humans/animals. Thus, for every control approach, existence of the VPP which may convert the locomotion from inverted pendulum motion to a regular virtual pendulum (VP) can be investigated. VPP is defined in Maus et al. (2010) as "the single point at which the total transferred angular momentum remains constant and the sum-of-squares difference to the original angular momentum over time is minimal, if the GRF is applied at exactly this point". In this paper, the VPP is found using the calculations described in Sharbafi and Seyfarth (2014). For every control approach, the existence of a VPP is given when the ground reaction forces intersect at a point above the center of mass.

2.3 RESULTS AND DISCUSSION

In this section, a 5-link model is simulated based on the average values of human body parameters extracted from the walking experiment (see Table 1). Similar to the experiments, 5 different gait speeds from 25%PTS to 125%PTS are simulated. As the preferred walking speed is about 75%PTS, first, we show the simulation results for this speed. The results and the design procedure are similar for the

other speeds. Then, the human walking experiment results are compared to the simulated model for 5 different speeds. In that respect, existence of VPP and the relation between its position and gait speed are investigated. Finally, the same virtual constraints are utilized for different sets of body parameters to evaluate the robustness.

2.3.1 HZD controller design

In this section, we describe the HZD controller design and the results of walking with 75%PTS. The first step in designing the controller is defining the virtual constraints. We utilize the leg and joint angles (ψ and q_1 to q_4) mean values of 21 different subjects' walking steps, as the references for computing the virtual constraints. As can be seen in Fig. 2, the joint angles are perfectly approximated with 5 degree polynomial functions of the leg angle. Unlike Ames (2012a) which approximates the states as functions of time and then approximate time from hip position and velocity, we use the leg angle directly to coordinate the joints internally. Therefore, the joint angles can be synchronized by the leg angle which makes the controller time-invariant and robust against perturbation and parameter changes. Although these functions are extracted from human walking experiments with body characteristics presented in Table 1, later, we apply the same virtual constraints for a different set of human body parameters and also for the parameters of Rabbit robot adopted from Westervelt et al. (2007) and they work in both cases.

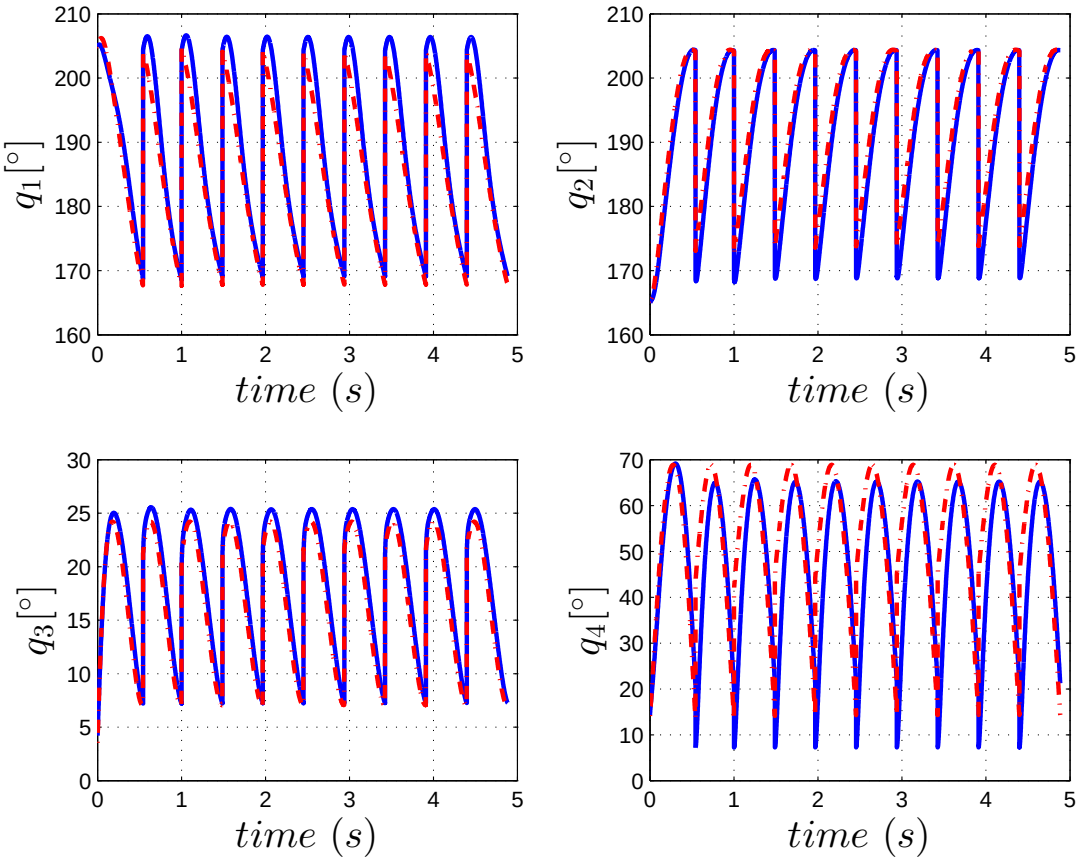

Figure 3: Hip and knee angles of the swing and stance legs (defined in Fig. 1) during 10 walking steps with $75\%PTS$. Blue line shows the angles computed based on human inspired virtual constraints and red dashed line are the simulation responses with 5-link model.

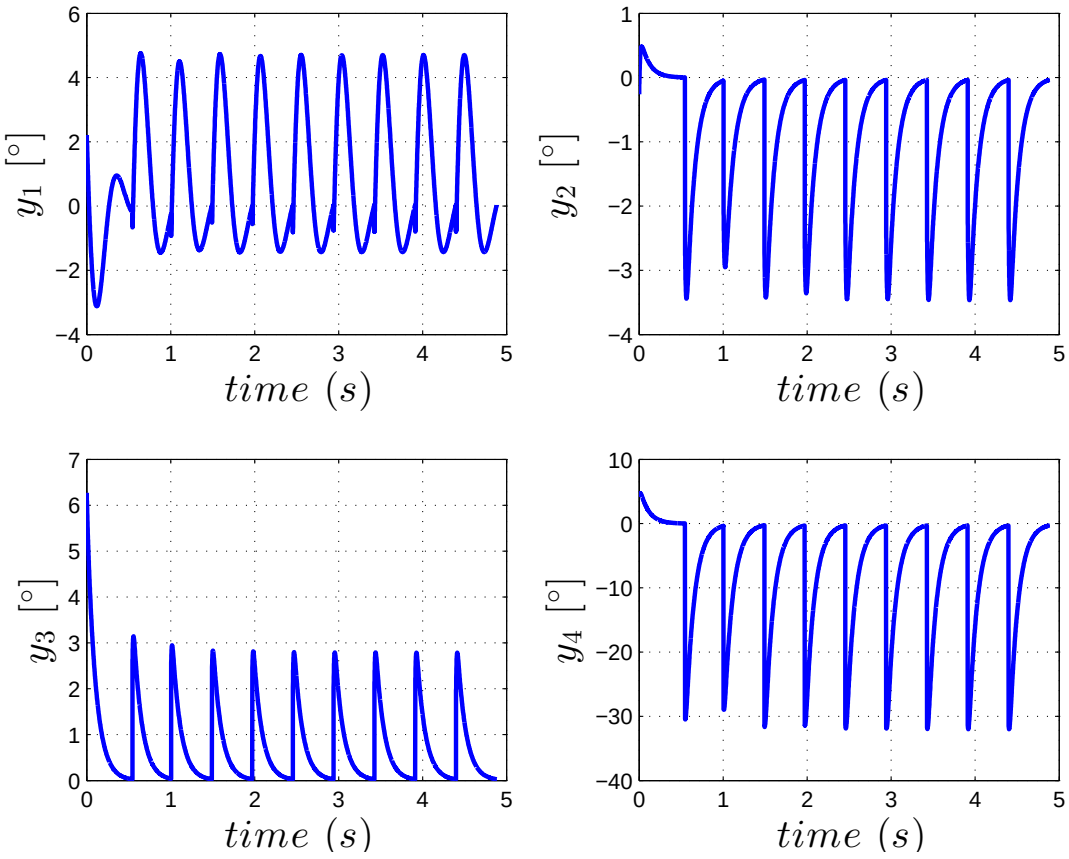

Figure 4: The outputs (5), defined by virtual constraints as the difference between the joint angles and the 5 degree polynomial of the leg angle (deviations from zero dynamics), during 10 walking steps with 75%*PTS*.

Since we do not optimize the virtual constraints to find an optimal controller with an attractive hybrid zero dynamics manifold, the resulted zero dynamics might not be hybrid invariant. To resolve this issue, we should check if a particular choice of parameters results in an exponentially stable walking cycle that is transversal to the switching surface S. Thus, it is needed to evaluate the restricted Poincaré map $\rho : S \cap Z \to S \cap Z$. Defining the vertical position of the swing foot by p_v^{sw}, the related Poincaré map should be checked on the following one dimensional surface

$$S \cap Z = \{(q, \dot{q}) | y = \dot{y} = 0, p_v^{sw} = 0\} \tag{6}$$

which gives 9 relations to compute the intersection of the zero dynamics manifold and switching surface. Therefore, considering $\dot{\psi}^-$ (the angular velocity of the stance leg before impact[4]), as the only remained unknown parameter, a one dimensional (local coordinate) representation of the Poincaré map can be computed as $\hat{\rho}(\dot{\psi}^-)$. Finding initial value $\dot{\psi}^{-*}$ which satisfies $\hat{\rho}(\dot{\psi}^{-*}) = \dot{\psi}^{-*}$ gives the fixed point of the Poincaré map[5]. With 75%*PTS*, the asymptotically stable walking cycle is achieved with $\dot{\psi}^- = 1.2\ rad/s$.

[4] Any joint angular velocity or combination of them can be selected. Here we chose $\dot{\psi}^-$ to have feeling about the motion speed.

[5] The procedure of computing the 1D Poincaré map $\hat{\rho}$ to check the existence and stability of the orbit is described for 3-segment model in Sec.6.6.1 of Westervelt et al. (2007). Here, the same method is aplied to the 5-link model.

Employing appropriate *PD* coefficients in controller (4), results in tracking the desired joint angles, computed from virtual constraints, as shown in Fig. 3. The periodic motion as a result of converging to the stable limit cycle is depicted in this figure. Since the outputs are defined by differences between the angles and their desired values, they determine deviations from zero dynamics manifold in different directions (joint angles). Fig. 4 shows that the outputs which should converge to zero get their maxima after impacts and then vanish during swing phase. The output regulation (to zero) is sufficiently fast to return to zero dynamics manifold before the next impact. It means that though the zero dynamics is not hybrid invariant, it is attractive enough to cope with the errors caused by impact. Therefore, with the virtual constraints, generated based on human walking experiments, a stable gait with regular walking speed (75% PTS) is obtained. As explained before, the stability of the system is verified using the Poincaré map analysis of the zero dynamics which is a one order system. With this approach, after satisfying input-output stability of the system with feedback linearization (controller (4)), the eigenvalue of the Poincaré map of the zero dynamic system is checked. With eigenvalue inside the unit circle, the stability of the complete system (10th order system) is guaranteed.

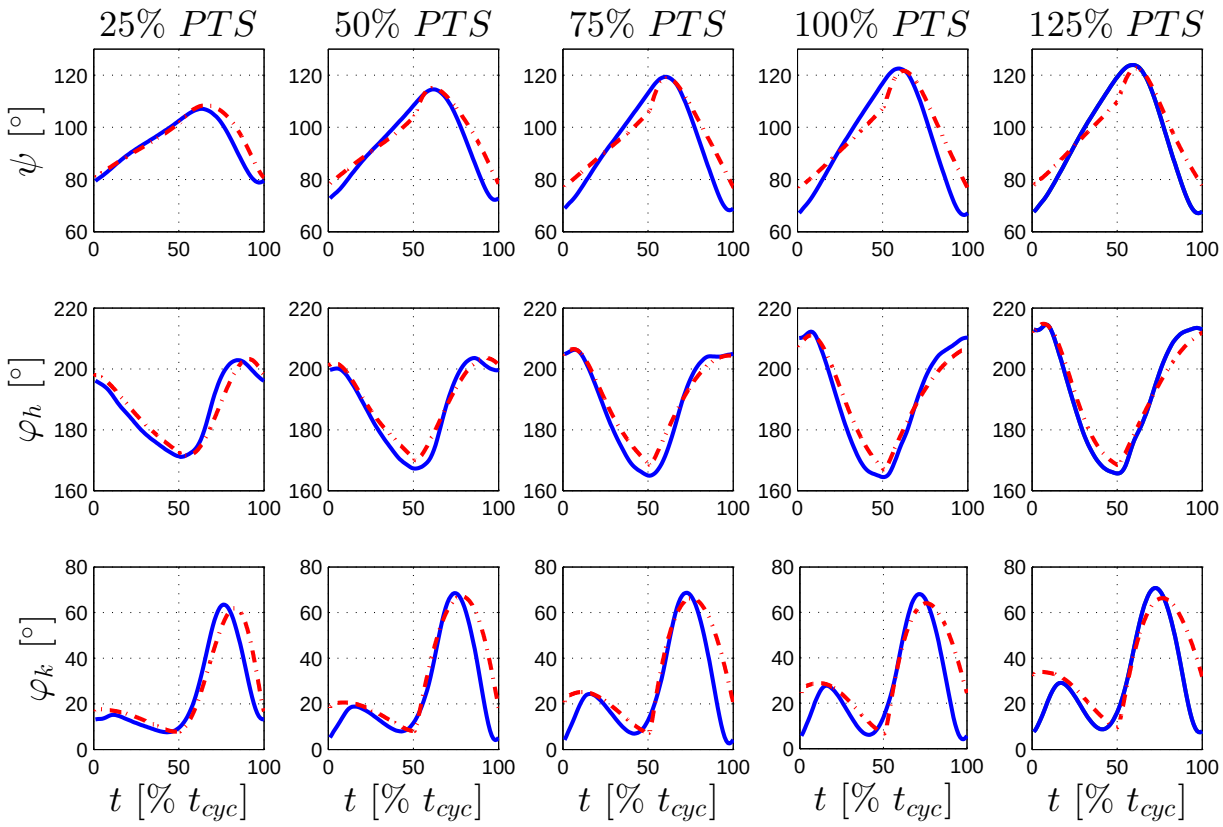

Figure 5: The leg, knee and hip angles (ψ, ϕ_k and ϕ_h) of one gait cycle for different speeds. The blue line is the human experiment and the red dashed line is the simulation response with the 5-link model.

2.3.2 Comparison with human experiments

In this section, the results of walking with HZD controller based on human experiment inspired virtual constraints are compared to experimental data for 5 different speeds. For each speed, we utilize the related experiment to extract an appropriate set of virtual constraints defined by four polynomials of

degree 5. This virtual constraints identification stage finally gives 20 polynomials of degree 5. Then, for each gait we employ the related virtual constraints to generate the stable movement. Fig. 5 displays the leg, hip and knee angles of the experiments and simulations during one gait cycle. It starts with the values for the stance leg and after 50% of the gait cycle the angles relate to the swinging leg. It is observed that the general trends of the experiment and simulation are similar for all gait speeds, especially for hip angle. The differences at the beginning and end of each step may come from modeling simplifications which consider instantaneous double support. The main important point is presenting a template for defining the virtual constraints based on human experiments which can stabilize the gait with similar movement patterns.

In order to investigate the kinetic behavior of the produced stable walking, we analyze the ground reaction force (GRF) and also employ the Virtual Pendulum (VP) concept as a feature in balancing the upper body. In Fig. 6, the GRFs directions are drawn with dashed lines from foot (center of pressure) when the coordinate system is centered at body CoM and the vertical axis shows the upper body direction. The VPPs computed for the simulation model and experiments (separately for each subject) are shown in this figure. As can be seen, the VPP exists in all gait speeds and the computed VPP points from simulations are in the neighborhood of the region found in human experiments, especially for walking faster than $25\%PTS$. Although with a fixed VPP, different gait speeds can be achieved Maus et al. (2010), here, with a fixed controller architecture, changing the virtual constraints may be considered as a way of changing the VPP to adapt with the motion speed. However, balancing (with VPP position) is not the only control mechanism for changing the speed. Another control layer also contributes to gait speed is leg adjustment which determines the step length and angle of attack and this contribution is sometimes more significant than postural control. Focusing more on Figs. 5 and 6 shows that for $75\%PTS$ (regular walking speed) and more, in which the angle of attack is almost constant (about 77°) and the step length changes are smaller than that of the slower gaits, the effect of VPP position on motion speed is more visible. For these speeds, the further VPP from CoM, the longer virtual pendulum and equivalently, the larger upper body oscillations, required for the faster motion. It seems that for slow motions, the speed is controlled by swing leg adjustment and when balancing should be performed in a slower manner, longer pendulum length is needed and the VPP moved more upward. However, the existence of VPP during walking shows that the proposed controller tries to mimic the kinetic behavior of human walking, in addition to kinematics.

2.3.3 Robustness against model parameters

In order to investigate robustness of the proposed controller, we apply it to two other body structures (see table. 2). The first parameter set corresponds to a human with 1.89 m height (with leg length 1 m) and 80 kg weight. The ratio between different segments' masses, inertias lengths and CoM positions are similar to the average value of Table. 1. The controller, proposed in the previous section, with the same parameters (virtual constraints and PD coefficients) is applied to the new body structure. It is noteworthy that a fixed controller works for different body characteristics. It shows that the virtual holonomic constraints are the basic rules of motion which should be considered to make stable walking and for each speed, irrelevant to body parameters, a specific set of virtual constraints is required.

Another example is the parameter configuration of the Rabbit robot Westervelt et al. (2007). Obviously, the structure and ratios of different segments' parameters are quite different to humans. Surprisingly, to stabilize the walking with this model, only the PD coefficients need to be adjusted. It means that with a fixed set of virtual constraints and only with tuning the convergence rate to the zero dynamics manifold

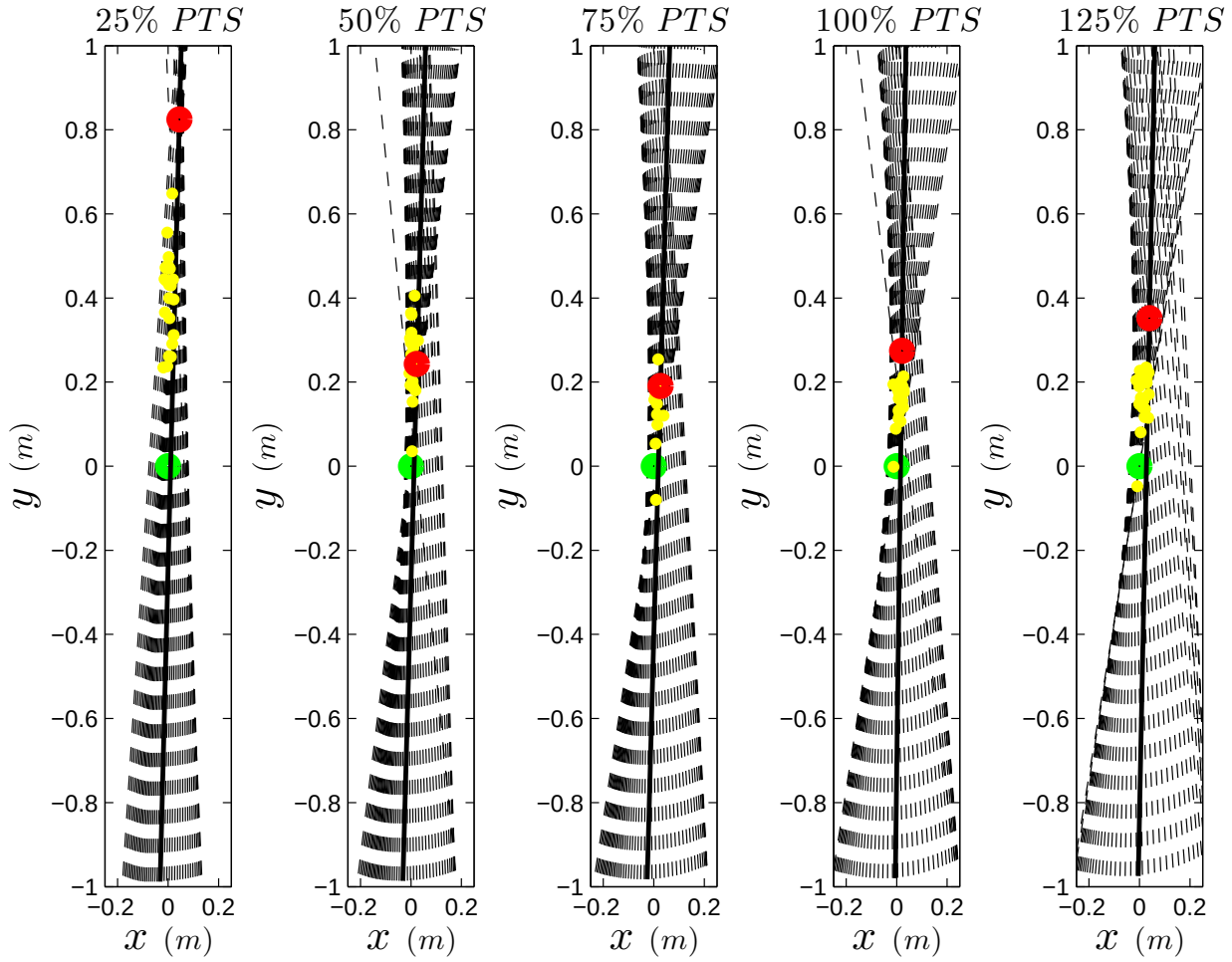

Figure 6: Alignment of the GRFs (ground reaction forces) during one step. The VPP point and CoM are shown by red and green circles, respectively. Yellow circles are the VPPs found for different subjects from human experiments.

which may be affected by the body parameters[6], stable walking is achievable. In other words, the basis of locomotion which is defined here with some relations between the states (synchronizing the joint angles variations using the leg angle) is determined for a specific motion with a diverse range of body characteristics.

2.4 CONCLUSION

Compared to other approaches to stabilize the legged robot locomotion, here imposing some holonomic constraints between different body parts is the design key. Satisfying internal relation between the joint angles based on a unifying variable such as the leg angle is the way of implementing the proposed approach to control a 5-link model walking in this paper. However, if there exist some basic rules of control design that can be fixed even if the structure varies, the control design problem is converted to detect these rules. On the other hand, humans/animals body is a sample of intelligent, efficient and robust controller which can be investigated to find the rules. Therefore, our approach for finding these

[6] The segments with different mass and inertias require different torques (equivalently different *PD* coefficients) to move similarly.

Table 2: 5-link model parameters with body characteristics of the Rabbit robot Westervelt et al. (2007) and a sample human Winter (2005)

Parameter	RABBIT	human	unit
Torso mass	12	54	
Thigh mass	6.8	8	kg
Shank mass	3.2	5	
Torso length	0.63	0.89	
Thigh length	0.4	0.5	m
Shank length	0.4	0.5	
Hip to torso CoM distance	0.24	0.33	
Hip to thigh CoM distance	0.11	0.21	m
Knee to shank CoM distance	0.24	0.3	
Torso inertia	1.33	10.6	
Thigh inertia	0.47	1.8	kgm^2
Shank inertia	0.2	1	

virtual constraints is employing human experiments. In that respect, the virtual relations between the joint angles and leg angles were developed based on experimental data. The controller satisfying these relations is able to stabilize walking in a wide range of body characteristics and speeds. It was shown that the controller for a robot (like Rabbit) can be obtained by satisfying the virtual constraints found in human gaits.

Another aspect in producing stable gait is mimicking humans' motion characteristics. It was also shown that with the proposed approach, in addition to similarity in kinematic behavior which was the first goal, the controlled model resembles some features of kinetic behavior of human gaits. The virtual pendulum property of human locomotion is a key feature in balancing exhibited by the HZD controller with human experiment inspired virtual constraints.

The results may suffer from inaccuracy in walking modeling like instantaneous double support. For example, one discrepancy from human locomotion is the effect of impact which can be seen as lack of swing leg retraction and jumps in speeds at touchdown moments. Completing the model to have a continuous double support and utilizing the derived control rules to empower the exoskeleton for stabilizing the motions with the least interference with human activities are the important future steps of this research.

2.5 AUTHOR CONTRIBUTIONS

Maziar A. Sharbafi is the main and corresponding author of this article responsible for the conception and design of modeling, analysis and interpretation of experimental data and writing of the manuscript. Andre Seyfarth was the supervisor of the project and contributed in discussions regarding interpretation of the results and writing the paper.

2.6 REFERENCES

Ames, A. D. (2012a). First steps toward automatically generating bipedal robotic walking from human data. *Lecture Notes in Control and Information Sciences*, 422:89–116.

Ames, A. D. (2012b). First steps toward underactuated human-inspired bipedal robotic walking. In *International Conference on Robotics and Automation (ICRA)*.

Full, R. J. and Koditschek, D. (1999). Templates and anchors: Neuromechanical hypotheses of legged locomotion on land. *Journal of Experimental Biology*, 22:3325–3332.

Geyer, H., Seyfarth, A., and Blickhan, R. (2003). Positive force feedback in bouncing gaits? *Proceedings of the Royal Society B*, 270.

Grizzle, J., Abba, G., and Plestan, F. (2001). Asymptotically stable walking for biped robots: Analysis via systems with impulse effects. *IEEE Transactions on Automatic Control*, 46:51–64.

Grizzle, J. W., Chevallereau, C., and long Shih, C. (2008). HZD-based control of a five-link underactuated 3d bipedal robot. In *47th IEEE Conference on Decision*, pages 5206–5213.

Grizzle, J. W., Hurst, J., Morris, B., won Park, H., and Sreenath, K. (2009). Mabel, a new robotic bipedal walker and runner. In *In Proc. of American Control Conference*, pages 2030–2036.

Grizzle, J. W. and Westervelt, E. R. (2008). Hybrid zero dynamics of planar bipedal walking. *Analysis and Design of Nonlinear Control Systems, Springer, Ed., A. Astolfi and L Marconi*, pages 223–237.

Ijspeert, A. J. (2008). Central pattern generators for locomotion control in animals and robots: A review. *Neural Networks*, 21:642–653.

Jiang, S., Patrick, S., Zhao, H., and Ames, A. D. (2012). Outputs of human walking for bipedal robotic controller design. In *American Control Conference (ACC)*.

Lipfert., S. W. (2010). *Kinematic and dynamic similarities between walking and running*. Verlag Dr. Kovaĉ,.

Maus, H. M., Lipfert, S., Gross, M., Rummel, J., and Seyfarth, A. (2010). Upright human gait did not provide a major mechanical challenge for our ancestors. *Nature Communications*, 1(6):1–6.

Morris, B. and Grizzle, J. W. (2009). Hybrid invariant manifolds in systems with impulse effects with application to periodic locomotion in bipedal robots. *IEEE Transaction on Automatic Contro*, 54(8):1751–1764.

Owaki, D., Koyama, M., Yamaguchi, S., Kubo, S., and Ishiguro, A. (2011). A 2-d passive-dynamic-running biped with elastic elements. *IEEE Transactions on Robotics*, 27(1):156–162.

Poulakakis, I. and Grizzle, J. W. (2009). The spring loaded inverted pendulum as the hybrid zero dynamics of an asymmetric hopper. *IEEE Transaction on Automatic Control*, 54(8):1779–1793.

Powel, M. J., Zhao, H., and Ames, A. D. (2012). Primitives for human-inspired bipedal robotic locomotion: Walking and stair climbing. In *International Conference on Robotics and Automation (ICRA)*.

Seyfarth, A., Geyer, H., Guenther, M., and Blickhan, R. (2002). A movement criterion for running. *Journal of Biomechanics*, 35(5):649–655.

Sharbafi, M. A., Maufroy, C., Ahmadabadi, M. N., Yazdanpanah, M. J., and Seyfarth, A. (2013). Robust hopping based on virtual pendulum posture control. *Bioinspiration and Biomimetics*, 8(3).

Sharbafi, M. A., Maufroy, C., Seyfarth, A., Yazdanpanah, M. J., and Ahmadabadi, M. N. (2012). Controllers for robust hopping with upright trunk based on the virtual pendulum concept. In *IEEE/RSJ International Conference on Intelligent Robots and Systems (Iros 2012)*.

Sharbafi, M. A. and Seyfarth, A. (2014). Stable running by leg force-modulated hip stiffness. In *IEEE International Conference on Biomedical Robotics and Biomechatronics (BioRob)*.

Shih, C., Grizzle, J. W., and Chevallereau, C. (2007). Asymptotically stable walking of a simple underactuated 3d bipedal robot. In *In Reprint 33rd Annual Conference of IEEE Industrial Electronics (IECON 2007)*, pages 1404–1409.

Sreenath, K., Park, H., Poulakakis, I., and Grizzle, J. W. (2010). A compliant hybrid zero dynamics controller for stable, efficient and fast bipedal walking on mabel. *International Journal of Robotics Research*.

VukobratoviÂt'c, M. and Stepanenko, Y. (1972). On the stability of anthropomorphic systems. *Mathematical Biosciences*, 15:1–37.

Westervelt, E. R., Grizzle, J., and Koditschek, D. E. (2003). Hybrid zero dynamics of planar biped walkers. *IEEE Transactions on Automatic Control*, 48:42–56.

Westervelt, E. R., Grizzle, J. W., Chevallereau, C., Choi, J. H., and Morris, B. (2007). *Feedback Control of Dynamic Bipedal Robot Locomotion*. Taylor & Francis, CRC Press.

Winter, D. A. (2005). *BioMechanics and motor control of human movement*. John Wiley & Sons, Inc, New Jersy, USA, 3 edition.

3 Article II: Template-based hopping control of a bio-inspired segmented robotic leg

Authors:

Jonathan Oehlke, Maziar Ahmad Sharbafi, Philipp Beckerle and André Seyfarth

Technische Universität Darmstadt

64289 Darmstadt, Germany

Published as a paper at the

2016 IEEE International Conference on Biomedical Robotics and Biomechatronics (BioRob)

ABSTRACT

In human hopping in place, the axial leg function is representable by a spring mass model. This description can be utilized to control robot hopping. In this paper, the SLIP (spring loaded inverted pendulum) model is employed as a template for the control of MARCO Hopper II, a robot with a two-segmented leg. Using VMC (virtual model control) a spring is emulated between the foot and hip joint. The required knee torque is generated by a cable-driven actuator to mimic the unilateral knee extensor. In ground contact, gravity acts as the antagonistic knee flexor. The paper describes an evolution of controllers operating on systems ranging from a simple SLIP to more complex simulation models and finally proposes a control strategy that yields stable hopping in the hardware setup. To compensate losses, energy management by tuning the virtual leg spring stiffness is utilized. The resulting hopping motion is similar to human motions with respect to the positions of foot and hip as well as the ground reaction force. A combination of the SLIP model with a control technique for segmented structures and the addition of a bio-inspired energy management method is the result of this work.

3.1 INTRODUCTION

Legged locomotion can be divided in three locomotion sub-functions Seyfarth et al. (2013): bouncing, leg swinging, balancing. Bouncing or hopping (axial leg function), which is the focus of this study, describes the elastic rebounding of the stance leg during ground contact to counteract gravity Blickhan (1989). Template models Full and Koditschek (1999) - although highly simplified in structure - are a very useful tool to understand how these sub-functions are controlled and coordinated, both in nature Full and Koditschek (1999) and legged robots Raibert (1986). Hopping is the only gait that is feasible with one leg and can be considered as a prerequisite movement for running. In vertical movement, the only required locomotor sub-function is hopping.

There are a lot of hopping robots in recent research. In Vu et al. (2015) a segmented robotic leg is presented which works with an actuated hip joint and a passive compliant knee joint. The proper tuning of the stiffness of the knee joint leads to an improved energy efficiency. Another segmented robotic leg is presented in Vanderborght et al. (2011). The focus lies on a compliant actuator with a stiffening spring. Experiments show an extended performance in comparison with an actuator without compliance. A segmented robotic leg of a bigger scale is presented in Hurst and Rizzi (2008). The research on this leg, that should be used for running and walking robots, also focuses on a compliant actuation system and a design that supports natural dynamics. A drawback is given by the fixed values of the used springs. Also, some older projects cope with (non-segmented) hopping robotic legs and methods that improve the efficiency of the mechanisms (see Ahmadi and Buehler (1999), Zeglin and Brown (1998)). All of them try to improve the energy efficiency of compliant segmented or straight robotic legs through different methods.

Applying conceptual models as templates for control may be a useful approach to fill the gap between human experiments and robot control Full and Koditschek (1999). For this, abstraction is the key feature in simplifying human locomotion problems, finding a solution and extending the simple control to the complex model, following the approach of “template and anchor” Full and Koditschek (1999). A spring-loaded inverted pendulum (SLIP) model Blickhan (1989) is a template model explaining the axial leg function in walking and running Geyer et al. (2006). Extended SLIP models, like ESLIP Ludwig et al. (2012) or the variable leg spring (VLS) model Riese et al. (2013), describe leg spring adjustments (stiffness, rest length) during stance phase. They provide better representations of human bouncing behavior, which can be used for the control of a system.

This paper extends the bio-inspired template based control implemented on the original 1D MARCO-Hopper Kalveram et al. (2012) to the new MARCO-Hopper II robot with segmented leg and knee ex-

tensor. The setup with a modular actuation system, enables the comparison of different actuator designs for realizing bio-inspired hopping movements. Regarding this goal, a virtual model control (VMC) Pratt et al. (2001) for mimicking SLIP based hopping by emulating a virtual spring behavior on MARCO-Hopper II (called hereafter MARCO II) in combination with a human-like energy management method Kalveram et al. (2012), is employed. The behavior of the system is influenced by the manipulation of the parameters of the virtual spring. Section 3.2 shows the development of this control strategy and the test-bed. In Section 3.3 simulation and experimental results are compared, which show comparable performance of MARCO II to human hopping and SLIP based hopping. Section 3.4 gives an insight in consequences and possible future approaches resulting from this work.

3.2 Methods

In this paper, template models are employed to fill the gap between biological and robotic locomotion.

Human hopping properties can be explained by a spring mass model Ludwig et al. (2012); Riese et al. (2013); Blickhan (1989). To mimic this behavior with a segmented structure a connection between the SLIP model and the multi-body system has to be found. The virtual model control is utilized to produce SLIP-like vertical hopping with MARCO II. The idea of virtual model control is to emulate virtual components behavior with real actuators. Hence, the required knee torque, as a function of the knee angle, is calculated to generate a spring-like (linear) relation between the axial leg force and the length of the virtual leg (defined by a line from hip to foot).

The approach is to move step by step from the SLIP model (spring loaded inverted pendulum: a point mass atop a mass-less spring) Blickhan (1989) (Fig. 1 b), over a segmented leg with an attached single mass (Fig 1 c), to a complete multi-body simulation model of MARCO II, as shown in Fig. 1 d. Here the actuator and transformation dynamics and also system losses (e.g., in the drive-train and the cable) are taken into account. Each system with ascending complexity is controlled to behave like a SLIP model. Finally the controller is implemented on the hardware setup. As a result a bio-inspired hopping controller on a two-segmented robotic leg can be implemented.

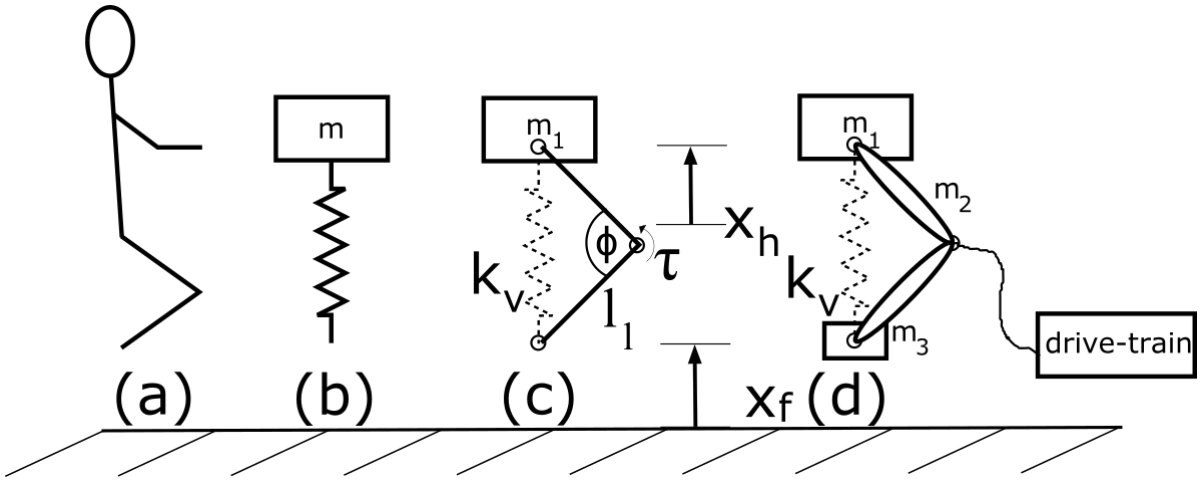

Figure 1: Evolution of models from human hopping to MARCO II. (a) Human vertical hopping can be described by (b) the SLIP model which can be extended using VMC to (c) a segmented leg mechanism with one (body) mass at the hip. The knee torque τ mimics the leg force represented by the virtual leg spring (with stiffness k_v). (d) Complete model of MARCO II with distributed masses, energy dissipation effects and drive train.

3.2.1 Test-bed Marco Hopper 2

In the SLIP model as a conservative model there is no need for the compensation of energy losses. On the opposite, stable hopping without energy management is not achievable in a real robotic system Kalveram et al. (2012). To investigate different energy management methods inspired from human hopping motions, a test-bed called MARCO (Mechanical adjustable reflexive-compliant) Hopper was developed Seyfarth et al. (2007) (Fig. 2(a)). Since the structures of MARCO, as the predecessor of MARCO II, and

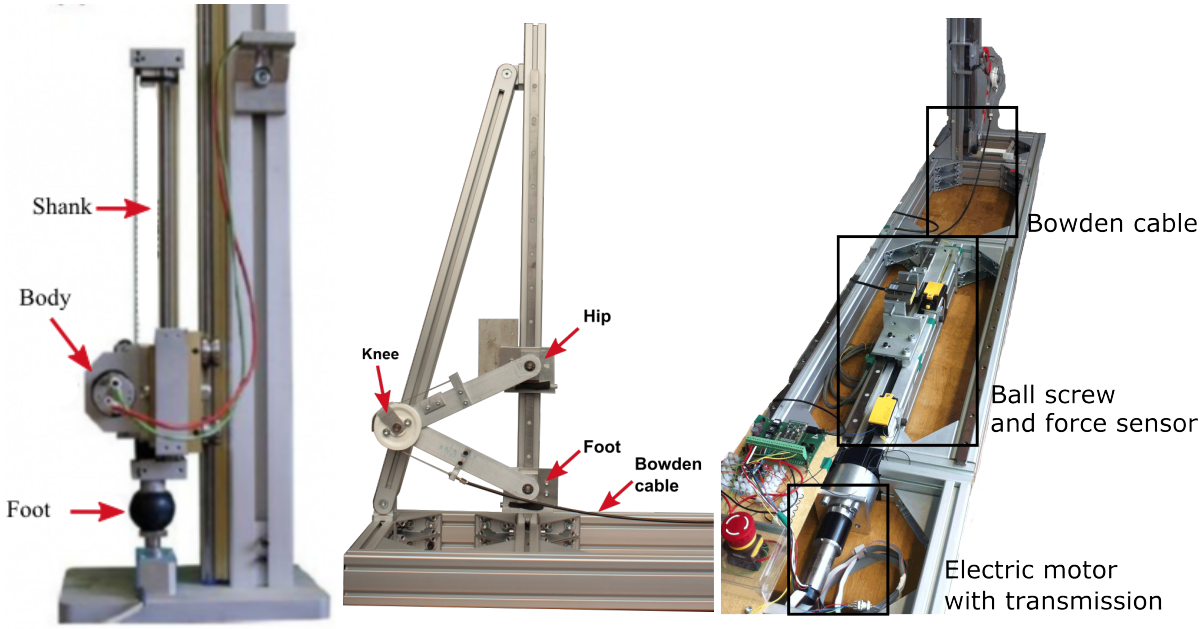

Figure 2: (a) MARCO-Hopper with prismatic leg (picture adopted from Kalveram et al. (2012)), (b) MARCO-Hopper II with a segmented leg and (c) the separate modular actuation mechanism (drive-train), connected by a cable.

the SLIP model are very similar, the applicability of the developed control strategies on more complex, segmented multi-body structures was an open question. A segmented robotic leg comes closer to the human role-model. The application of bio-inspired control strategies on such a test-bed is another step to successful biomimetics. In order to respond this question a new version of that robot, called MARCO Hopper II (Fig. 2(b)) was developed at TU Darmstadt, Germany[7]. MARCO II consists of two links mimicking shank and thigh (with length l_l) that are connected by a roller bearing (knee joint). A mass (m_1) at the top point resembles the body. The knee is actuated via a cable (with stiffness k_C) attached to a pulley (with radius r). The actuator of the system in combination with a transmission and a ball screw is placed outside of the leg to separate its inertia from the moving parts of the leg (Fig.2(c)). The positions of the hip and the foot are calculated with the angular data of the thigh measured by an IMU (inertia module unit) and a potentiometer position sensor, respectively. The ground reaction force and the actuator force (in the drive-train) are measured with strain gauge force sensors. Force sensing happens only for the analysis of the system. Only the position data is required to mimic a spring-mass behavior with the two-segmented leg of MARCO II. The drive-train can be adapted to different actuation systems such as Serial Elastic Actuation (SEA) or other soft actuation concepts. In the current rigid version, a

[7] http://wiki.ifs-tud.de/adp_laufrobotik/adp_2013

geared electric motor with the maximum power of 200 W and a maximum current of 10.5 A is utilized. More details about the MARCO II hardware setup are described in Table. 1.

Table 1: Properties of the test-bed and control parameters

motor	maxon EC-4pole, $P = 200$ W
transmission	maxon GP 42 C, $i = 91/6$
ball screw	item KGT VK14, $i = 314$
length segments leg	$l_\mathrm{l} = 0.25$ m
mass at the hip, „body-mass“	$m_1 = 1.1$ kg
mass of a segment	$m_2 = 0.1$ kg
mass of the foot	$m_3 = 0.3$ kg
stiffness cable	$k_C = 556650$ N/m
radius pulley	$r = 0.034$ m
mass m SLIP model	$m = 1$ kg
basic virtual stiffness k_0	$k_0 = 65.4$ N/m
basic injected energy ΔW	$\Delta W = 5$ J

3.2.2 Control concept

With the virtual model control (VMC) approach Pratt et al. (1997), the effects of a spring with the stiffness k_v between hip and foot are mimicked, as shown in Fig. 1 c. The torque τ at the knee is controlled in a manner to have the same effect on the leg as a spring would have. This connection is given by the comparison of the dynamic equations of both systems. It is calculated as follows:

$$\tau = 2\ \cos\left(\frac{\phi}{2}\right) l_\mathrm{l} k_\mathrm{v} (l_0 - x_\mathrm{h} + x_\mathrm{f}) \tag{1}$$

in which, ϕ, l_0, x_h and x_f are the knee angle, the virtual spring rest length, the positions of hip and foot, respectively. This approach is valid for a mass-less segmented leg with one mass at the hip m_1, shown in Fig. 1(c). Although this relation for the complete model of MARCO II including distributed masses in the legs (shown in Fig. 1 (d)) is more complex, the same principle will be held. A system with the masses of the body, m_1, the leg segment m_2 and the foot m_3 mimic the behavior of a single mass oscillator m (see Fig. 1), if the torque τ is generated with the following law:

$$\tau = 2\cos\left(\frac{\phi}{2}\right) l_l \left(\frac{k_v (l_0 - x_h + x_f)}{m}\left(m_1 + \frac{3}{4}m_2\right) + \frac{m_2 g}{4}\right) \tag{2}$$

The desired hopping condition (i.e. hopping height) can be determined by tuning the virtual spring parameters (rest length l_0 and the stiffness k_v). In all trials (simulation and experiments) the initial condition ($x_h = x_0$ and $x_f = 0$) is a compressed position with zero initial speed (called MC, maximum compression). The virtual spring rest length is adjusted to the maximum leg length of MARCO II; $l_0 = 0.5$ m. Starting from a fixed MC, this rest length results in the highest hopping height for each stiffness. Thus, the hopping height can be adjusted by k_v.

In the SLIP model, the hopping frequency is determined by $\omega = \sqrt{\frac{k}{m}}$, which is the natural frequency of the system. Hopping is given when the foot leaves the ground. This condition is given when the hip

position and hence leg length get higher than the rest length of the virtual spring. To satisfy this condition, the energy stored in the spring in the initial condition (x_0) should be higher than $mg(l_0 x_0)$ and thus:

$$k_v > \frac{2mg}{l_0 - x_0} \tag{3}$$

Satisfying this condition besides Eq. 1, controls a desired hopping motion in a SLIP model and more complex multi-body models. It is notable that like the SLIP model, in which the spring just pushes (positive force in upward direction), in MARCO II the actuator can only extend the knee through pulling the cable connected to the pulley at the knee (similarly, upward force direction).

A block diagram of the control approach is presented in Fig. 3. The control concept is shown with

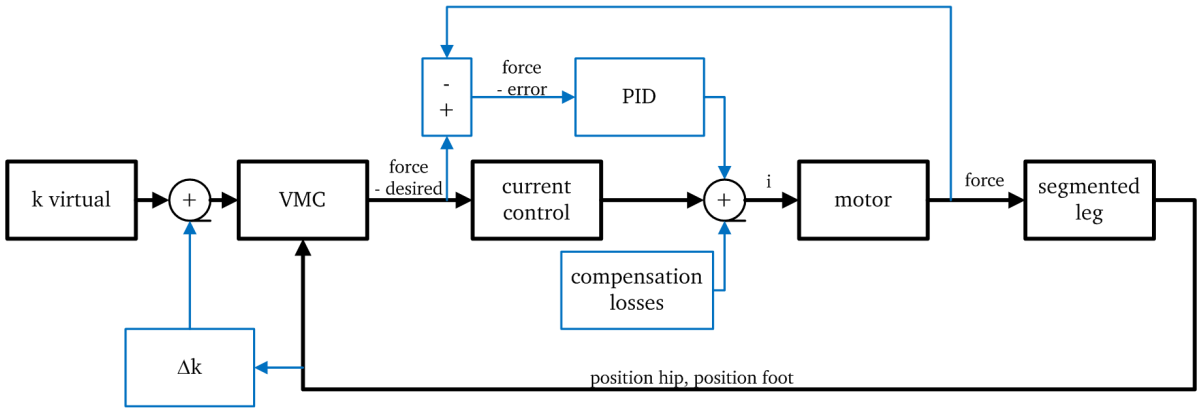

Figure 3: Control block diagram of MARCO 2. Black parts (lines and boxes) show the basic control mechanism for SLIP-based virtual model control (VMC). The blue parts include additional alternatives for energy management and force control. Equations to calculate the desired force at the cable and a simplified drive train model are contained in the VMC block. The current control adjusts the desired current in the motor. All control schemes are performed online.

black lines, in which the VMC uses the positions of the hip and foot (their difference is the current length of the virtual spring) and the virtual stiffness to find the desired knee torque. To command the required knee, the corresponding current is calculated using a motor model. This can be considered as a feed-forward control term since there is no feedback considered for tracking the desired torque. The only feedback is the actual leg length for determining the related torque. An extended control approach is shown via the blue lines in Fig. 3. This additional feedback loop is able to use measured force (the force attacking the cable) to adapt the virtual stiffness. As impact through ground contact and system friction cause losses it is possible to compensate them with complementary control terms to enhance the hopping performance. For the experiments shown here the force-feedback is not used, but the possibility of enhancing the performance with a force-feedback loop is given.

Because at every hop the impact at ground contact and friction in the system causes losses, a kind of energy management is required to achieve stable hopping in the real system. The first option is to calculate the lost energy and to inject the exact amount by increasing the motor current. Since the model is is complex and has several uncertainties, calculating the precise amount of losses is not practicable. It was shown that for SLIP-based control of the MARCO-Hopper, injecting a constant amount of energy in each bounce results in stable hopping Kalveram et al. (2012). The strategy for injecting energy in this work is to change the virtual spring stiffness during the movement in two different ways.

Bang-bang control of virtual stiffness:

In this approach, the virtual spring stiffness k_v switches between zero and a positive value k_v satisfying Eq. 3. The system initiates at the lowest position x_0 with a vertical speed equal to zero and with a nonzero virtual stiffness k_v. During the upward motion the stiffness switches to zero when the leg is completely stretched (leg length is equal to the rest length); which means that the required torque at the knee becomes zero. The inertial forces/torques of body, thigh, and shank make the robotic leg leave the ground. Because the virtual stiffness is still zero the structure can to fall freely downward after reaching the apex point. The virtual spring stiffness switches back to k_ν when the hip point reaches the lowest point. At this point the virtual spring reaches maximum compression (MC). With this approach the highest possible amount of energy with fixed values for spring rest length l_0, maximum stiffness k_ν and initial hip position x_0 is injected Kalveram et al. (2012). In other words, if a fixed amount of energy should be injected, this is the minimum required change in the stiffness that is necessary if x_0 and l_0 are fixed. However, there is a discontinuity in the required axial force (respectively in knee torque) when the virtual spring stiffness switches from zero to k_ν at MC. A discrete change in the desired knee torque is not desirable for the actuator and is also not biologically inspired. So the second approach to smooth the knee torque pattern is presented. The switching from k_ν to zero at the apex point does not result in a discrete jump of the knee torque. The virtual spring force is zero when the leg length is equal to the rest length l_0.

Continuous change of the spring stiffness:

The linear stiffness increment of virtual spring stiffness suggested by *Kalveram* et al. for MARCO-Hopper Kalveram et al. (2012) is used here. In this approach, a certain amount of energy is injected into the system during each hopping cycle to compensate losses and to reach a certain hopping height. It was shown that adding a fixed amount of energy ΔW to the hopper system can converge to a periodic stable vertical hopping if ΔW is greater than an unknown but existing threshold. The threshold can be determined, if the losses during a hopping cycle are known. Perturbations of the motion and changes in mechanical parameters make the prediction of the losses difficult. So the injected amount of energy is adjusted during experiments to achieve a hopping motion. The adjustment of the spring stiffness starts with $k_\nu = k_0$ at MC (x_0) and is increased by adding the additional term Δk (see Fig. 3). k_0 serves as a hopping condition extracted from the SLIP model, while Δk compensates losses and unmodeled effects.

$$\begin{aligned} k_v &= k_0 + \Delta k \\ \text{with: } \Delta k &= \frac{6\,\Delta W}{(l_0 - x_0)^3}((x_h - x_f) - x_0) \end{aligned} \tag{4}$$

The additional term in the stiffness calculation Δk has a linear relation to the difference between the actual leg length $(x_h - x_f)$ and the initial hip height (x_0). Thus, during moving upward this amount will increase linearly. The proportionality factor that includes ΔW derives from a biologically reasonable mathematical formulation of the additional force acting in the manipulated spring. In Kalveram et al. (2012) it was shown that with this formulation the injected amount of energy ΔW is equal to the same amount of energy injected in a SLIP model if the spring reaches the rest length during each hopping cycle. For the derivation of this formulation see Kalveram et al. (2012). The virtual stiffness is set to zero during the downward motion similar to the bang-bang approach. In this approach the fixed term of the stiffness (k_0) is found from the SLIP model. It is the stiffness that leads to a movement reaching the rest length of the virtual spring. The injection of a fixed amount of energy ΔW, by increasing the stiffness by the term Δk during the travel of the hip from x_0 to the rest length, determines the hopping height. A value for the injected energy was found iteratively by experiments with the test-bed. The tested range of values is between 1-8 J.

3.2.3 Simulation model

In order to implement a human-inspired hopping control on the hardware setup, several simulation models with ascending complexity as shown in Fig. 1 have been developed. The SLIP model is used as a benchmark and as the template for desired hopping behavior. A model of a segmented leg without details of hardware setups (e.g., drive train) helps to investigate the applicability of the control concept to the segmented leg mechanism. Then, with the detailed multi-body model the controller is validated to be implemented on the real system. With this model, the influence of the actuation mechanism on the performance of the controlled system can be shown, to find solutions coping with issues expected from the hardware setup. For simulation models, MATLAB SIMULINK and SIMMECHANICS with the ODE23 solver are used. Friction forces were modeled with an adapted model basing on a *Stribeck*-model presented in KrÃd'mer and Kempkes (2014). The ground impact model bases on a realistic non-linear spring-damper model presented in Vu et al. (2015).

3.3 Results and discussion

Subsequently, the results of applying the bio-inspired hopping control on different levels of simulation models and a hardware setup are presented. Stable hopping with MARCO II is depicted and compared with a simulated multi-body system to show the validity of the model which is comparable to human hopping experiments.

3.3.1 Performance of the control approach

Starting from a desired hopping motion of the SLIP model, a desired torque in the segmented leg mechanism without drive-train can be found (see Eq. 2). This torque pattern can ideally mimic similar hopping if there are no losses or they can be estimated and compensated. The model of the segmented leg helps to understand the basic multi-body dynamics of MARCO II and is the counterpart to the SLIP model. The next step is to evaluate the control on a multi-body model with drive-train (the complete model of MARCO II). The complexity of the model increases when including losses, mass distribution, transformation and other limitations. Only the basic parameters of the SLIP model (e.g., initial conditions, spring rest length and basic stiffness k_0) are considered in control to avoid this complexity. In Fig. 4 a comparison between a single hop performed with the SLIP model and with the multi-body model of MARCO II is shown. The injected energy is $\Delta W = 5\ J$ and the parameters are set to values found in the hardware setup or in identification phase (m_1, m_2 and m_3, bearing friction coefficient, the cable efficiency, the impact model at touchdown and also at the knee stop etc.). The results show that both movements have the same duration and reach comparable apex heights (see Fig. 4 a). In the SLIP model the movement is symmetric whereas in the multi-body system the robot moves upward faster than falling downward. The reason is the asymmetric implemented stiffnesses in these two phases (see Fig. 4 b). During the upward movement energy is injected by increasing the virtual stiffness of the system. This energy might be even higher than losses in this phase. During falling the virtual stiffness is equal to zero and counteracted by forces like friction.

3.3.2 Comparison with human hopping

In Fig. 5 a the hip position and the ground reaction force F_{GRF} are shown for four hops of the segmented leg model (without drive train). This movement, which is generated based on the SLIP model, is stable and comparable to the human hopping motions shown in Fig. 5 b (adopted from Kalveram et al. (2012)). The movement patterns of the hip position (frequency about $f = 1,5$ Hz and the form) show comparable

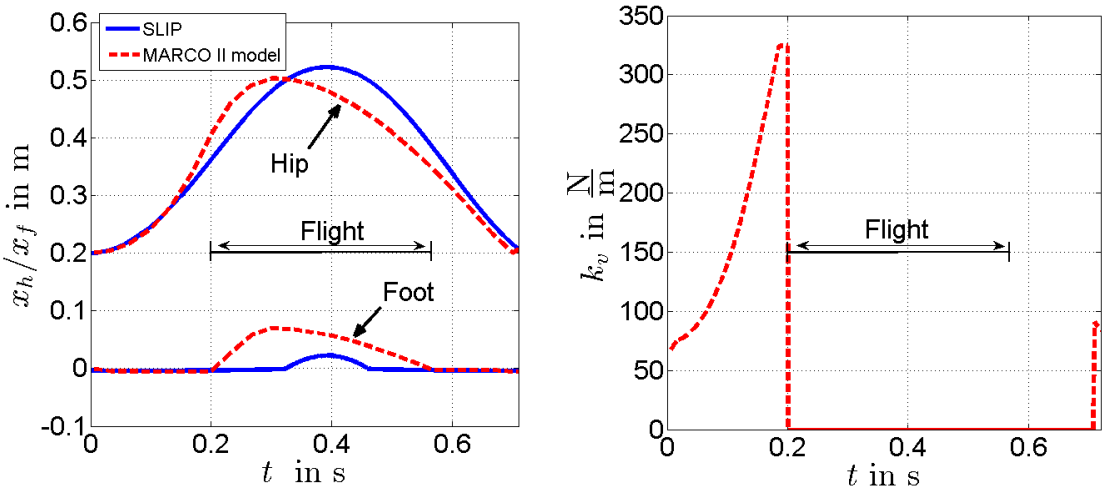

(a) (b)

Figure 4: (a) Comparison of a hopping motion by the SLIP model (solid line) and the multi-body model of MARCO II (dashed line). A fixed amount of energy ($\Delta W = 5$ J) is injected through a stiffness increment during upward movement. The basic stiffness k_0 is the same for both models. (b) Course of the virtual stiffness k_v during hopping motion. From MC the stiffness starts with $k_v = k_0$, is raised during the straightening of the leg and switched to zero when the leg reaches its apex point.

results for the simulation (a) and the experiment with human subjects (b). Also the ground reaction force patterns are similar. Absolute values of the amplitudes come not close to each other, because the masses and the dimensions also differ between a human and the model of MARCO II. None the less this comparison shows, that if the actuator can generate the desired torque at the knee joint, human-like hopping is achievable with the proposed bio-inspired control approach. However, with the constraints in the hardware setup, similar hopping conditions are not achievable with the current version of MARCO II: results obtained by using the same parameters and the complete multi-body model of MARCO II with drive train are shown in Fig. 6 a. Here the complete simulation model (solid line) and an experiment with MARCO II (dashed line) are compared. With the complete simulation model stable hopping can be achieved and the resulting motion comes close to the previous one, shown in Fig. 5 a. Hopping height and hopping frequency are decreased. This happens because of limitations in the drive train, which prevent the actuator to produce the desired knee torque. Actuator limitations decrease the quality of the control in the actual version of MARCO II. From another point of view the produced hopping can be considered as human-like hopping (because it can be produced by a SLIP model) with different resulting conditions (e.g., frequency). Therefore, doing human hopping experiments with a larger range of hopping conditions or releasing the hardware constraints may help find more similar behavior in humans and the robot.

3.3.3 Experimental results of control ideas

Also in Fig. 6 simulation results (solid line) are compared to experimental results with MARCO II (dashed line). After the tuning of the control parameters in the model and the test-bed, similar hopping behaviors are achieved. The actuator system reaches its performance limitations during the experiments. For higher hopping results some changes on the hardware have to be made. Regarding imprecise torque control of the actuator, which suffers from noisy measurement of the torque, the internal torque control mechanism and inherent delay of the sensory-motor system, the results are not precisely reproducible in

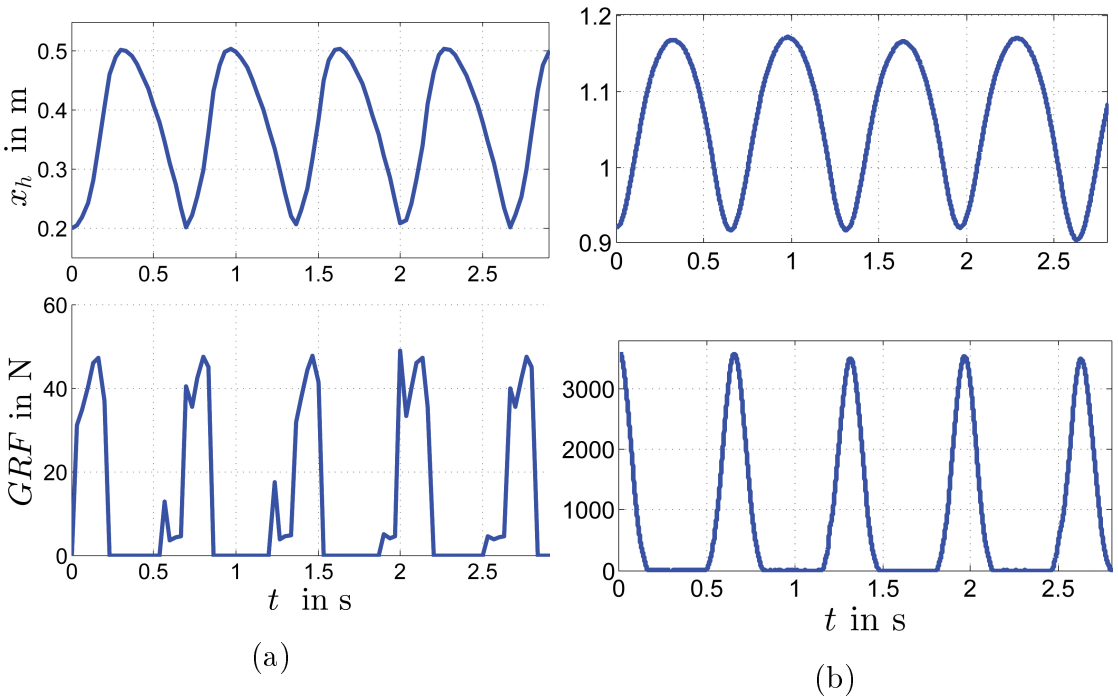

Figure 5: Stable hopping with (a) multi-body model without drive-train and (b) human experiments (adopted from Kalveram et al. (2012)). Hip position (x_h) and ground reaction force (GRF) are shown for five hops. Injected energy is $\Delta W = 5$ J in the simulation model.

the simulation model. To resolve this issues, some modifications of the structure (regarding the friction), more precise sensors and a more powerful motor-controller are required. However, stable hopping can be achieved with applying the simple proposed control approach on the existing hardware setup. Therefore, the applicability of the bio-inspired control approach on the real system is demonstrated by this results.

3.4 Conclusion

This paper contributes on using bio-inspired template models that describe human locomotion to control robotic systems focusing on the imitation of human hopping. To overcome the gap between biological and robotic locomotor system design and control, axial leg function is modeled by a virtual spring between hip and foot and utilized to generate knee torques that facilitate stable hopping.

Considering an actuator that only mimics a knee extensor shows that this bio-inspired feed-foward locomotion control approach is feasible in hopping and efficiently exploits system dynamics and interaction with the environment. Through the only variable parameter, virtual stiffness k_v or injected energy ΔW respectively, the hopping motion can be adjusted. As the basic control strategy, this energy management method is designed to mimic human behavior. With this approach and the reduced number of required sensor data (positions of the leg segments), the control approach is easy to understand, realize, and tune.

Limitations in achieving the simulated performance within the test-bed are due to mechanical issues of the real system. Although the preliminary results shown in this paper might not be optimal, they show that the control approach is promising for further investigation and implementation in various robotic systems. Such might benefit from simplifying control by using template models in legged locomotion.

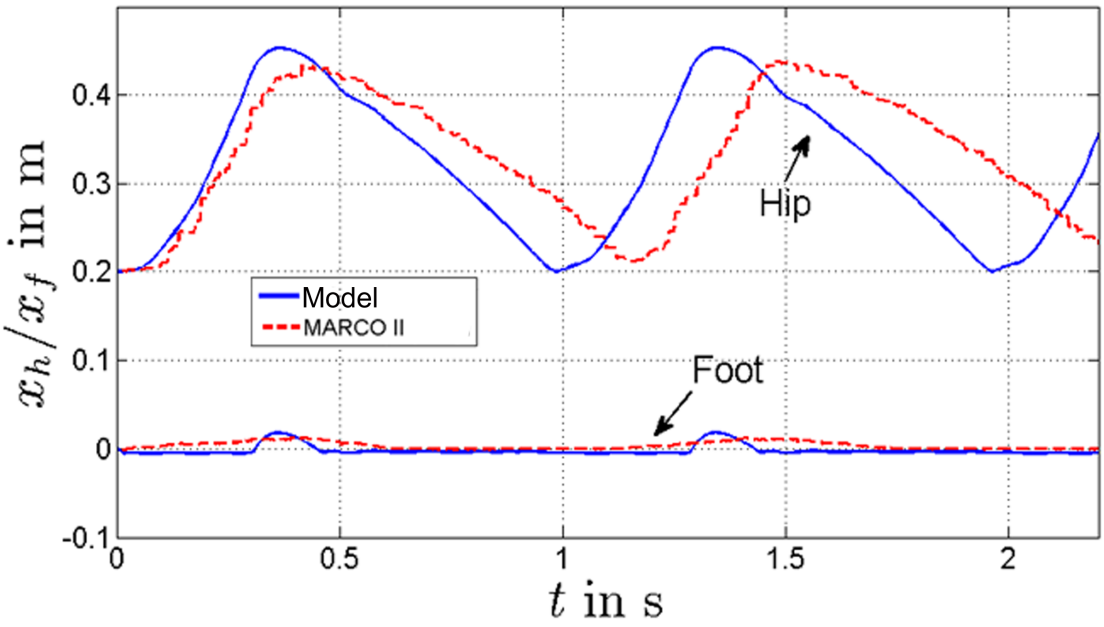

Figure 6: Comparison between hopping motions of the multi-body model with drive train (solid line) and an experiment with MARCO II (dashed line). The same parameter set as used before result in lower hopping height and frequency.

The applicability of the template-based control using VMC in producing stable human-like movement with a simple mechanism of pulling a cable, could further be extended to more complex systems. Future works might transfer it to robots with musculoskeletal structures or assistive devices.

3.5 ACKNOWLEDGMENT

This research was supported in part by the EU project BALANCE under Grant Agreement No. 601003 and the German Research Foundation (DFG) under grants No. SE1042/8.

3.6 AUTHOR CONTRIBUTIONS

Jonathan Oehlke was the main author contributing in making the simulation models, implementation on the robot and writing the paper. Maziar A. Sharbafi is the corresponding author of the article who presented the article in the conference. He designed the template based stance leg control concept and supervised design of simulations, analysis and interpretation of experimental data and highly contributed to writing the manuscript. Philipp Beckerle was supervising the engineering design of Marco-Hopper-II and the implementation of the control algorithms on the hardware. He has contributed in discussions and improvements of modeling, control design, resolving hardware issues and writing the paper. Andre Seyfarth was the supervisor of the project and contributed to developing concepts and models and writing the paper.

3.7 REFERENCES

Ahmadi, M. and Buehler, M. (1999). The ARL monopod II running robot: Control and energetics. In *Robotics and Automation, 1999. Proceedings. 1999 IEEE International Conference on*, volume 3, pages 1689–1694. IEEE.

Blickhan, R. (1989). The spring-mass model for running and hopping. *Journal of Biomechanics*, 22(11):1217–1227.

Full, R. J. and Koditschek, D. (1999). Templates and anchors: Neuromechanical hypotheses of legged locomotion on land. *Journal of Experimental Biology*, 22:3325–3332.

Geyer, H., Seyfarth, A., and Blickhan, R. (2006). Compliant leg behaviour explains basic dynamics of walking and running. *Proceedings of the Royal Society B*, 273(1603):2861–2867.

Haeufle, D. F. B., Grimmer, S., and Seyfarth, A. (2010). The role of intrinsic muscle properties for stable hoppingâĂŤstability is achieved by the forceâĂŞvelocity relation *Bioinspiration and Biomimetics*, 5(1):267–274.

Hurst, J. and Rizzi, A. (2008). Series compliance for an efficient running gait. *IEEE Robotics & Automation Magazine*, 15(3):42–51.

Kalveram, K. T., Haeufle, D. F. B., Seyfarth, A., and Grimmer, S. (2012). Energy management that generates terrain following versus apex-preserving hopping in man and machine. *Biological Cybernetics*, 106(1):1–13.

KrÃd'mer, A. and Kempkes, J. (2014). Modellierung und Simulation von nichtlinearen Reibungseffekten bei der Lageregelung von Servomotoren.

Ludwig, C., Grimmer, S., Seyfarth, A., and Maus, H.-M. (2008). Multiple-step model-experiment matching allows precise definition of dynamical leg parameters in human running. *Journal of Biomechanics*, 42:2472–2475.

Muybridge, E. (1955). *The Human Figure in Motion*. New York: Dover Publications Inc.

Piazza, S. J. and Delp, S. L. (1996). The influence of muscles on knee flexion during the swing phase of gait. *TJournal of Biomechanics*, 29(6):723–33.

Pratt, J., , Chew, C.-M., Torres, A., Dilworth, P., and Pratt, G. (2001). Virtual model control: An intuitive approach for bipedal locomotion. *The International Journal of Robotics Research*, 20(2):129–143.

Pratt, J., Dilworth, P., and Pratt, G. (1997). Virtual model control of a bipedal walking robot. In *Robotics and Automation, 1997. Proceedings., 1997 IEEE International Conference on*, volume 1, pages 193–198. IEEE.

Raibert, M. H. (1986). *Legged Robots that Balance*. MIT Press, Cambridge MA.

Riese, S. and Seyfarth, A. (2013). Stance leg control: variation of leg parameters supports stable hopping. *Bioinspiration and Biomimetics*, 7(1).

Seyfarth, A., Grimmer, S., Maus, H.-M., Haeufle, D., Peuker, F., and Kalveram, K.-T. (2013). *Biomechanical and Neuromechanical Concepts for Legged Locomotion*. Routledge.

Seyfarth, A., Kalveram, K. T., and Geyer, H. (2007). Simulating muscle-reflex dynamics in a simple hopping robot. In *Autonome Mobile Systeme 2007*, pages 294–300. Springer.

Thorson, I., Svinin, M., Hosoe, Sh., Asano, F., and Taji, K. (2007). Design considerations for a variable stiffness actuator in a robot that walks and runs. In *Autonome Mobile Systeme 2007*, pages 294–300. Springer.

Thorson, I., Svinin, M., Hosoe, Sh., Asano, F., and Taji, K. (2007). Design considerations for a variable stiffness actuator in a robot that walks and runs. In *Robotics and Mechatronics Conference (RoboMec), 2007*.

Vanderborght, B., Verrelst, B., Van Ham, R., Van Damme, M., Lefeber, D., Meir, B., Duran, Y., and Beyl, P. (2006). Exploiting natural dynamics to reduce energy consumption by controlling the compliance of soft actuators. *The International Journal of Robotics Research (IJRR)*, 25(4):343–358.

Vanderborght, B., Tsagarakis, N. G., Van Ham, R., Thorson, I., and Caldwell, D. G. (2011). MACCEPA 2.0: compliant actuator used for energy efficient hopping robot Chobino1d. *Autonomous Robots*, 31(1):55–65.

Vu, H., Pfeiffer, R., Iida, F., and Yu, X. (2015). Improving energy efficiency of hopping locomotion by using a variable stiffness actuator. *IEEE/ASME Transactions on Mechatronics*, PP(99):1–1.

Zeglin, G. and Brown, B. (1998). Control of a bow leg hopping robot. In *Robotics and Automation, 1998. Proceedings. 1998 IEEE International Conference on*, volume 1, pages 793–798. IEEE.

4 Article III: VBLA, a Swing Leg Control Approach for Humans and robots

Authors:

Maziar Ahmad Sharbafi and André Seyfarth

Technische Universität Darmstadt

64289 Darmstadt, Germany

Published as a paper at the

2016 IEEE/RSJ International Conference on Humanoid Robots (Humanoids)

ABSTRACT

Experiments on human subjects, data analyses and modeling can help the engineers design and develop high performance humanoid robots and assistive devices. In an abstract level bipedal locomotion can be considered as a combination of three sub-functions: stance, swing and posture control. In this paper, we focus on swing leg adjustment searching for a bio-inspired method working well on simulation models and robots. In that respect, velocity based leg adjustment method (VBLA) is presented to find the desired leg angle in different gaits. Our investigations are based on analyses of human walking, perturbed hopping experiments, beside simulation studies on bipedal running and walking. Compared to some other approaches the VBLA can better explain human leg adjustment in different gaits, gives higher robustness against parameter variations and is practical and easy to implement on robots.

4.1 INTRODUCTION

Human locomotion is a complex task, which involves many levels of structural and control components. The ability to perform efficient and robust locomotion is crucial condition for real-world legged robots. Inspired from nature and Raibert's hopper Raibert (1986), we can consider legged locomotion to be composed of three locomotor sub-functions Seyfarth et al. (2013): stance leg axial function, leg swinging and posture balancing. This distribution of tasks to different elements of the legged system and their interaction simplifies mechanical design and control.

Because of the limited number of legs which need to hit the ground in a sequential manner, an appropriate leg swinging is critical in bipedal gaits. Leg swinging contributes to locomotion dynamics in many ways: (i) determining stance phase dynamics as a result of the landing condition, (ii) shaping the system states to achieve versatile gaits with selected gait type, footfall pattern, step length, step frequency, robustness and efficiency (iii) distribution of energies in forward, lateral and vertical directions, e.g., acceleration or changes in locomotion direction, (iv) perturbation recovery, overcoming unwanted ground contacts, e.g., obstacle avoidance. However, employing conceptual models (templates Full and Koditschek (1999)) in addition to simplify the complex problem of bipedal locomotion can address all these items. One of these templates is the spring-loaded inverted pendulum model (SLIP) Blickhan (1989) Full and Koditschek (1999) representing principal features of human locomotion which was frequently applied to the robotic counterparts. In the SLIP model, the stance leg axial function is addressed by a massless spring connected to a point mass representing the body mass concentrated at center of mass (CoM). Adjusting the swing leg to reach a fixed angle at touchdown (angle of attack) results in stable gaits Seyfarth et al. (2002)

Unlike running and walking Geyer et al. (2006), stable hopping cannot be achieved with a fixed angle of attack with respect to ground. Although using a fixed angle of attack with respect to the ground can stabilize running Seyfarth et al. (2002) and walking Geyer et al. (2006), the region of attraction for the stable gait is quite small Seyfarth et al. (2003). In addition, it is not robust against perturbation e.g., the desired fixed attack angle in hopping in place is 90° which results in unstable hopping that cannot resist even a tiny perturbation. Small region of attraction and sensitivity to running velocity and control parameters exist in common leg adjustment methods which are mostly based on Raibert approach Raibert (1986). In Peuker et al. (2012), Peuker et al. showed that employing the relative angle of the CoM velocity with respect to gravity vector results in more robust gaits, even in 3d. In contrast to Seipel and Holmes (2005), Peuker et al. showed lateral leg placement with respect to body coordinate (using CoM velocity and gravity to build the sagittal plane) instead of world coordinate (defined by desired running direction) can predict stable running solutions for a large range of attack angles. Inspired from this stu-

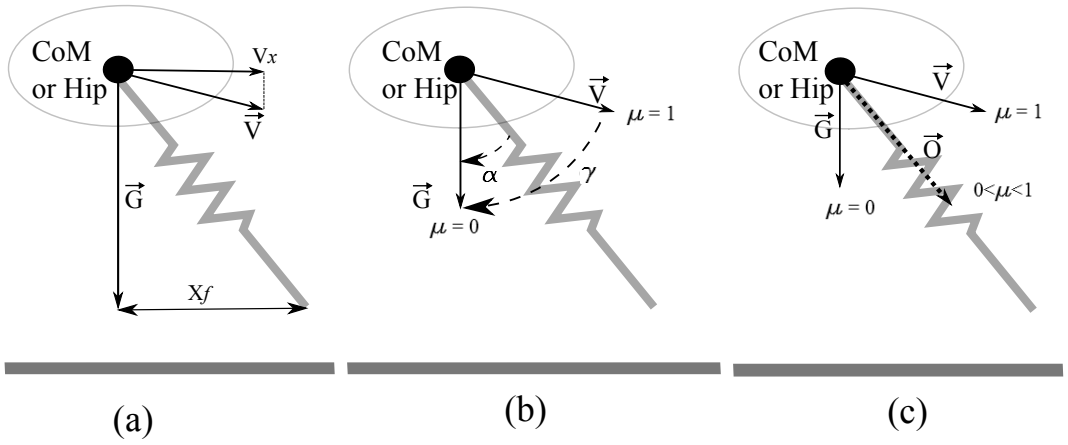

Figure 1: Different leg Adjustment approaches: a) Raibert, b) Peuker c) VBLA.

dy, we investigate a new developed swing leg control approach, called velocity based leg adjustment[8] (VBLA) and compare that with Peuker's and Raibert's methods. Sensitivity to parameter variations, applicability to different gaits, ability to describe human swing leg control are the features that we consider for comparison. In order to implement these approaches on a real robot a sensor to measure the CoM velocity is required (e.g., IMU). More details about characterizing analytically the sensory cost based on SLIP model can be found in Altendorfer et al. (2004).

The rest of the paper is organized as follows. In Sec. 4.2, the methods including the controller formulation, simulation models and experimental setup are described. Results of simulations and experimental data analyses are presented in Sec. 9.4. Finally, Sec. 4.4 concludes the paper.

4.2 METHODS

Swing leg adjustment is one of the main three sub-functions in locomotion which plays an important role in stabilizing gait during swing/flight phase. In contrast to steady state gaits, fixed angle of attack does not work on uncertain (e.g. on rough terrain) and perturbed gaits. In order to adapt the leg angle during leg swinging to increase robustness against perturbations, state feedback can be used Raibert (1986). In most of such control strategies, the foot landing position is adjusted based on the horizontal velocity Poulakakis and Grizzle (2009) Sato (2004). In this section, we present three control approaches for swing leg adjustment, describe the experimental setups for perturbed hopping and walking, and explain how we evaluate each method's ability in predicting human swing leg adjustment strategy.

4.2.1 Leg adjustment during swing phase

Three leg adjustment approaches are shown in Fig. 1. In Raibert approach Raibert (1986) the foot landing position is adjusted based on the Center of Mass (CoM) horizontal speed v_x and its desired value v_x^d as follows:

$$x_f = k' \frac{v_x T_s}{2} + k(v_x - v_x^d) \tag{1}$$

in which, k and k' are control constants and T_s is the stance time. The output of this controller is the horizontal distance between the desired foot point at touchdown and hip point named x_f (see Fig. 1a).

[8] Note that the two other approaches also use CoM velocity, while the new approach is the only which utilizes the vector of velocity. Since the velocity is a vector, we do not mention it velocity vector based leg adjustment for preventing repetition.

Since for SLIP model the equations are not integrable during stance phase, T_s is an estimation of the stance time, obtained by solving it just for vertical direction. This results in a fixed period for different horizontal velocities corresponding to a fixed vertical speed.
Therefore, in steady state condition with a fixed stance time T_s and the motion speed equal to the desired speed, Eq. 1 will be simplified to:

$$x_f = \mu \upsilon_x \tag{2}$$

in which $\mu = k'T_s/2$. For simulation studies we use Eq.1, whereas in experimental data analyses which is in steady state, Eq. 2 is employed. For hopping in place that the desired speed is zero ($\upsilon_x^d = 0$), Eq.1 can be simplified to Eq.2, in which $\mu = k'T_s/2 + k$.

Recently, various strategies were investigated by Peuker et al. Peuker et al. (2012) stating that leg placement with respect to the CoM velocity vector $\vec{V}$ and the gravity vector $\vec{G}$ yielded the most robust and stable hopping and running motions. Defining the angles of the gravity vector with the velocity vector and leg orientation by γ and α, respectively (shown in Fig. 1b), this method gives the leg orientation by

$$\alpha = \mu\gamma \tag{3}$$

where μ is a constant between 0 and 1. In VBLA, the leg direction is given by vector $\vec{O}$ as a weighted average of the CoM velocity vector $\vec{V}$ and the gravity vector $\vec{G} = [\,0,\ -g]^T$ (Fig. 1c).

$$\vec{O} \ = \ \mu\vec{V} + (1-\mu)\vec{G} \tag{4}$$

where weighting constant μ accepts values between 0 and 1. In the original version of VBLASharbafi et al. (2012), we employed dimensionless equations in which $\vec{V} = [\upsilon_x, \upsilon_y]^T/\sqrt{gl}$ and $G = [0,-1]^T$. However, the normalization (constant) coefficients can be sumarrized in μ and tuning this parameter in Eq. (2) is sufficient for leg adjustment while it looks simpler too. In the next section one example for tuning μ based on body parameters is presented for perturbed hopping.

4.2.2 Simulation model

The simulation model used in this paper is the SLIP model for running/hopping and BSLIP (Bipedal SLIP) for walking Geyer et al. (2006). In these models a point mass M is placed atop of one (or two) massless spring with stiffness k_s and rest length l_0. Defining the leg (spring) length by l, the spring force $F_s = k_s(l_0 - l)$ and the gravitational force $F_G = Mg$ are the only elements determining the motion dynamics. Using SLIP model, it can be shown that with the following equation, dead beat response is achievable via VBLA for perturbed hopping. Dead beat response of SLIP model using appropriate leg adjustment is analytically shown in Carver (2003). With VBLA, the following μ results in dead beat response for perturbed hopping

$$\mu = \frac{1}{1+T_s}. \tag{5}$$

4.2.3 Experiments

Here we explain the setups and analyzing methods for human perturbed hopping and walking experiments.

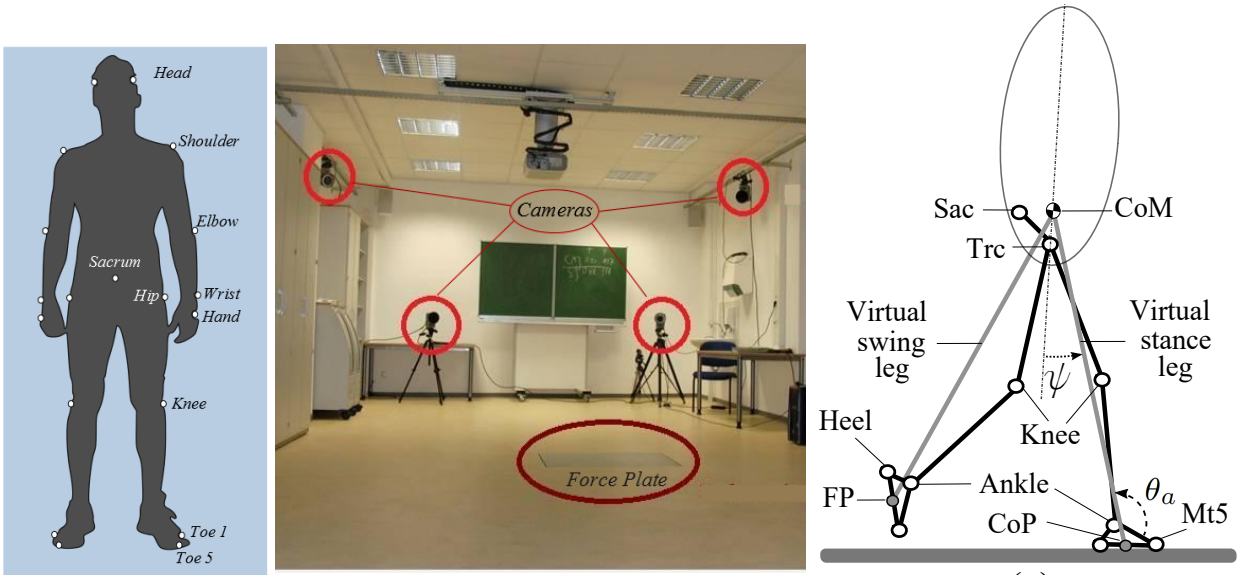

(a) (b) (c)

Figure 2: Experimental settings (a) marker positions for perturbed hopping, (b) high speed motion capture cameras and force plate for perturbed hopping (c) Marker positions for walking experiments: the lower back (sacrum, Sac), the hip (greater trochanter, Trc), the knee (lateral knee joint gap), the toe (5th metatarsal joint, Mt5), the heel (calcaneus), and the ankle (lateral malleolus). The virtual stance leg is defined from center of mass (CoM) to center of pressure (CoP). The virtual swing leg is defined from CoM to foot point (FP) which is half way between Mt5 and Heel. The figure is adopted from Lipfert. (2010).

Perturbed hopping experiment:

Proper selection of μ in VBLA can result in dead beat response for perturbed hopping with SLIP model. Thus, with this approach it is possible to remove all perturbations at most in two steps. The perfect results of applying this method beside VPPC (Virtual Pendulum Posture Controller) to SLIP model with upper-body (called TSLIP for Trunk+SLIP) are reported in our previous work Sharbafi et al. (2012).

We did an experiment to investigate which method approximates the human leg adjustment best. In this experiment, the subject hops in place with arms akimbo and suddenly a perturbation occurs at apex by pushing him/her from behind. The pushing point is near sacrum which is an approximation of CoM. The kinematic behavior of the body is derived using markers shown in Fig. 2a. We use a force-plate to measure GRF during stance phase. CoM motion was obtained by integrating the GRFs twice. Initial values for velocity and position of CoM were obtained from the sacrum position Gard et al. (2004). The markers positions, cameras and the force-plate are shown in Fig. 2b.

To evaluate the aforementioned methods, the velocity at touch down and the leg orientation (the vector from the CoM to the foot contact point with the ground) are detected. In order to approximate control parameter μ in different approaches (Eq. 2,3 and 2) a least square approximation is used. The first two methods can be represented by a linear relation $a = \mu b$ between input (b) and output (a). In Raibert

approach, $a = x_f$ and b is the horizontal velocity. For the second approach, $a = \alpha$ and $b = \gamma$. However, for VBLA we need some manipulation to translate Eq. 2 to a linear relation:

$$\begin{aligned} \frac{O_y}{O_x} &= \frac{\mu V_y - (1-\mu)g}{\mu V_x} \Rightarrow \\ \underbrace{gO_x}_{n} &= \mu \underbrace{(O_x V_y + gO_x - O_y V_x)}_{m} \end{aligned} \tag{6}$$

So, considering $a = n$ and $b = m$ the targeted linear relation is obtained.

Walking experiment:

The data was collected in walking experiments on a treadmill (type ADAL-WR, Hef Tecmachine, Andrezieux Boutheon, France) at different speeds. Motion capture data (Qualisys, Gothenburg, Sweden) from 11 markers and ground reaction force data (12 piezo-electric force transducers within the treadmill) as shown in Fig. 2c. Twenty one subjects (11 female, 10 male) were asked to walk at different percentages of their preferred transition speeds (PTS)[9]. The treadmill speed which equals the average velocity during strides was employed as the walking speed. The subjects were between 22 to 28 years old with $1.73 \pm 0.09m$ height and $70.9 \pm 11.7kg$ weight. Kinematic and kinetic data processing was described in Lipfert. (2010).

For this experiment, we investigate which of three control approaches can better describe human swing leg adjustment. We calculate the control parameter (μ) for different control approaches and compared the parameter variations for different subjects at different speeds. For walking at a certain speed, the controller which has the smallest variance (for a range of subjects) can represent a unified approach for swing leg adjustment regardless the body parameters (e.g., weight and height).

4.3 RESULTS

In this section, we investigate which of three control approaches (Raibert Raibert (1986), Peuker Peuker et al. (2012) and VBLA Sharbafi et al. (2012)) introduced in Sec. 4.2.1 can better describe human swing leg adjustment. First, we show the simulation results for running and walking. Then, the abilities of the control approaches to predict human perturbed hopping and walking experiments are compared.

4.3.1 Simulations: running

In this section, we compare the methods regarding the region of attraction, sensitivity to running velocity and control parameters in running and hopping with SLIP model. With fixed values for the control parameters (μ in VBLA and Peuker approach and k and k' for the Raibert approach) we can achieve stable running at a certain range of speeds. We start the simulation at apex with initial speed (v_x^0) and stop it if the model falls or stably run 50 steps.

As the model is energy conservative, for a specific set of initial conditions (energy level) the controllers adjust the compromise between the final speed (v_x^*) and the apex height. Therefore, the ratio (r) between the final and the initial speed (v_x^*) shows the ability of the controller in keeping the speed which can be considered as a performance index ($r = 0$ means instability).

In Fig. 3, the stable solutions achieved by appropriate combinations of control parameters and initial speeds are shown with colors representing the speed ratio $r = \frac{v_x^*}{v_x^0}$. In Raibert approach we set the desired speed equal to the initial speed (not reached in many cases $r < 1$) and the speeds above $6m/s$ are not

[9] PTS is the preferred speed for transition between running and walking which is typically about $1.9 - 2.1\ m/s$ for humans Lipfert. (2010) .

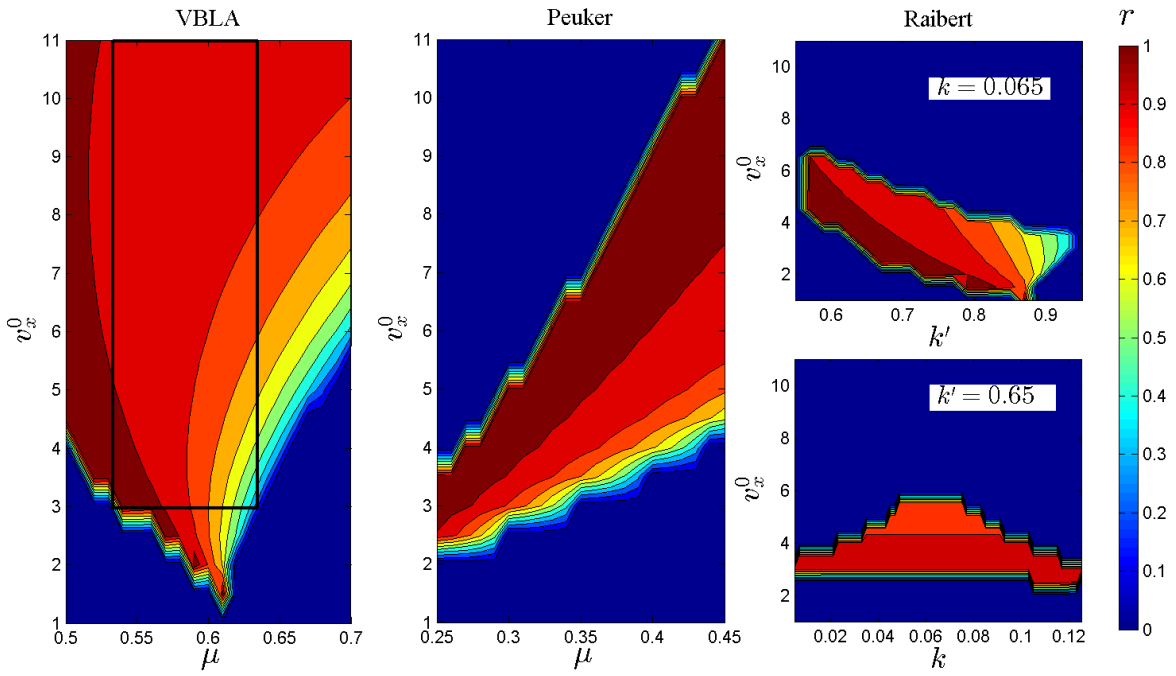

Figure 3: Performance and stability of different methods. The colors show the ratio of final to initial horizontal velocity $r = \frac{v_x^*}{v_x^0}$. The dark blue area $(r = 0)$ shows the instability.

achievable. In VBLA, the stable range is larger than the two other methods and the sensitivity to control parameter variations is smaller than them. For example with any control parameter $0.53 \leq \mu \leq 0.64$ the model never falls if the initial speed is above 3 m/s (shown by the rectangle in Fig. 3 (left). In addition, a large range of speeds can be achieved just by one value of $\mu = 0.52$ with $r = 1$. It means that with this control parameter, every initial speed from $3.4m/s$ to $11m/s$ can be kept without needing to change the controller. Of course, by increasing μ (not to more than 0.65) the speed can be decreased while the gait is still stable. The control parameter with the largest acceptable range of initial speed is $\mu = 0.61$, which can handle running from 1.5 m/s to 11 m/s, much larger than this value for the other methods.

4.3.2 Simulations: walking

As pointed in Geyer et al. (2006), the maximum achievable speed with BSLIP model is about $1.4m/s$. This constraint avoids havinga large speed range as obtained for running. However, this covers humans slow to moderate walking speeds. As can be seen in Fig. 8, considerably large region of stability is obtained with a combination of VBLA parameter μ and leg (normalized) stiffness K_N. It means that the control approach is quite robust against model uncertainties and also perturbations (e.g., variations in motion speed). It is shown that stiffer legs need larger μ meaning steeper leg at touchdown. In other words, we can keep the motion speed with different combinations of swing leg control and leg repulsion behavior. In the left figure, the minimum achievable walking speed depicts that for a fixed stiffness, the motion speed can be adjusted by μ. The middle figure shows the tolerable variations of speed for stable walking. It is observed that larger range of walking speeds can be achieved in the middle of the stable region in which a kind of linear relation between μ and K_N can be distinguished. The control parameters found in this region are able to produce stable walking with wider speed ranges. Finally, the fastest obtainable walking speed has more uniformly distribution over μ and K_N. However, for walking with a

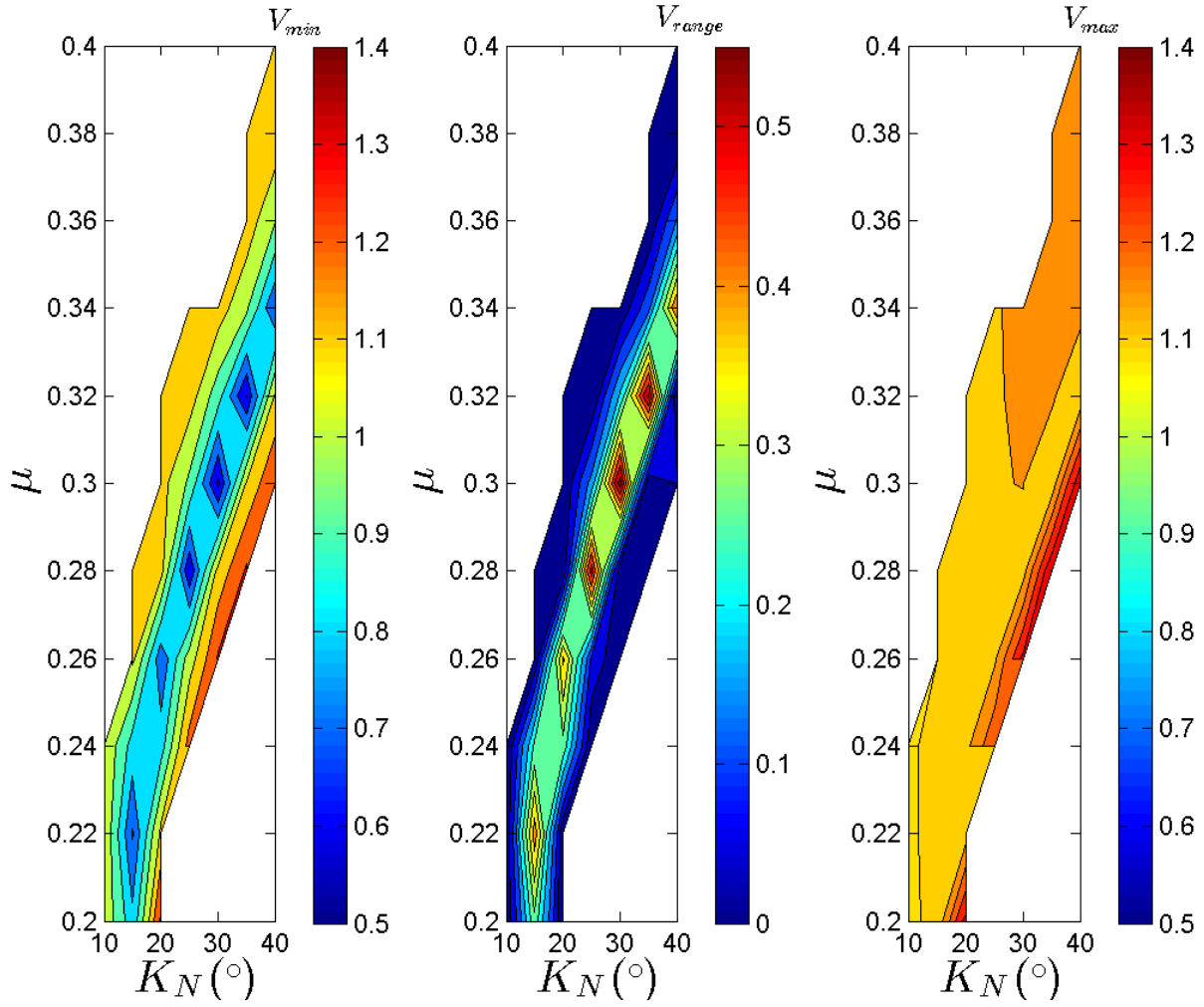

Figure 4: Maximum, range of and minimum speed achieved using BSLIP model with VBLA. The colored area shows the stable region while the colors show the values for minimum, variation range and maximum achievable speeds. The relation between normalized stiffness (K_N) and VBLA coefficient μ to have stable walking is shown.

moderate speed similar to humans normal walking speed, the legs should be stiffer and and the attack angle should be larger (smaller μ) than what are needed for slow walking.

4.3.3 Experiment: perturbed hopping

For this experiment, the parameters (a and b) are computed for three control approaches as described in Sec. 4.2.3. For each approach, these parameters are plotted against each other for different trials in Fig. 5. Then, using the least square we fit a linear relationship between two parameters. As can be seen, VBLA has the best matching to the data meaning that it can predict human leg adjustment by a fixed value of μ better than two other approaches. In addition, Table. 1 shows the statistical information about these data. The closer R^2 correlation index to one, the better fitting of data points to a line. This value is about 0.95 for VBLA, showing an appropriate matching of the data to this method. At each TD moment, related control parameter is also obtained by $\mu = a/b$. The variance of this number (normalized to its average) for different trials show how well that approach can explain human leg adjustment in different experiments. Table. 1 shows that the minimum variance beside the maximum R^2 correspond to VBLA.

Table 1: Different approaches statistical characteristics

Method	μ	R^2 **index**	**Variance**
Raibert	0.1614	0.6753	0.0182
Peuker	0.2865	0.763	0.0248
VBLA	0.6881	0.9486	0.0162

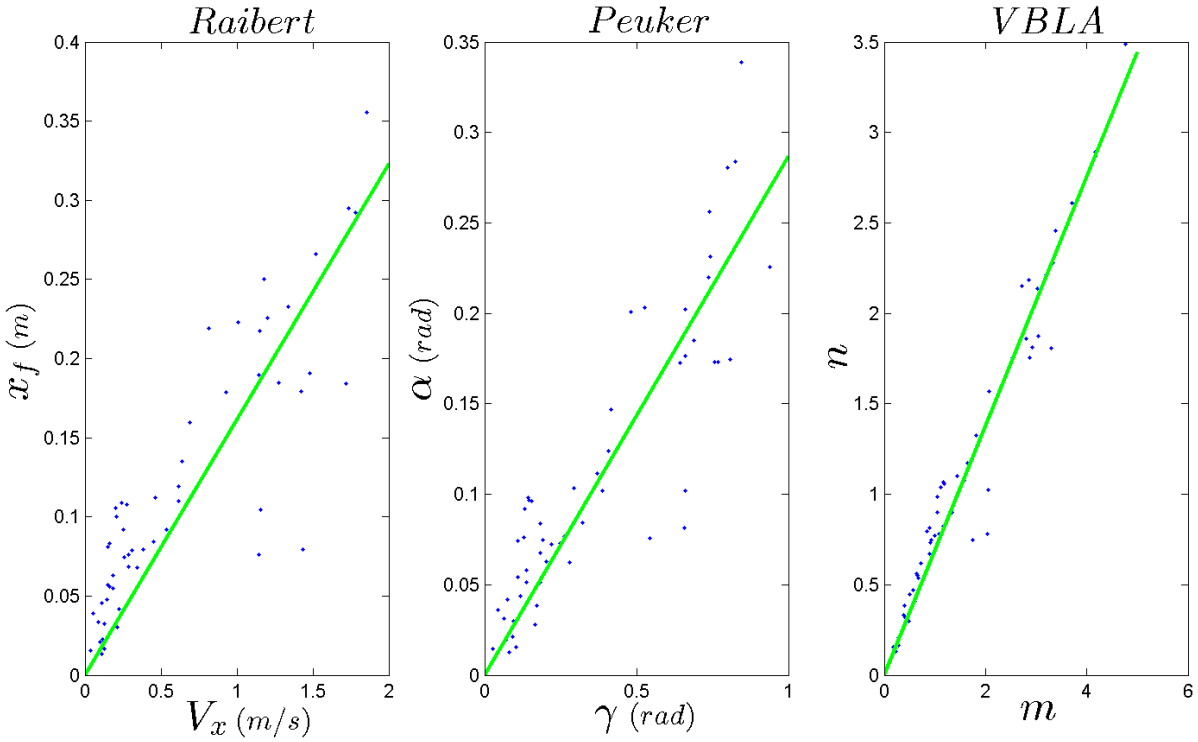

Figure 5: Human perturbed hopping experimental results analyses for different control approaches (blue dots). A linear relationship is fitted to the data points shown by green line.

4.3.4 Experiment: human walking

In this section, we investigate different control approaches to explain human swing leg adjustment in walking. For each approach, the control parameter is obtained by fitting the related equation (e.g., Eq. 2 for VBLA) to the experimental data at different speeds for all subjects (Fig. 6). The average values (bold black lines) show a monotonic trend in changing control parameter to increase the gait speed for all control approaches except from $100\%PTS$ to $125\%PTS$ in the Peuker approach. VBLA parameter variations versus speed shows almost a linear relation between μ and motion speed. It indicates that for faster walking the contribution of the velocity vector in computing the desired angle of attack is reduced. Thus, for increasing speed, we need to reduce μ which results in a larger (more vertical) angle of attack.

If one control approach can explain human swing leg adjustment better than others, the parameter of that approach calculated for different subjects at a specific speed should have the least deviation. Therefore, in order to find the most similar swing leg adjustment method to humans (regardless of the body parameters) the standard deviations (normalized to mean values) are compared in Fig. 7. The VBLA has the lowest variance among different approaches. It means this approach is the most human-like leg adjustment approach. For all approaches the normal walking speed has the lowest variance among

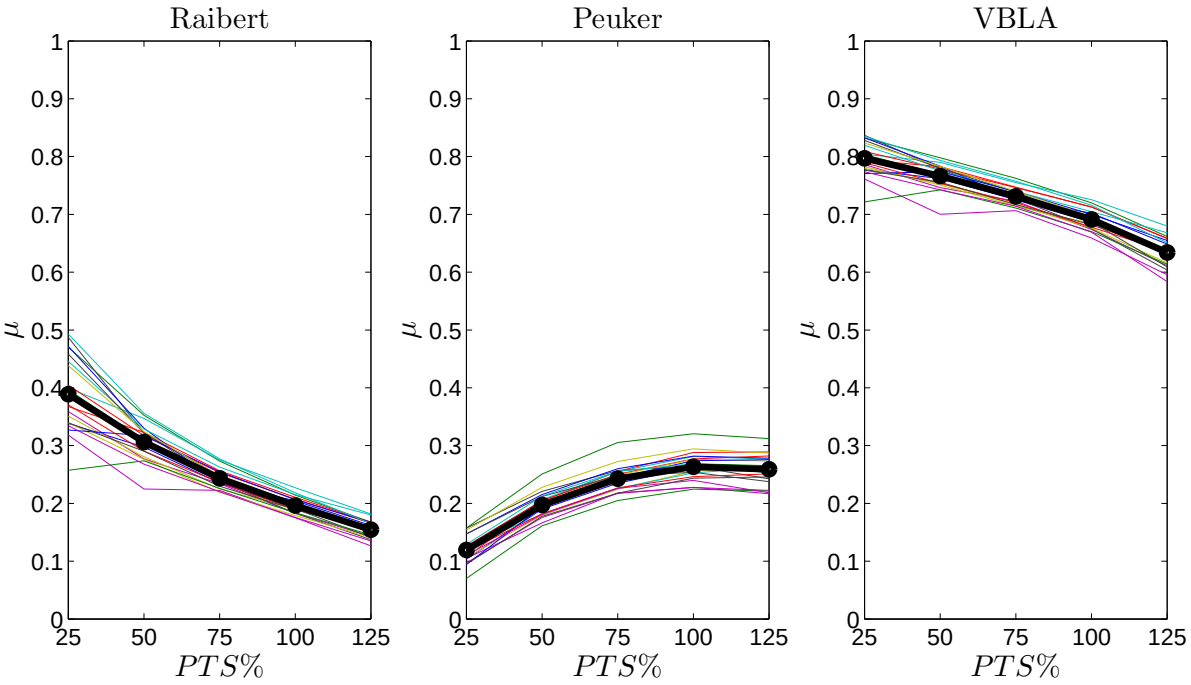

Figure 6: Different leg adjustment parameter (μ) changes versus speed in human walking (21 subjects). Thick lines show the mean value.

different speeds. This shows that velocity dependent swing leg adjustment techniques match better to experimental data at human normal walking speeds.

4.4 CONCLUSIONS

In this paper we compared three different control strategies for swing leg adjustment: Raibert controller Raibert (1986), Peuker approach Peuker et al. (2012) and VBLA (velocity based leg adjustment studies) Sharbafi et al. (2012) in simulations and human gait experiments. It was shown that VBLA is the best in mimicking human leg adjustment in walking perturbed hopping, achieve the largest range of running velocities by a fixed controller and provide a robust walking in simulation model with BSLIP model. From analytical point of view the main advantage of this approach is that it uses both elements of the velocity vector, the magnitude and the angle (or horizontal and vertical elements). This provides ability to react properly to any perturbations and increase the region of stability. This was tested by SLIP and BSLIP model for running and walking, respectively. As an important task in locomotion, it can be merged with other control techniques for stance phase like balancing and leg length adjustment for more complex models, e.g., with extended trunk TSLIP for running and hopping (Sharbafi et al. (2012)) and BTSLIP for walking (Sharbafi and Seyfarth (2015)).

From experimental side of view, VBLA can unify the human-like swing leg adjustment control at a certain speed, for human subjects with different body parameters in walking and perturbed hopping. This model was also implemented on simulation model of BioBiped robot as one of the locomotion sub-function controllers resulting in stable forward hopping Sharbafi et al. (2014). In addition to control of bipedal robots, this method can be easily implemented on exoskeleton to assist (impaired) humans in foot placement.

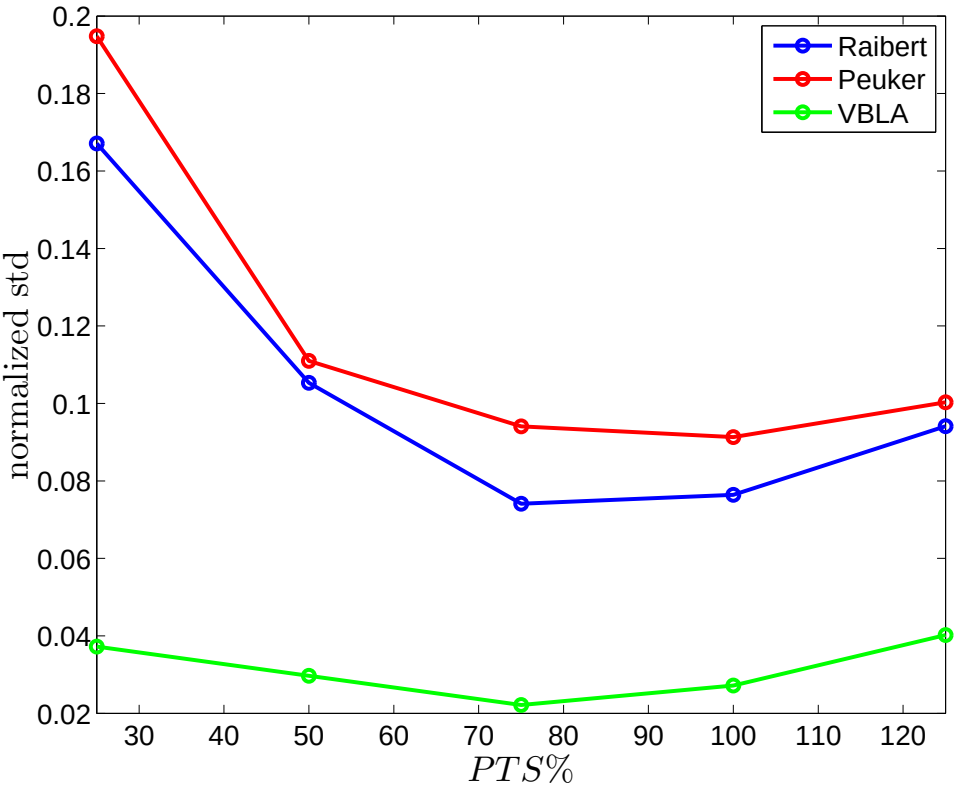

Figure 7: Leg adjustment parameter (μ) standard deviation of 21 subjects normalized to the average value for different leg adjustment approaches. The lower the number the more uniform the swing leg controller for different subjects at each speed.

4.5 ACKNOWLEDGMENT

This research was supported in part by the German Research Foundation (DFG) under grants No. SE1042/8 and in part by the EU project BALANCE under Grant Agreement No. 601003.

4.6 AUTHOR CONTRIBUTIONS

Maziar A. Sharbafi is the main and corresponding author of the article. He developed the new model of posture control and was responsible for the conception and design of simulations, analysis and interpretation of experimental data and writing of the manuscript. Andre Seyfarth was the supervisor of the project and contributed to developing concepts and models. He has also supported writing the paper.

4.7 REFERENCES

Altendorfer, R., Koditschek, D. E., and Holmes, P. (2004). Stability analysis of legged locomotion models by symmetry-factored return maps. *The International Journal of Robotics Research*, 23(10–11).

Blickhan, R. (1989). The spring-mass model for running and hopping. *Journal of Biomechanics*, 22(11):1217–1227.

Carver, S. (2003). *Control of a Spring-Mass Hopper*. PhD thesis, Cornell University, Ithaca, NY.

Full, R. J. and Koditschek, D. (1999). Templates and anchors: Neuromechanical hypotheses of legged locomotion on land. *Journal of Experimental Biology*, 22:3325–3332.

Gard, S. A., Miff, S. C., and Kuo, A. D. (2004). Comparison of kinematic and kinetic methods for computing the vertical motion of the body center of mass during walking. *Human Movement Science*, 22:597 – 610.

Geyer, H., Seyfarth, A., and Blickhan, R. (2006). Compliant leg behaviour explains basic dynamics of walking and running. *Proceedings of the Royal Society B: Biological Sciences*, 273:2861–2867.

Lipfert., S. W. (2010). *Kinematic and dynamic similarities between walking and running*. Verlag Dr. Kovaĉ,.

Peuker, F., Maufroy, C., and Seyfarth, A. (2012). Leg adjustment strategies for stable running in three dimensions. *Bioinspiration and Biomimetics*, 7(3).

Poulakakis, I. and Grizzle, J. W. (2009). The spring loaded inverted pendulum as the hybrid zero dynamics of an asymmetric hopper. *IEEE Transaction on Automatic Contro*, 54(8):1779–1793.

Raibert, M. H. (1986). *Legged Robots that Balance*. MIT Press, Cambridge MA.

Sato, A. (2004). A planar hopping robot with one actuator: design, simulation, and experimental results. In *IEEE/RSJ International Conference on Intelligent Robots and Systems (IROS)*.

Seipel, J. and Holmes, P. (2005). Running in three dimensions: Analysis of a point-mass sprung-leg model. *The International Journal of Robotics Research*, 24(8).

Seyfarth, A., Geyer, H., Günther, M., and Blickhan, R. (2002). A movement criterion for running. *Journal of biomechanics*, 35(5):649–655.

Seyfarth, A., Geyer, H., and Herr, H. (2003). Swing-leg retraction: a simple control model for stable running. *The Journal of Experimental Biology*, 206:2547–2555.

Seyfarth, A., Grimmer, S., Häufle, D., Maus, H.-M., Peuker, F., and Kalveram, K.-T. (2013). Computer models and robot validation. *Routledge Handbook of Motor Control and Motor Learning*, page 90.

Sharbafi, M. A., Maufroy, C., Seyfarth, A., Yazdanpanah, M. J., and Ahmadabadi, M. N. (2012). Controllers for robust hopping with upright trunk based on the virtual pendulum concept. In *IEEE/RSJ International Conference on Intelligent Robots and Systems (IROS)*.

Sharbafi, M. A., Radkhah, K., von Stryk, O., and Seyfarth, A. (2014). Hopping control for the musculoskeletal bipedal robot: Biobiped. In *2014 IEEE/RSJ International Conference on Intelligent Robots and Systems*, pages 4868–4875. IEEE.

Sharbafi, M. A. and Seyfarth, A. (2015). Fmch: a new model to explain postural control in human walking. In *IEEE/RSJ International Conference on Intelligent Robots and Systems (IROS)*. IEEE.

5 Article IV: Reconstruction of human swing leg motion with passive biarticular muscle models

Authors:

Maziar Ahmad Sharbafi, Aida Mohammadi Nejad Rashty, Christian. Rode and André Seyfarth

Lauflabor Locomotion Laboratory, TU Darmstadt, Darmstadt, Germany
School of Electrical and Computer Engineering, College of Engineering, University of Tehran, Iran
Department of Motion Science at Friedrich-Schiller-University Jena

Published as a paper in

Human Movement Science, ELSEVIER 2017.

ABSTRACT

Template models, which are utilized to demonstrate general aspects in human locomotion, mostly investigate stance leg operation. The goal of this paper is presenting a new conceptual walking model benefiting from swing leg dynamics. Considering a double pendulum equipped with combinations of biarticular springs for the swing leg beside spring-mass (SLIP) model for the stance leg, a novel SLIP-based model, is proposed to explain human-like leg behavior in walking. The action of biarticular muscles in swing leg motion helps represent human walking features, like leg retraction, ground reaction force and generating symmetric walking patterns, in simulations. In order to stabilize the motion by the proposed passive structure, swing leg biarticular muscle parameters such as lever arm ratios, stiffnesses and rest lengths need to be properly adjusted. Comparison of simulation results with human experiments shows the ability of the proposed model in replicating kinematic and kinetic behavior of both stance and swing legs as well as biarticular thigh muscle force of the swing leg. This substantiates the important functional role of biarticular muscles in leg swing.

KEYWORDS

Bipedal walking, biarticular muscles, swing leg adjustment, conceptual models.

5.1 INTRODUCTION

Template models such as the inverted pendulum (IP) (Cavagna et al., 1963) (Cavagna and Margaria, 1966) and the spring-mass model (SLIP, spring-loaded inverted pendulum) (Blickhan, 1989) can help understand principles inherent in human locomotion (Full and Koditschek, 1999) and demonstrate them in robotic counterparts. Many studies on these two basic models concentrate on the description of ground reaction forces (GRF) and center of mass (CoM) trajectories and neglect the effects of swing leg dynamics when the leg is massless (Seyfarth et al., 2002; Alexander, 1976; Hemami and Golliday, 1977; Wisse et al., 2006; Geyer et al., 2006). In the swing phase of walking, beside ground clearance, the main function of the swing leg is providing an appropriate foot placement, i.e. achieving a suitable leg configuration, a desired angle of attack, and leg retraction. Although the swing leg's mass also affects whole body motion, in most studies this effect is ignored and the swing leg movement is simplified to provide an appropriate angle of attack and the focus is on stance leg, CoM movement and GRF (Knuesel et al., 2005; Kuo, 2007).

In (Mochon and McMahon, 1980), Mochon et al. presented a model comprising a stiff stance leg and a segmented swing leg. They showed that the passive model with 2-segmented swing leg can better represent features (e.g., swing time course) of human walking compared with single pendulum. However, the vertical GRF of the model is different from experiments because the modelling constraints (e.g., stiff stance leg). Equipping the IP model with an elastic spring in the stance leg, the SLIP model could mimic GRF and COM movement and non-instantaneousness double support of human locomotion (Geyer et al., 2006). Still, swing leg movement is a missing part in SLIP model and many of its extensions (e.g., to 3d SLIP (Seipel and Holmes, 2005) or with extended foot (Maykranz and Seyfarth, 2014)). In (OĆonnor, 2009), a new SLIP-based model with additional mass in both legs, curved feet and hip rotational spring was introduced. In this study, OĆonnor investigated different parameters' effects on stability of different types of gaits while integrating feedback (reflex) and feedforward control (CPG). Nevertheless, it has not yet been attempted to focus on human-like swing leg control and effects of segmented leg on overall motion dynamics while maitining simplicity in modelling by employing conceptual models.

In this paper, we combine a segmented swing leg with the spring-loaded inverted pendulum model for the stance leg to represent the swing phase of human-like walking (Fig. 1a). Such a new simple model can potentially explain significant features of human walking which could so far be described in complex models including detailed leg muscles like (Geyer and Her, 2010). Therefore, we can achieve a

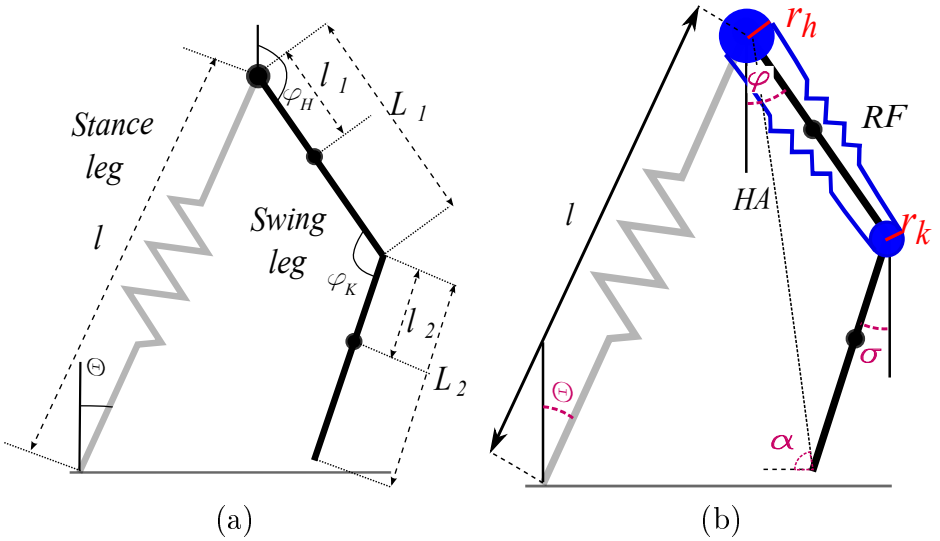

Figure 1: (a) DPS model during swing phase. (b) Addition of biarticular muscles to DPS.

target behavior inspired from human walking, and simplicity in modeling and control. We can also apply simple control methods developed using this model to robots and prostheses (see (Sharbafi et al., 2016) for implementing the controller on BioBiped robot).

Judging from human leg muscle activities in the swing leg movement, biarticular hip muscles rectus femoris (RF) and hamstrings (HA) seem to be the main contributors in the swing phase of walking (Nilsson et al., 1985). By modeling these two muscles with biarticular springs, we aim at a better mechanical understanding of their activities in producing stable gait. In addition, such a passive mechanism may also replicate strong correlation observed between RF and HA in human swing leg movement (Prilutsky et al., 1998), as a consequence of body mechanics.

The goal of this study is to identify the role of elastic biarticular thigh muscles (represented as springs) on swing leg dynamics, the appropriate spring parameters and morphology such that the model can mimic human swing leg motion in walking. With the proposed model, we investigate the role of HA and RF, by comparing the leg's behavior with and without muscles. Human walking data are used (Lipfert, 2010) to determine the initial conditions of the swing phase (at lift-off) and for comparison with simulation results. The influences of muscle lever arm ratio, muscle stiffness and muscle rest lengths on the COM motion and swing leg behavior are demonstrated. It is observed that with passive elastic biarticular muscles, walking motion characteristics, like swing leg retraction and symmetric stance leg behavior around mid-stance are obtainable.

5.2 METHODS

5.2.1 Model

In this section, we describe the walking model shown in Fig. 1. It is assumed that the segments of the swing leg have a distributed mass while the stance leg is massless. The model properties are adapted to anthropometric data (Winter, 2005) and are summarized in Table 1. Human walking is characterized by alternating double support and single support phases, and the CoM is approximately at the hip (Maus et al., 2010). In the model, during double support phase, the whole mass is represented by a point mass at the hip; in the single support phase, the mass at the hip is body mass reduced by the mass of the swing

leg segments. Since the focus of this study is on swing leg dynamics, double support is not playing a significant role in our analyses. However, for completing the walking step, the bipedal SLIP model is used to describe the double support and we implement a switching between springy leg and two segmented leg, as described in 8.5.1.

First, we describe the hybrid "**DPS**" model including double pendulum (**DP**) for the swing leg and **S**LIP for the stance leg (Fig. 1a). Later, we add biarticular springs (muscles) to the two segmented swing leg, as shown in Fig. 1b. Considering $q = [l;\theta;\varphi;\sigma]$ as depicted in this figure, we write Lagrange equations that give the dynamical system equations for the single support phase of motion[10],

$$D(q)\ddot{q} + C(q,\dot{q})\dot{q} + G(q) = BF \tag{1}$$

in which D and C are the inertia and the Coriolis matrices, respectively. G is the gravity vector and B is a constant matrix that maps the force vector F to the generalized forces. Hence, defining the state vector $x = [q;\dot{q}]$ gives the following relation for the continuous mode of the robot motion:

$$\dot{x} \;=\; \begin{bmatrix} \dot{q} \\ D^{-1}(q)[-C(q,\dot{q})\dot{q} - G(q) + BF] \end{bmatrix} \tag{2}$$

In the proposed model, the hip and knee torques can be considered as (external) control input, placed in force vector F. Hip torque is exerted between thigh and a virtual trunk which is assumed to be upright during swing phase. Physical interpretation of such a model for the upper body could be considering a flywheel with a large (infinite) inertia at the hip point. An upright trunk approximates the normal upper body posture in human locomotion (Maus et al., 2010). The detailed equations are presented in the 8.5.1 and hereafter we focus more on the biarticular muscle modeling.

In this model, the biarticular muscles are represented by passive unidirectional springs (only able to exert pulling force), connected from upper body to shank (Fig. 1b). With this formulation, torques produced by rectus femoris (RF) and hamstrings (HA) in knee and hip can be computed based on the spring lengths. Suppose the lever arms and the rest angles at hip and knee are described by r_h, r_k, φ_{h0} and φ_{k0}, respectively. Then, the elongation in RF (from rest length) will be

$$\Delta l^{RF} = r_h(\varphi_h - \varphi_{h0}) - r_k(\varphi_k - \varphi_{k0}) \tag{3}$$

in which φ_h and φ_k are the hip and knee angles as shown in Fig. 1a. Then, the net torques generated by the RF acting at the thigh (τ_φ^{RF} in direction of φ, the third variable of q) and the shank (τ_σ^{RF} in direction of σ, the forth variable of q) are computed as follows:

$$\begin{cases} \tau_\varphi^{RF} = k_{RF}(r_h - r_k)max(\Delta l^{RF}, 0) \\ \tau_\sigma^{RF} = k_{RF} r_k max(\Delta l^{RF}, 0) \end{cases} \tag{4}$$

where *max* function shows that the spring is unidirectional, and k_{RF} is the stiffness of the RF spring. Defining lever arm ratio $r = \frac{r_h}{r_k}$ and new constants $k_{Rh} = k_{RF} r_h^2$ and $\varphi_{RF0} = \varphi_{h0} - \frac{\varphi_{k0}}{r}$, equations (5) and (6) result in

$$\begin{cases} \tau_\varphi^{RF} = k_{Rh}(1 - \frac{1}{r})max(\theta_{sw} - \varphi_{RF0}, 0) \\ \tau_\sigma^{RF} = \frac{k_{Rh}}{r} max(\theta_{sw} - \varphi_{RF0}, 0) \end{cases} \tag{5}$$

[10] Sign ";" concatenates the matrices vertically; i.e. $[a;b] := [a^T b^T]^T$, where super index T means transpose.

where $\theta_{sw} = \varphi_h - \frac{\varphi_k}{r}$. For equal shank and thigh lengths and if the lever arm ratio r is equal to 2, then this new angle θ_{sw} has a physical meaning which is the virtual leg angle (α) measured between the virtual leg (through hip and leg tip) and the horizontal axis (Fig. 1b). This geometrical relation in a leg model can simplify the control of swing leg movement. Therefore, with such a configuration, if the virtual leg angle α is larger than a certain angle φ_{RF0}, RF works by extending the knee and flexing the hip[11]. By antagonistic arrangement the net torque provided by the HA is similar to the RF. Thus, defining k_{HA} and φ_{HA0} as the hamstrings stiffness and rest angle, the produced torque by this muscle will be:

$$\begin{cases} \tau_{\varphi}^{HA} = -k_{Hh}(1-\frac{1}{r})max(\varphi_{HA0} - \theta_{sw}, 0) \\ \tau_{\sigma}^{HA} = -\frac{k_{Hh}}{r} max(\varphi_{HA0} - \theta_{sw}, 0) \end{cases} \tag{6}$$

in which $k_{Hh} = k_{HA} r_h^2$.

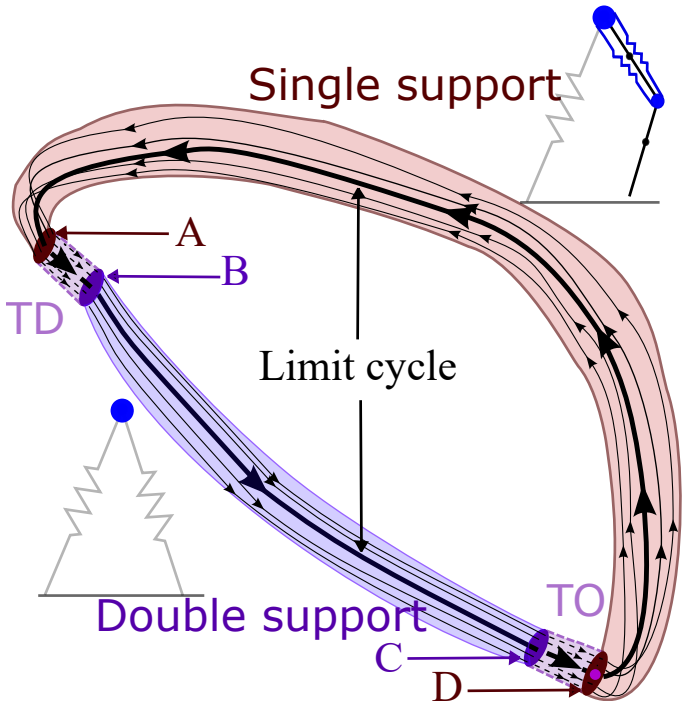

Figure 2: Schematic representation of the stability region for a complete step of the hybrid model, including DPS for single support and BSLIP for double support. Considering the curves illustrating the phase portrait (e.g., for CoM states), arrows represent phase trajectories where the bold line is the limit cycle. A, B, C and D show the allowable region to have stable gait for swing phase, touchdown (TD), stance phase and takeoff (TO), respectively. If in each of these phases (continuous swing and stance phases (solid lines) or discrete TD and TO (dashed lines)) the phase trajectories end in an allowable region, the stability conditions are simplified to satisfying structural constraints e.g., avoiding knee hyper extension.

[11] The lever arm ratio in human hamstring and rectus femoris in straight configuration are 2 and 1.25, respectively (Loram and Lakie, 2002).

5.2.2 Stability

A walking step can be divided into two continuous (single support and double support) phases switching to each other through discrete mapping at touchdown (TD) and takeoff (TO), as shown in Fig. 2. For a specific gait condition (e.g., speed), we define a region of stability around a nominal stable limit cycle[12] as follows: for any initial condition inside the stability region, the states never leave this region. This definition can be considered as an extension of Lyapunov stability (Isidori, 1995). Therefore, allowable regions A, B, C, D can be defined for evaluating stability, as shown in Fig. 2. The discrete phases are determined by system dynamics (see 8.5.1) and are not controllable. Hence, the controllers which bring any state inside D to A and any state inside B to C result in stable walking, if the constraint conditions (e.g., preventing knee hyper extension) are satisfied. As a result, the controller for single (double) support phase is stabilizing if it transfers any point in region D (B) to a point in region A (C). With this definition, motion control in swing phase is separated from stance phase and they are not affected by each other. In this study, the goal is mimicking human-like swing leg movement via a conceptual model. Therefore, to prevent swing leg movement to be affected by double support dynamics and control, we define an allowable region A (for the swing phase) based on D, while region D is determined as a neighborhood of initial conditions. The swing phase stability is analyzed, starting from takeoff moment (TO) and ending at touchdown (TD).

The initial conditions including the stance leg length and angle, thigh and shank angles of the swing leg and their derivatives are adopted from the average value of human walking experiments (21 subjects (Lipfert, 2010)). Using subindices $_{TO}$, $_{TD}$ for takeoff and touchdown moments and defining the desired angle of attack α_{att} and an acceptable error range[13] of $\delta = 2^\circ$, the swing motion is called stable if

1. the swing leg hits the ground in the predefined range

$$|\alpha_{TD} - \alpha_{att}| < \delta \tag{7}$$

2. the stance leg angle at touchdown is close to this angle at takeoff with opposite sign

$$|\theta_{TO} + \theta_{TD}| < \delta \tag{8}$$

3. the knee angle is less than 180° during the whole swing leg motion.

$$\varphi_K < 180 \tag{9}$$

4. swing leg retraction happens before touchdown.

Leg retraction means that the virtual leg angular speed at touchdown is positive. Such a backward rotation of the swing leg before touchdown is observed in human walking patterns at different speeds (Poggensee et al., 2014). Swing leg retraction is detected when the following condition holds:

$$\forall\, t,\ t_{TD} - \Delta t < t < t_{TD} \mid \quad \dot{\alpha}(t) > 0, \tag{10}$$

[12] It is not necessary to reach a limit cycle. Any cyclic movement (even with neutral stability) can be considered to define the stable region. In this study, the reference periodic trajectory (cycle) is found based on an average human gait cycle at the desired speed.

[13] This value is chosen based on experimental results. In human walking at normal speed (about $1.5 m/s$), the standard deviation of attack angle through different steps is between $0.7^\circ - 2^\circ$ for different subjects. The acceptable error range δ in our model is set to 2° to match the experiments.

Table 1: Initial conditions of simulation adopted from walking experiment.

Variable	Symbol	Value [units]
Stance leg length	l_0	0.98 $[m]$
Stance leg angle	θ_0	-14 $[^\circ]$
Thigh angle	φ_0	-10 $[^\circ]$
Shank angle	σ_0	-48 $[^\circ]$
stance leg length changes	$\dot{l}_0$	-0.14 $[m/s]$
Stance leg angular speed	$\dot{\theta}_0$	80 $[^\circ/s]$
Thigh angular speed	$\dot{\varphi}_0$	130 $[^\circ/s]$
Shank angular speed	$\dot{\sigma}_0$	-133 $[^\circ/s]$

in which Δ is the required time to find the retraction speed at touch down. From human walking and running experiments (Poggensee et al., 2014), the swing leg retraction speed is calculated as the average angular velocity $20ms$ before TD. Thus, $\Delta = 20ms$ is selected for our simulations.

A similar approach can be considered for adjusting spring parameters in the BSLIP model to keep stability for the double support phase.

5.2.3 Experiment and simulation

The data was collected in human walking on a treadmill (type ADAL-WR, Hef Tecmachine, Andrezieux Boutheon, France). Motion capture data (Qualisys, Gothenburg, Sweden) from 11 markers and ground reaction force data (12 piezo-electric force transducers within the treadmill) were collected. 21 subjects (11 female, 10 male) were asked to walk at 75% of their preferred transition speed (PTS)[14]. The treadmill speed which equals the average velocity during strides was employed as the walking speed. The subjects were between 22 to 28 years old with $1.73 \pm 0.09m$ body height and $70.9 \pm 11.7kg$ body weight.

For simulation, the initial conditions are adopted from walking experiments with 75%PTS (about 1.55 m/s) as shown in Table 2. The virtual stance leg is defined by a line from the CoM (center of mass) to the CoP (center of pressure) and the length is normalized to the virtual spring rest length ($L0$). In the experimental data, the virtual spring leg is at its rest length when the swing leg switches to stance leg at touchdown. Normalizing the body parameters to this rest length, sets the rest length to 1 for the simulations. The beginning of the single support phase coincides with the end of the double support phase. Hence, the stance leg is compressed at the initial configuration. The model parameters are set to match the characteristics of a human body with $75kg$ weight and $1.89m$ height (meaning $1m$ leg length) as shown in Table 1.

5.3 RESULTS

In this section we show the simulation results of the single support phase and compare the kinematic behavior with human walking data. The analyses are shown for different values of biarticular springs stiffness and rest lengths with the lever arm ratio $r = 2$. With this ratio, the biarticular muscles only contribute to change the leg angle and not on leg length (leg length is changing based on system dynamics) which can simplify realization and control of the model. All results are shown for a fixed set of parameters for the stance leg while different values for the swing leg parameters (the spring rest length and stiffness) are examined to find stable gaits.

[14] PTS is the preferred speed for transition between walking and running which is typically about $1.9 - 2.1\ m/s$ for humans (Lipfert, 2010) .

Table 2: Model parameters based on human body characteristics. The segments' parameters are computed based on (Winter, 2005).

Parameter	Symbol	Value [units]
Body mass	m	75 [kg]
Thigh mass	m_1	7.275 [kg]
Shank mass	m_2	4.5 [kg]
Stance leg rest length	L_0	1 $[m]$
Thigh length	L_1	0.5 $[m]$
Shank length	L_2	0.5 $[m]$
Hip to thigh CoM distance	l_1	0.22 $[m]$
Knee to shank CoM distance	l_2	0.22 $[m]$
Stance leg stiffness	K_s	30000 $[N/m]$
Gravitational acceleration	g	9.81 $[m/s^2]$

5.3.1 DPS stability

In this section, we investigate the effects of biarticular muscle parameter adjustment on stability. As explained in section 5.2.1, with $r = 2$, each of the biarticular muscles contributes to a certain range of virtual leg angles (α in Fig.1(b)). Therefore, φ_{RF0} and φ_{HA0} (the virtual rest angles of RF and HA) determine the range in which each of RF or HA produces force (for $\alpha > \varphi_{RF0}$ and $\alpha < \varphi_{HA0}$, RF and HA muscles contribute to swing leg movement, respectively).

In Fig. 3, for different ratios of RF to HA stiffness ($r_k = \frac{k_{RF}}{k_{HA}}$) stable regions for biarticular muscles rest angles are shown while different colors correspond to different stiffnesses of the hamstrings (k_{HA}). Increasing r_k moves the stable region (upward) towards larger RF rest angles. Therefore, higher stiffness of the RF (compared with HA) is compensated by shortening its contribution to the swing leg movement. The stable regions become smaller for r_k larger than 1. More precisely, if the RF is stiffer than the HA, smaller regions for desired rest angles are found which means the muscles must be tuned more accurately. Negative slope observed in stable regions illustrates that larger φ_{RF0} -corresponding to less contribution of the RF- requires smaller φ_{HA0}, meaning less contribution of the HA. In addition, the lighter color on the right-bottom side of each drawing demonstrates the need of softer muscles when the HA and RF rest angles are higher and lower, respectively. If the muscles are softer, they should work for longer fraction of the swing phase. The stable region above the dashed lines show dead zone, a range for the virtual leg angle in which none of RF and HA produces force. The large regions below this line demonstrates overlap between working regions of hip biarticular muscles. Although this means producing opposing forces, the resulting nonlinear hip torque-angle relation helps provide desired swing leg behavior.

5.3.2 Muscle forces

Looking at rest angles in Fig. 3 shows that the hamstrings produce force (as hip extensor/knee flexor) before the swing leg passes vertical configuration, as $90^\circ < \varphi_{HA0}$. The related rest angle for rectus femoris depends on r_k, expressing which muscle is stiffer. When RF is stiffer ($r_k = 2$), considerable stable regions are found with $90^\circ < \varphi_{RF0}$, meaning RF muscle finishes producing force much before the swing leg reaches vertical orientation. Hence, there will be low overlap between HA and RF opposing forces. However, when the HA stiffness is equal or larger than RF ($r_k \leq 1$), a kind of complementary behavior is observed between the two muscles such that for a considerable part in stable regions $\varphi_{HA0} + \varphi_{RF0} \approx 180^\circ$. Such a behavior can be observed in the force, generated by the hip biarticular muscles with DPS model

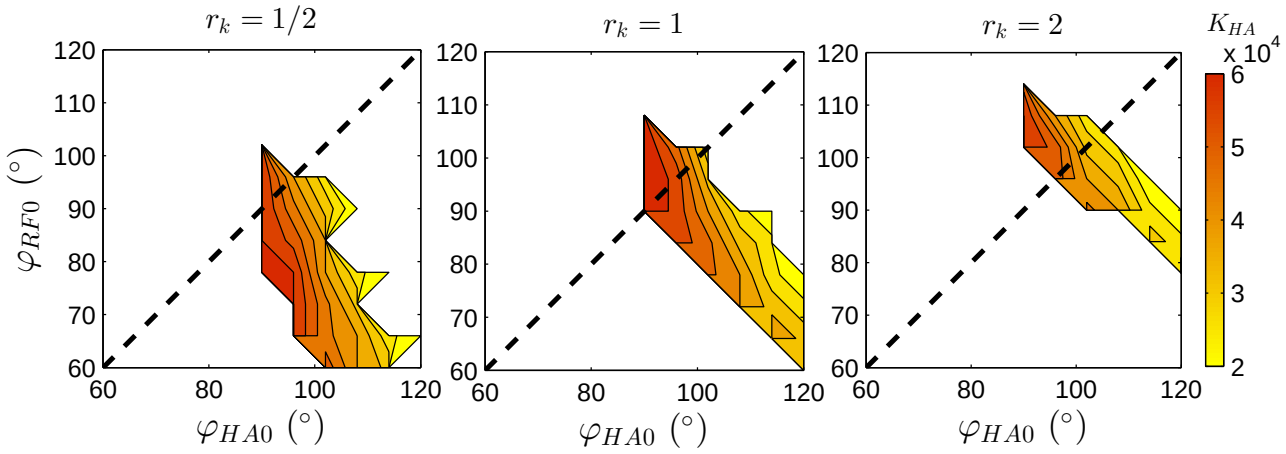

Figure 3: combinations of biarticular muscle's rest lengths are shown by colored areas for different RF to HA stiffness ratio (r_k). Colors show different levels of stiffness in HA spring. The dashed lines show the border between having overlap (below line) and dead zone (above line) for hip biarticular muscle actuations.

in Fig. 5 which is similar to human biarticular muscle forces in swinging the leg (Prilutsky et al., 1998). Hamstrings force decreases at the last 20% of the swing phase because of leg retraction. Investigating a wide range of spring parameters yields high variance in behavior of stabilizing couples of passive biarticular thigh muscles in the simulation model. However, lower overlap or more similar behavior to human muscles can be obtained by selecting appropriate stiffness and rest length for biarticular springs.

5.3.3 Kinematic behavior

The swing leg, knee and hip angles of the DPS model and human walking experiment data are depicted in Fig. 5. The DPS model can produce angular movement of the swing leg similar to human ones. The virtual leg angle (α) is decreasing during swing phase until shortly before touchdown. Such a backward movement of the swing leg (swing leg retraction) providing for lower impacts, and is observed in both simulation model and human walking. Knee flexion in the beginning of the swing phase results from releasing energy stored during previous stance phase at push-off. RF reduces the flexion speed and finally after passing about 30% of swing phase, knee extension starts and continues until the late 10% of the motion. Swing leg movement results in less actuation of RF and later initiates and then increases HA actuation, which yields reducing knee extension speed to reach a certain knee angle before touchdown. Hip flexion at the beginning of the swing phase results from pre-stretch of the RF due to the initial conditions. In simulation, hip flexion and extension are more pronounced than in human experiments. In both experiments and simulations, hip extension starts at late swing phase.

In Fig. 6, the stance leg's angle and length are shown for simulation and experiments. For both, the leg angle increases linearly (from θ_0 to around $-\theta_0$) resulting in symmetric stance leg behavior. The leg length changes in the DPS model oscillate with a higher frequency than in the experiments. Concluding, with a passive mechanism, both stance and swing leg movements can be approximated.

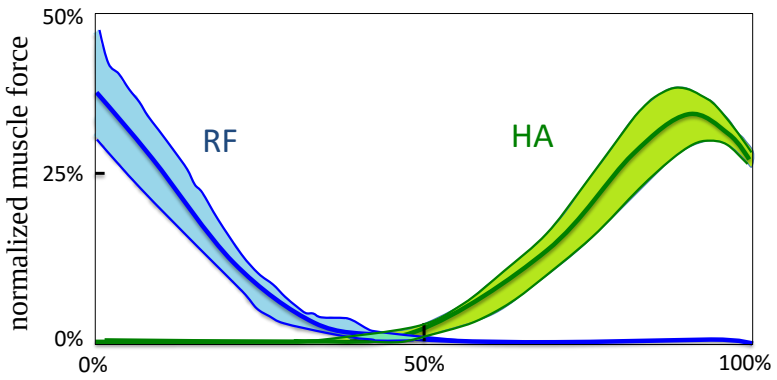

(a)

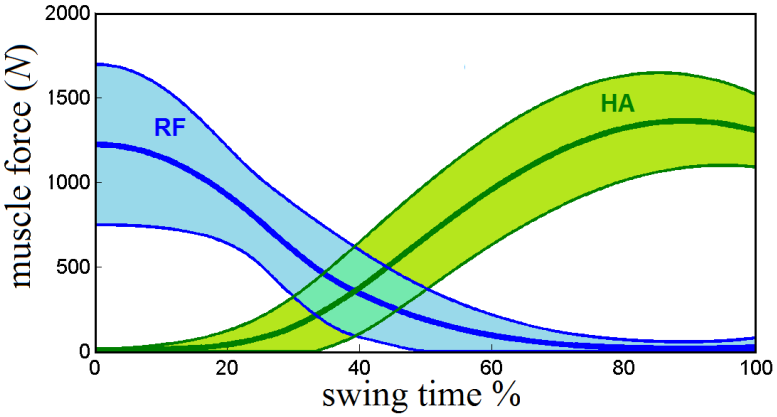

(b)

Figure 4: Hip biarticular muscle forces during swing phase of walking (a) at speed 1.8 (m/s) of human experiment (data adopted from (Prilutsky et al., 1998)) (b) at speed 1.55 (m/s) in simulation. The mean values (solid lines) and standard deviation (thin lines) of all stable simulations are shown.

5.3.4 Kinetic behavior

Fig. 7 shows the ground reaction forces (GRF) of the DPS model compared to experimental data. Although swing leg movement changes the GRF by accelerating and decelerating leg segments, the DPS model can approximate the GRF patterns in both horizontal and vertical directions. Increasing GRF in horizontal direction fits well to experimental data. Most of the typical M-shape GRF in vertical direction (in human walking) occurs during the swing phase meaning that the vertical GRF has one early and one late peak separated by a minimum around mid-stance (Geyer et al., 2006). Such a pattern is also observed in the DPS model except an earlier second peak and a stronger decrease in GRF of the simulation model than in experiments. This may be related to the linear stiffness in the stance leg and the lack of a foot which hampers push off in SLIP based models.

The role of swing leg movement is not only providing a certain angle of attack and ground clearance, but also a noticeable contribution to the GRF (Zhao and Seyfarth, 2015). Fig. 8 shows the simulation and experiment results. It can be seen that during the swing phase of human walking, swing leg force is in phase with the GRF in vertical direction while it is out of phase in horizontal direction. The magnitude of the swing leg force is about 25% of GRF at normal walking speeds. Similar contribution of the swing leg movement in GRF can be observed in the proposed model.

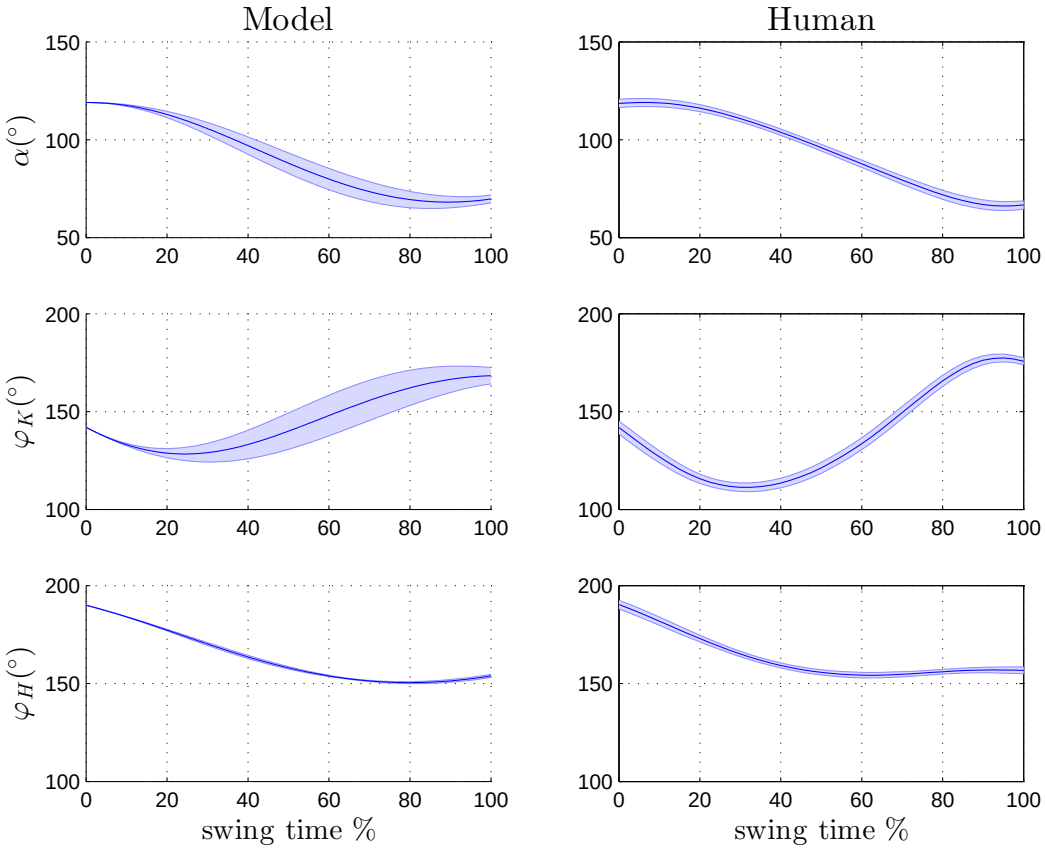

Figure 5: Virtual leg, knee and hip angles of the swing leg during swing phase (40% of the gait cycle) for regular walking speed (about 1.55 m/s) for DPS model and humans. Thick lines and shaded areas show the mean and standard deviation, respectively.

5.4 DISCUSSION

In this paper we investigated how biarticular muscles may contribute to the control of the swing leg in bipedal walking. We found that swing leg dynamics can be tuned by a presetting the stiffness and rest length of two antagonistic spring-like operating muscles resulting in stable walking. With this approach we obtain similar behavior as in human walking regarding a) muscle forces, b) swing and stance leg kinematics and c) ground reaction forces.
The muscle lever arm ratio, stiffness and rest lengths for RF and HA are important parameters affecting the motion. In this study, we explored the influence of the latter two on leg swinging while the lever arm ratio was fixed ($r = 2$). Appropriate combinations of rest length and stiffness were found to achieve a completely passive leg swinging for stable walking.

The introduced DPS model can mimic human-like swing leg movement, GRF, and muscle forces. Investigating different rest lengths and stiffnesses for passive elastic RF and HA yielded strong correlation between these predicted muscle actions in the swing phase and human muscle activities (Prilutsky et al., 1998). Here, we designed a mechanical template to suggest appropriate swing leg muscle activities. On the one hand, the results in Fig. 3 indicates a joined action of RF and HA muscles which can also be observed in Fig. 5. On the other hand, the stiffness of the biarticular thigh muscles will tune the duration of the swing leg rebound and thus the duration of muscle activity.

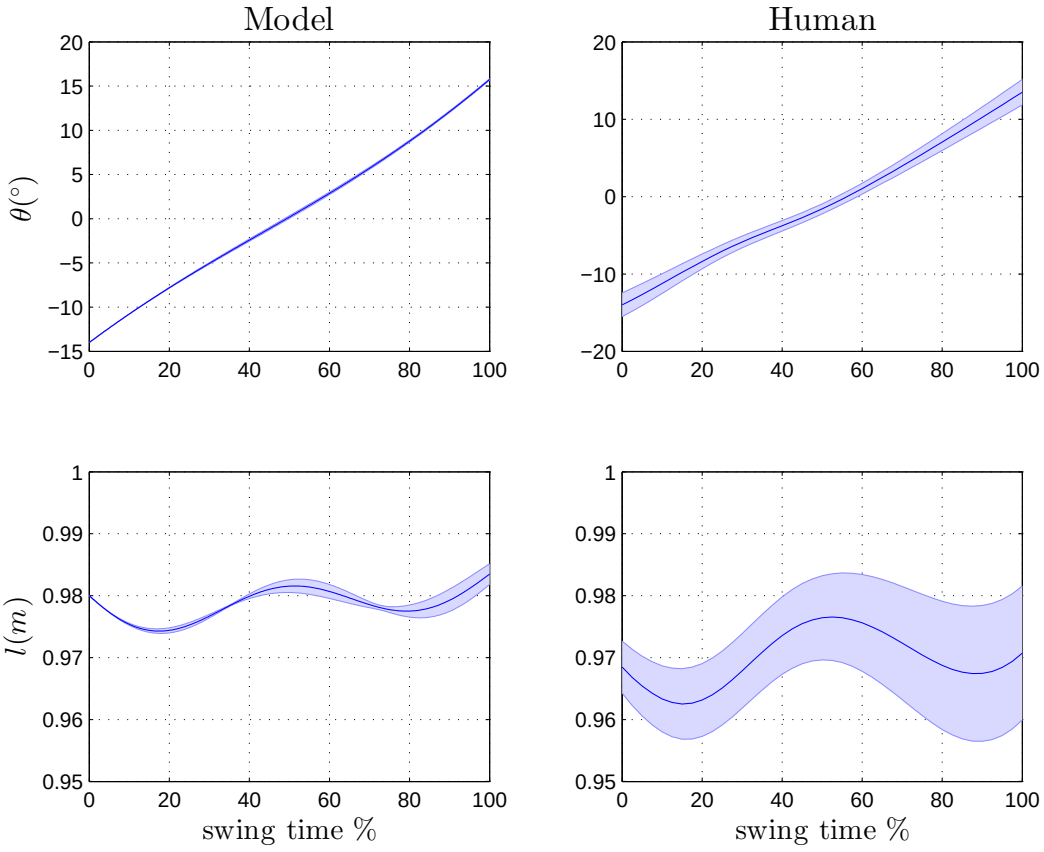

Figure 6: Stance leg's angle and length during swing phase (40% of the gait cycle) for regular walking speed (about 1.55 m/s) for DPS model and humans. Thick lines and shaded areas show the mean and standard deviation, respectively.

In contrast to previous studies (Desai and Geyer., 2013; Geyer and Her, 2010), the proposed conceptual model indicates benefits allowing for a simple realization of the swing-phase in robots with segmented legs. The biarticular springs do not need to be adjusted during the swing phase. Moreover, small human-like overlap between biartiular working periods can be achieved by tuning rest lengths and stiffness or by using biarticular springs.

Furthermore, the predicted kinematics of the swing and stance legs in the DPS model are comparable with their counterparts in human walking (Lipfert, 2010). Thus, the model demonstrates that ground clearance, leg retraction, reaching the desired angle of attack and preventing knee hyper extension can largely be achieved, passively. This indicates that the swing leg movement could be realized energy efficient in bipedal locomotion of robots. In other words, if the system is properly designed and adjusted, the passive dynamics of the system includes control and just a small amount of energy may be required for fine tuning in order to cope with perturbations or uncertainties.

Biarticular elastic muscles create a spring-driven pendulum which results in a swing-leg adjustment similar to a contact angular acceleration prior to touchdown, as previously described by Vejdani et al (Vejdani et al., 2013). The adjustment of the leg orientation before touchdown could further be supported by the two-joint muscle in the lower leg (m. gastrocnemius). This leg angle adjustment was found in human running over uneven ground (Müller and Blickhan, 2010). It results in an additional adjustments in knee angle and foot orientation prior to landing which was not considered in our study.

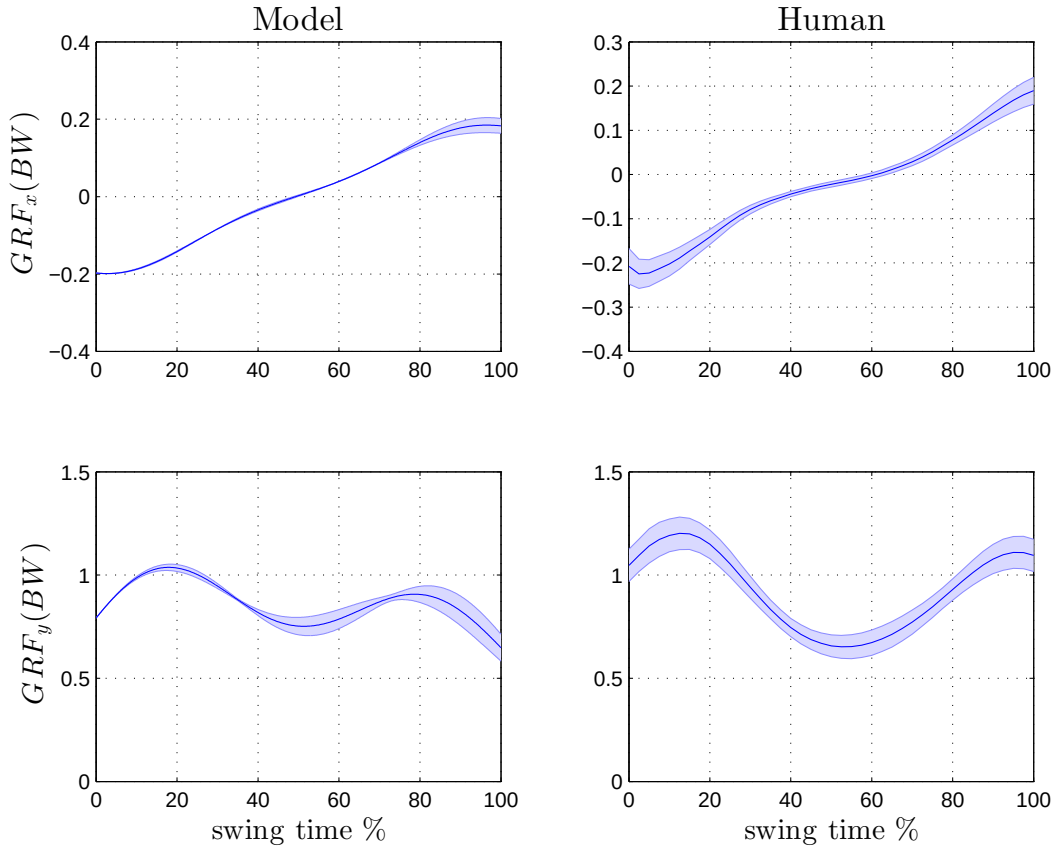

Figure 7: GRF during swing phase (40% of the gait cycle) for regular walking speed (about 1.55 m/s) for DPS model and humans. Thick lines and shaded areas show the mean and standard deviation, respectively.

With some concessions, ground reaction forces can be replicated by the DPS model with the segmented swing leg movement (with mass and inertia). This is due to the fact that the force generated by the swing leg movement is synchronized with that of the stance leg and with the CoM movement. The contribution of swing leg movement to the horizontal and vertical component of the GRF is in out-of-phase and in-phase with that of the rest of the body, respectively. This means that the swing leg contributes to the M-shaped vertical GRF. By counteracting in the horizontal GRF component of the stance leg it helps balancing the upper body which is also in accordance with findings in human walking experiments (Zhao and Seyfarth, 2015). Given the similarity in walking dynamics (e.g. GRF patterns) between the DPS model and human walking, the predicted stability with compliantly tuned segmented swing legs could also be beneficial for gait stability in humans.

In conclusion, our results show the importance of considering biarticular muscles to better understand human locomotion control. The presented model can explain i) humans' energy efficient swing leg adjustment using passive mechanisms with little energy required for presetting and fine tuning of muscles, ii) stabilizing leg adjustment providing ground clearance, leg retraction and accurate setting of attack angle while preventing knee hyper extension and iii) low control effort for swing leg adjustment based on mechanical properties of the muscles.

The function of biarticular muscles needs to be further investigated (e.g., the influence of lever arm ratios on the motion) to improve the design of bipedal locomotor systems (e.g. as in the humanoid robot

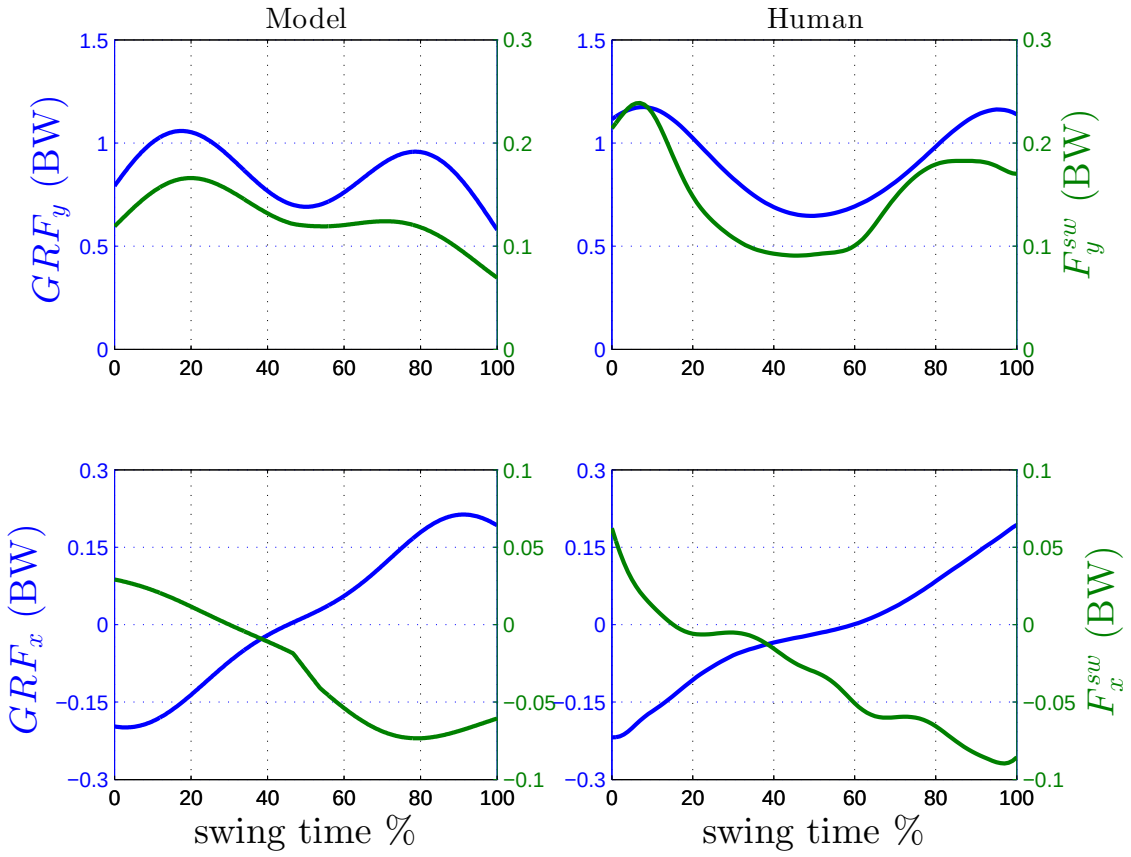

Figure 8: Swing leg force contribution to GRF during walking (at 1.55m/s) for the model and humans. Subscripts x and y denote the force in vertical and horizontal directions and superscript *sw* stands for swing leg force. All forces are normalized by body weight (BW). The experimental data is the average value for nine subjects.

BioBiped 3) and future assistive devices (e.g. prosthetic or orthotic systems and exoskelettons). For this, the proposed model needs to be extended to the whole gait including stance and swing phase. In that respect, application of this method in swing leg adjustment of the BioBiped robot in forward hopping was tested using the detailed simulation model of the robot (Sharbafi et al., 2016). This was the first step of implementing the proposed design and control on a complete detailed gait model. The same approach can be implemented for other gaits.

The compliantly tuned segmented swing leg (DPS model) establishes a novel template model for a mechanical pattern generator (MPG) for the swing leg. This pattern generator complements the previously identified mechanical pattern generators described as spring-mass system (SLIP model, (Blickhan, 1989)) for COM gait pattern generation and as a virtual pendulum (VPP model, (Maus et al., 2010)) for upright body balance. Future research will need to show how these three MPGs can work together in different gaits (e.g. walking, running) and different gait conditions (e.g. step length, uneven terrain). As all three MPGs are harmonic oscillators, they result in similar motion patterns. Theses patterns need to be controlled though modulated muscle activity. This could either be realized by central pattern generators (CPG, (Ijspeert, 2008)) or based on reflexes ((Geyer et al., 2003)). The individual contributions of these neural circuits (CPGs vs. reflexes) in the generation of the three identified MPGs are not yet well understood and awaits for future research.

5.5 APPENDIX

5.5.1 Mathematical model of DPS

In order to find the dynamic equations of the DPS model shown in Fig.1, we first calculate the potential (P) and kinetic (K) energy of the system which are used to find the Lagrangian ($L = K - P$)

$$\frac{d}{dt}(\frac{\partial L}{\partial \dot{q}}) - \frac{\partial L}{\partial q} = 0 \tag{11}$$

Here we consider the leg spring and biarticular springs as external source of force and torques, which determine the effective force vector BF. Defining total mass $M = m + m_1 + m_2$, $M' = (m_1 l_1 + m_2 L_1)$, J_1 and J_2 as thigh and shank inertia (computed from uniform distribution of the mass along the segments), respectively, gravity vector and the inertia and Coriolis matrices are computed as follows:

$$G = \begin{bmatrix} Mg\cos(\theta) \\ -Mgl\sin(\theta) \\ M'g\sin(\varphi) \\ m_2 l_2 g\sin(\sigma) \end{bmatrix} \tag{12}$$

$$D = \begin{bmatrix} M & 0 & M'\sin(\theta_\varphi) & m_2 l_2 \sin(\theta_\sigma) \\ 0 & Ml^2 & M'l\cos(\theta_\varphi) & m_2 l_2 l\cos(\theta_\sigma) \\ M'\sin(\theta_\varphi) & M'l\cos(\theta_\varphi) & (m_1 l_1^2 + m_2 L_1^2 + J_1) & m_2 l_2 L_1 \cos(\varphi - \sigma) \end{bmatrix} \tag{13}$$

$$C = \begin{bmatrix} 0 & -Ml\dot{\theta} & M'\dot{\varphi}\cos(\theta_\varphi) & m_2 l_2 \dot{\sigma}\cos(\theta_\sigma) \\ Ml\dot{\theta} & Ml\dot{l} & M'l\dot{\varphi}\sin(\theta_\varphi) & -m_2 l_2 l\dot{\sigma}\sin(\theta_\sigma) \\ M'\cos(\theta_\varphi)\dot{\theta} & M'\cos(\theta_\varphi)\dot{l} - M'\sin(\theta_\varphi)l\dot{\theta} & 0 & m_2 l_2 L_1 \sin(\varphi - \sigma)\dot{\sigma} \\ m_2 l_2 \cos(\theta_\sigma)\dot{\theta} & m_2 l_2 \cos(\theta_\sigma)\dot{l} - m_2 l_2 l\sin(\theta_\sigma)\dot{\theta} & 0 & -m_2 L_1 l_2 \dot{\varphi}\sin(\varphi - \sigma) \end{bmatrix} \tag{14}$$

$$\begin{aligned} BF &= \begin{bmatrix} K_s max(L_0 - l, 0) \\ 0 \\ K^{RF}(r_h^{RF} - r_k^{RF})max(r_k^{RF}\Delta l^{RF}, 0) - K^{HA}(r_h^{HA} - r_k^{HA})max(r_k^{HA}\Delta l^{HA}, 0) \\ K^{RF} r_k^{RF} max(r_k^{RF}\Delta l^{RF}, 0) - K^{HA} r_k^{HA} max(r_k^{HA}\Delta l^{HA}, 0) \end{bmatrix} \\ &= \begin{bmatrix} F_S \\ 0 \\ \tau_\varphi^{RF} + \tau_\varphi^{HA} \\ \tau_\sigma^{RF} + \tau_\sigma^{HA} \end{bmatrix} \end{aligned} \tag{15}$$

where $\theta_\varphi = \theta + \varphi$, $\theta_\sigma = \theta + \sigma$, r_h^{HA}, r_k^{HA},r_h^{RF}, r_k^{RF}, k^{RF} and k^{HA} are HA and RF lever arm at hip, knee, HA and RF stiffness, respectively.

Bipedal SLIP (BSLIP) as a model for the double support phase and switching conditions between single and double support phases are described hereafter. In the double support phase of the BSLIP model, the body mass (M) is concentrated at the hip, and both legs are modeled as massless springs.

Thus, the double support model can be defined by positions of the hip $[x,\ y]$ and the front leg $[x_f,\ 0]$ with respect to the hind leg, as follows:

$$\begin{cases} M\ddot{x} &= K_s max(L_{0h}-l_h,0)\frac{x}{l_h} + K_s max(L_{0f}-l_f,0)\frac{x-x_f}{l_f} \\ M\ddot{y} &= K_s max(L_{0h}-l_h,0)\frac{y}{l_h} + K_s max(L_{0f}-l_f,0)\frac{y}{l_f} - g \end{cases} \tag{16}$$

Here, subindices $_h$ and $_f$ depict the related parameters for the hind and front legs, respectively.

$$\begin{cases} l_h &= \sqrt{x^2+y^2} \\ l_f &= \sqrt{(x-x_f)^2+y^2} \end{cases} \tag{17}$$

Switching between DPS and BSLIP model is defined using the following constraints:

- positions of the feet and the hip are kept.
- Total mass is fixed.
- speed vector at hip is kept.
- The system total energy is kept.

Switching from DPS to BSLIP:

$$\begin{cases} x &= l\sin(\theta) \\ y &= l\cos(\theta) \\ x_f &= l\sin(\theta) + L_1\sin(\varphi) - L_2\sin(\sigma) \\ \dot{x} &= \dot{l}\sin(\theta) + l\dot{\theta}\cos(\theta) \\ \dot{y} &= \dot{l}\cos(\theta) - l\dot{\theta}\sin(\theta) \end{cases} \tag{18}$$

L_{0f} is set to the stance leg rest length of the DPS model and L_{0h} is calculated such that the total energy does not change with switching the model.

Switching from BSLIP to DPS: For the DPS model,

$$\begin{cases} l &= \sqrt{(x-x_f)^2+y^2} \\ \theta &= \arctan(\frac{x-x_f}{y}) \\ \varphi &= \arccos(\frac{L_{0h}^2+L_1^2-L_2^2}{2L_1L_{0h}}) - \gamma \\ \sigma &= \arccos(\frac{y-L_1\cos(\varphi)}{L_2}) \end{cases} \tag{19}$$

in which $\gamma = \arctan(\frac{x}{y})$ is the hind leg angle. The (angular) speeds are computed by differentiation from (19) with the additional constraint of keeping the system energy constant.

5.6 ACKNOWLEDGMENT

This research was supported in part by the German Research Foundation (DFG) under grants No. SE1042/8 and in part by the EU project BALANCE under Grant Agreement No. 601003.

5.7 AUTHOR CONTRIBUTIONS

Maziar A. Sharbafi was responsible for the conception and design of simulations, analysis and interpretation of data and writing of the manuscript. Aida Mohammadinejad Rashty provided all simulations, data analysis and interpretation of results. She has also contributed in writing the paper. Christian Rode participated in providing the research structure, discussions and partially supervision of the work. He has also a large contribution in writing and revising the paper and discussions. Andre Seyfarth was supervising the research and also supported writing and revision of the article.

5.8 REFERENCES

Alexander, R. M. (1976). Mechanics of bipedal locomotion. *Perspectives in experimental biology*, 1:493–504.

Blickhan, R. (1989). The spring-mass model for running and hopping. *Journal of Biomechanics*, 22(11):1217–1227.

Cavagna, G. and Margaria, R. (1966). Mechanics of walking. *Journal of Applied Physiology*, 21(1):271–278.

Cavagna, G., Saibene, F., and Margaria, R. (1963). External work in walking. *Journal of Applied Physiology*, 18(1):1–9.

Desai, R. and Geyer., H. (2013). Muscle-reflex control of robust swing leg placement. In *IEEE International Conference on Robotics and Automation, (ICRA 2013)*.

Full, R. J. and Koditschek, D. (1999). Templates and anchors: Neuromechanical hypotheses of legged locomotion on land. *Journal of Experimental Biology*, 22:3325–3332.

Geyer, H. and Herr, H. (2010). A muscle-reflex model that encodes principles of legged mechanics produces human walking dynamics and muscle activities. *IEEE Transactions on Neural Systems and Rehabilitation Engineering*, 18(3):263 – 273.

Geyer, H., Seyfarth, A., and Blickhan, R. (2003). Positive force feedback in bouncing gaits? *Proceedings of the Royal Society of London B: Biological Sciences*, 270(1529):2173–2183.

Geyer, H., Seyfarth, A., and Blickhan, R. (2006). Compliant leg behaviour explains basic dynamics of walking and running. *Proc. Roy. Soc. B*, 273(1603):2861–2867.

Hemami, H. and Golliday, C. L. (1977). The inverted pendulum and biped stability. *Mathematical Biosciences*, 34(1):95–110.

Ijspeert, A. J. (2008). Central pattern generators for locomotion control in animals and robots: a review. *Neural Networks*, 21(4):642–653.

Isidori, A. (1995). *Nonlinear Control Systems*. Springer-Verlag, Berlin, 3 edition.

Knuesel, H., Geyer, H., and Seyfarth, A. (2005). Influence of swing leg movement on running stability. *Human Movement Science*, 24:532–543.

Kuo, A. D. (2007). The six determinants of gait and the inverted pendulum analogy: A dynamic walking perspective. *Human Movement Science*, 26(4):617–656.

Lipfert, S. W. (2010). *Kinematic and dynamic similarities between walking and running*. Verlag Dr. kovac, Hamburg Germany.

Loram, I. D. and Lakie, M. (2002). Direct measurement of human ankle stiffness during quiet standing: the intrinsic mechanical stiffness is insufficient for stability. *The journal of physiology*, 545(3):1041–1053.

Maus, H. M., Lipfert, S., Gross, M., Rummel, J., and Seyfarth, A. (2010). Upright human gait did not provide a major mechanical challenge for our ancestors. *Nature Communications*, 1(6):1–6.

Maykranz, D. and Seyfarth, A. (2014). Compliant ankle function results in landing-take off asymmetry in legged locomotion. *Journal of theoretical biology*, 349:44–49.

Mochon, S. and McMahon, T. A. (1980). Ballistic walking. *Journal of Biomechanics*, 13:49 – 75.

Müller, R. and Blickhan, R. (2010). Running on uneven ground: leg adjustments to altered ground level. *Human movement science*, 29(4):578–589.

Nilsson, J., Thorstensson, A., and Halbertsma, J. (1985). Changes in leg movements and muscle activity with speed of locomotion and mode of progression in humans. *Acta Physiologica Scandinavica*, 123(4):457–475.

OĆonnor, S. M. (2009). *The Relative Roles of Dynamics and Control in Bipedal Locomotion*. PhD thesis, University of Michigan.

Poggensee, K. L., Sharbafi, M. A., and Seyfarth, A. (2014). Characterizing swing-leg retraction in human locomotion. In *International Conference on Climbing and Walking Robots (CLAWAR 2014)*.

Prilutsky, B. I., Gregor, R. J., and Ryan, M. M. (1998). Coordination of two-joint rectus femoris and hamstrings during the swing phase of human walking and running. *Experimental Brain Research*, 120(4):479–486.

Seipel, J. and Holmes, P. (2005). Running in three dimensions: Analysis of a point-mass sprung-leg model. *The International Journal of Robotics Research*, 24(8):657–674.

Seyfarth, A., Geyer, H., Guenther, M., and Blickhan, R. (2002). A movement criterion for running. *Journal of Biomechanics*, 35(5):649–655.

Sharbafi, M. A., Rode, C., Scholz, S. K. D., Moeckel, R., Radkhah, K., von Stryk, G. Z. A. M. O., and Seyfarth, A. (2016). A new biarticular actuator design facilitates control of leg function in biobiped3. *Bioinspiration & Biomimetics*, 11(4):046003.

Vejdani, H. R., Blum, Y., Daley, M. A., and Hurst, J. W. (2013). Bio-inspired swing leg control for spring-mass robots running on ground with unexpected height disturbance. *Bioinspiration & biomimetics*, 8(4):046006.

Winter, D. A. (2005). *BioMechanics and motor control of human movement*. John Wiley & Sons, Inc, New Jersy, USA, 3 edition.

Wisse, M., Atkeson, C. G., and Kloimwieder, D. K. (2006). *Dynamic stability of a simple biped walking system with swing leg retraction*. Springer Berlin Heidelberg.

Zhao, G. and Seyfarth, A. (2015). Contributions of stance and swing leg movements to human walking dynamics. In *submitted to the International Conference on Climbing and Walking Robots (CLAWAR)*, pages 4868–4875. IEEE.

6 Article V: Hopping control for the musculoskeletal bipedal robot: BioBiped

Authors:

Maziar Ahmad Sharbafi Katayon Radkhah, Oskar von Stryk and André Seyfarth

Technische Universität Darmstadt

64289 Darmstadt, Germany

Published as a paper at the

2014 IEEE/RSJ International Conference on Intelligent Robots and Systems (IROS)

ABSTRACT

Bipedal locomotion can be divided into primitive tasks, namely repulsive leg behavior (bouncing against gravity), leg swing (protraction and retraction) and body alignment (balancing against gravity). In the bipedal spring-mass model for walking and running, the repulsive leg function is described by a linear prismatic spring. This paper adopts two strategies for swinging and bouncing control from conceptual models for the human-inspired musculoskeletal BioBiped robot. The control approach consists of two layers, velocity based leg adjustment (VBLA) and virtual model control to represent a virtual springy leg between toe and hip. Additionally, the rest length and stiffness of the virtual springy leg are tuned based on events to compensate energy losses due to damping. In order to mimic human locomotion, the trunk is held upright by physical constraints. The controller is implemented on the validated detailed simulation model of BioBiped. In-place as well as forward hopping and switching between these two gaits are easily achieved by tuning the parameters for the leg adjustment, virtual leg stiffness and injected energy. Furthermore, it is shown that the achieved motion performance of in-place hopping agrees well with that of human subjects.

6.1 INTRODUCTION

Robots can help to demonstrate and prove concepts on human locomotion such as concepts based on springlike leg behavior. Starting from simple models, hopping is a simple 1D motion which can be described with the SLIP (Spring Loaded Inverted Pendulum) model (Blickhan, 1989). Then, a first basic mechanical function in human locomotion is rebounding on compliant legs, which can be described by a leg spring like running (Seyfarth et al., 2002) and walking (Geyer et al., 2006).

Simple conceptual models, coined “templates” (Full and Koditschek, 1999) have proved to be very helpful for describing and analyzing legged locomotion. In that respect, developing bipedal robots based on human morphology and locomotion can be inspired by these simple models (Raibert, 1986)(Saranlıet al., 2001), in spite of their high level of abstraction. Another interesting property of the SLIP is its asymptotic stability against perturbations conserving energy, even with a constant angle of attack (Seyfarth et al., 2002).

In (Pratt, 2000), Pratt presented the Virtual Model Control (VMC) approach to create virtual forces when the virtual components interact with a robot system (Pratt et al., 2001). Due to the complexity of the robots and, of course humans, the implementation of stabilizing strategies is a challenge. However, fundamental strategies to gain stability can be deduced from very simple models. Hence, in this paper VMC is employed to represent a virtual spring between toe and hip in order to resemble the SLIP model.

The second control level, which is needed when the motion is planar instead of 1D, is leg adjustment. Unlike running (Seyfarth et al., 2002) and walking (Geyer et al., 2006), stable hopping in 2D cannot be achieved with a fixed angle of attack with respect to the ground. So, to recover from any perturbation, a robust method to find the appropriate leg direction during the flight phase is necessary for hopping in place. In literature, the leg adjustment strategies are mostly following the Raibert approach (Raibert, 1986) in which the foot landing position is adjusted based on the horizontal velocity (e.g. (Sato, 2004)(Poulakakis and Grizzle, 2009)). Recently, Peuker et al. (Peuker et al., 2012) investigated different strategies and showed that applying both CoM velocity and gravity vectors result in very robust hopping and running with SLIP model. In this paper we utilized Velocity Based Leg Adjustment (VBLA) introduced in (Sharbafi et al., 2012) which is an improved version of Peuker’s approach(Peuker et al., 2012).

Further, hip springs support faster steps and accelerate swing leg motion (Kuo, 2002)(Hobbelen and Wisse, 2007). The latter effect may equally be achieved by implementing elastic tendons between the upper body and the legs (Kuo, 2007). The compliant coupling of the upper body and legs is also existent

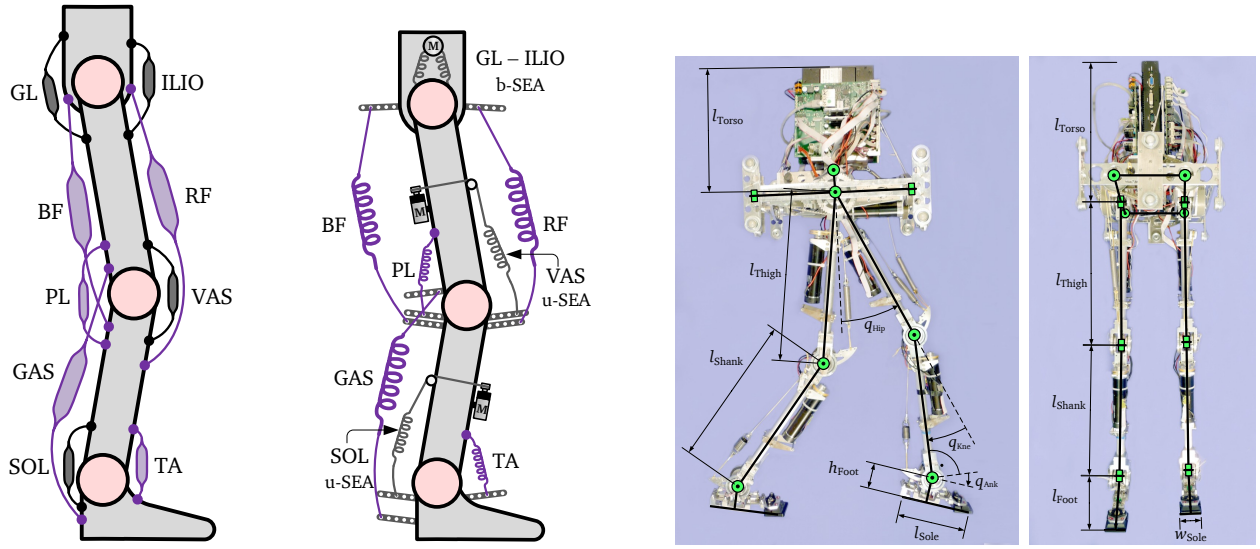

(a) (b) (c)

Figure 1: Technical realization of BioBiped1 and its actuation from left to right: (a) Essential human muscle groups during locomotion: Actuated tendons are indicated by dark grey color, while passive tendons are marked in purple; (b) constructed version of BioBiped1's actuation with u-SEA and b-SEA denoting a unidirectional and bidirectional series elastic actuator, respectively (Radkhah et al., 2012); (c) real robot platform with its main kinematic and dynamic parameters given in Table 1. Pictures are taken from (Radkhah, 2014).

in the human body, e.g the Rectus femoris and Hamstring muscles (see Fig.1a). We also have implemented these biarticular muscles in the BioBiped robot which is our test bed for evaluating the control approaches.

From (Maus et al., 2010), it is concluded that upright trunk is a key feature for human locomotion. Because of the robot limitations, balancing is not considered in this paper. Thus, we keep the trunk upright by some constraining mechanisms. Implementing a proper posture control strategy like VPP (Maus et al., 2010) is targeted with a redesigned robot.

In this study, a controller which is designed based on template models is presented for hopping in place and forward hopping just with tuning a few parameters. This controller is applied to BioBiped, a biologically inspired, musculoskeletal bipedal robot consisting two 3-segmented legs and a rigid trunk that can tilt for- and backwards as shown in Fig. 1c. Projection of the robot model on the conceptual model, designing the controller for the simplified model and extending it to the complex model are different steps of the proposed control approach. Energy management via event based control, leg adjustment and position control construct different parts of the controller. Similarity of the robot structure and controlled motion to humans and changing the hopping speed with leg angle adjustment and energy compensation just with tuning few parameters are the main contributions in this paper. The results from a detailed simulation model of the robot show the performance of the proposed method. The comparison with human hopping in place which help to improve the robot structure in the next generations[15] toward designing a controlled robot mimicking human locomotion.

6.2 METHODS

[15] Two versions of BioBipeds were already manufactured and BioBiped III is in the designing step.

Table 1: Main kinematics and dynamics data of the BioBiped1 robot.

Dimensions and Masses	
Segment lengths	$l_{Torso} = 269\,\text{mm}$; $l_{Thigh} = 330\,\text{mm}$; $l_{Shank} = 330\,\text{mm}$; $l_{Foot} = 122\,\text{mm}$
Foot dimensions	$h_{Foot} = 67\,\text{mm}$; $l_{Sole} = 165\,\text{mm}$; $w_{Sole} = 40\,\text{mm}$
Leg length	0.727 m (from hip to sole with extended leg)
Segment masses	$m_{Torso} = 5.332\,\text{kg}$; $m_{Thigh} = 0.843\,\text{kg}$; $m_{Shank} = 0.804\,\text{kg}$; $m_{Foot} = 0.342\,\text{kg}$
Total mass	$\sim 9.2\,\text{kg}$ (the CoM is located at $\sim 0.14\,\text{m}$ above the hip joint)

6.2.1 Simulation Model

The BioBiped1 robot, built within the BioBiped project[16], represents a biologically inspired robot featuring a highly compliant actuation system (Radkhah et al., 2011). It is about 1.1 m tall in extended position with the body mass of 10 kg. For the main kinematics and dynamics data we refer to Table 1. Both legs have rotational degrees of freedom (DoF), one in hip, knee and ankle joint along the pitch axis.

6.2.2 Actuation concept and its technical realization

BioBiped's actuation is inspired by the human musculoskeletal system, in which monoarticular and biarticular muscles, i.e. muscles that span two joints, work together (Radkhah et al., 2011). In Fig. 1a we have depicted nine muscle groups mainly acting in sagittal plane during human locomotion. The monoarticular muscles contribute to the task of power generation (Gregoire et al., 1984). Each joint is coupled to a pair of monoarticular muscles: *I*liopsoas (ILIO) - *G*luteus Maximus (GL) in the hip, *P*opliteus (PL) - *V*astus lateralis (VAS) in the knee and *T*ibilias anterior (TA) - *S*oleus (SOL) in the ankle for the respective flexion and extension. The biarticular muscles are known to transfer energy from proximal to distal joints and to synchronize joint function of hip, knee and ankle (Jacobs et al., 1996). The muscles *R*ectus femoris (RF) and *B*iceps Femoris (BF) cross both the hip and knee joint. While RF acts as combined knee extensor and hip flexor, BF behaves exactly the other way. The knee and ankle joints are coupled by the *G*astrocnemius (GAS).

As for the technical realization, all the biarticular and monoarticular flexing muscles are represented as passive tendons with a built-in extension spring, i.e. they act completely passively based on the actual joint configurations and external forces. All other muscles, the pair in the hip as well as the knee and ankle extensors, are actively integrated. A bidirectional series elastic actuator connecting the hip joint to the motor via a timing belt supports actively both the flexion and extension. In the knee and ankle the geared electric motors are coupled to the joints by an elastic tendon consisting of a Dyneema tendon with built-in spring. For attaching the tendons at the joints several different attachment points are available. This leg actuation concept introduces varying lever arms and transmission ratios aside from highly nonlinear joint torques and stiffnesses.

[16] See the project page `http:\www.biobiped.de`

The geared rotary electric direct-current motors were appropriately selected prior to the robot's construction using a model-based motion generation and control method (Radkhah and von Stryk, 2011). For more details regarding the actuation decisions we refer to (Radkhah et al., 2011).

6.2.3 Detailed physical modeling and simulation

A detailed simulation model of the real robot was developed in order to efficiently design and test different control strategies prior to direct experimentation on the real robot. The simulation model was developed in MATLAB with Simulink and SimMechanics using object-oriented design to ease the analyses and data management (Lens et al., 2011). The multi-body system (MBS) dynamics model contains the rigid whole-body structure and the actuation dynamics. These two levels are consistently connected by the corresponding transmitted torques. Additionally, a detailed ground contact model considering collision, friction and stiction force is included to simulate realistic ground reaction forces with high time-resolution within reasonable computational time (Lens et al., 2011). The rigid body dynamics of the robot consists of a torso and two 3-joint-link serial chains representing the legs that are attached to the torso. The simulation of the generated SimMechanics model is performed by means of a single numerical solver provided by Simulink, without model switching to enable the analysis of impact peak forces and the simulation of flight phases. For the main kinematics and dynamics data of the rigid skeleton we refer to Table 1. The highly complex dynamics models of the active and passive monoarticular tendons were derived from the classical mechanical principle of virtual displacement and work to determine the motor and joint torques, the nonlinearly changing lever arms and transmission stiffnesses of the tendons (Radkhah et al., 2012). All models including the full MBS dynamics model and the realistic ground contact model were experimentally validated and shown to match the behavior of the real robot.

6.2.4 Control Approaches

The controller performs different tasks to the joints' actuators during stance and flight. According to human hopping in place, the main source of energy injection is the ankle joint, and knee and hip joints do not move considerably (Lipfert., 2010). Thus, the duty of knee and hip joints is setting the joints' angles to adjust the leg during flight phase and tracking the desired configuration during stance.

Bouncing via approximated VMC:

By simplification of the robot model with segmented leg to the SLIP model, we try to produce similar leg behavior during stance phase. Defining a virtual leg from hip to foot tip, the leg motion can be described by its angle and length (see Fig. 2). In SLIP model, the leg force is produced by $F_s = k_s(l - l_0)$, in which k_s, l and l_0 are the leg stiffness, length and rest length, respectively.

Suppose that the angle between the foot and the virtual leg direction remains about constant[17]. Then, in order to produce leg force similar to SLIP ankle torque needs to be proportional to F_s during the stance phase $\tau = k(l - l_0)$, where k, l and l_0 are the stiffness, leg length and rest length of the virtual leg. With this ankle torque, an approximation of the Virtual Model Controller is realized which turns the leg model close to SLIP. The virtual leg length l is estimated using the joint angles.

In the real robot, damping exists which should be compensated during stance phase. In our controller, the virtual leg rest length and stiffness are changed at mid-stance moment. With this technique, the leg force (respectively, ankle joint torque) remains continuous, while the stored energy increases. In the E-

[17] This assumption is verified later in the results and the angles' definitions are explained more in Sec.8.2.2.

SLIP model (Ludwig et al., 2012), it was shown that to add a specific amount of energy ΔE at mid stance moment, stiffness and rest length should change as follows:

$$l_0^{new} = \frac{2\Delta E}{k^{old}(l - l_0^{old})} \tag{1}$$

$$k^{new} = \frac{k^{old}(l - l_0^{old})}{(l - l_0^{new})} \tag{2}$$

With these new values, the energy losses are compensated and stable motion can be generated. Without energy compensation, the system will loose energy and fall. Although the amount of lost energy is not known, with this energy compensation approach, it converges to a new equilibrium point. The initial value of leg rest length is computed by the virtual leg length with desired leg configuration, at the first touch down moment. For leg stiffness, the initial value k_0 is set by the designer. We consider a range adopted from human leg stiffness (Farley and Morgenroth, 1999) which is scaled by weight ratio of human to robot and results in $500 < k_0 < 3500$.

Leg adjustment during the swing phase:

As mentioned before, in (Peuker et al., 2012) a new leg placement strategy was presented as the a robust and stable approach for hopping and running motions with the SLIP model. In this approach the angle between the CoM velocity and the gravity vectors are employed to determine the desired leg angle. Hence, increasing the CoM velocity without changing the direction of this vector never changes the desired leg angle which is the main drawback of this method. In (Sharbafi et al., 2012), to solve this problem, a modified version of this strategy was introduced as:

$$\begin{aligned} \vec{V} &= [v_x, v_y]^T \; ; \; \vec{G} = [0, -g]^T \\ \vec{O} &= \mu \vec{V} + (1 - \mu)\vec{G} \end{aligned} \tag{3}$$

in which the leg direction is given by vector $\vec{O}$, a weighted average of the CoM velocity vector $\vec{V}$ and the gravity vector $\vec{G}$ (See Fig. 3a). The weight of each vector is determined by coefficient $0 < \mu < 1$. When $\mu = 1$, the leg is parallel to the CoM velocity vector and, for $\mu = 0$, the leg is exactly vertical. In the rest of the paper, we will refer to this strategy as the Velocity-Based Leg Adjustment VBLA. Unlike Peuker's approach which considers the angle of velocity vector, in VBLA, using both magnitude and angle of the velocity vector increase the robustness of the method against high perturbations.

The advantages of the new method are shown for running and hopping with SLIP model (Sharbafi et al., 2013b). Its similarity to human hopping strategy in coping with perturbation was shown in (Sharbafi and Seyfarth, 2013). With this approach, running in a large range of velocities can be obtained. During flight phase, the desired knee and ankle angles are set to fixed values which are determined beforehand. The leg angle (α) is obtained by $\alpha' + \delta$ as shown in Fig. 3b. Since during motion δ does not considerably change, this is approximated by the following equation.

$$\bar{\alpha} = \varphi_1 + \frac{\varphi_2}{2} + \delta_0 \tag{4}$$

Here, δ_0 is a fixed value to approximate δ in Fig. 3b which is set to 10° in the rest of this paper and the remaining part equals to α'. Therefore, the leg angle is adjusted using hip actuator. At each instance, the desired leg angle is computed via Eq. (3) and by measuring knee angle φ_2, the desired hip angle (φ_h) is given by

$$\varphi_h = tan^{-1}(\frac{O_y}{O_x}) - \frac{\varphi_2}{2}. \tag{5}$$

Finally, other target angles are set to fixed values and position control is obtained using PD controllers.

Balancing, locomotion with upright trunk':

Upright upper body is a crucial aspect of human/animal locomotion (Maus et al., 2010). Balancing the trunk is an important elementary task in legged locomotion. In this paper, due to design limitations of the robot the trunk is kept upright via a constraining mechanism. This is because of low inertial (short distance between hip and trunk CoM) of the trunk with respect to the legs. This will be resolved in the next generation of Bio-Biped robot. However, in the rest of the paper, we consider upright trunk, which is satisfied by physical constraints. Therefore the trunk can move in sagittal plane, but cannot rotate. This is in the same direction with our hopping experiments on a fixed or moving treadmill with BioBiped robot whose trunk is constrained with a frame preventing rotation[18]. This is the intermediate step to do freely hopping on treadmill.

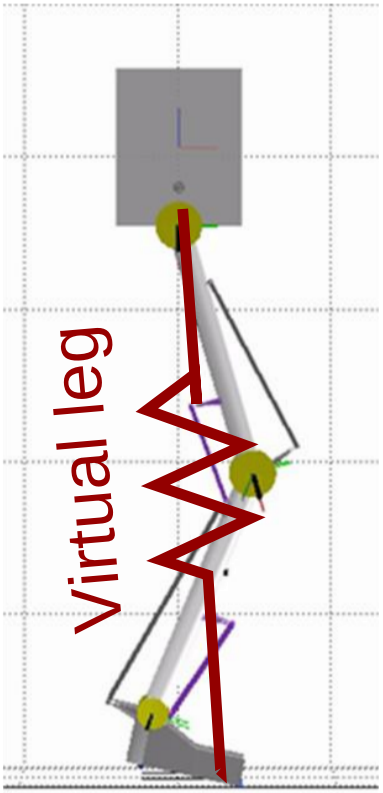

Figure 2: The musculoskeletal leg is represented by a virtual leg from hip to foot tip.

6.2.5 Human Hopping Experiment

Since BioBiped is a bio-inspired robot, comparison with human hopping is helpful to improve the future generations of this robot and also can show how close we are in design and control to produce gaits compared to humans' gaits. We have done hopping experiments with 6 different subjects with body masses between 61 kg and 84 kg and heights between 1.60 m and 1.85 m. The task was hopping in place and kinematic data and force data were measured by a Qualisys motion capture system and a Kistler force plate, respectively. Each experiment takes 30 seconds, starting with 5 seconds standing, 20 seconds hopping and finishing with 5 seconds standing. With the kinematic data we estimated leg angle and leg length from 5^{th} metatarsal joint (the joint at the smallest toe) and trochanter (hip point) markers. Center of mass is also estimated by integrating twice ground reaction forces with initial position and velocity of sacrum (Gard et al., 2004).

6.3 RESULTS

With the controller presented in the previous section, not only hopping in place and forward bipedal hopping can be produced, but also switching from one task to another is possible. With respect to specific initial conditions, Changing μ, virtual leg stiffness and injected energy ΔE result in different gaits. The simulation starts from apex point in which the robot falls down with zero vertical velocity and the initial conditions include leg desired configuration, initial hopping height and horizontal velocity.

In the first experiment, the motion starts with zero horizontal velocity, hopping height equal to 20 cm, $\mu = 0.82$, $k_0 = 2000\ N/m$ and $\Delta E = 5\ J$. Stable hopping in place is achieved as it is shown in Fig. 4.

[18] See `http:\www.biobiped.de` for some videos showing the experimental setup. The control approach in the experiments is different from the proposed approach in this paper.

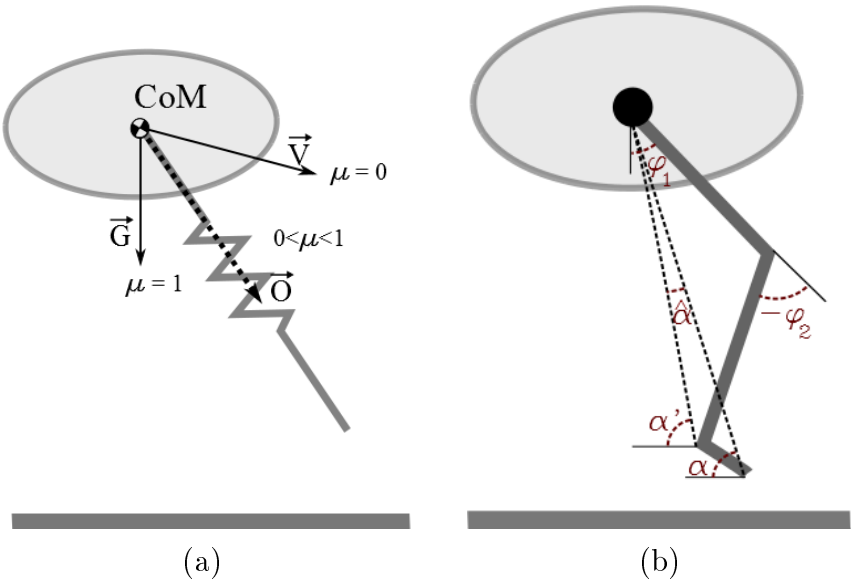

Figure 3: (a) Velocity Based Leg Adjustment. (b) Virtual leg angle estimation in 3-segmented leg.

In this motion, the CoM speed is slightly larger than zero during flight phase which is compensated by a sharp negative peak in stance phase. It is qualitatively similar to human hopping, shown in Fig. 5. The vertical displacement and speed are very similar. In human hopping in place, the horizontal speed is not exactly zero and it might be positive or negative and if the subject hops with closed eyes, he/she cannot keep the hopping point. This phenomena can be seen in Fig. 6, where the CoM position changes during time with different manners for different subjects. The results are comparable to what obtained with BioBiped, in which at each moment reduction in magnitude of CoM speed is important, not returning to the starting position. Different patterns for hopping in place can be produced by changing the aforementioned parameters μ, k_0 and ΔE (see Fig. 6).

In Fig. 7, the leg angle and length are drawn during the gait. The approximation of the leg angle ($\bar{\alpha}$) is very close to the real value. It means that δ in Fig. 3b is almost constant. The same accuracy is observed in all other experiments too. In both human and BioBiped hopping in place, the leg angle starts to decrease after take off and increase to values close to the beginning of the flight phase before touch down. In robot motion the variation is more than it for human hopping. In the stance phase small changes observed in leg angle from beginning to end. In contrary to human motion, the stance phase is shorter in BioBiped hopping.

Considering different leg lengths of human and robot, comparison of the leg length patterns show that they are similar in stance phase. Higher leg length at take off than at touch down shows increasing the leg rest length during stance phase as in (Ludwig et al., 2012). In flight phase, decreasing the length occurs in both cases, with different strategies. In human gait, it shortens moderately, but in robot motion it starts with a sharp drop and then increasing smoothly.

In the next experiment, forward hopping with different horizontal speeds are achieved. Again finding the correct combination of control parameters is the key to reach the desired speed. This makes a trade off between braking with leg adjustment and thrusting via ankle energy injection approach. Fig. 9 shows the results for hopping with 1 m/s. This illustrates the ability of regulating the horizontal speed to a fixed value.

In the last experiment, the robot falls with zero velocity; by adjusting the parameters $\mu = 0.9$, $\Delta E = 20$ and $k_0 = 3000$ switching from hopping in place to forward hopping occurs (See Fig. 10). After 10

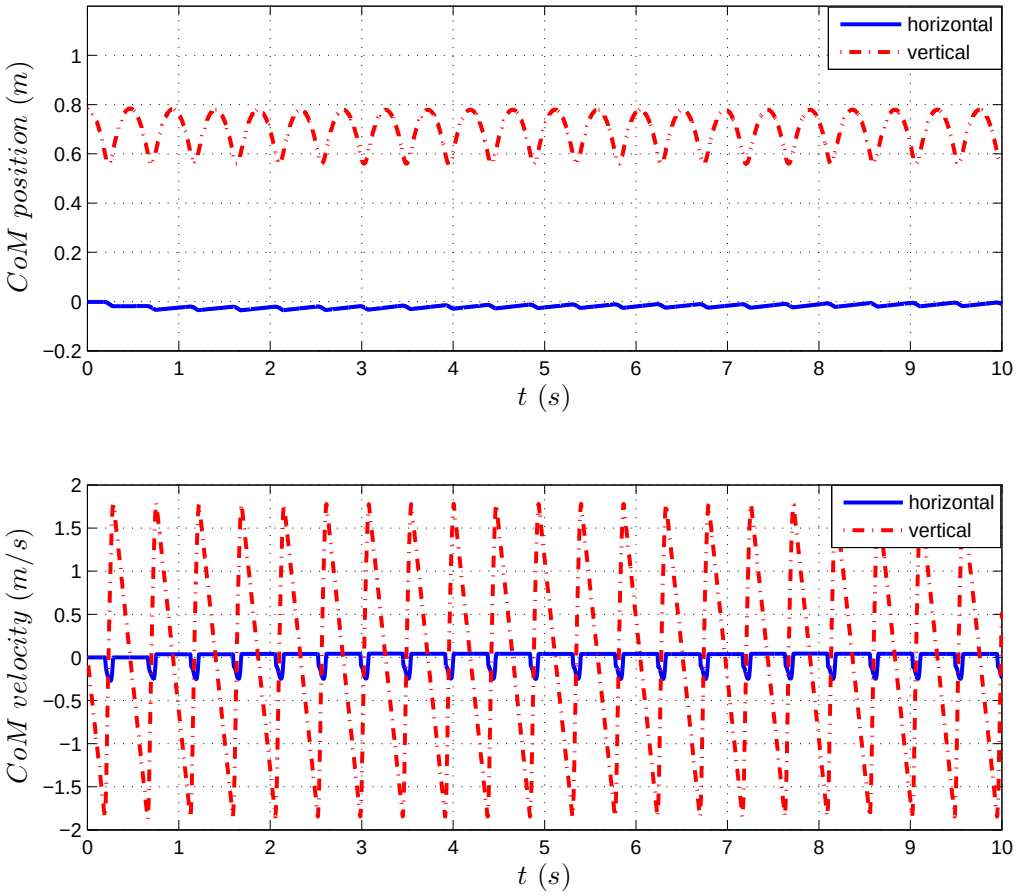

Figure 4: CoM position and velocity for hopping in place with BioBiped.

seconds, reducing leg adjustment coefficient and injected energy to $\mu = 0.75$ and $\Delta E = 1$ results in decreasing system energy and more vertical leg which are needed for hopping with zero speed. The CoM horizontal speed and position illustrate this switching gait. Lower hopping height in the beginning and end of motion shows the lower energy of the system which resulted from smaller ΔE and more vertical leg orientation.

6.4 DISCUSSION

SLIP model based ankle joint torque control with changing stiffness and spring rest length to manage the energy of the system is employed for stance phase of hopping of BioBiped robot. The VBLA is utilized for leg adjustment in flight phase to tune the motion velocity and perturbation attenuation. The other angles are set to predefined values. With this control approach robust hopping is obtained and different speeds can be attained just with tuning the parameters.

With such a simple controller, a set of two leg motions[19] is provided to the BioBiped as a bioinpired robot. Note that the upright trunk configuration is provided by physical constraints (frame). Similarity between human and robot hopping in place is illustrated in the first part of the results. Without visual feedback, zero velocity is not possible for human. Even with open eyes, more that 15 centimeters horizontal deviation from starting point were observed in 10 seconds of the presented experiments. Since the

[19] Moving two legs for forward hopping or hopping in place.

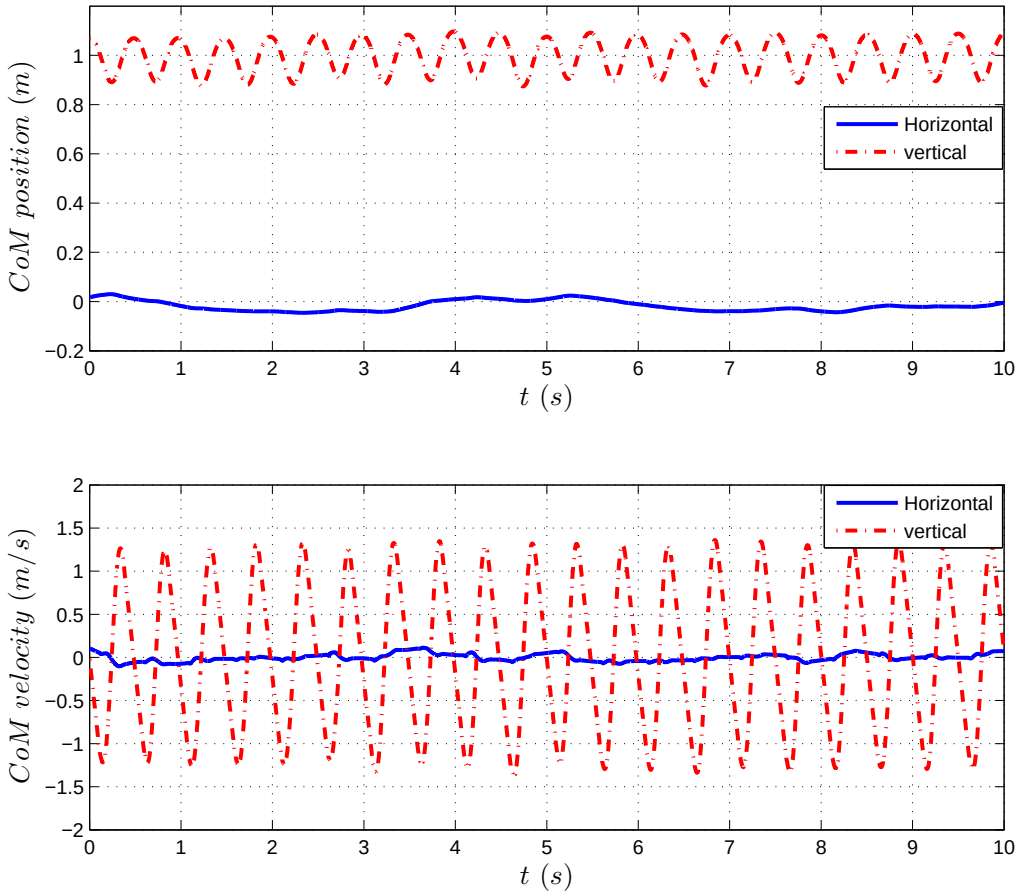

Figure 5: CoM position and velocity for hopping in place of human.

subjects are asked to hop with their preferred height and frequency, different gaits patterns are observed. Changing the gait patterns is easily achieved with varying parameters of the robot controller. It can be concluded that the required information for human hopping is absolutely low. Injecting a fixed amount of energy corresponding to the hopping height and a mechanism to adjust the leg with respect to velocity vector which can be prepared by a mechanical structure are the two basic requirements. In this study, the energy is just added by ankle joint as a push off force, but the knee and even the hip joint can also contribute to distribute the required torque during stance phase. It might yield other hopping patterns changing the stance and flight duration.

The leg behavior including length and angle changes are qualitatively similar between humans and the model predictions. With the stiff leg, considered in Fig. 7, stance phase is shorter than the swing phase. This ratio may be other way around when the leg spring is sufficiently soft. Flight phase duration is mostly related to the hopping height tuned by the injected energy. Therefore, by adjusting the virtual leg stiffness and injected energy, hopping with shorter flight phase and longer stance phase can be achieved. The ration between duration of stance and flight phases is also different depending on the selected human gait, even if they hop with the same frequencies. It depends mostly on how much knee and ankle joints are used to store and return the energy.

The second achievement was producing forward hopping with a constant speed. The results show that if the initial speed is close to the desired ones, sufficient push off ankle torque and appropriate leg angle are provided. This means that the controller requires a proper mapping between the coefficients

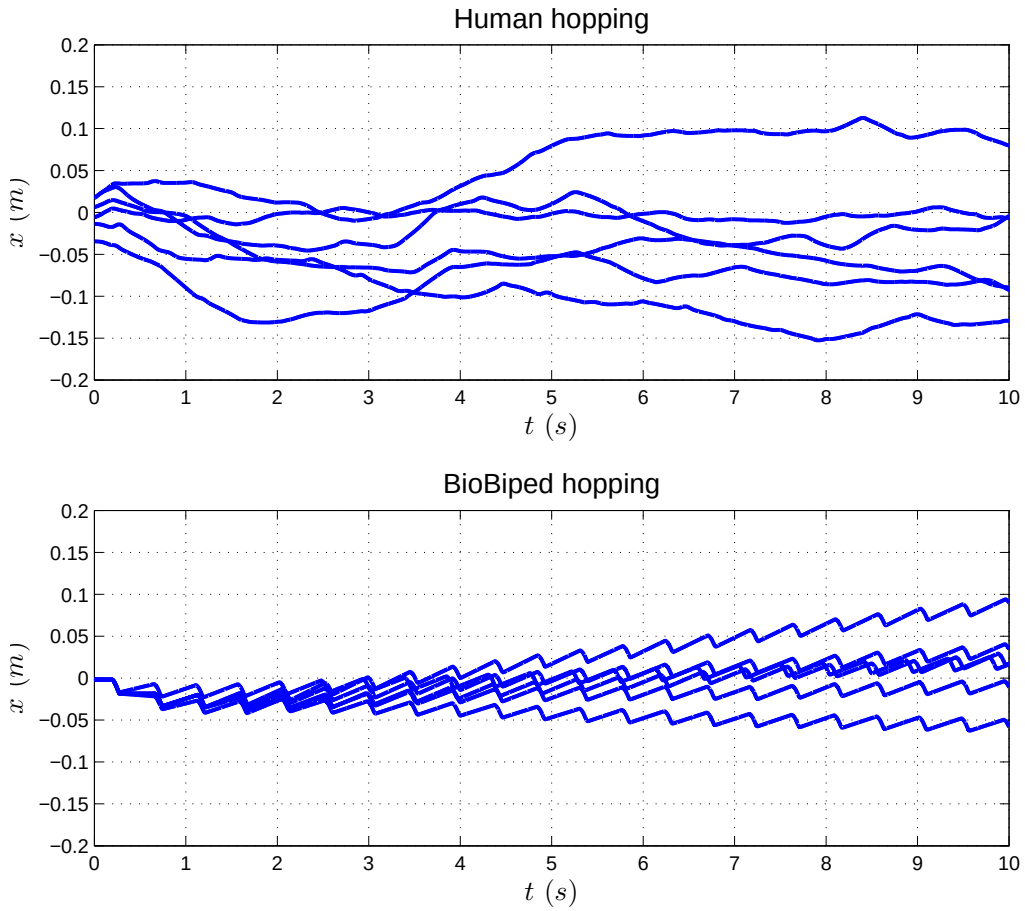

Figure 6: CoM horizontal motion comparison between human and BioBiped. The robot motion patterns change with changing control parameters μ, k_0 and ΔE.

and desired motion. Then, for faster motion, first required to produce sufficient forward speed. Then, by tuning the parameters the new speed can be realized. In other words, changing the fixed point and moving the states inside the basin of attraction of new fixed point can change the gait speed. This approach simplifies the control and the speed when is automatically realized by a correct set of parameters.

Finally, switching between different gait speeds is accomplished based on the aforementioned scheme. Here, we showed that when the states are in the region of attraction of two different fixed points with different parameters and desired speeds, changing the parameters is enough to change the speed. Hence, with changing the parameters you differ the equilibrium solution (it is a limit cycle, which can be represented as a fixed point by using a Poincaré section) from one to another and since the states of the system are placed in the region of attraction of both fixed points, it can easily switch between them by parameter adjustment.

As the next step we aim at implementing the proposed approach to make a stable running or one leg hopping. Trunk stabilization could be achieved with approaches like Virtual Pendulum Posture control (VPPC) in which the torques are produced such that the ground reaction forces are redirected toward the virtual pivot point (VPP) (Maus et al., 2010). This strategy is similar to human and animal locomotion and could be employed for trunk stabilization during stance phase.

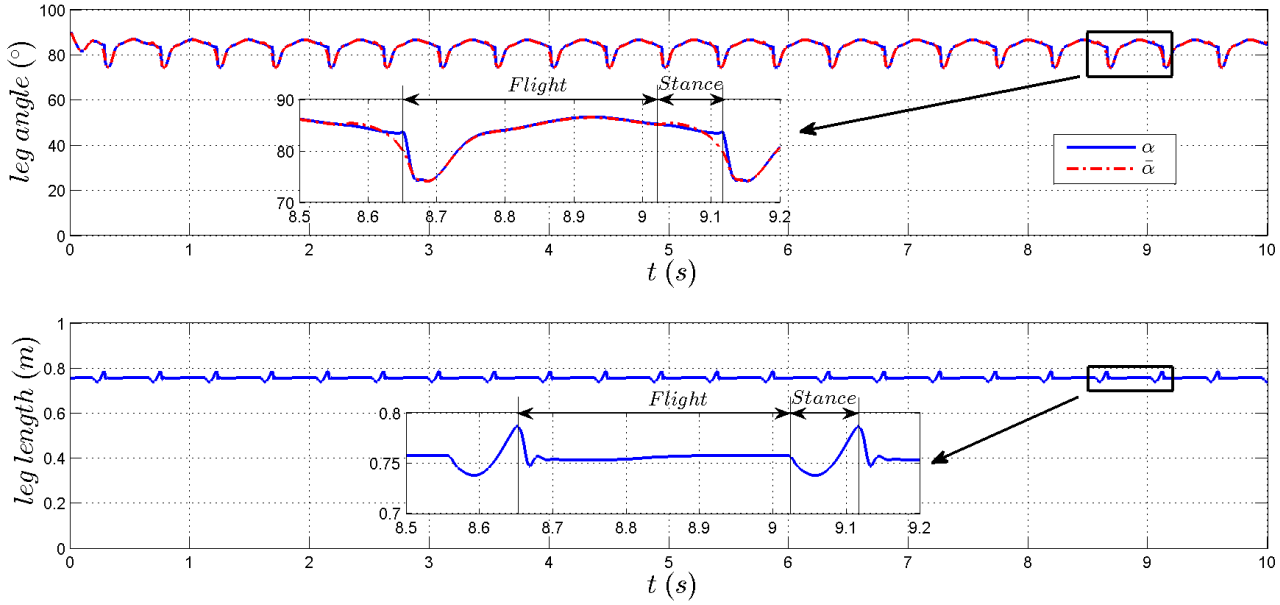

Figure 7: Leg angle and leg lengths for hopping in place of BioBiped robot. Approximation of leg angle which is used for leg adjustment is also shown in top figure.

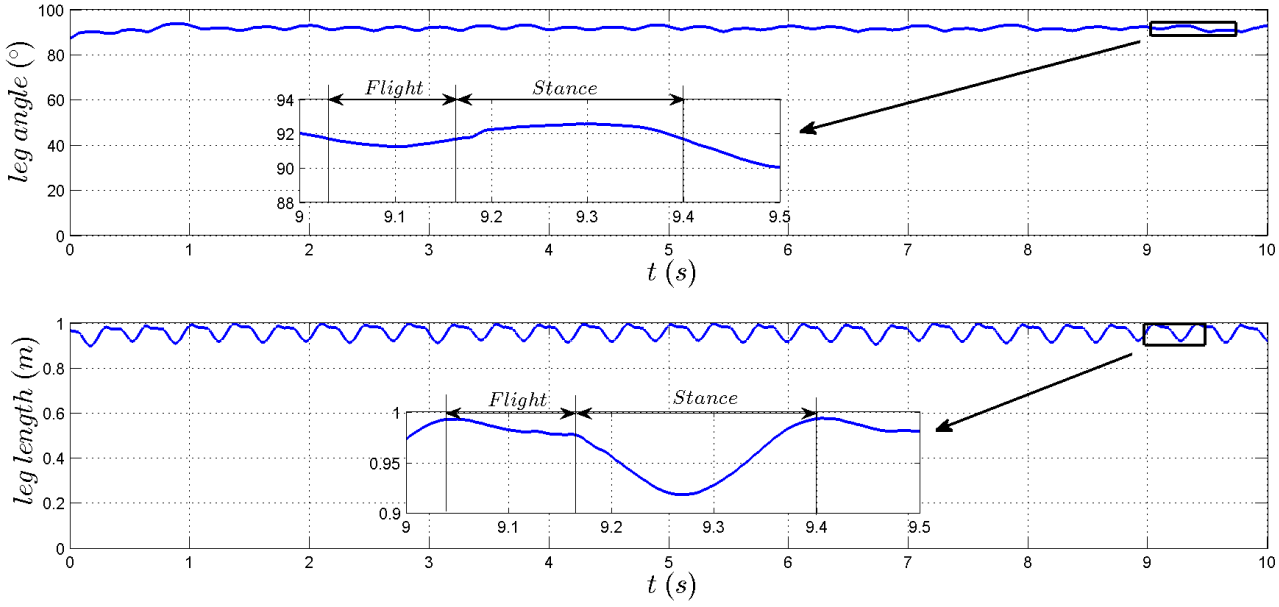

Figure 8: A sample of human leg kinematics in hopping.

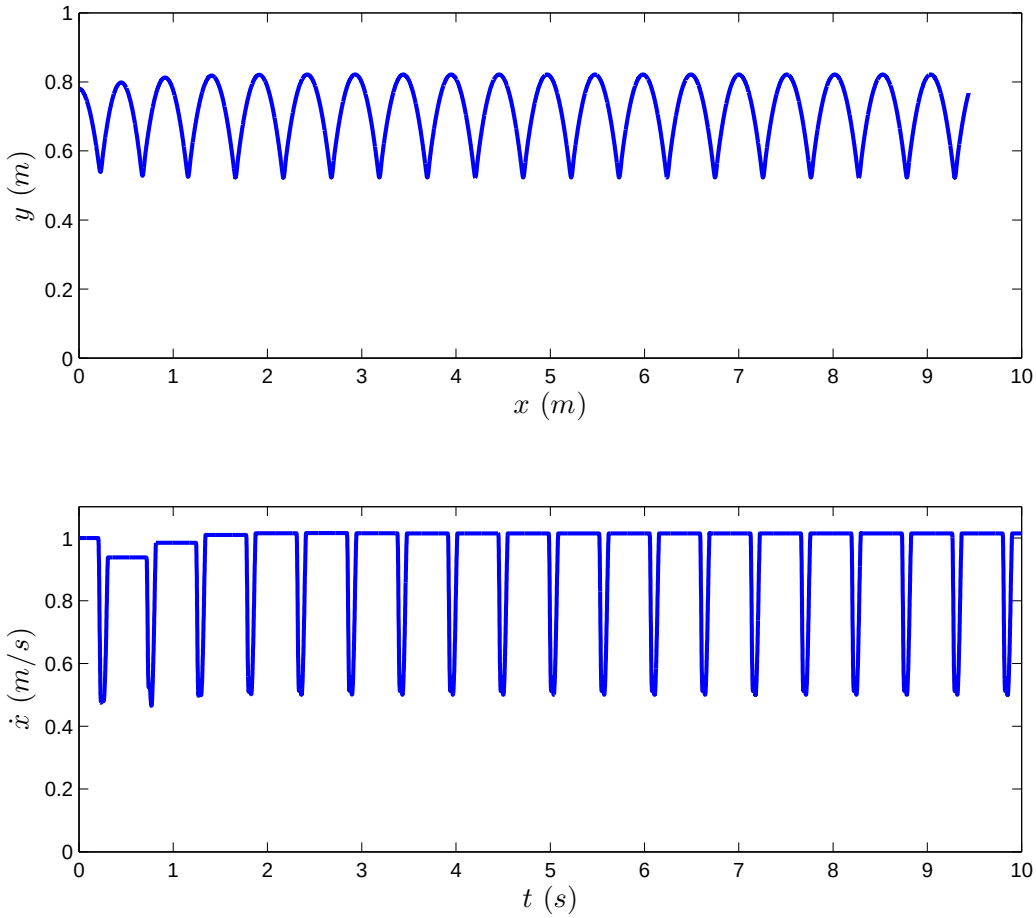

Figure 9: CoM position and velocity in forward hopping of BioBiped.

6.5 ACKNOWLEDGMENT

This research has been supported by the German Research Foundation (DFG) under grants no. SE 1042/6-2.

6.6 AUTHOR CONTRIBUTIONS

Maziar A. Sharbafi is the main and corresponding author of the article. He was responsible for the conception and design of simulations and experiments, analysis and interpretation of data and writing of the manuscript. Katayon Radkhah developed the multi-body simulation model of the robot which was used for forward hopping control. She has partially contributed to the conception and control through successful adaption of control strategies from conceptual models and their validation by a detailed multibody-system dynamics simulation for a version of the musculoskeletal BioBiped robot. She has significantly contributed in writing the paper and discussions. Oskar von Stryk and Andre Seyfarth were the supervisors of the project from the two groups involved in this project and contributed to discussions and commenting writing the article.

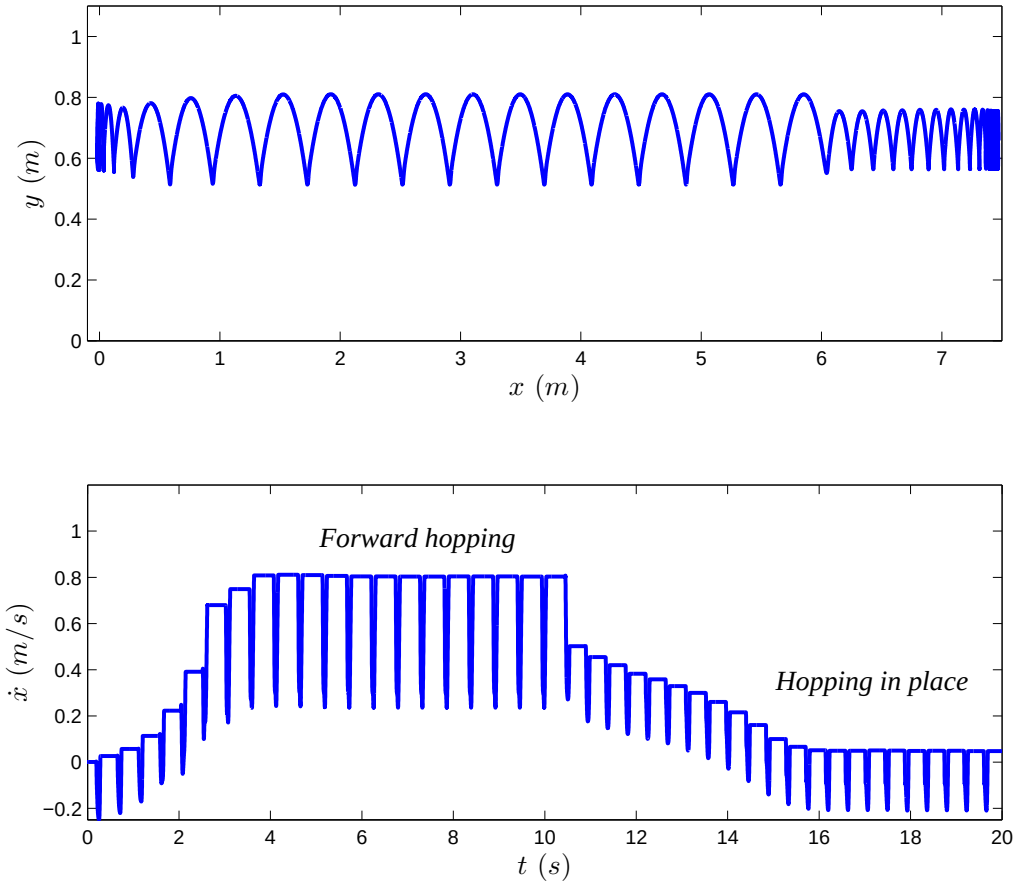

Figure 10: CoM motion and velocity of switching between hopping in place and forward hopping with BioBiped.

6.7 REFERENCES

Blickhan, R. (1989). The spring-mass model for running and hopping. *Journal of Biomechanics*, 22(11):1217–1227.

Farley, C. and Morgenroth, D. (1999). Leg stiffness primarily depends on ankle stiffness during human hopping. *Journal of Biomechanics*, 32:267–273.

Full, R. J. and Koditschek, D. (1999). Templates and anchors: Neuromechanical hypotheses of legged locomotion on land. *Journal of Experimental Biology*, 22:3325–3332.

Gard, S. A., Miff, S. C., and Kuo, A. D. (2004). Comparision of kinematic and kinetic methods for computing the vertical motion of the body center of mass during walking. *Human Movement Science*, 22:597–610.

Geyer, H., Seyfarth, A., and Blickhan, R. (2006). Compliant leg behaviour explains basic dynamics of walking and running. *Proceedings of the Royal Society B*, 273(1603):2861–2867.

Gregoire, L., Veeger, H., Huijing, P., and van Ingen Schenau, G. (1984). Role of mono-and biarticular muscles in explosive movements. *International journal of sports medicine*, 5(06):301–305.

Hobbelen, D. G. E. and Wisse, M. (2007). A disturbance rejection measure for limit cycle walkers: The gait sensitivity norm. *IEEE Transactions on Robotics*, 23(6):1213–1224.

Jacobs, R., Bobbert, M. F., and van Ingen Schenau, G. J. (1996). Mechanical output from individual muscles during explosive leg extensions: The role of biarticular muscles. *Journal of biomechanics*, 29(4):513–523.

Kuo, A. D. (2002). Energetics of actively powered locomotion using the simplest walking model. *Journal of Biomechanical Engineering*, 124:113–120.

Kuo, A. D. (2007). The six determinants of gait and the inverted pendulum analogy: A dynamic walking perspective. *Human Movement Science*, 26(4):617–656.

Lens, T., Radkhah, K., and Von Stryk, O. (2011). Simulation of dynamics and realistic contact forces for manipulators and legged robots with high joint elasticity. In *Advanced Robotics (ICAR), 2011 15th International Conference on*, pages 34–41. IEEE.

Lipfert., S. W. (2010). *Kinematic and dynamic similarities between walking and running*. Verlag Dr. Kovaĉ,.

Ludwig, C., Grimmer, S., Seyfarth, A., and Maus, H. (2012). Multiple-step model-experiment matching allows precise definition of dynamical leg parameters in human running. *Journal of Biomechanics*, 45(14):2472–5.

Maus, H. M., Lipfert, S., Gross, M., Rummel, J., and Seyfarth, A. (2010). Upright human gait did not provide a major mechanical challenge for our ancestors. *Nature Communications*, 1(6):1–6.

Peuker, F., Maufroy, C., and Seyfarth, A. (2012). Leg adjustment strategies for stable running in three dimensions. *Bioinspiration and Biomimetics*, 7(3).

Poulakakis, I. and Grizzle, J. W. (2009). The spring loaded inverted pendulum as the hybrid zero dynamics of an asymmetric hopper. *IEEE Transaction on Automatic Control*, 54(8):1779–1793.

Pratt, J. (2000). *Exploiting Inherent Robustness and Natural Dynamics in the Control of Bipedal Walking Robots*. PhD thesis, Massachusetts Institute of Technology.

Pratt, J. E., Chew, C. M., Torres, A., Dilworth, P., and Pratt, G. (2001). Virtual model control: An intuitive approach for bipedal locomotion. *International Journal of Robotics Research*, 20(2):129–143.

Radkhah, K. (2014). *Advancing musculoskeletal robot design for dynamic and energy-efficient bipedal locomotion*. PhD thesis, Technische Universität.

Radkhah, K., Lens, T., and von Stryk, O. (2012). Detailed dynamics modeling of biobiped's monoarticular and biarticular tendon-driven actuation system. In *Intelligent Robots and Systems (IROS), 2012 IEEE/RSJ International Conference on*, pages 4243–4250. IEEE.

Radkhah, K., Maufroy, C., Maus, M., Scholz, D., Seyfarth, A., and Von Stryk, O. (2011). Concept and design of the biobiped1 robot for human-like walking and running. *International Journal of Humanoid Robotics*, 8(03):439–458.

Radkhah, K. and von Stryk, O. (2011). Actuation requirements for hopping and running of the musculoskeletal robot biobiped1. In *Intelligent Robots and Systems (IROS), 2011 IEEE/RSJ International Conference on*, pages 4811–4818. IEEE.

Raibert, M. H. (1986). *Legged Robots that Balance*. MIT Press, Cambridge MA.

Saranlı, U., Buehler, M., and Koditschek, D. (2001). Rhex: a simple and highly mobile robot. *International Journal of Robotic Research*, 20(7):616–631.

Sato, A. and Beuhler, M. (2004). A planar hopping robot with one actuator: Design, simulation, and experimental results. In *4 IEEE/RSJ International Conference on Intelligent Robots and Systems*.

Seyfarth, A., Geyer, H., Guenther, M., and Blickhan, R. (2002). A movement criterion for running. *Journal of Biomechanics*, 35(5):649–655.

Sharbafi, M. A., Ahmadabadi, M. N., Yazdanpanah, M. J., and Seyfarth, A. (2013). Novel leg adjustment approach for hopping and running. In *Dynamic Walking*.

Sharbafi, M. A., Maufroy, C., Seyfarth, A., Yazdanpanah, M. J., and Ahmadabadi, M. N. (2012). Controllers for robust hopping with upright trunk based on the virtual pendulum concept. In *IEEE/RSJ International Conference on Intelligent Robots and Systems (Iros 2012)*.

Sharbafi, M. A. and Seyfarth, A. (2013). Human leg adjustment in perturbed hopping. In *AMAM*.

7 Article VI: Stable running by leg force-modulated hip stiffness

Authors:

Maziar Ahmad Sharbafi and André Seyfarth

Technische Universität Darmstadt

64289 Darmstadt, Germany

Published as a paper at the

2014 IEEE International Conference on Biomedical Robotics and Biomechatronics (BioRob)

ABSTRACT

Balancing the upper body as one of the main features in human locomotion is achieved by actuation of the compliant hip joints. Using leg force feedback to adjust the hip spring is presented as a new postural control technique. This method results in stable and robust running with the conceptual SLIP model which is extended by addition of a rigid trunk for upper body. Besides providing stability, this approach can represent the virtual pendulum (VP) concept which was observed in human/animal locomotion. Even more, the duality of this controller with virtual pendulum posture controller (VPPC) was mathematically shown. Such a mechanism could be also interpreted as a template for neuromuscular model.

7.1 INTRODUCTION

Upright upper body is found in human (Muybridge, 1955) and animal locomotion (Maus et al., 2010). Recently the virtual pendulum concept was proposed for postural control, based on experimental findings in human and animal locomotion (Maus et al., 2010). It was shown that during stance phase, the ground reaction forces are intersecting in a virtual support point above center of mass (CoM), namely virtual pivot point (VPP) (Maus et al., 2010) or divergent point (DP) (Gruben and Boehm, 2012). From control point of view, this concept can be employed to balance the trunk. Producing hip torque such that redirects the ground reaction forces to a predefined VPP could be an appropriate control approach. This technique was already utilized to generate stable walking/running (Maus et al., 2010). Some extensions of the model to adjust the VPP in each step for robust hopping were developed (Sharbafi et al., 2013), named virtual pendulum posture control (VPPC).

Stabilizing the gait and implementing the VP concept were already accomplished in walking (Rummel and Seyfarth, 2010), running and hopping (Sharbafi et al., 2013a) with a passive hip compliance. In the latter study, performance of hybrid zero dynamics (HZD) controller and VPPC were compared to a passive structure with compliant hip. It was shown that with combination of springs and damper in hip during stance phase, robust running and hopping with performance close to two other approaches can be achieved. Although mimicking the VPP with such a passive structure is an important step to implement VP concept mechanically, this approach has two drawbacks. First, the virtual pivot point produced by hip compliance could be placed close to the optimal location for stable and robust VPPC. However, there it is no established method to find the appropriate compliance characteristics to point out a specific VPP in accordance to a pre-designed VPPC. Second problem comes from nonzero hip torques at take off and touch down which causes discontinuities in hip torque at these moments (switching between flight and stance phases). This second point prevents the proposed method to be applied as a controller in practice and deviates the hip torque from desired one, produced by VPPC or HZD. Although the conceptual models are not mechanically feasible, their controller can be extended to a physical model (Raibert, 1986)(Poulakakis and Grizzle, 2009). Having such large hip torques (the highest value in stance phase) at take off and touchdown does not match to the typically much smaller hip torque during swing phase(Piazza and Delp, 1996).

In this study we want to resolve these drawbacks by using leg force feedback to adjust the stiffness. Variable stiffness were utilized for changing the natural dynamics of the system in order to attain different speeds or optimizing the energy consumptions like (Vanderborght et al., 2006)(Thorson et al., 2007) and (Hurst, 2008). However, here the goal is representing a mechanism for tuning the hip stiffness in order to resembling a feature in human balance control. It is illustrated that an acceptable approximation of VPPC torque can be realized by hip compliance + leg force feedback. In that respect, the hip torque can mimic the activities of muscles between upper body and legs, like hamstring and rectus femoris.

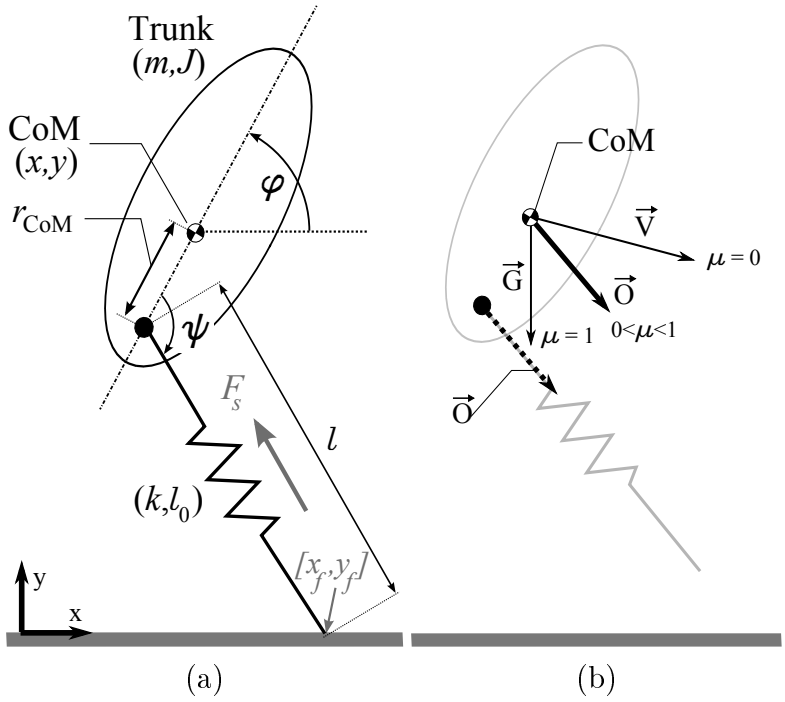

Figure 1: (a) TSLIP model with a rigid trunk and a leg modeled as a massless prismatic spring. (b) Velocity-based leg adjustment (VBLA) during flight phase.

7.2 METHODS

7.2.1 Simulation model

The simulation model which is used in this study is an extension of Spring Loaded Inverted Pendulum (SLIP) model with addition of a rigid trunk representing the upper body. In this model, called TSLIP (Sharbafi et al., 2012) for Trunk-SLIP, the leg is modeled by a massless spring (like in SLIP) and the trunk represents a rigid upper body with mass m and moment of inertia J as shown in Fig. 1a. In (Poulakakis and Grizzle, 2007) a similar model was introduced namely ASLIP, for "Asymmetric SLIP". However, as this term can also designate a SLIP model with asymmetric leg properties, we prefer to use the appellation TSLIP. The model parameters are set to match the characteristics of a human with 80 kg weight and 1.89 m height (see Table 1). Running dynamics (gait cycle) has two phases: *flight* and *stance*. Flight phase is described by the ballistic motion of the Center of Mass (CoM) when the leg does not touch the ground. The only control parameter in this phase is the leg orientation which can be arbitrarily adjusted, because the leg is massless. This angle has no effect on flight phase and just influences the touch down moment and configuration and respectively, the motion in the next stance phase.

$$\begin{cases} m\ddot{x} &= 0 \\ m\ddot{y} &= -g \\ J\ddot{\varphi} &= 0 \end{cases} \tag{1}$$

Stance phase starts by touchdown (TD), the moment that the distal end of the leg hits the ground and ends with takeoff (TO) when the $GRF = [GRF_x\ GRF_y]$ has no vertical component ($GRF_y = 0$). In this phase, $F_s = k\ (l_0 - l)$ gives the spring force along the leg axis, where l, l_0 and k are respectively the

Table 1: Model parameters

Parameter	symbol	value [units]
trunk mass	m	80 [kg]
trunk moment of inertia	J	4.58 [kg m^2]
distance hip-CoM	r_{CoM}	0.1 [m]
leg stiffness	k	16000 [N/m]
leg rest length	l_0	1 [m]
Nominal hopping/running height	y^*	2.5 [cm]

current leg length, leg rest length and the spring stiffness. Defining the states x, y and φ as the CoM horizontal and vertical positions and the trunk orientation, respectively; the hip point ($X_h = [x_h,\ y_h]$) which is positioned below CoM with distance r_h is obtained as follows

$$\begin{aligned} x_h &= x - r_h \cos\varphi \\ y_h &= y - r_h \sin\varphi \end{aligned} \tag{2}$$

The hip torque τ is determined by the controller (VPPC or passively by compliant hip) for stabilizing the posture of the trunk during stance phase. The hip torque and the leg spring force produce the ground reaction force in interaction with the ground by

$$\begin{aligned} GRF_x &= F_s \tfrac{x_h}{l} + \tfrac{\tau y_h}{l^2} \\ GRF_y &= F_s \tfrac{y_h}{l} - \tfrac{\tau x_h}{l^2} \end{aligned} \tag{3}$$

Considering g as the gravity acceleration, the motion in the stance phase equations is described by

$$\left\{ \begin{array}{lcl} m\ddot{x} &=& GRF_x \\ m\ddot{y} &=& GRF_y - g \\ J\ddot{\varphi} &=& \tau + r_h(GRF_x \sin\varphi - GRF_y \cos\varphi) \end{array} \right. \tag{4}$$

7.2.2 Control approaches

For the TSLIP model, the controller is combined of leg adjustment in flight phase and hip torque control during stance phase as described in previous section. In leg adjustment, the leg angle during swing phase is controlled, while considering the massless leg simplifies it to determining the leg angle at touchdown moment, namely “angle of attack”. During the stance phase, a controller determines the required hip torque for stabilization of the motion, especially balancing the upper body. In the following, a short summary of the leg adjustment approach is presented and we concentrate more on trunk stabilization which is done by hip torque control.

Leg adjustment during the flight phase:

The easiest leg adjustment approach is setting the leg angle to a fixed value. Although using a fixed angle of attack with respect to the ground can stabilize running (Seyfarth et al., 2002) and walking (Geyer et al., 2006), the region of attraction for the stable gait is quite small. This drawback which results in to low robustness and sensitivity to running velocity changes and control parameters exist in other common leg adjustment methods (mostly based on Raibert approach (Raibert, 1986)). In most

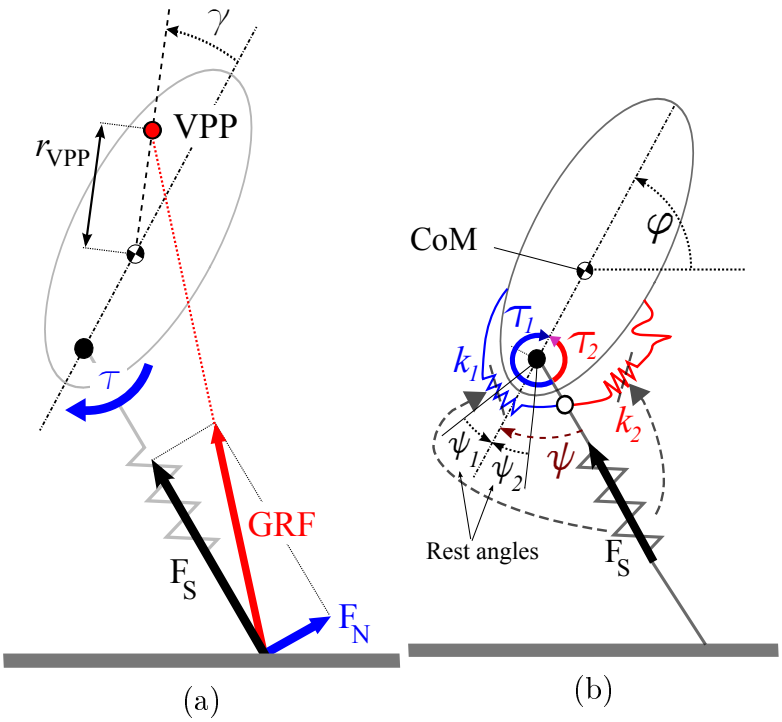

Figure 2: (a) Virtual pendulum-based posture control (VPPC) during stance phase. (b) Hip spring adjustment, to implement VP.

of the leg adjustment strategies the foot landing position is adjusted based on the horizontal velocity (Poulakakis and Grizzle, 2009) (Sato, 2004). In this paper, VBLA (Velocity Based Leg Adjustment) presented in (Sharbafi et al., 2012) is used as a robust method. This method can mimic human leg adjustment strategies for perturbed hopping (Sharbafi and Seyfarth, 2013) and achieve a large range of running velocities by a fixed controller (Sharbafi et al., 2013b). In VBLA, the leg direction is given by vector $\vec{O}$ as a weighted average of the CoM velocity vector $\vec{V}$ and the gravity vector $\vec{G} = [0, -g]^T$ (Fig. 1b).

$$\vec{O} \;=\; (1-\mu)\vec{V} + \mu\vec{G} \tag{5}$$

with weighting constant μ between 0 and 1.

VPPC for hip torque control:

Intersection of ground reaction forces (GRF) during stance phase in a point above the CoM (VPP) was shown in human/animal walking and running (Maus et al., 2010). This idea could be employed to design a controller producing hip torque which redirects GRFs toward a predefined VPP located above CoM (Fig. 2b). In that respect, the trunk behavior is transformed, from an inverted pendulum mounted at the hip to a regular virtual pendulum (VP) suspended at the VPP.

Knowing the leg spring force F_s, the hip torque τ, required for producing the normal force (F_N) to redirect GRF to VPP, is computed as follows (See Fig. 2b).

$$\tau = F_s\, l\, \frac{r_h sin\psi + r_{VPP} sin(\psi - \gamma)}{l + r_h cos\psi + r_{VPP} cos(\psi - \gamma)} \tag{6}$$

in which r_{VPP}, γ and ψ are the distance between VPP and CoM, the VPP angle and the angle between the leg and the upper body, respectively. With this equation, balancing the upper body is performed,

without measuring anything with respect to the environment, e.g. the absolute trunk orientation φ. The internal body sensors are sufficient to find the leg force F_s and angle ψ which are employed in the proposed controller (10). In the following, we set γ to zero to have the VPP on the trunk axis which is also sufficient for regular (without perturbation) human/animal locomotion (Maus et al., 2010). This assumption simplifies (6) to

$$\tau = F_s\, l\, \frac{(r_h + r_{\mathrm{VPP}})sin\ \psi}{l + (r_h + r_{\mathrm{VPP}})cos\ \psi} \tag{7}$$

Passive hip control':

In the passive compliant hip control approach, the hip torque τ is produced by hip springs and damper. According to Fig. 2a, the two unidirectional springs work in opposite directions in different regions of angle between trunk and leg ψ. With constant values for rest angles ψ_1 and ψ_2, stiffnesses k_1 and k_2 and damping ratio d the hip torque is computed by

$$\tau = k_1 max(0, \psi - \psi_1) + k_2 min(0, \psi - \psi_2) - d\dot{\psi}. \tag{8}$$

This mechanism represents human-like muscles, hamstring and rectus femoris[20]. The damping effect is considered to compensate the energy injected in each step by preloading the springs. It is removed when the leg force feedback is added in the following.

Adapting hip compliance using leg force:

In the proposed passive compliant hip mechanism, one of the springs (with respect to the angle of attack) should be preloaded at touch down which means sudden increment in the energy of the system which makes the model physically infeasible. In order to mimic the hip torque patterns produced by VPPC, the leg force F_s is utilized as the feedback signal for hip spring stiffness (k_i, $i = 1, 2$) adjustment.

$$k_i = k_i^0 \frac{F_s}{F_s^n} \tag{9}$$

where k_i^0s and F_s^n are the initial values of hip springs' stiffnesses and normalization value for the leg force, respectively. How this adaptive hip compliance can approximate VPPC[21] is described in Appendix. 8.5.1. It was already suggested that the lengths of knee (vastus) muscle and biarticular muscles (hamstring and rectus femoris) correspond the virtual leg (the virtual line connecting hip to ankle) length and angle (Desai and Geyer., 2013). Therefore, this method presents a mechanical representation to implement the VP concept for postural stabilization of running, without requiring any extra measurements.

7.2.3 Evaluating VPP existence in a controlled motion

As mentioned before, VPP is a concept which was observed in human/animal upper body balancing. For every control approach, existence of the VP concept can be investigated. VPP is defined (Maus et al., 2010) as "the single point at which the total transferred angular momentum remains constant and the sum-of-squares difference to the original angular momentum over time is minimal, if the GRF is applied at exactly this point". In this paper, for the hip compliance (with or without leg force feedback) this point is found using the calculations described in Appendix. 8.5.2. For every control approach, the existence of a VPP is given when the GRFs clearly intersect at a point above the center of mass.

[20] These human muscles are biarticular which need two-segment leg. Hip springs can be interpreted as a mechanical representation of these muscles and can be extended in future to models with segmented legs.

[21] To resemble VPPC with VPP on the trunk axis, the rest angles may be set to zero.

7.3 RESULTS

In this section, stability in running with VBLA for leg adjustment and VPPC, hip compliance with and without leg force feedback are investigated. As a standard model, TSLIP for running with parameters of Table 1 is simulated in MATLAB/SIMULINK 2012b using ode45 solver. The hip torque-angle behavior is analyzed and the ground reaction forces vectors during stance phase which demonstrate the VPP concept are also shown.

7.3.1 Torque angle analysis

Stable running at $3m/s$ is achieved by a range of control parameters. Similar results are found for other speeds, just by changing the parameters and initial conditions. Hereafter, all hip control approaches are combined with VBLA for leg adjustment with $\mu = 0.43$. The first controller is VPPC with $r_{\text{VPP}} = 8cm$ which can stabilize the motion. This value is selected based on finding a trade off between eigenvalue minimization and robustness maximization as explained in (Sharbafi et al., 2013).

For the second approach, two different combinations are set for hip compliance which can stabilize the motion:

- Type 1 (overlap between springs working area): springs stiffnesses $k_1 = k_2 = 300\frac{Nm}{rad}$, rest angles $\psi_1 = -\psi_2 = -5^\circ$ and damping $d = 0.5\frac{Nms}{rad}$.
- Type 2 (with dead zone): springs stiffnesses $k_1 = k_2 = 350\frac{Nm}{rad}$, rest angles $\psi_1 = -\psi_2 = 2^\circ$ and $d = 0.5\frac{Nms}{rad}$.

Leg force is utilized for hip spring stiffness adjustment using Eq. (8) with initial springs stiffnesses $k_1^0 = k_2^0 = 250\frac{Nm}{rad}$, rest angles $\psi_1 = -\psi_2 = 0^\circ$ without damping.

In Fig. 3, hip torque and trunk angle are shown during one step, from apex to apex. The gait duration is normalized to 1. It is observable that for all control types, the trunk angle with respect to ground φ does not deviate considerably from vertical orientation. In passive hip springs this deviation is less than 4° and for VPPC and hip spring + force feedback which are very close to each other, it is less than 1°. Such a low angular motion is also observed in human locomotion (Muybridge, 1955). The trend is also similar to what humans do when after reaching apex (middle of flight phase), the upper body is slightly bending forward until touch down. Then, it starts leaning backward until takeoff and again moves forward until the next apex.

Fig. 3(bottom) illustrates the torque changes which has nonzero values during stance phase when no torque is needed for moving the massless leg in flight phase. For passive hip springs, jumps from zero to the highest produced hip torques, in addition to make the model impractical, make the trend different from VPPC and also human hip torque actuations, except around mid-stance. These drawbacks are resolved using leg force feedback which prepares torque pattern very similar to VPPC. This is expected from argumentation in Sec. 7.2.2 and Appendix. 8.5.1.

In Fig. 4, the hip torque is drawn versus the angle between upper body and leg (ψ). This shows how the hip torque relates to hip angle. The dead zone and overlap of the springs are illustrated in this figure. It is conclude from this figure that with leg force feedback, it is possible to mimic VPPC torque-angle relation.

7.3.2 VPP representation with Hip spring

The VPP is computed for the model with compliant hip (with and without leg force compliance) by the equations presented in Appendix. 8.5.1. The computed VPP for different methods and the ground

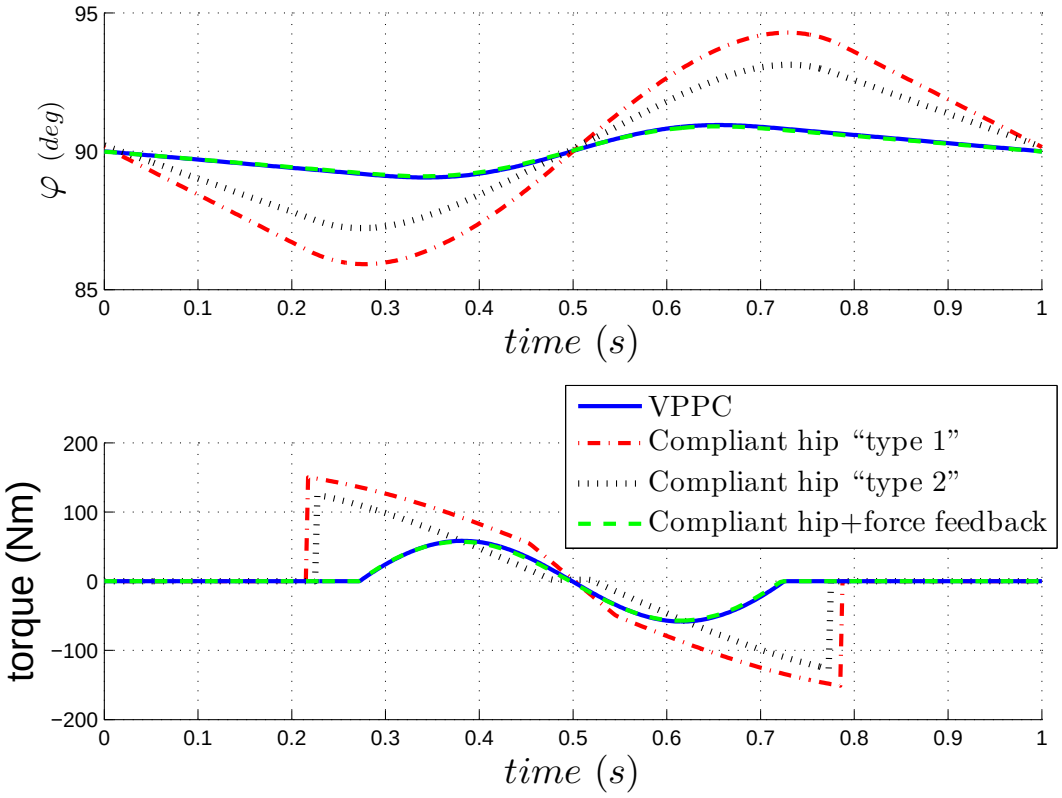

Figure 3: Steady state (top) trunk angle and (bottom) hip torque trajectories during gait cycle.

reaction forces are shown in CoM coordinate system in Fig. 1. Here, CoM is the origin and the ground reaction forces, originating at the center of pressure are displayed at different time instances. The estimated location of the VPP measured over running steps, is depicted by red point above the CoM. For the hip compliance type 1, the related r_{VPP} is 34cm which is more than 4 times this value for VPPC. This distance is 16.6cm for the second type of hip compliance which is about half of this value for the first type. Having dead zone in the middle of torque angle behavior makes both the motion behavior (Fig. 4) and VPP point closer to what achieved by VPPC. Although the GRFs almost intersect in VPP, it is not very precise. Adaptation of the hip spring stiffness via leg force both reduces the the related r_{VPP} and makes a more focused VPP from ground reaction forces. No out-layer forces like Figs. 5a and 5b exists in Fig. 5c.

7.4 DISCUSSION

In this paper, an approach for implementing the virtual pendulum posture control (VPPC) is presented via addition of leg force feedback to tune the hip spring stiffness. In VPPC, trunk and leg angles are not required and just the angle between them should be known beside the leg force. On the other hand, we found useful properties of applying hip spring and damper in stabilizing hopping and running motion from our previous studies (Sharbafi et al., 2013a). It was demonstrated that employing such a compliant hip gives similar torque patterns in the middle of stance phase and comparable robustness against perturbations with respect to VPPC. These two points of view concluded a need for tuning the hip spring to produce torque-angle behavior similar to VPPC in whole stance phase. In other words, we replaced

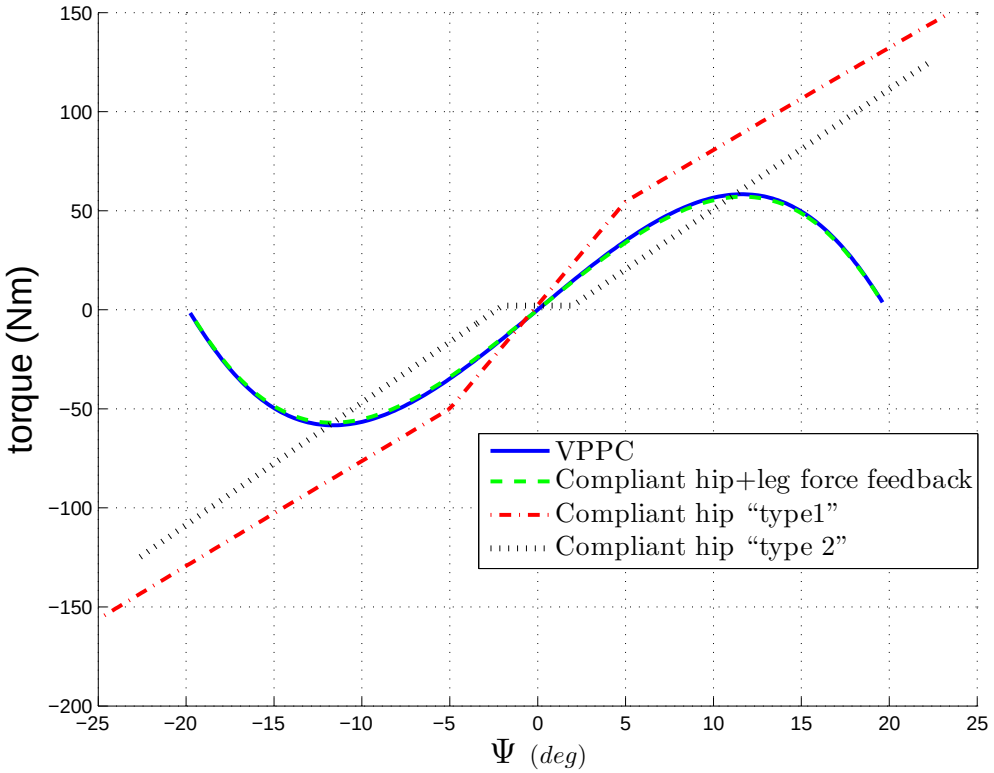

Figure 4: Hip torque-angle diagrams for different control approaches.

damping and nonlinear spring relation with variable stiffness mechanism. In that respect, using the leg force feedback to adjust the hip spring stiffness helped to mimic the exact behavior of VPPC controller. Accordingly, with a passive mechanism beside an internal measurement of the leg property like leg length, a robust controller to balance the upper body is produced[22]. Existence of such kinds of sensors for measuring leg configuration in human body was already shown (Desai and Geyer., 2013) (e.g. knee muscle measures the leg length).

By this method for hip control, in addition to reproducing the torque-angle pattern of VPPC, the exact VPP can be implemented with precise positioning of the intersection point of ground reaction forces. Therefore, to apply this controller in reality, the stabilizing and even robust VPPC controller can be designed and then, the parameters of the related mechanism for hip spring+leg force feedback can be obtained.

The idea of compliance adjustment was also introduced in Hill type muscle modeling (Hill, 1938) when it is triggered by an activation function $A(t)$ as

$$F_m = A(t)F_l(l_m)F_v(\dot{l}_m)F_{max} \tag{10}$$

in which, l_m is the muscle length and F_m, F_l, F_v and F_{max} are the muscle force, the force-length relation, the force-velocity relation and the maximum isometric contraction force of the muscle, respectively. Therefore, the presented mechanism is like a Hill type muscle model for hip torque control which utilizes the leg force as activation function. Eq. (6) can be easily mapped to Eq. (10) considering spring relation with zero rest length for F_l, unity function for F_v, $F_{max} = \frac{1}{F_s^n}$ and $A = F_s$. The proposed functions for force-length and force-velocity relation were also suggested by Haeufle et al (Haeufle et al., 2010).

[22] The robustness is inherited from VPPC which was shown in (Sharbafi et al., 2013).

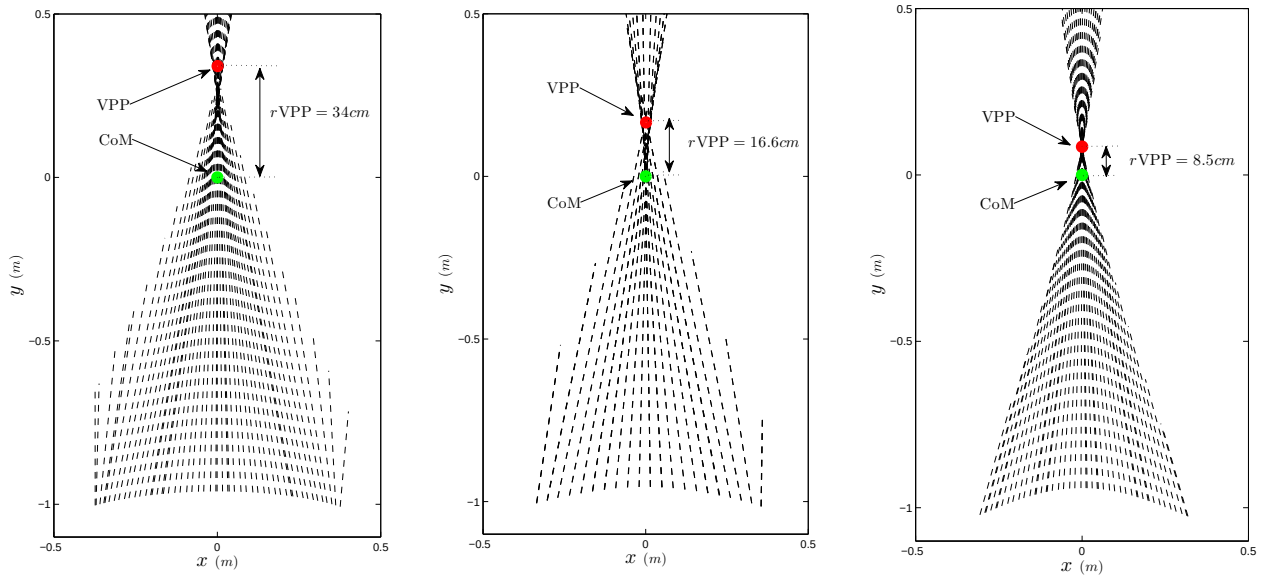

Figure 5: VPP of running for a) compliant hip type 1 b) compliant hip type 2 c) hip spring+leg force feedback.

The presented model could be interpreted as a muscle model with an activation function determined based on feedback signal of another muscle. For example, in human body, the hip muscles (hamstring and rectus femoris) may change their properties based on vastus muscle length which measures the leg length. The function of such a biologically motivated hip control could be simulated based on a series-elastic-actuator concept as proposed by (Robinson et al., 1999).

In this paper the focus was on establishing new, biologically plausible control mechanisms for upright trunk posture in locomotion. Based on an extension of the conceptual SLIP model, we were able to identify that leg force feedback is appropriate to tune compliant hip function. This finding can be translated into neural circuits between different leg muscles helping to establish balance during locomotion. Similar neuro-muscular networks have been previously suggested for repulsive leg function (e.g. in bouncy tasks like hopping, (Geyer et al., 2003)). The similarity of the proposed networks for balance and spring-like leg function suggest that different functional requirements for locomotion could be implemented by applying similar sensor-motor relations to different connections (e.g. between single-joint and two-joint muscles for balance) within the neuro-muscular system. In this respect, the VPP approach proved to be a very useful “navigation tool"to identify appropriate control schemes, which could be used for both technical and biological systems.

7.5 APPENDIX

7.5.1 Approximation of VPPC with hip compliance+leg force feedback

Considering r as the distance between VPP and hip which means ($r = r_{\text{VPP}} + r_h$), from Eq. (10) the hip torque produced by VPP is obtained by:

$$\tau_{\text{VPP}} = F_s \, l \, \frac{r \, sin\psi}{l + r \, cos\psi} \tag{11}$$

For angles ψ less than 30° the error of approximating $sin\psi$ with ψ is less than 6%. In human, the distance between the CoM of upper body and the hip (r_h) is less than 10% of the leg length (Winter, 2005). The VPP distance (r_{VPP}) is also not more than 20 *cm* which is around 20% of the leg length (Maus et al., 2010). In our simulation the optimal value was 8 *cm*. When difference between $\cos\psi$ and one is less than 0.125 for ψ smaller than 30°, approximating $l + r\cos\psi$ with $l + r$ does not make error more than 3%. It is remarkable that these approximation errors happen in the same direction (both are positive or negative) which reduce total error of the following approximation to less than 1.5%. With such a close approximation, the VPP torque can be written as:

$$\tau_{\text{VPP}} \approx F_s \; l \; \frac{r\psi}{l+r} \tag{12}$$

On the other hand, setting $\psi_1 = \psi_2 = 0$ and combining Eqs. (7) and (8) gives the following hip torque relation for hip spring+leg force feedback.

$$\tau_h = \begin{cases} k_1^0 \frac{F_s}{F_s^n}\psi & \psi > 0 \\ k_2^0 \frac{F_s}{F_s^n}\psi & \psi < 0 \end{cases} \tag{13}$$

It can be easily seen that using the following equation for initial stiffness k_i^0, equalizes the hip torques in two methods (τ_h and τ_{VPP}).

$$k_i^0 = \frac{lr}{(l+r)} F_s^n \tag{14}$$

Note that, Eq. (8) demonstrates a kind of interpretation of normalizing the leg force and considering zero rest angles, the leg force modulated compliance torque may also be written as follows.

$$\tau_h = \frac{lr}{(l+r)} F_s \psi = k(F_s)\psi \tag{15}$$

Which means the hip actuator is a compliance having variable stiffness with a linear relation to leg force.

7.5.2 Finding VPP during stance phase

First of all, we need to compute the GRFs in the coordinate system centered at CoM and with vertical axis in trunk orientation. Then defining $[x,y]$, $[x_f,y_f]$ and φ as the position of CoM, foot contact and the trunk angle (See Fig. 1a), the foot point in the new coordinate system ($P^c := [x_f^c, y_f^c]$) is computed by

$$\begin{cases} x_f^c &= (x_f - x)\sin\varphi - (y_f - y)\cos\varphi \\ y_f^c &= (x_f - x)\cos\varphi - (y_f - y)\sin\varphi \end{cases} \tag{16}$$

Also the GRF in the new coordinate system ($F^c := [F_x^c, F_y^c]$) is computed as follows:

$$\begin{cases} F_x^c &= GRF_x \sin\varphi - GRF_y \cos\varphi \\ F_y^c &= GRF_x \cos\varphi - GRF_y \sin\varphi \end{cases} \tag{17}$$

The torque generated by F^c exerted at P^c around the origin (CoM) is computed by outer product ($\times$) of these two vectors:

$$\tau^c = F_x^c y_f^c - F_y^c x_f^c = F^c \times P^c \tag{18}$$

Assume that vectors $\vec{F}_x$, $\vec{F}_y$, $\vec{X}$ and $\vec{Y}$ are composed of concatenating the related values F_x^c, F_y^c, x_f^c and y_f^c during stance phase in 4 columns, respectively. Then, the summation of torques produced by GRFs during stance phase is obtained by

$$\tau = \vec{F}_y^T \vec{Y} - \vec{F}_x^T \vec{X} \tag{19}$$

where upper index $(.)^T$ stands for transpose. The first condition in existence of VPP is having a constant total transferred angular momentum (Maus et al., 2010) which should be equal to τ. Suppose that vector $\vec{F} = [F_x, F_y]$ represents the average of GRFs during stance phase. Each point on a line l with slope $\frac{F_y}{F_x}$ and distance from origin $d = \frac{\tau}{|\vec{F}|}$ has total transferred angular momentum equal to τ. This line is defined by $l : y = ax + b$ where a and b are as follows:

$$\begin{cases} a = \frac{F_y}{F_x} \\ b = sign(F_x) d \sqrt{1 + a^2} \end{cases} \tag{20}$$

Exerting force $\vec{F}$ from any point on this line produces torque τ. For the second condition, the VPP point should be found such that applying the GRF at that point minimizes the sum-of-squares difference to the original angular momentum over time. With some mathematical manipulation, the VPP is obtained by the following relation:

$$\begin{cases} x_{\text{VPP}} = (\alpha^T \alpha)^{-1} \alpha^T \beta \\ y_{\text{VPP}} = a x_{\text{VPP}} + b \end{cases} \tag{21}$$

in which considering "."for element-wise multiplication of two vectors, α and β are defined as follows:

$$\begin{cases} \alpha := \vec{F}_x a - \vec{F}_y \\ \beta := \vec{F}_x . (\vec{Y} - b) - \vec{F}_y . \vec{X} \end{cases} \tag{22}$$

7.6 ACKNOWLEDGMENT

This research was supported in part by the EU project BALANCE under Grant Agreement No. 601003 and the German Research Foundation (DFG) under grants No. SE1042/8.

7.7 AUTHOR CONTRIBUTIONS

Maziar A. Sharbafi is the main and corresponding author of the article. He developed the new model of posture control and was responsible for the conception and design of simulations, analysis and interpretation of experimental data and writing of the manuscript. Andre Seyfarth was the supervisor of the project and contributed to developing concepts and models and writing the paper.

7.8 REFERENCES

Desai, R. and Geyer., H. (2013). Muscle-reflex control of robust swing leg placement. In *IEEE International Conference on Robotics and Automation, (ICRA 2013)*.

Geyer, H., Seyfarth, A., and Blickhan, R. (2003). Positive force feedback in bouncing gaits? *Proceedings of the Royal Society B*, 270.

Geyer, H., Seyfarth, A., and Blickhan, R. (2006). Compliant leg behaviour explains basic dynamics of walking and running. *Proceedings of the Royal Society B*, 273(1603):2861–2867.

Gruben, K. G. and Boehm, W. L. (2012). Force direction pattern stabilizes sagittal plane mechanics of human walking. *Human Movement Science*, 31(3).

Haeufle, D. F. B., Grimmer, S., and Seyfarth, A. (2010). The role of intrinsic muscle properties for stable hopping âĂŞ stability is achieved by the force-velocity relation. *Bioinspiration and Biomimetics*, 5(1).

Hill, A. V. (1938). The heat of shortening and the dynamic constants of muscle. *Proceedings of the Royal Society B*, 126.

Hurst, J. W. (2008). *The Role and Implementation of Compliance in Legged Locomotion*. PhD thesis, Robotics Institute, Carnegie Mellon University.

Maus, H. M., Lipfert, S., Gross, M., Rummel, J., and Seyfarth, A. (2010). Upright human gait did not provide a major mechanical challenge for our ancestors. *Nature Communications*, 1(6):1–6.

Muybridge, E. (1955). *The Human Figure in Motion*. New York: Dover Publications Inc.

Piazza, S. J. and Delp, S. L. (1996). The influence of muscles on knee flexion during the swing phase of gait. *Journal of Biomechanics*, 29(6):723–33.

Poulakakis, I. and Grizzle, J. (2007). Formal embedding of the spring loaded inverted pendulum in an asymmetric hopper. In *in Proc. of the European Control Conference*, Kos, Greece.

Poulakakis, I. and Grizzle, J. W. (2009). The spring loaded inverted pendulum as the hybrid zero dynamics of an asymmetric hopper. *IEEE Transaction on Automatic Control*, 54(8):1779–1793.

Raibert, M. H. (1986). *Legged Robots that Balance*. MIT Press, Cambridge MA.

Robinson, D. W., Pratt, J. E., Paluska, D. J., and Pratt, G. A. (1999). Series elastic actuator development for a biomimetic walking robot. In *IEEE/ASME International Conference on Advanced Intelligent Mechatronics*.

Rummel, J. and Seyfarth, A. (2010). Passive stabilization of the trunk in walking. In *International Conference on Simulation, Modeling and Programming for Autonomous Robots*, Darmstadt, Germany.

Sato, A. and Beuhler, M. (2004). A planar hopping robot with one actuator: Design, simulation, and experimental results. In *4 IEEE/RSJ International Conference on Intelligent Robots and Systems*.

Seyfarth, A., Geyer, H., Guenther, M., and Blickhan, R. (2002). A movement criterion for running. *Journal of Biomechanics*, 35(5):649–655.

Sharbafi, M. A., Ahmadabadi, M. N., Mohammadinejad, M. J. Y. A., and Seyfarth, A. (2013a). Compliant hip function simplifies control for hopping and running. In *IEEE/RSJ International Conference on Intelligent Robots and Systems (Iros 2013)*.

Sharbafi, M. A., Ahmadabadi, M. N., Yazdanpanah, M. J., and Seyfarth, A. (2013b). Novel leg adjustment approach for hopping and running. In *Dynamic Walking*.

Sharbafi, M. A., Maufroy, C., Ahmadabadi, M. N., Yazdanpanah, M. J., and Seyfarth, A. (2013c). Robust hopping based on virtual pendulum posture control. *Bioinspiration and Biomimetics*, 8(3).

Sharbafi, M. A., Maufroy, C., Seyfarth, A., Yazdanpanah, M. J., and Ahmadabadi, M. N. (2012). Controllers for robust hopping with upright trunk based on the virtual pendulum concept. In *IEEE/RSJ International Conference on Intelligent Robots and Systems (Iros 2012)*.

Sharbafi, M. A. and Seyfarth, A. (2013). Human leg adjustment in perturbed hopping. In *AMAM*.

Thorson, I., Svinin, M., Hosoe, S., Asano, F., and Taji, K. (2007). Design considerations for a variable stiffness actuator in a robot that walks and runs. In *In Proc. of the Robotics and Mechatronics Conference (RoboMec)*.

Vanderborght, B., Verrelst, B., Ham, R. V., Damme, M. V., Lefeber, D., Duran, B. M. Y., and Beyl, P. (2006). Exploiting natural dynamics to reduce energy consumption by controlling the compliance of soft actuators. *The International Journal of Robotics Research (IJRR)*, 25(4):343–358.

Winter, D. A. (2005). *BioMechanics and motor control of human movement*. John Wiley & Sons, Inc, New Jersy, USA, 3 edition.

8 Article VII: FMCH: a new model for human-like postural control in walking

Authors:

Maziar Ahmad Sharbafi and André Seyfarth

Technische Universität Darmstadt

64289 Darmstadt, Germany

Published as a paper at the

2015 IEEE/RSJ International Conference on Intelligent Robots and Systems (IROS)

ABSTRACT

Spring loaded inverted pendulum (SLIP) model used simple spring mass mechanism to explain leg function and ground reaction force in legged locomotion. Balancing the upper body can be addressed by addition of a rigid trunk to this template model. The resulting model is not conservative and needs hip torque to keep the trunk upright during locomotion, like humans. Leg force modulated compliant hip (FMCH) is our new model for postural control in walking which employs the leg force feedback to adjust the hip compliance. Such an application of positive force feedback presents a new template for neuromuscular model. This method provides stable and robust walking in simulations and also mimics human-like kinetic behavior. Analyzing human walking experiment shows that FMCH can explain the hip torque-angle relation for different walking speeds. Finally, this approach may physically implement the virtual pendulum (VP) concept, observed in human/animal locomotion.

8.1 INTRODUCTION

Simple, conceptual models are very useful tools in describing and analyzing human/animal locomotion. Such models which are called “templates” (Full and Koditschek, 1999) benefit from high level of abstraction in explaining locomotion features. Additionally, many successful legged robots are developed (Raibert, 1986)(Saranlıet al., 2001) based on template models. They are also utilized as explicit templates for control (Poulakakis and Grizzle, 2009). Spring-loaded inverted pendulum (SLIP) is one of the most popular templates (Blickhan, 1989)(McMahon and Cheng, 1990). In SLIP, whole body mass is concentrated in one point (center of mass (CoM)) and the leg behavior is modeled by a massless spring. This model and its extension to have the second spring during double support (BSLIP for Bipedal SLIP) can describe human gaits, such as hopping/running (Blickhan, 1989) and walking (Geyer et al., 2006), respectively.

In spite of all advantages of (B)SLIP model, since the upper body is represented by a point mass, it cannot address postural control whereas vertical body alignment plays a key role in stabilization of human locomotion (Maus et al., 2010). For that purpose, the SLIP must be extended to include a model of the upper body. An extension of the SLIP with a rigid trunk was introduced as TSLIP (for Trunk-SLIP) (Sharbafi et al., 2013) or ASLIP, for “Asymmetric SLIP” (Poulakakis and Grizzle, 2007)[23]. The model that we use in this paper is based on BTSLIP (Bipedal TSLIP), shown in Fig. 1.

In contrary to most of posture control approaches which are based on control of the trunk orientation with respect to an absolute referential frame (Raibert, 1986)(Poulakakis and Grizzle, 2009)(Hyon and Emura, 2005), Maus et al. (Maus et al., 2008) proposed a postural controller which uses the angle between leg and trunk. This controller was based on an innovative concept for posture stabilization, coined Virtual Pendulum (VP), based on observations in a variety of animals including humans (Maus et al., 2010). One passive alternative for balance control using the same angle for postural control is having rotational springs at hip joint. Stabilizing the gait and implementing the VP concept were already accomplished in walking (Rummel and Seyfarth, 2010), running and hopping (Sharbafi et al., 2013a) with a passive hip spring. Looking at humans hip torque-angle behavior shows that linear spring cannot explain human-like postural control in walking. In addition, nonzero force at moment of touchdown which results in discrete actuation makes the control approach impractical.

From another point of view, humans neuromuscular system can be implemented in mechanical models considering different relations between the generated force, muscle length and velocity (e.g., Hill-type muscle model (Hill, 1938)) besides some sensory feedback signals (as muscle reflexes) which control the actuator parameters like model presented in (Geyer and Her, 2010). In (Geyer et al., 2003), stable

[23] Here we will use TSLIP because Asymmetric SLIP can also apply to a SLIP model with asymmetric leg properties.

hopping was achieved using positive force feedback to stimulate the muscle. Later, Günther et al., introduced a new muscle model in which damping effect of the muscle is tuned based on muscle force (Günther and Schmitt, 2010). Using spring (damper) mechanism and tuning the parameters may transfer part of the knowledge of neuromuscular models to the templates. Inspired from the muscle models and reflex system, we propose FMCH (force modulated compliant hip) for postural control. In this model the hip stiffness is adjusted based on the leg force feedback signal. With FMCH we (i) achieve stable walking with upright trunk needless to measure absolute leg (or body) angle with respect to ground (ii) present an acceptable explanation of human postural control (mimicking human hip torque pattern (iii) suggest a mechanical representation of postural control method based on template models (iv) introduce a new concept in muscle reflex system which can be used to realize human locomotion.

8.2 METHODS

8.2.1 Simulation model

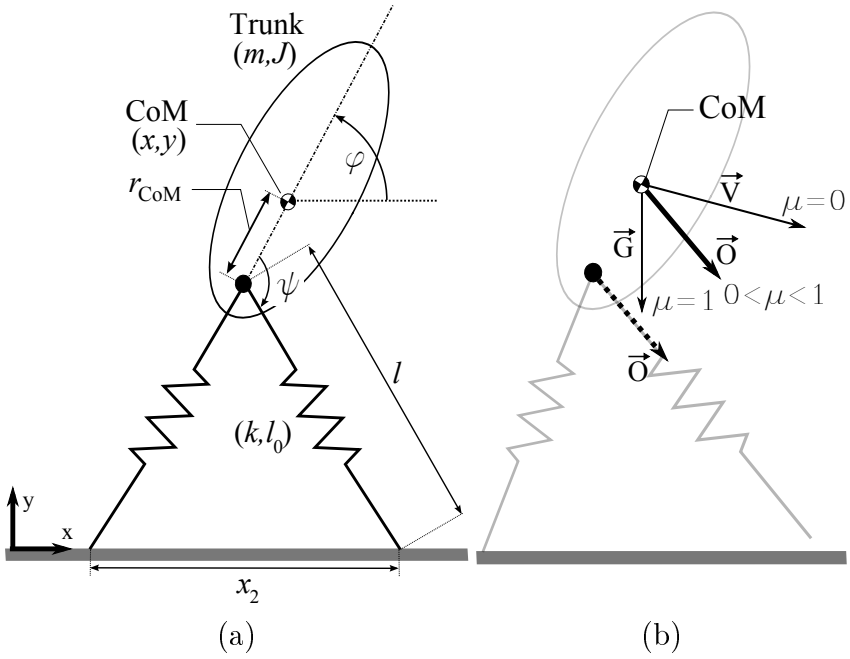

Figure 1: (a) TSLIP model with a rigid trunk and a leg modeled as a massless prismatic spring. (b) Velocity-based leg adjustment (VBLA) during flight phase.

The simulation model which is used in this study is based on BTSLIP model, shown in Fig. 1. In BTSLIP model, legs are modeled by massless springs and a rigid trunk represents the upper body with mass m and moment of inertia J. Walking dynamics (gait cycle) has two phases: *single support (SS)* and *double support (DS)*.

SS starts at takeoff moment of a leg and ends at touchdown of the same leg. Touchdown (TD) is defined as the moment that the distal end of the leg hits the ground and takeoff is when the leg leaves the ground. In SS, one leg is in contact with the ground, called stance leg and the swing leg moves virtually (no change in dynamics when the leg is massless) to finish the SS with hitting the ground with desired angle (angle of attack). Here, the hip torque exerted between trunk and stance leg and the swing leg angle are the two control parameters.

TO is detected when the ground reaction force ($GRF = [GRF_x\ GRF_y]$) has no vertical component ($GRF_y = 0$). In this phase, $F_s = K_s\ (l_0 - l)$ gives the spring force along the leg axis, where l, l_0 and K_s are respectively the current leg length, leg rest length and the spring stiffness. Defining the states x, y and φ as the CoM horizontal and vertical positions and the trunk orientation, respectively; the hip point ($X_h = [x_h,\ y_h]$) which is positioned below CoM with distance r_h is obtained as follows

$$\begin{aligned} x_h &= x - r_h \cos\varphi \\ y_h &= y - r_h \sin\varphi \end{aligned} \tag{1}$$

The hip torque τ is determined by the controller (compliant hip) for stabilizing the posture of the trunk. The hip torque and the leg spring force produce the ground reaction force in interaction with the ground by

$$\begin{aligned} GRF_x &= F_s \frac{x_h}{l} + \frac{\tau y_h}{l^2} \\ GRF_y &= F_s \frac{y_h}{l} - \frac{\tau x_h}{l^2} \end{aligned} \tag{2}$$

Considering g as the gravity acceleration, the motion dynamic in the SS is described by

$$\left\{ \begin{array}{lcl} m\ddot{x} &=& GRF_x \\ m\ddot{y} &=& GRF_y - g \\ J\ddot{\varphi} &=& \tau + r_h(GRF_x \sin\varphi - GRF_y \cos\varphi) \end{array} \right. \tag{3}$$

When the swing leg in SS hits the ground the second stance leg appears (hereafter we show the parameters related to this leg by subindex $_2$), meaning DS starts and it ends with TO of first stance leg leg (shown by $_1$). In this phase, the controller produces torques (τ_1 and τ_2) between legs and trunk to keep the system stable. Defining the position of the second stance leg by $[x_2,\ 0]$, the dynamic model of DS will be as follows:

$$\left\{ \begin{array}{lcl} m\ddot{x} &=& GRF_{x1} + GRF_{x2} \\ m\ddot{y} &=& GRF_{y1} + GRF_{y1} - g \\ J\ddot{\varphi} &=& \tau_1 + \tau_2 + r_h(GRF_{x1} + GRF_{x2})\sin\varphi \\ & & -r_h(GRF_{y1} + GRF_{y2})\cos\varphi \end{array} \right. \tag{4}$$

where

$$\left\{ \begin{array}{lcl} GRF_{x1} &=& F_{s1}\frac{x_h}{l} + \frac{\tau_1 y_h}{l_1^2} \\ GRF_{y1} &=& F_{s1}\frac{y_h}{l} - \frac{\tau_1 x_h}{l_1^2} \\ GRF_{x2} &=& F_{s2}\frac{x_h - x_2}{l} + \frac{\tau_2 y_h}{l_2^2} \\ GRF_{y2} &=& F_{s2}\frac{y_h}{l} - \frac{\tau_2 x_h}{l_2^2}. \end{array} \right. \tag{5}$$

8.2.2 Control approaches

In single support phase of walking with the BTSLIP model, the controller is combined of leg adjustment for the swing leg and hip torque control between stance leg and trunk (τ). The double support does not have freely swing leg movement and two hip torques τ_1 and τ_2 should be produced by the motion controller. VBLA (Velocity based leg adjustment) is our control strategy for swing leg and FMCH is the approach for hip torque control.

Leg adjustment during the swing phase:

The easiest leg adjustment approach is setting the leg angle to a fixed value. Although using a fixed angle of attack with respect to the ground can stabilize running (Seyfarth et al., 2002) and walking (Geyer et al., 2006), the region of attraction for the stable gait is quite small. This drawback which equals to low robustness and high sensitivity to gait speed changes and control parameters exist in other common leg adjustment methods (mostly based on Raibert approach (Raibert, 1986)). In order to concentrate on balancing of the trunk, we need to have a robust leg adjustment method. In most of the leg adjustment strategies, the foot landing position is adjusted based on the horizontal velocity (Poulakakis and Grizzle, 2009) (Sato, 2004). In this paper, VBLA (Velocity Based Leg Adjustment) presented in (Sharbafi et al., 2012), is used as a robust method. This method can mimic human leg adjustment strategies for perturbed hopping (Sharbafi and Seyfarth, 2013) and achieve a large range of running velocities by a fixed controller (Sharbafi et al., 2013b). Here, we use this method for walking.

In VBLA, the leg direction is given by vector $\vec{O}$ as a weighted average of the CoM velocity vector $\vec{V}$ and the gravity vector $\vec{G} = [0, -g]^T$ (Fig. 1b).

$$\vec{O} \quad = \quad (1-\mu)\vec{V} + \mu\vec{G} \tag{6}$$

where weighting constant μ accepts values between 0 and 1.

FMCH for hip torque control:

We consider a bi-directional rotational spring between trunk and each leg. With the configuration showed in Fig. 1(a) for double support phase, the hip torques of leg i is determined by

$$\tau_i = k_i(\psi_i - \psi_i^0) \tag{7}$$

in which k_i and ψ_i^0 are the hip stiffness and rest angle for leg i, respectively, and ψ_i is the angle between trunk and leg i as shown in Fig. 1(a). In FMCH control approach we use the leg force for modulating hip stiffness.

$$k_i = k_i^0 \frac{F_s^i}{F_s^n}, \quad i = 1,2 \tag{8}$$

where k_i^0, F_s^i ans F_s^n are the default values for hip spring stiffness, leg force and normalization value for leg force, respectively. In (Sharbafi and Seyfarth, 2014), we showed that for a single leg in contact with ground (with length l), if k_i^0 is computed by the following equation and $\psi_i^0 = 0$, then a the GRF goes through a point on trunk axis whose distance to hip is equal to r.

$$k_i^0 = \frac{lr}{(l+r)} F_s^n \tag{9}$$

Having an intersection point for GRFs during whole gait cycle, placed above CoM, is found in human walking, called VPP (virtual pivot point) (Maus et al., 2010). For the TSLIP model shown in Fig. 1(b), the required torque to redirect the GRF toward VPP, is

$$\tau_{VPP} = F_s \, l \, \frac{r_h \, sin\psi + r_{\text{VPP}} \, sin(\psi - \gamma)}{l + r_h \, cos\psi + r_{\text{VPP}} \, cos(\psi - \gamma)} \tag{10}$$

in which r_{VPP} and γ are the VPP distance to CoM and deviation angle from trunk axis, respectively, as shown in Fig. 1(b). In Appendix. 8.5.1, it is shown that FMCH can approximate VPP out of trunk axis if the hip spring rest angle is computed as follows

$$\psi_0 = \frac{r_{\text{VPP}}\gamma}{r}. \tag{11}$$

Therefore, if the gain for adapting hip stiffness is adaptively adjusted based on leg length (see Eq. 8), leg force feedback can be employed to precisely control VPP. Since the stance leg length changes are minor in walking, l can be replaced by its average value $\bar{l}$. Therefore, from Eqs (7) to (9), based on the following equation, FMCH controller only needs to measure the leg force to adjust hip stiffness

$$\tau_i = cF_s^i(\psi_i - \psi_i^0) \tag{12}$$

and it can also properly approximate VPP if the constant gain (c) is computed as follows

$$c = \frac{\bar{l}r}{(\bar{l}+r)} \tag{13}$$

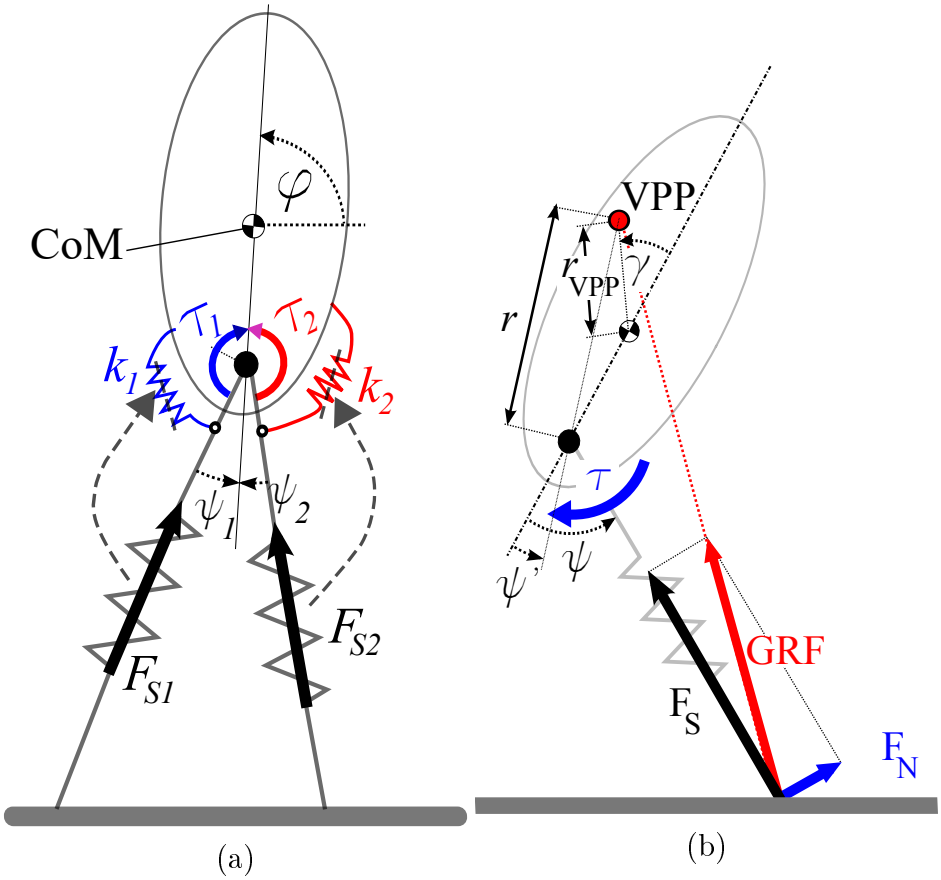

Figure 2: (a) FMCH for double support. (b) Virtual pendulum-based posture control (VPPC) during stance phase.

8.2.3 Walking experiment

We investigated the ability of FMCH in replicating human virtual hip torque in walking. The virtual hip torque is the torque between upper body and the virtual leg (the line between hip and COP (center of pressure)). Since the single support is the major part of walking cycle (about 80%) (Lipfert., 2010), we look at this phase of walking in the experimental data. Another reason is that with just one leg in contact with the ground the error can be characterized better because there is just one controller for balancing. For such analysis, we compute the ratio between hip torque and leg force ($r_F^\tau = \frac{\tau_h}{F_S}$) and draw r_F^τ versus hip angle ψ (between stance leg and trunk). The more linear behavior, the more fitting with FMCH concept.

The data was collected in walking experiments on a treadmill (type ADAL-WR, Hef Tecmachine, Andrezieux Boutheon, France) at different speeds. Motion capture data (Qualisys, Gothenburg, Sweden) from 11 markers and ground reaction force data (12 piezo-electric force transducers within the treadmill) were collected. Twenty one subjects (11 female, 10 male) were asked to walk at different percentages of their preferred transition speeds (PTS)[24]. The treadmill speed which equals the average velocity during strides was employed as the walking speed. The subjects were between 22 to 28 years old with $1.73 \pm 0.09m$ height and $70.9 \pm 11.7kg$ weight.

8.2.4 FMCH for finding VPP location

As mentioned before, VPP is a concept which was observed in human/animal upper body balancing. For every control approach, existence of the VP concept can be investigated. VPP is defined (Maus et al., 2010) as "the single point at which the total transferred angular momentum remains constant and the sum-of-squares difference to the original angular momentum over time is minimal, if the GRF is applied at exactly this point". In (Sharbafi and Seyfarth, 2014) the mathematical details to find VPP based on this definition was presented.

Based on FMCH concept, we propose a new method to compute VPP from experimental data. The first step is fitting a line to $r_F^\tau - \psi$ curve (e.g., with least square approach). Then, the rest angle ψ^0 and coefficient c in Eq. (3) are found. Using the average length of the virtual leg $\bar{l}$, Eqs. (11) and (13), r, γ and finally r_{VPP} are calculated. For more details see Appendix. 8.5.1.

8.3 RESULTS

In this section, first, the results of stable walking using VBLA for leg adjustment and FMCH for posture control are shown in simulation model. Then the experimental data analyzed based on FMCH for hip torque control. Explaining the human balance control and also examining the accuracy of FMCH in finding VPP are shown.

8.3.1 Simulation results

BTSLIP for walking, explained in Sec. 8.2.1, is simulated in MATLAB/SIMULINK 2013b using ode45 solver. The system initiates in single support when the stance leg is vertical (mid-stance). At this moment the stance leg is compressed and leg length (l_{in}) is less than the spring rest length. The model parameters are set to match the characteristics of a human with 80 kg weight and 1.89 m height (Table 1). For different walking speeds $0.5 - 1.3[m/s]$, different combinations of VBLA coefficient ($0.2 \leq \mu \leq 0.4$),

[24] PTS is the preferred speed for transition between running and walking which is typically about $1.9 - 2.1\ m/s$ for humans (Lipfert., 2010) .

leg spring stiffness ($10 \leq k_N \leq 40$), hip stiffness ($0.1 \leq c \leq 0.5$) and rest angle ($0 \leq \psi \leq 0.1$) result in stable motion[25].

Table 1: Model parameters

Parameter	symbol	value [units]
trunk mass	m	80 [kg]
trunk moment of inertia	J	4.6 [kg m^2]
distance hip-CoM	r_{CoM}	0.1 [m]
Normalized leg stiffness	k	40
leg rest length	l_0	1 [m]
Gravitational acceleration	g	9.81 [m/s^2]

Fig. 3 shows the hip torque of each leg (τ_1 and τ_2) and the total torque ($\tau = \tau_1 + \tau_2$) for a sample set of control parameters and initial conditions (see Table .2). The results are shown for one gait cycle starting with double support (touchdown) and ending with single support (before the next touchdown). The hip torque pattern of each leg are similar to what found in human walking (Maus et al., 2010). Similar patterns for different leg in opposite directions with a phase shift results in smaller net torque on trunk. The main difference is having double support longer than what is observed in human walking at this speed. The torque between each leg and trunk is smooth (with no jump like in passive hip spring (Rummel and Seyfarth, 2010)), resulting from modulating hip stiffness by leg force.

Table 2: Initial conditions and control parameters

Parameter	symbol	value [units]
speed	V_0	1 [m/s]
initial leg length	l_{in}	0.99 [m]
normalized hip spring stiffness	c	0.26
hip spring rest length	ψ_0	0[°]
VBLA coefficient	μ	0.34 [m]
Normalized leg stiffness	K_N	40

8.3.2 FMCH approximation of hip torque in human walking

In this section we use the FMCH model to explain human posture control. If Eq. (3) holds for human hip torque control, relation of $r_F^\tau = \frac{\tau_h}{F_S}$ with ψ will be linear. In Fig. 6, these relations are shown for different walking speeds (from $25\% - 125\%PTS$). It is observed that the curves can be approximated by straight lines. The hip stiffness (c) and rest angle (ψ_0), found from the line slope and its intersection with horizontal axis, are shown in Fig. 5. The hip stiffness decreases with increasing the motion speed except from $100\%PTS$ to $125\%PTS$. It means that for faster movement more oscillations are allowed for the upper body, except for very fast walking. However, at $125\%PTS$ running is preferred to walking, requiring stiffer hip. The trend is the same for rest angle in the opposite direction.

[25] With SLIP-based models with fixed leg spring stiffness, fast walking (speed more than $1.3[m/s]$) is not achievable

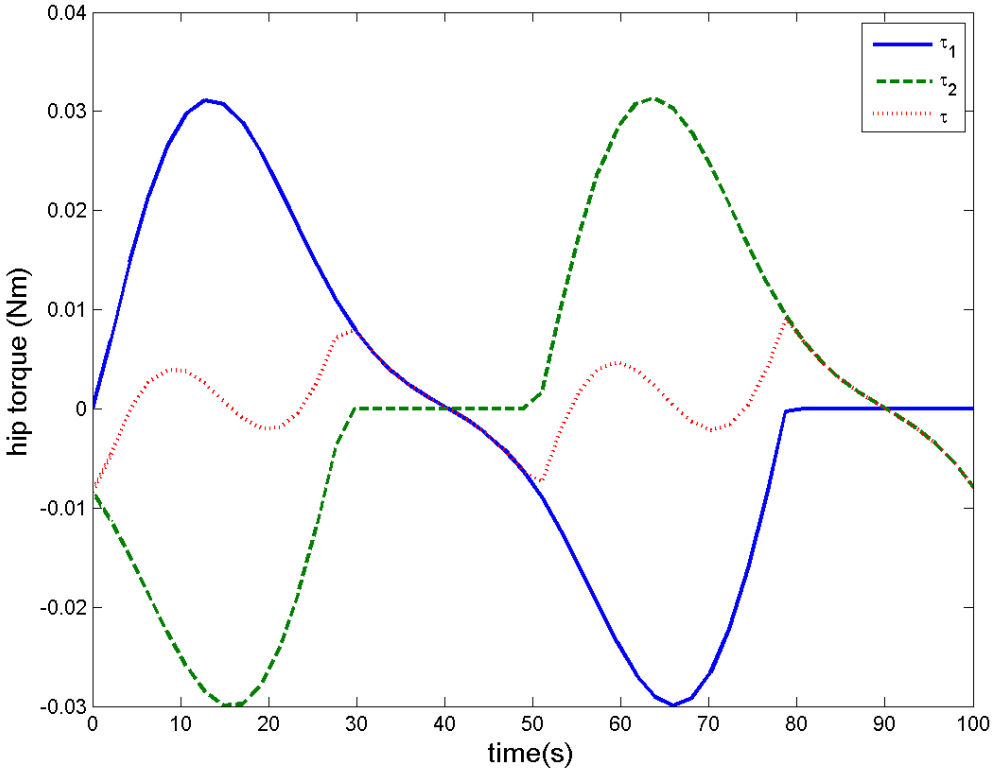

Figure 3: Hip torques of different leg (τ_1 and τ_2) and total hip torque τ for a complete gait cycle of walking at $1[m/s]$ with FMCH model.

Based on the parameters found for the FMCH model, the normalized hip torque (to body weight and length) found in experiment and the approximation of FMCH are drawn in Fig. 6. It is shown that the model can predict the hip torque using a modulating hip compliance by simple reflex from leg force. Some deviations from the prediction are observed at the the beginning of the cycle for fast walking. It might be the effect of large push off at high speeds which will be handled after passing 20% of swing phase (single support). It is observed that the FMCH model can properly explain the hip torque control strategy in humans.

8.3.3 VPP estimation by FMCH

In (Maus et al., 2010), the method mentioned in Sec.8.2.4 is presented to find VPP (for mathematical details see (Sharbafi and Seyfarth, 2014)). Here, we use the new method to find the VPP based on FMCH model as explained in Appendix. 8.5.2. The ground reaction forces are plotted from CoP by dashed lines in Fig. 7 where the coordinate system centered at CoM and aligned with upper body orientation are shown. The CoM and the estimated VPP are also shown with green and red circles, respectively. It is clear that the estimation of VPP by FMCH is the focus point in these graphs. Hence, VPP can be physically implemented by FMCH model, just using leg force feedback.

8.4 DISCUSSION

Using oscillatory behavior of spring mass system, SLIP as a template model can describe bouncing property of legged locomotion. Here, we presented another template model for balancing, comprised

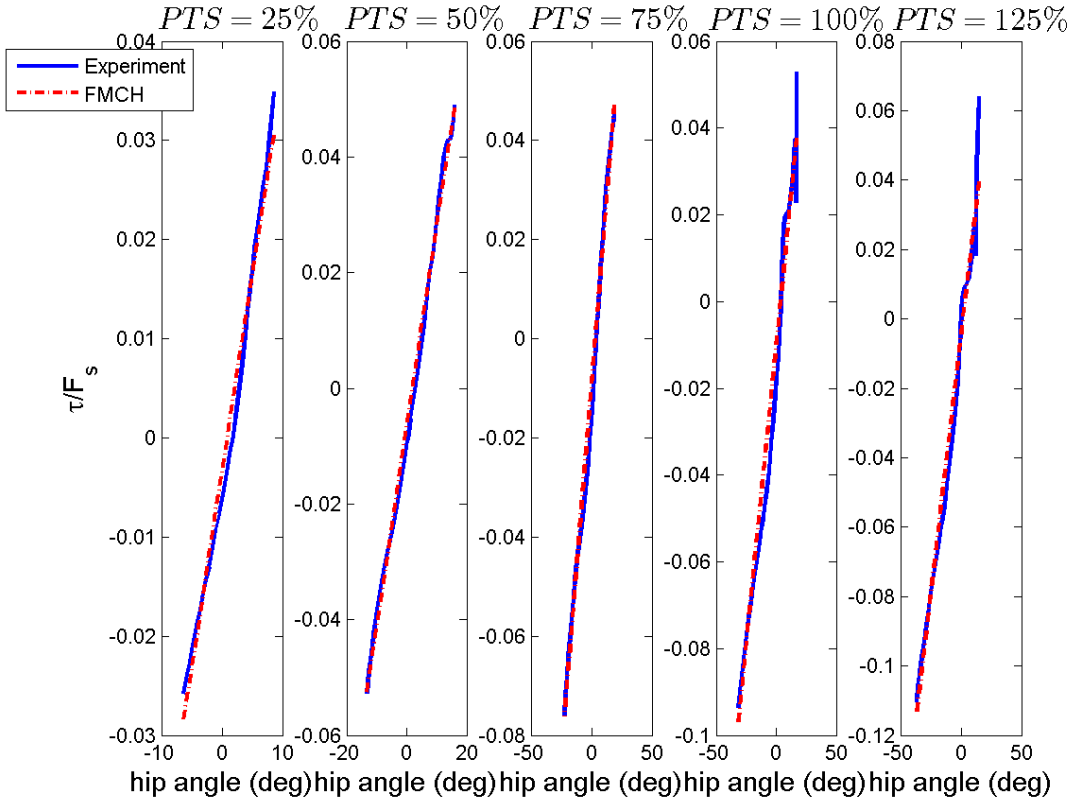

Figure 4: Hip torque τ_h to leg force ratio (r_F^τ) versus hip angle (ψ). Solid line is the experimental result and dashed line shows the fitted FMCH model.

of a (rotational) spring and inverted pendulum (as oscillatory system) with feedback signal to adjust the stiffness. The new template, called *FMCH*, employs feedback signal for tuning the property of the passive mechanical system (spring) similar to reflex model in neuro-muscular system (Geyer et al., 2003). Instead of force-velocity (Günther and Schmitt, 2010) or stimulation (Geyer et al., 2003), we suggest to adapt stiffness as force-length property, based on muscle reflex.

With FMCH model, we can explain the hip torque control in human walking. The closer linear relation between hip torque over leg force (introduced by r_F^τ) and hip angle, the better representation of human posture control by FMCH. Thus, linear curves in Fig. 6 support the idea of using leg muscle reflex for hip muscle control. In addition, existence of such kinds of sensors for measuring leg configuration in human body was already shown (Desai and Geyer., 2013), e.g., the hip bi-articular muscles may change their properties based on vastus muscle length measuring the leg force, in human body.

Changing the stiffness and rest angle of hip spring with respect to motion speed shows that the balance control strategy may contribute to gait speed adjustment, except for very fast walking. This property besides leg angle and stiffness adjustment can precisely control the motion speed.

Finally, with mathematical relation between the hip normalized stiffness and rest length and position of VPP with respect to CoM (the distance and angle from upper body axis), we proposed a method to find VPP based on FMCH model. The main benefit of such calculations appears when the VPP changes during gait e.g., to recover from perturbations or to change the gait speed. In such cases VPP adaptation can be detected from slope changes in $r_F^\tau - \psi$ curves.

8.5 APPENDIX

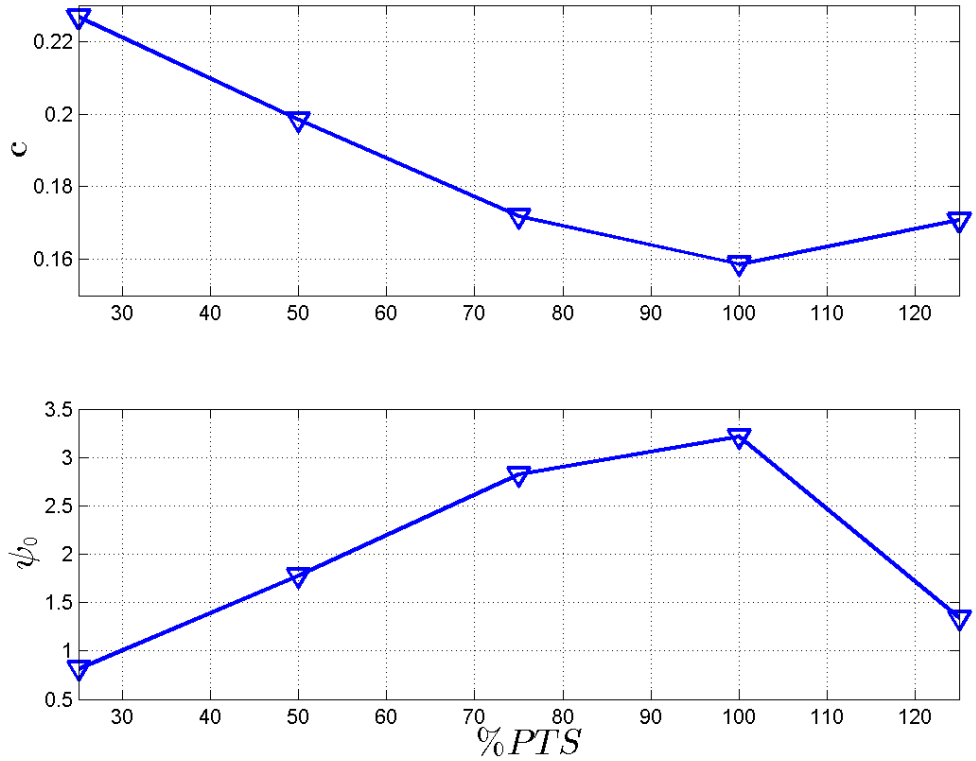

Figure 5: Variations of normalized hip stiffness (c) and rest angle (ψ_0) according to walking speeds.

8.5.1 Relation between FMCH and VPP

From Fig. 1, the distance between VPP and hip (r) is

$$r = \sqrt{r_{\text{VPP}}^2 + r_h^2 + 2 r_h r_{\text{VPP}}\, cos\gamma} \tag{14}$$

In addition, the angle between line from VPP to hip and trunk axis ψ' can be found by

$$\psi' = \arctan \frac{r_{\text{VPP}}\, sin\gamma}{r_h + r_{\text{VPP}}\, cos\gamma}. \tag{15}$$

If VPP angle $\gamma < 20°$, (14) and (15) can be approximated by

$$\begin{cases} r &= r_{\text{VPP}} + r_h \\ \psi' &= \frac{r_{\text{VPP}}\gamma}{r} \end{cases} \tag{16}$$

Eq. (10) gives the required torque τ_{VPP} to have GRF going through VPP. For hip angle range during walking ($\psi < 30°$), this equation can be approximated by the following equation with error less than 1.5%

$$\tau_{VPP} \approx F_s\, l\, \frac{(r_h + r_{\text{VPP}})\psi - r_{\text{VPP}}\gamma)}{l + r_h + r_{\text{VPP}}} = F_s\, l\, \frac{r(\psi - \psi')}{l + r} \tag{17}$$

Setting the hip rest angle to ψ' (meaning $\psi_0 = \psi'$) and replacing l by its average during single support results in the hip torque generated by FMCH. The approximation error for parameter ranges used in walking is less than 2%.

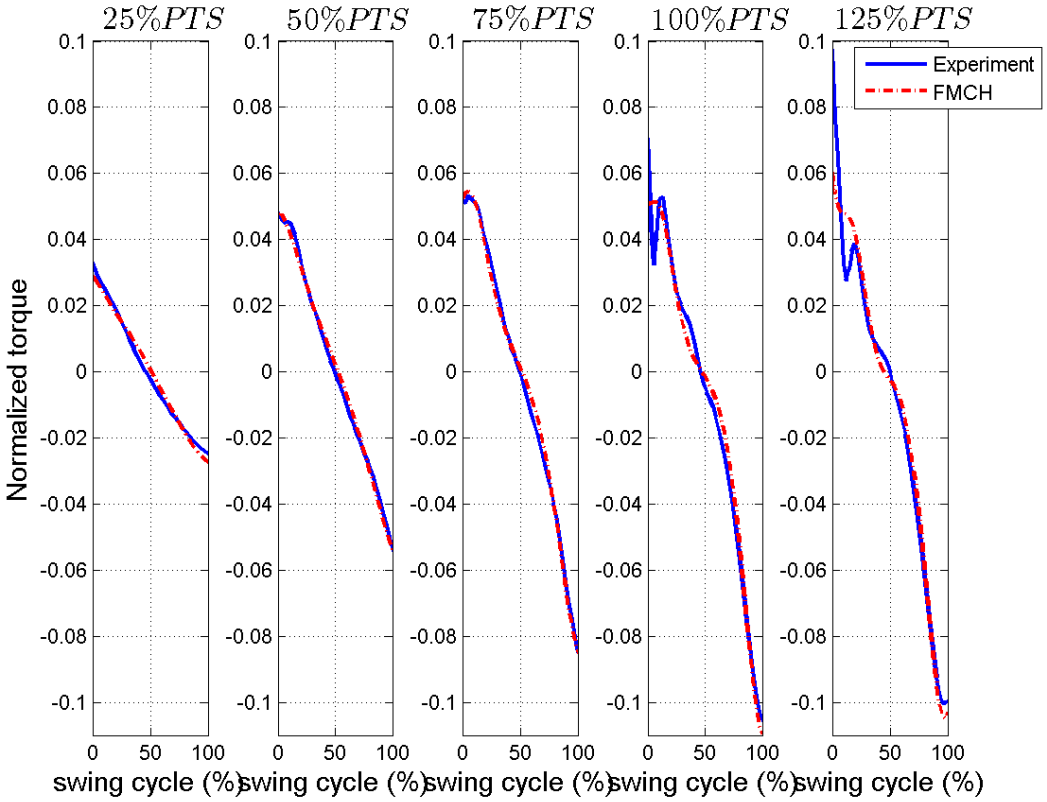

Figure 6: Normalized hip torque to body weight and leg length during single support cycle.

8.5.2 Approximating VPP with FMCH

First, we find FMCH parameters (c and ψ_0) from linear approximation of $r_F^\tau - \psi$ curve. Then, r as the approximated distance of VPP to hip is computed by the following equation

$$r = \frac{\bar{l}c}{(\bar{l}-c)} \tag{18}$$

in which $\bar{l}$ is the average leg length in single support. From (11), (3) and (18) the VPP parameters are calculated as

$$\begin{cases} r_{\text{VPP}} &= r - r_h \\ \gamma &= \frac{r\psi_0}{r_{\text{VPP}}} \end{cases} \tag{19}$$

8.6 ACKNOWLEDGMENT

This research has been supported in part by the German Research Foundation (DFG) under grants no. SE 1042/6-2 and STR 533/7-2 and in part by the EU project BALANCE under Grant Agreement No. 601003.

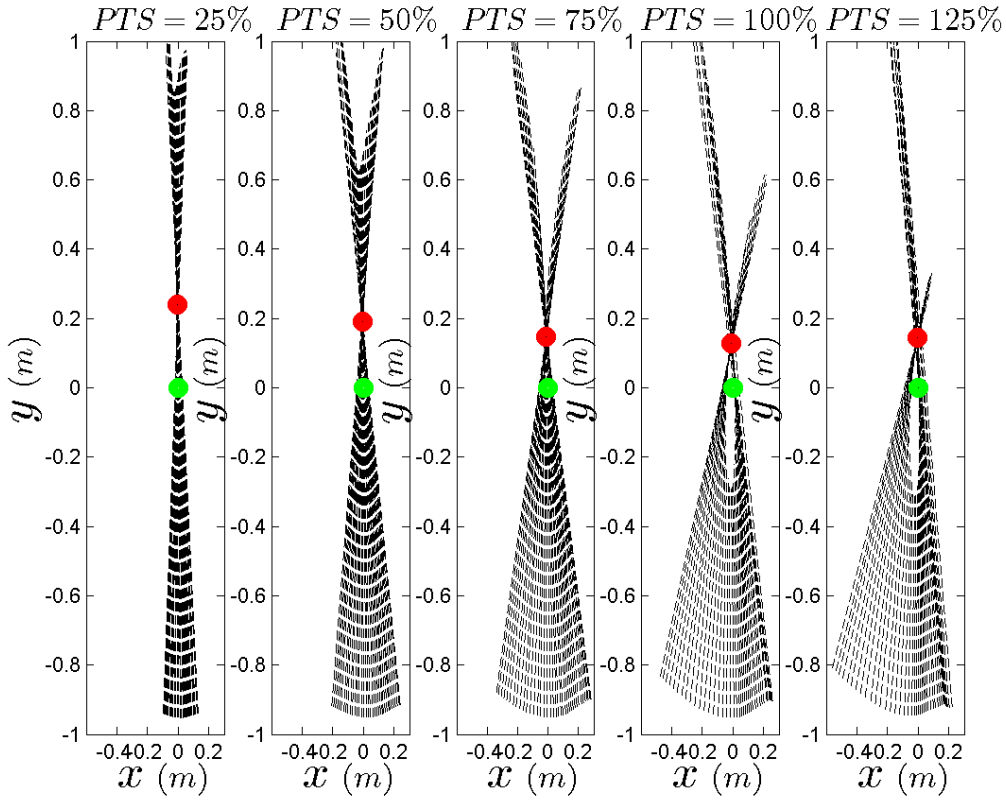

Figure 7: Ground reaction forces from CoP. The coordinate system is centered at CoM (green circle) and aligned with trunk orientation. Red circles show VPPs, estimated by FMCH.

8.7 AUTHOR CONTRIBUTIONS

Maziar A. Sharbafi is the main and corresponding author of the article. He developed the new model of posture control and was responsible for the conception and design of simulations, analysis and interpretation of experimental data and writing of the manuscript. Andre Seyfarth was the supervisor of the project and contributed to developing concepts and models. He has also supported writing the paper.

8.8 REFERENCES

Blickhan, R. (1989). The spring-mass model for running and hopping. *Journal of Biomechanics*, 22(11):1217–1227.

Desai, R. and Geyer., H. (2013). Muscle-reflex control of robust swing leg placement. In *IEEE International Conference on Robotics and Automation, (ICRA 2013)*.

Full, R. J. and Koditschek, D. (1999). Templates and anchors: Neuromechanical hypotheses of legged locomotion on land. *Journal of Experimental Biology*, 22:3325–3332.

Geyer, H. and Her, H. (2010). A muscle-reflex model that encodes principles of legged mechanics produces human walking dynamics and muscle activities. *IEEE Transactions on Neural Systems and Rehabilitation Engineering*, 18(3):263–273.

Geyer, H., Seyfarth, A., and Blickhan, R. (2003). Positive force feedback in bouncing gaits? *Proceedings of the Royal Society B*, 270.

Geyer, H., Seyfarth, A., and Blickhan, R. (2006). Compliant leg behaviour explains basic dynamics of walking and running. *Proceedings of the Royal Society B*, 273(1603):2861–2867.

Günther, M. and Schmitt, S. (2010). A macroscopic ansatz to deduce the hill relation. *Journal of theoretical biology*, 263(4):407–418.

Hill, A. V. (1938). The heat of shortening and the dynamic constants of muscle. *Proceedings of the Royal Society B*, 126.

Hyon, S.-H. and Emura, T. (2005). Symmetric walking control: Invariance and global stability. In *IEEE International Conference on Robotics and Automation (ICRA)*, pages 1455–1462, Barcelona, Spain.

Lipfert., S. W. (2010). *Kinematic and dynamic similarities between walking and running*. Verlag Dr. Kovaĉ,.

Maus, H. M., Lipfert, S., Gross, M., Rummel, J., and Seyfarth, A. (2010). Upright human gait did not provide a major mechanical challenge for our ancestors. *Nature Communications*, 1(6):1–6.

Maus, H. M., Rummel, J., and Seyfarth, A. (2008). Stable upright walking and running using a simple pendulum based control scheme. In *Advances in Mobile Robotics*.

McMahon, T. and Cheng, G. (1990). The mechanics of running: How does stiffness couple with speed? *Journal of Biomechanics*, 23:65–78.

Poulakakis, I. and Grizzle, J. (2007). Formal embedding of the spring loaded inverted pendulum in an asymmetric hopper. In *in Proc. of the European Control Conference*, Kos, Greece.

Poulakakis, I. and Grizzle, J. W. (2009). The spring loaded inverted pendulum as the hybrid zero dynamics of an asymmetric hopper. *IEEE Transaction on Automatic Control*, 54(8):1779–1793.

Raibert, M. H. (1986). *Legged Robots that Balance*. MIT Press, Cambridge MA.

Rummel, J. and Seyfarth, A. (2010). Passive stabilization of the trunk in walking. In *International Conference on Simulation, Modeling and Programming for Autonomous Robots*, Darmstadt, Germany.

Saranlı, U., Buehler, M., and Koditschek, D. (2001). Rhex: a simple and highly mobile robot. *International Journal of Robotic Research*, 20(7):616–631.

Sato, A. and Beuhler, M. (2004). A planar hopping robot with one actuator: Design, simulation, and experimental results. In *4 IEEE/RSJ International Conference on Intelligent Robots and Systems*.

Seyfarth, A., Geyer, H., Guenther, M., and Blickhan, R. (2002). A movement criterion for running. *Journal of Biomechanics*, 35(5):649–655.

Sharbafi, M. A., Ahmadabadi, M. N., Mohammadinejad, M. J. Y. A., and Seyfarth, A. (2013a). Compliant hip function simplifies control for hopping and running. In *IEEE/RSJ International Conference on Intelligent Robots and Systems (Iros 2013)*.

Sharbafi, M. A., Ahmadabadi, M. N., Yazdanpanah, M. J., and Seyfarth, A. (2013b). Novel leg adjustment approach for hopping and running. In *Dynamic Walking*.

Sharbafi, M. A., Maufroy, C., Ahmadabadi, M. N., Yazdanpanah, M. J., and Seyfarth, A. (2013c). Robust hopping based on virtual pendulum posture control. *Bioinspiration and Biomimetics*, 8(3).

Sharbafi, M. A., Maufroy, C., Seyfarth, A., Yazdanpanah, M. J., and Ahmadabadi, M. N. (2012). Controllers for robust hopping with upright trunk based on the virtual pendulum concept. In *IEEE/RSJ International Conference on Intelligent Robots and Systems (Iros 2012)*.

Sharbafi, M. A. and Seyfarth, A. (2013). Human leg adjustment in perturbed hopping. In *AMAM*.

Sharbafi, M. A. and Seyfarth, A. (2014). Stable running by leg force-modulated hip stiffness. In *IEEE International Conference on Biomedical Robotics and Biomechatronics (BioRob 2014)*.

9 Article VIII: A new biarticular actuator design facilitates control of leg function in BioBiped3

Authors:

Maziar Ahmad Sharbafi, Christian Rode, Stefan Kurowski, Dorian Scholz, Rico Möckel, Katayon Radkhah, Guoping Zhao, Aida Mohammadinejad Rashty, Oskar von Stryk and Andre Seyfarth

Technische Universität Darmstadt

64289 Darmstadt, Germany

Published as a paper in

Boinspiration and Biomimetics, IOP Publishing Ltd, 2016.

ABSTRACT

Bioinspired legged locomotion comprises different aspects, such as (i) benefiting from reduced complexity control approaches as observed in humans/animals, (ii) combining embodiment with the controllers and (iii) reflecting neural control mechanisms. One of the most important lessons learned from nature is the significant role of compliance in simplifying control, enhancing energy efficiency and robustness against perturbations for legged locomotion. In this research, we investigate how body morphology in combination with actuator design may facilitate motor control of leg function. Inspired by the human leg muscular system, we show that biarticular muscles have a key role in balancing the upper body, joint coordination and swing leg control. Appropriate adjustment of biarticular spring rest length and stiffness can simplify the control and also reduce energy consumption. In order to test these findings, the BioBiped3 robot was developed as a new version of BioBiped series of biologically inspired, compliant musculoskeletal robots. In this robot, three-segmented legs actuated by mono- and biarticular series elastic actuators mimic the nine major human leg muscle groups. With the new biarticular actuators in BioBiped3, novel simplified control concepts for postural balance and for joint coordination in rebounding movements (drop jumps) were demonstrated and approved.

9.1 INTRODUCTION

A large number of roboticists and biologists explore bio-inspired design and control of legged robots. Advantages of having compliant legs are well accepted both in biomechanical studies of animal (Alexander, 2002) and human locomotion (Geyer et al., 2006) as well as in legged robot movement (Grizzle et al., 2009; Raibert, 1986). Improving energy efficiency (Alexander, 1990), robustness against perturbations (Raibert, 1986; Alexander, 1990), achieving higher speeds(Alexander, 2002), overcoming bandwidth limitations of actuators (Spagna et al., 2007) and simplifying control (Kubow and Full, 1999), are some of the main advantages gained by compliant design. Pneumatic actuators (Hosoda et al., 2010; Vanderborght et al., 2008), compliant mechanisms (e.g., leaf spring (Grizzle et al., 2009) or archery bow (Brown and Zeglin, 1998; Altendorfer et al., 2001)), series elastic actuators (SEA) with coiled springs (Pratt and Krupp, 2004), and emulated compliance (impedance control) with hydraulic actuators (Raibert et al., 2008; Semini et al., 2011) or electric motors (Seok et al., 2014) are the most common engineering solutions to achieve compliant legs in robots. One of the simplest leg morphologies based on the spring mass model of locomotion (Blickhan, 1989; Full and Koditschek, 1999) is the prismatic leg (Raibert, 1986; Ahmadi and Buehler, 2006). With such a high level of abstraction, just some basic concepts of locomotion can be investigated. However, conceptual models like the SLIP (spring loaded inverted pendulum) (Blickhan, 1989) can also be utilized as templates for design and control of legged robots with more complex body structure (e.g., segmented leg with two (Grizzle et al., 2009; Hutter et al., 2010) or three segments (Sharbafi et al., 2014)). Although compliant legs seem to be crucial in legged locomotion there is certainly more we can learn from natural leg morphology when designing and controlling bio-inspired legged robots. With appropriate body design, more freedom in maneuverability alongside simplicity in control may be achieved.

In the BioBiped project [26], we are working on designing biologically inspired robots with leg musculoskeletal structures similar to humans in order to apply locomotion concepts for representing human-like motor control in different gaits. The three-segmented legs of the BioBiped robots are equipped with compliant mono-/biarticular structures that mimic the main nine human leg muscle groups. They are implemented by series elastic actuators (SEA) consisting of cables and springs in combination with electrical actuators or just passive springs.

[26] www.biobiped.de

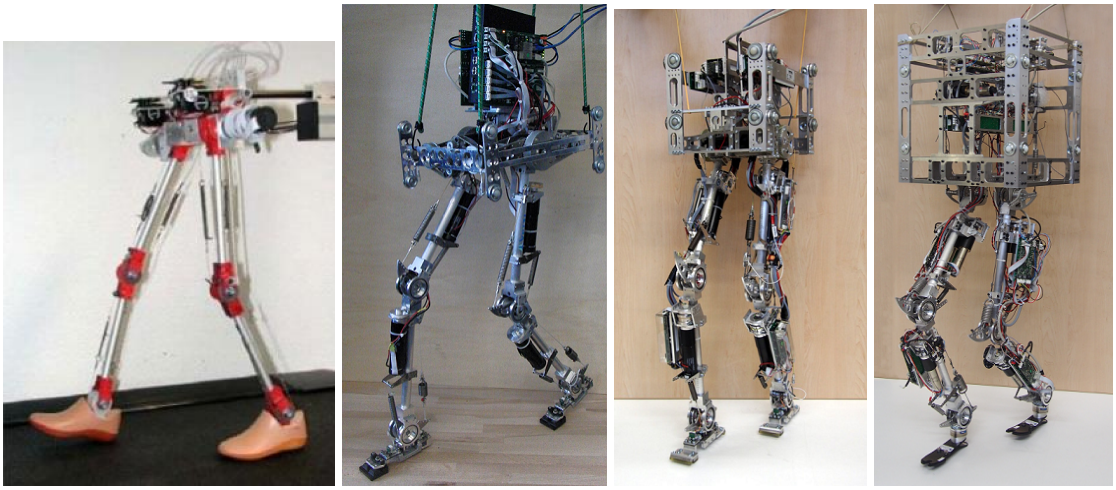

(a) (b) (c) (d)

Figure 1: Different generations of the musculoskeletal BioBiped robot series and its predecessor: (a) JenaWalker II, (b) BioBiped1 (2) BioBiped2 (c) BioBiped3.

In the first and second versions of BioBiped robots, monoarticular knee and ankle extensors besides hip muscle were active. However, biological studies on humans show that biarticular muscles have a key role in the single support phase of locomotion (Prilutsky et al., 1998). In addition, recent simulation studies by us and colleagues illustrate the importance of biarticular muscles in simplifying control in leg swinging (Sharbafi et al., 2017) and postural balance (Lakatos et al., 2014). Based on these evidences and experimental results with previous versions of BioBiped on hopping, active biarticular muscles have been introduced into the new version of our BioBiped robot, BioBiped3. With this new design we may adjust biarticular muscle parameters to (i) decouple rotational leg function from axial leg function in the stance phase, (ii) achieve swing leg control with biarticular muscles decreasing energy consumption, and (iii) benefit from synchronizing segment movements based on the system dynamics (Scholz, 2015; Scholz et al., 2012).

Recently, bio-inspired leg designs with musculoskeletal architecture were applied to legged robots (Klein and Lewis, 2009; Lewis and Klein, 2008; Liu et al., 2015). As a result, novel robot designs with both biarticular and monoarticular actuators were realized (Hosoda et al., 2010; Liu et al., 2015). However, in these studies biarticular actuation is mainly employed for coordination between two joints and transferring energy from one joint to another. Here, we benefit from biarticular actuation in different aspects to facilitate the control of locomotion sub-functions (bouncing, leg swinging and balancing) (Seyfarth et al., 2012). Compared to pneumatic muscles, which are mainly used in bio-inspired bipedal robot designs (Hosoda et al., 2010; Liu et al., 2015), SEA provides controllability in addition to elasticity.

9.2 BIOBIPED ROBOT

The goal of the BioBiped project was to investigate and realize human-like stable locomotion in humanoid robots (Radkhah et al., 2011). In contrast to conventional rigid bipeds, BioBiped robot series (shown in Fig. 1) are developed based on compliant musculoskeletal bipedal systems using series elastic actuators (SEA) as replacement for biological muscles. In JenaWalker II ÙŚ(Fig. 1a), the predecessor of the BioBiped robot series, a single electric motor at the hip was utilized to actuate each leg in which energy is transferred to other joints through passive springs resembling human muscles. The BioBiped project aims at providing more advanced testbeds for experimental evaluation of hypotheses from biomechanics

and investigate bio-inspired mechanisms' roles in different leg functionalities, required in locomotion. It offers the flexibility to change various mechanical configurations like spring stiffnesses, attachment points and the addition or removal of certain structures to compare different hardware setups. Also, it features a vast range of on-board sensors to not only allow for real-time control, but also provide additional data for monitoring and offline analysis. To reach aforementioned targets, we planned two steps, (i) development and application of conceptual models in a real robot mimicking human locomotion and (ii) searching for an appropriate mechanical structure in a robot to represent human muscle functions in locomotion. Therefore, in the BioBiped series of robots, the robot leg morphology (e.g., segments' length ratio) is designed based on human leg properties.

In order to achieve human-like motion performance on a robot with comparable power to weight ratio, SEAs with the potential to store and release energy in their elastic components are utilized. Placing the spring between gear head and the joint, results in passive protection of the gears and motors from impacts. In the new design, besides considering more flexibility in actuation and more precise measurements, we corrected some deviations from anthropomorphic characteristics of previous BioBiped versions.

9.2.1 Hardware structure

The BioBiped3 is a two-legged musculoskeletal robot with elastic joint actuation. Each leg is constructed as a chain of three rigid segments (thigh, shank, and foot) connected by three 1-DOF joints (hip pitch, knee pitch, and ankle pitch) per leg (see Fig. 2 and Table. 1). The actuation is performed by serial elastic actuators (SEA). For this, conventional DC-motors change the lengths of attached cables, which are in series with linear springs, to move the respective joints. The springs' stiffnesses are between 2.4 kNm^{-1} and 19.4 kNm^{-1}. Since with these SEAs we cannot change spring stiffnesses online during experiments we adjust the springs' rest lengths using motor position control. With this continuous rest length adjustment we can emulate different (or nonlinear) stiffnesses. There is no limitation for changing the rest lengths if they are inside the maneuverable range of the joints. Physical constraints (e.g., mechanical lock at the knee for preventing hyper extension) may just reduce maneuverability and as a result will limit adjustable rest length ranges. The wire-driven actuation can generate only pulling forces similar to biological muscles. Thus, for mimicking the human musculoskeletal system, we use antagonistic actuators to pull the leg segments forward and backwards. A main advantage of the wire-driven actuation is the flexibility of the structure, e.g., to adapt the lever arms and springs. Currently, the power supply (24 V, 40 A) is external, but the robot is designed to have an on-board battery.

The torso of the BioBiped3 houses three actuators for each leg (Fig. 2a). One of them is used to actuate the hip joint. For antagonistic actuation, two cables are applied to the same hip motor, such that one of these cables is shortened depending on the direction of rotation. The other two motors are used to mimic the biarticular structures Rectus Femoris (RF) and Hamstrings (HAM) and actuate both hip and knee joints. Each thigh houses two actuators, shown in Fig. 2a. One actuator, which corresponds to the Vastus (VAS) muscle, is used to perform the extension motion of the knee. The second motor of the thigh is applied to actuate the biarticular Gastrocnemius (GAS) muscle. The shank houses one motor corresponding to the Soleus (SOL) muscle for extending the ankle. The retraction motion (flexion) in knee (Popliteus, PL) and ankle (Tibialis Anterior, TA) are implemented using antagonistic passive springs. The properties of the mechanical design of BioBiped3 are presented in Table. 1. More technical information about BioBiped3 is presented in Scholz (2015). Locking the motor position in a SEA mimics a passive spring while switching off the (backdrivable) motors results in damper-like behavior of the motors. Therefore, we can employ all muscles as (passive) spring, serial spring-damper or (active) compliant actuators depending on their contributions in a specific task, except PL and TA which are just passive springs.

Table 1: Main characteristics of the BioBiped3 robot. Biarticular muscles RF, HAM and GAS refer to Rectus Femoris, Hamstrings and Gastrocnemius, respectively. Monoarticular muscles TA, SOL, VAS, GM, IL and PL represent Tibialis Anterior, Soleus, Vastus, Gluteus Maximus, Iliopsoas and Popliteus, respectively. The active cable transmission and the body design are shown in Fig. 2.

Dimensions and masses	
Segment lengths	$l_{trunk} = 0.37$ m; $l_{thigh} = 0.33$ m; $l_{shank} = 0.33$ m; $l_{foot} = 0.16$ m
Segment masses	$m_{trunk} = 8.7$ kg; $m_{thigh} = 2$ kg; $m_{shank} = 1.2$ kg; $m_{foot} = 0.4$ kg
Foot	Ossur Flex Foot Junior from carbon fiber
Leg length	0.7 m (from hip to sole with extended leg)
Total mass	15.9 kg
Body CoM	0.01 m above the hip joint
Actuation	
Motors	12 maxon EC-powermax 22, brushless, 120 W, gear ratio 51:1
Active	SEA for RF, HAM, SOL, VAS, GL, IL, GAS
Passive	passive springs for TA, PL
Stiffnesses	adjustable
Sensors	
IMU	ADIS 16364 with 6 axes
Encoders	motor positions: incremental & absolute
	joint positions: absolute
Force sensors	ATI F/T Sensor: Mini45; 6 axes sensor below ankle joint
Control system	
Hardware	13 custom made microcontroller boards;
	EtherCAT communication
Software	Orocos Real-Time Toolkit
	Robot Operating System (ROS)

9.2.2 Software architecture

For the BioBiped3 robot, a flexible control infrastructure is implemented. Embedded electronics distributed among the robot read out position and force sensors and provide low-level motor control. All electronics are connected via an EtherCAT communication bus that allows reading sensory data and sending control commands at a rate of 1 kHz into/from a standard or embedded PC. Higher level control is implemented on this PC in C++ using an Orocos Real-Time Toolkit and the ROS Robot Operating System. Non-real-time applications for user interfaces, monitoring, and analyzing data from robot operation are implemented in Python.

9.2.3 Modifications in BioBiped design

Based on simulation and experimental studies on previous versions of the BioBiped robot, we considered the following modifications in the BioBiped3 design (a summary is presented in Table.2).

- **Hip actuation:** We found the hip actuation mechanism based on pushing springs and a timing belt too inefficient and unpredictable. Furthermore, the maximum spring compression of the series elastic element was too limited and it was impossible to change the spring coefficients. The new

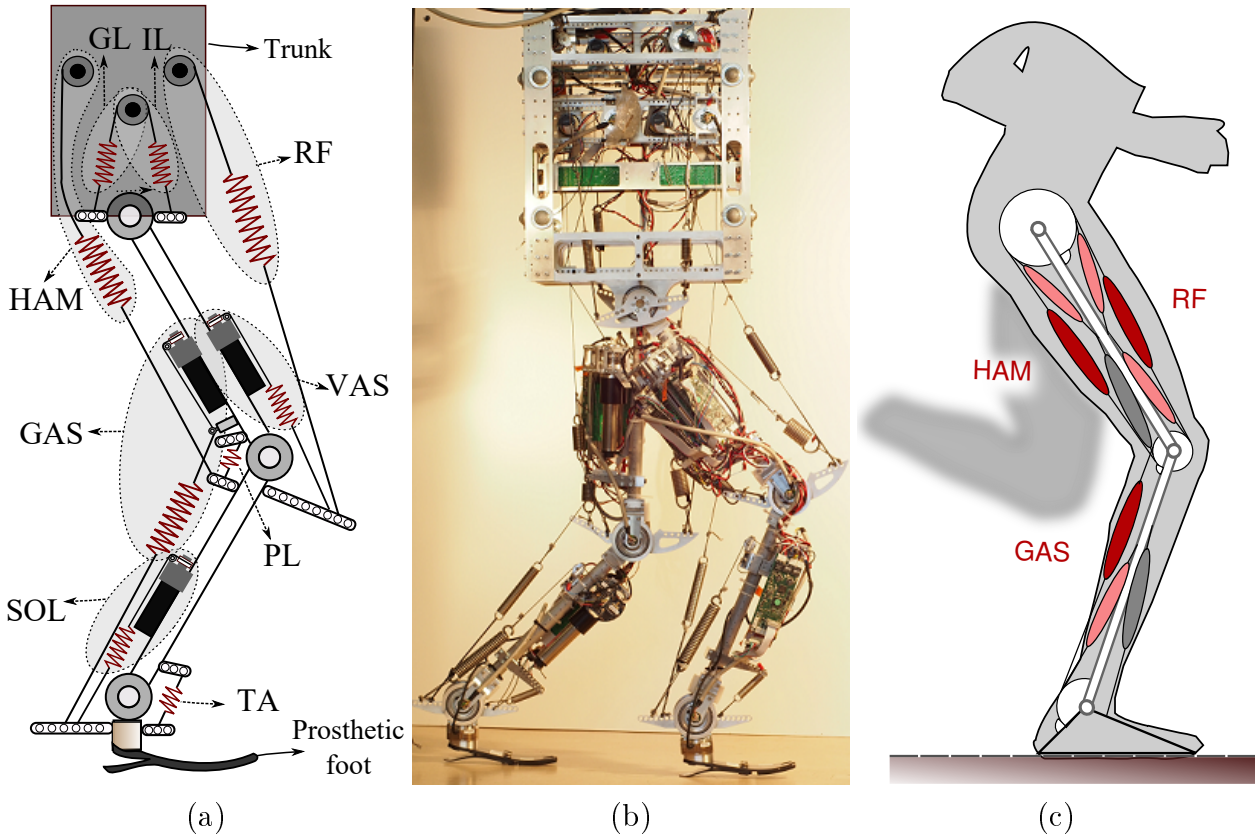

Figure 2: The BioBiped3. (a) Schematic of trunk, one leg, foot, and actuators. This figure shows the structure used in developing the multi-body system (MBS) simulation model and to manufacture the real robot. (b) Real robot in standing configuration. (c) Schematic bio-inspired BioBiped3 sagittal plane actuation. New active serial elastic actuators (red, passive in Biobiped2), active monoarticular serial-elastic actuators (light red), and passive monoarticular muscles (grey).

design is based on the actuation concept of the BioRob manipulator in which one motor is considered to pull the lever arm in two antagonistic directions through two springs (see Fig. 2a). Thus, spring coefficients can easily be adapted and maintained.

- **Foot design:** The feet in BioBiped1 and BioBiped2 are bending under high ground contact forces. This results in plastic deformation and leads to limited capabilities. The new robot includes prosthetic feet. These are made from carbon fiber with a thin 2 mm rubber layer underneath. They are constructed to withstand high ground reaction forces, especially at impacts. In addition, they can easily be exchanged to test other prosthetic foot models.

- **Force sensors:** In the previous versions, the ground reaction force sensors evaluate the applied force based on the deflection of the feet. This approach is neither sufficient for precise calibration, nor deterministic due to the plastic deformation of the feet. The new construction includes off-the-shelf 6-axis force sensors (see Table. 1 for details) with sufficient capabilities to identify the applied forces.

- **Active biarticular muscles:** Simulation studies beside experimental results revealed that active biarticular structures can improve the performance of the robot. In the new design six motors are considered for each leg, instead of three in the previous versions. Two of the additional motors

Table 2: Modifications in BioBiped3

Problem	Solution
Flexibility in hip actuation	Antagonistic SEA design
Foot design	Prosthetic foot
Low quality force sensors	Industrial force sensor
Passive biarticular muscles	Actuated biarticular muscles
Efficiency of motors	Brushless DC motor
Not anthropomorphic CoM	Larger and heavier trunk
Higher inertia of leg than trunk	Larger and heavier trunk

are applied to actuate biarticular thigh structures. In addition, the last motor can be used to actuate either the Gastrocnemius or the knee flexor.

- **Efficient motors:** We replaced the brushed DC motors with 120 W brushless motors. As a result, we increased power density and actuation to suffice for the increased total weight of the robot construction.
- **Anthropomorphic CoM:** The overall center of mass of the previous robots was slightly below the hip rotation axis. This is not corresponding to the dynamical properties of the human body. For this reason, and also in order to house the additional actuators, the dimensions of BioBiped3 torso were increased. With these measures, the robot CoM shifted to above the hip rotation axis which is more anthropomorphic.
- **Higher trunk inertia:** The larger trunk containing more mechanical devices (e.g. six motors) also increased the inertia of the trunk leading to higher trunk inertia than leg inertia which facilitates swing leg control without losing the upright trunk orientation.

Among all these modifications, using active biarticular muscles is the crucial step that can facilitate robot control especially when mimicking human behavior in locomotion. In the next section, we elaborate on the significance of biarticular muscles for this based on simulation and experimental analysis.

9.3 ACTIVE BIARTICULAR MUSCLES FOR SIMPLIFIED MOTOR CONTROL

The design of the musculoskeletal system is the outcome of a long evolution (Bobbert and van Soest, 2000). The human musculoskeletal system is equipped not only with muscles spanning one joint (monoarticular muscles), but also with muscles spanning two joints, called biarticular muscles (Fig. 2c). The causes for these muscles pose a long-standing research problem. Leonardo da VinciâĂŹs lion robot (equipped with a central motor pulling strings) already illustrated what Cleland (Cleland, 1867) termed the “ligamentous action” of biarticular muscles, namely that heavy muscles can be located proximally while transferring energy to the distal end of the limbs. This reduces inertia of fast moving limbs and thus contributes to efficient legged gait. Further, the joint coupling can increase the working range and improve the working point of monoarticular muscles (Schenau, 1989). Recent research could demonstrate that biarticular muscles can facilitate i) balancing (Lakatos et al., 2014), ii) control of the leg swing phase (Dean and Kuo, 2008; Sharbafi et al., 2017), and iii) generating the whole running motion (Lakatos et al., 2014).

The following Sections 9.3.1 to 9.3.4 motivate and outline human/robot experiments and simulations that substantiate the claim that may clarify whether biarticular muscles facilitate motor control. The corresponding results are shown in Sections 9.4.1 to 9.4.4.

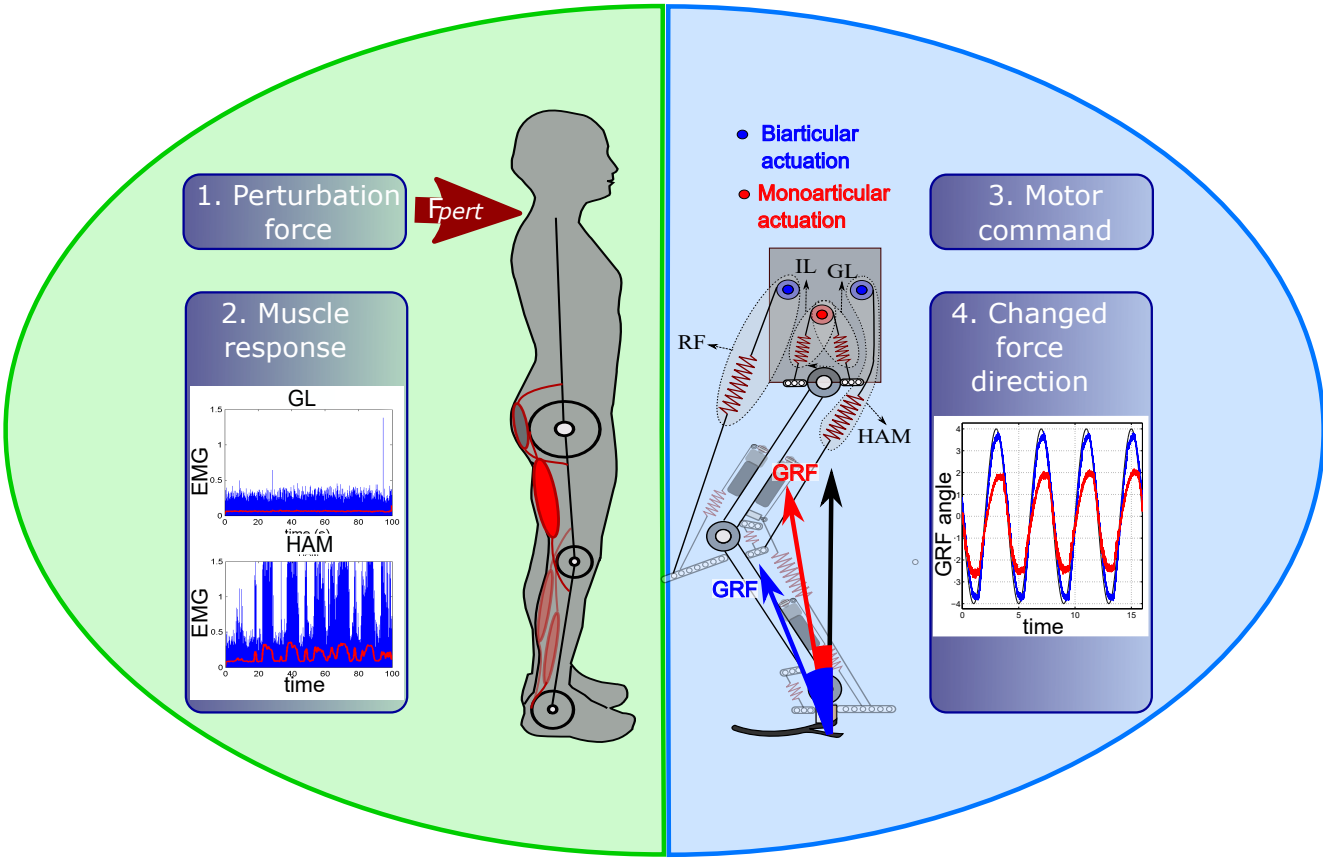

Figure 3: Experimental analysis of muscle functions in human standing and transfer to robot experiment. (1) Horizontal forces applied to the human result in (2) corresponding increases in EMG of biarticular muscles like HAM but inconsistent or no changes of monoarticular muscles like GL. (3) Introducing muscle forces through motor patterns in the robot lead to (4) responses in leg force orientation. The unique feature of biarticular muscles to respond to and to create horizontal forces was found in humans and in the robot.

9.3.1 Stance leg

Biarticular muscles can generate considerable components of ground reaction force perpendicular to the leg axis (line from ankle to hip joint) in the sagittal plane (Hof, 2001; Schenau, 1989). Perpendicular leg force is associated with postural control. A conceptual musculoskeletal arrangement with 2:1 hip to knee and ankle to knee moment arm ratios of biarticular muscles and equal thigh and shank lengths enables exclusive regulation of perpendicular leg force independent of the knee angle via biarticular muscles (Lakatos et al., 2014). At the same time, the length change of the biarticular thigh muscles depends on the virtual leg angle (orientation of leg axis) with respect to the trunk. Biarticular thigh muscles do produce ground reaction force contributions matching those produced by hip torques in a model with telescopic leg. Moreover, when the biarticular thigh muscles are modeled as spring, they resemble a hip spring in a telescopic leg model (Maus et al., 2010). This means that control concepts like the virtual pivot point (VPP) developed with models with trunk and massless telescopic legs (Maus et al., 2010) can be seamlessly transferred to models with trunk and massless *segmented* legs.

In recent human standing experiments we evaluated whether the conceptual musculoskeletal arrangement can explain muscle EMG (electromyography) activity (Tokur et al., 2015). Subjects were repeatedly exposed to a static external force applied at different positions of the body in the sagittal plane, and were

instructed to hold their position. Assuming that the static torques can be balanced by either the action of biarticular muscles or by the action of monoarticular muscles, clear hypotheses can be drawn which muscles should increase in EMG activity. The concept of facilitating posture control using biarticular muscles in both human and robot experiments are illustrated schematically in Fig. 3.

To further elaborate on the function of biarticular muscles during locomotion, we implemented this conceptual design into a rigid-body model (trunk and three-segmented legs).With the help of biarticular muscles, human running can be decomposed into a set of tasks which can be directly addressed (Lakatos et al., 2014). This was demonstrated using a simple control scheme for a 7-link model (trunk and three leg segments with mass) capable of human-like bipedal running. The model was equipped with biarticular thigh and shank SEAs, and a knee SEA. The morphology, followed the conceptual morphology described above, is associated with elastic decoupling of axial and perpendicular leg function that enabled the task decomposition. These results support the suggested role of biarticular leg muscles in achieving postural balance.

9.3.2 Swing leg

Biarticular muscle force shows a characteristic pattern during the swing phase in human walking (Prilutsky et al., 1998). In (Sharbafi et al., 2017), we combined the spring-loaded inverted pendulum (SLIP) model (Blickhan, 1989) for the stance leg with a double pendulum model representing the swing leg which is called DPS (Double pendulum +SLIP, depicted in Fig. 4). It was shown (Sharbafi et al., 2017) that tuned biarticular springs can replicate the muscle forces during the swing phase while at the same time the double pendulum reproduces the kinematic pattern of the human swing leg motion. Given adequate initial conditions of the swing leg segments at the beginning of the swing phase, the parameters of the biarticular springs (e.g. their rest lengths) may be set prior to the swing phase to yield human-like swing leg motion. Thus, in a robot with locking mechanism, the spring rest length can be adjusted and locked at takeoff to have a completely passive swing leg in walking.

In order to evaluate the applicability of this swing leg control, we tested it in the BioBiped multi-body model for forward hopping. In (Sharbafi et al., 2014), we applied the VMC (virtual model control) to mimic a virtual spring between the hip and the foot for axial leg function (bouncing) control and VBLA (velocity based leg adjustment) (Sharbafi et al., 2012) for swing leg control in forward hopping. Since the focus is on swing leg adjustment, to handle posture control the upper body is physically constrained to be upright, similar to the alternate hopping experiment on a treadmill [27]. During the flight phase the knee actuator adjusts the leg length with controlling the knee angle (to 146° inner joint angle in this experiment) using a PID controller. In VBLA, the monoarticular hip actuator adjusts the orientation of the leg axis (from hip to ankle) with respect to the horizontal axis (leg angle α), computed from the CoM velocity vector. The control quality was tested by starting from hopping in place, switching to forward hopping with a certain speed and returning to zero speed, by changing the VBLA parameter (Sharbafi et al., 2014).

In the here presented BioBiped3 simulation study, the monoarticular hip muscles are removed during the flight phase and the swing leg is controlled using adjustable biarticular (RF and HAM) thigh springs. The biarticular thigh muscles (represented as a SEA in BioBiped3) work only if the SEA spring is loaded. With hip to knee lever arm ratio of 2 to 1 for these muscles and equal thigh and shank length, this requires that the leg angle α is above (or below) a corresponding rest angle as shown in Fig. 4b, i.e. $\alpha > \alpha_{RF0}$ for RF and $\alpha < \alpha_{HAM0}$ for HAM. To implement this approach in the BioBiped3 model, we adjust these two rest angles to achieve a certain speed. Therefore, similar to the passive rebound experiment (Sec. 9.3.4),

[27] See `https://www.youtube.com/watch?v=ew_qhFEh6TM`

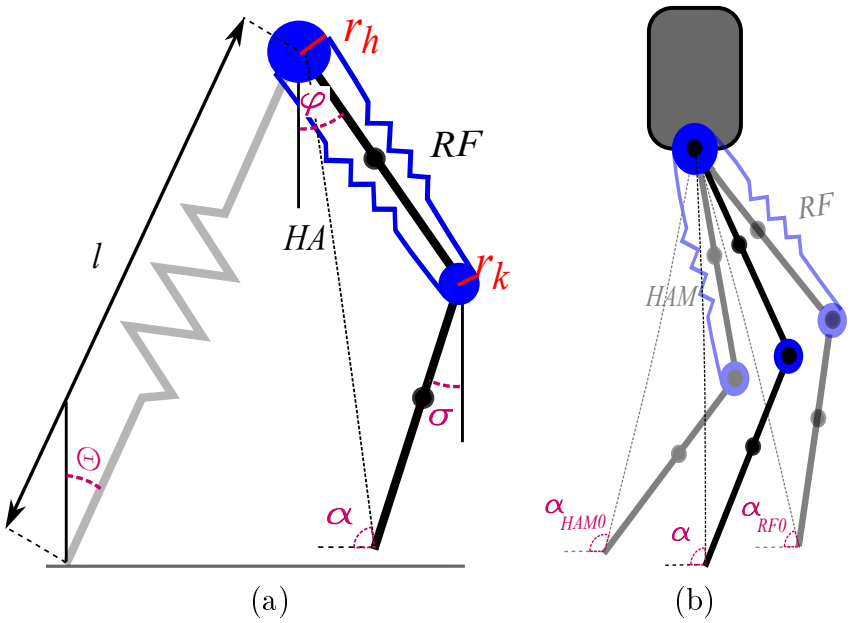

Figure 4: (a) DPS (double pendulum+SLIP) model with additional biarticular springs for swing leg control Sharbafi et al. (2017). (b) Definition of leg angle (α) RF and HAM rest angles (α_{RF0} and α_{HAM0}) when the hip to knee lever arm ratio is 2 to 1 and the thigh and shank lengths are equal.

by locking motor positions during the swing phase, all muscles (except GL/IL which are removed) are simplified to become passive springs and the robot behaves like a passive elastic structure. In this control strategy, to reach a certain speed, the thigh biarticular muscles' rest angles are adjusted once (with a step-like signal at the first takeoff after getting a new speed) and kept until a new desired speed is set. In contrast to VBLA, we do not need to measure the CoM velocity to find the desired angle of attack. Therefore, no sensor is required except the foot force sensor for detecting the takeoff.

9.3.3 GRF direction control experiment

In order to demonstrate the advantages of using biarticular HAM and RF muscles for stance leg control (compared to monoarticular IL and GL muscles), we conducted GRF direction control experiments in the BioBiped3 robot during stance. Each experiment includes either (i) active biarticular thigh (HAM/RF) SEAs, or (ii) active monoarticular hip (IL/GL) SEAs. Hip to knee moment arm ratios for both biarticular SEAs are about 2:1. A sine trajectory is set as the desired GRF direction for both legs. The robot trunk is constrained in a frame and could only move up or down. IL/GL SEA motor is off (acting as a damper because the motor is back-drivable) during the experiment of controlling GRF direction with biarticular SEAs. Biarticular SEAs are removed during the experiment of controlling GRF direction with IL/GL SEAs. In both cases, all other joints' SEAs (except knee VAS) act as passive springs (fixed motor position control). With ankle force sensor feedback, a simple PID controller is implemented for active motors. PID parameters were tuned for different experiments, separately.

To investigate how the knee angle affects the results, the experiments are performed in two different knee configurations:

1. static (standing): VAS motor shaft position is fixed. VAS act as a passive spring. Knee angle is about 26 degree during the experiment.

2. dynamic (squatting): VAS motor shaft position is controlled by a sinusoidal wave with frequency 0.125 Hz. Knee angle changes from 14 degree to 41 degree during the experiment.

9.3.4 Joint synchronization with biarticular structures

In order to achieve maximum jumping performance, a sequential extension of leg joints from proximal to distal is required (Bobbert and van Ingen Schenau, 1988). Using an articulated physical model of the vertical jump, Bobbert et al (Bobbert et al., 1987) showed that the timing of the GAS activation is critical to obtain a maximum effect. By transferring energy between joints, biarticular RF and GAS helps the monoarticular extensors (at hip and knee) to remain active until take-off without damaging the joints (Bobbert and van Ingen Schenau, 1988). In addition, in human hopping in place, GAS muscle activation provides a rapid ankle extension which has a large effect on the vertical velocity (by translating the stored energy into velocity) resulting in greater hopping heights.
Here, we design a vertical passive rebound experiment with the BioBiped3 robot to analyze the GAS rest length effect on synchronizing ankle and knee joints and energy management at impact. In this experiment, we drop the robot from a certain height (h_0 of 7.5 cm and 15 cm, two trials for each height) and investigate the role of the GAS in recoiling the energy to the system to gain higher hopping height after rebounding. All motors are locked in fixed positions, representing muscles with passive springs having fixed rest lengths and stiffnesses. GAS muscle is also passive, but the rest length is changed from one trial to the next. We decrease the GAS rest length (l_0^{GAS}) from 0 cm to -5 cm while $l_0^{GAS} = 0$ cm gives no interaction from GAS. Therefore, the robot mimics a passive structure using motor position control.

9.4 RESULTS

In this section we present the results of the different human/robot experiments and simulations outlined in Sec. 9.3. In Sec. 9.4.1, *a human perturbed standing experiment* shows the important contribution of biarticular muscles in posture control through the *stance leg*. Then, DPS and BioBiped MBS simulation models are employed in Sec 9.4.2 to generate *stable walking and forward hopping* using passive biarticular thigh muscles for *swing leg control*. *GRF direction control experiments* with BioBiped3 in Sec. 9.4.3 show how biarticular muscles help *facilitate leg force control*. Finally, the *passive rebound experiment with BioBiped3* in Sec. 9.4.4 demonstrates *synchronization of adjacent joints* by the biarticular GAS muscle.

9.4.1 Human perturbed standing experiment

In perturbed standing experiment the EMG is utilized to identify the muscle contribution to perturbation recovery. Sample responses for monoarticular GL and biarticular HAM muscles are shown in Fig. 3 (see more details in (Tokur et al., 2015)). The EMG of the biarticular muscles increased consistently, as expected in the theoretical model. Monoarticular muscles did not show a consistent EMG response. This indicates that biarticular muscles are the main contributors in the production of required torques to withstand the external force. This is in line with previous findings on the role of biarticular muscles in postural control (Hof, 2001; Schenau, 1989). The contribution of monoarticular muscles for balance control needs further investigations. For instance, in our static experiment they might be used to fine-tune the static joint torques due to deviations of human muscle arrangement from conceptual design. We take advantage of these insights in the design and control of the novel BioBiped3 robot (see Sec. 9.4.3).

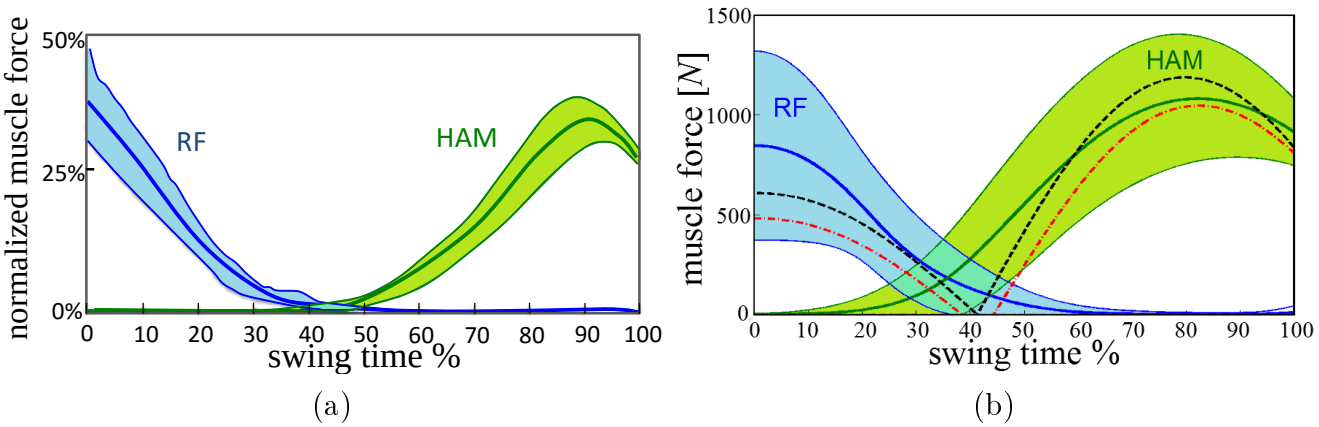

Figure 5: Biarticular thigh muscle forces during swing phase of walking (a) at speed 1.8 m/s of human experiment (data adopted from (Prilutsky et al., 1998)) (b) at speed 1.55 m/s of stable simulations with different combinations of rest length and stiffness for RF and HAM. The mean values and standard deviation are shown with solid and thin lines, respectively. Dashed lines indicate parameter combinations that result in no overlap between RF and HAM forces similar to human data.

9.4.2 Swing leg control

The addition of passive biarticular thigh muscles with an appropriate set of rest length and stiffness to the DPS model can produce human-like leg kinematics during swing phase of walking (Sharbafi et al., 2017). Fig. 5 shows that the biarticular muscle force patterns in the simulation model are similar to human biarticular muscles (during the swing phase), and stable walking can be achieved in a large range of biarticular thigh muscle parameters. Although the overlap between working regions of RF and HAM in simulations is more than the negligible (with very low forces) range in the human experiments, there are sets of parameters which result in no overlapping. Two samples of such behavior are depicted with dashed lines in Fig. 5; red with no-force region from 38% to 44% of swing time and black with no-force moment at 41% of swing time. In the BioBiped3 robot, the ability to adjust the biarticular muscle rest length enables us to test this simple swing leg control strategy for different gaits in hardware.

Besides providing a certain angle of attack and ground clearance, the swing leg also has a noticeable contribution to the GRF (Zhao and Seyfarth, 2015). As can be seen in Fig. 6, during the swing phase of human walking, swing leg force is in phase with the GRF in vertical direction while it is out of phase in horizontal direction. Swing leg force magnitude is about 25% of GRF at regular walking speeds. This means that the swing leg partially supports the vertical GRF and with counteracting in the horizontal direction helps balancing the upper body. Similar contribution of the swing leg movement in GRF can be observed in the DPS model equipped with biarticular passive springs having appropriate stiffness and rest angles. Therefore, adjustment of biarticular muscles (springs) in the swing leg will also support GRF control and balancing.

The same simple control approach for leg swing like in the DPS model, applied to the BioBiped MBS model for forward hopping, results in stable forward hopping with adjustable speed (as explained in Sec. 9.3.2). Fig. 7 shows the result of changing hopping speed using this technique. The simulated robot movement starts from zero horizontal speed (hopping in place) and we tune the RF and HAM rest lengths to certain values (shown in Table. 3) which results in moving forward. Note that these parameters are adjusted once and are kept constant until the next speed change. With that we achieve forward hopping

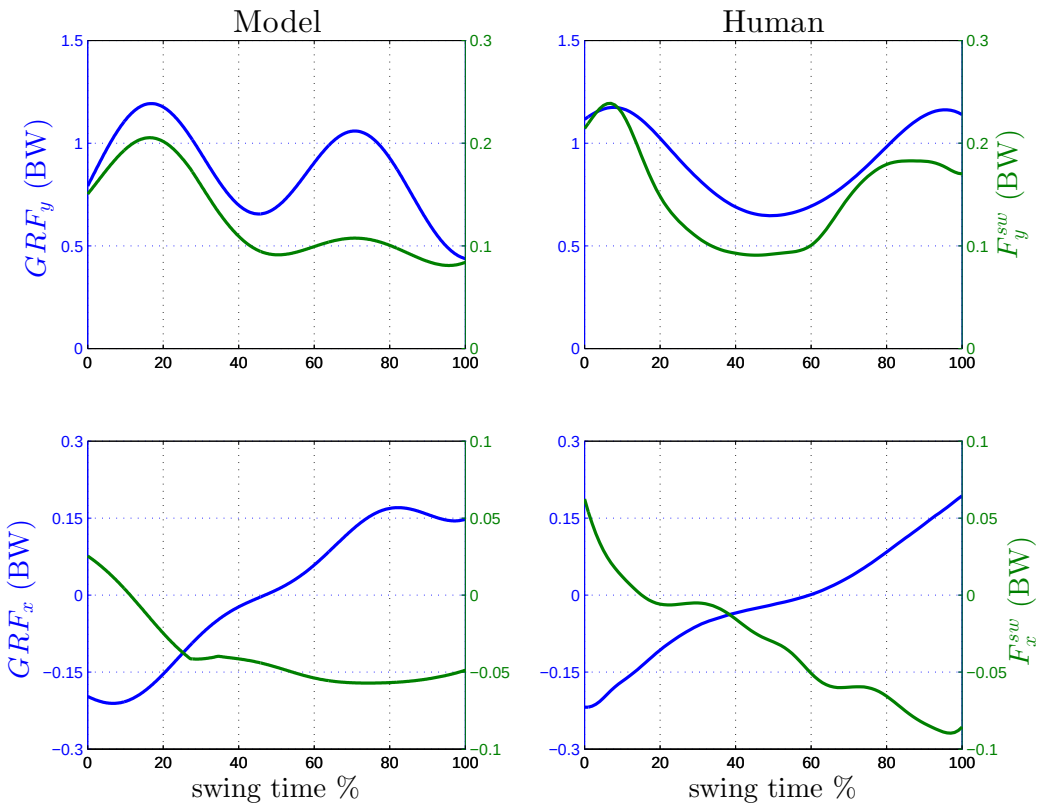

Figure 6: Swing leg force contribution to GRF during walking (at 1.55m/s) in the DPS model with biarticular thigh springs (left column) and in human experiments (right column). Subscripts x and y denote the force in vertical and horizontal directions and superscript sw stands for swing leg force. All forces are normalized by body weight (BW). The experimental data is the average value for nine subjects (see details of experiment in (Zhao and Seyfarth, 2015)).

at 1.5 m/s speed with passive swing leg adjustment. After five seconds both muscles rest lengths are decreased (Table. 3). This results in larger (smaller) working region of RF (HAM), which changes the angle of attack and swing leg angular velocity to return to hopping in place. Unlike feedback control for swing leg adjustment (e.g., VBLA), here we just set the biarticular muscles' rest angles to achieve different speeds and even changing the gait.

9.4.3 GRF direction control in BioBiped3

In this section, we show the results of GRF direction control during standing and squatting. As both legs are operating in parallel, only the results of one leg are presented in Fig. 8 and Fig. 9. The first experiment was the static standing. In Fig. 8(left), tracking of the GRF angle with monoarticular and biarticular muscles without changing the leg configuration is shown. Control with biarticular muscles is more precise in adjusting leg force direction than control with monoarticular ones. Note that, if the monoarticular muscle force increases to improve the tracking of GRF direction, the resulting axial leg forces (due to cross-talk) interferes with leg length control (through knee angle control with VAS). This means that VAS control would need to compensate for the cross-talk to preserve axial leg configuration. In order to control the GRF direction with monoarticular muscles and also keeping the static conditi-

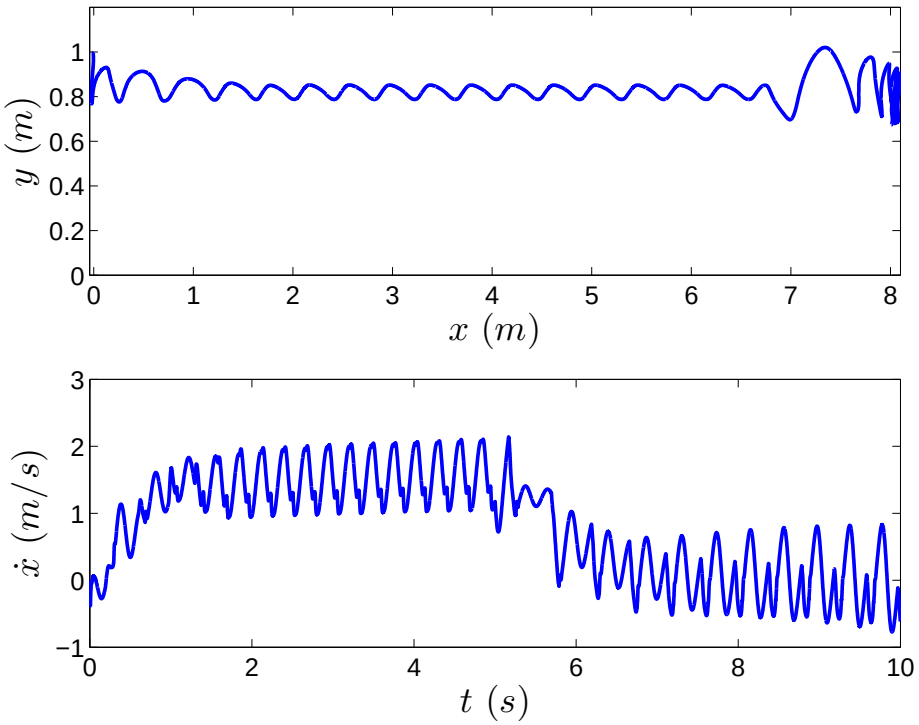

Figure 7: Trunk CoM motion in sagittal plane (top) and horizontal speed (bottom) in switching between hopping in place and forward hopping with the BioBiped multi-body-system (MBS) model (Radkhah, 2013) (shown in Fig. 2a) using adjustable passive biarticular thigh muscles. Simulation starts with switching from hopping in place to forward hopping. Swing leg control changes at $t = 5$ to return again to hopping in place.

on (without movement), additional energy in the knee actuator is needed. With monoarticular muscle control, not only the tracking error of GRF directon in control is much higher than that in control with biarticular ones but also variations in the GRF magnitude and in the knee angle are much higher. Fig. 9 shows similar results for the squatting (dynamic) motion. Higher errors in control with monoarticular muscles and larger oscillations in GRF magnitude can be observed in this figure. The reason for larger oscillations in control with monoarticular muscles is its interference with knee actuator controller. However, the knee actuator is able to handle such effects which results in less than 2 degrees differences between knee angles in two cases. The smaller the deviations from the desired GRF direction when using monoarticular muscles, the larger the errors in the kinematic behavior of the knee.

9.4.4 Passive rebound experiments with BioBiped3

The passive rebound experiments show how biarticular actuators can support the axial leg function by synchronizing adjacent joints. Fig. 10 shows the knee angle versus the ankle angle for one leg during the first rebound of the robot. A linear relation between these two angles means synchronized joints operation. In an extreme case, if the knee vs. ankle joint angles' graph becomes a straight line, it signifies that the two joints are completely synchronized and will move (extend/flex) together. With this definition, the knee and ankle joints are synchronized during falling for different GAS rest lengths, in contrast to rebound. The largest deviation from the linear relationship occurs when we remove GAS ($l_0^{GAS} = 0$ cm) while the smallest deviation is achieved with ($l_0^{GAS} = -4$ cm). This value also results in maximum rebounding height (2 *cm*) as shown in the attached video, while the largest variation corresponds to the

Table 3: Thigh biarticular muscle parameters (stiffness k and rest angle α) in forward hopping speed adjustment.

Parameter	Acceleration	Deceleration
α_{RF0}	90°	60°
α_{HAM0}	105°	100°
k_{RF}	12000 N/m	12000 N/m
k_{HAM}	12000 N/m	12000 N/m

lowest rebounding height. Synchronous joint operation is efficient as a positive (negative) joint work occurs in both joints at the same time. With this, internal energy losses by transferring positive work from one joint to negative work of the adjacent joint are avoided.

9.5 DISCUSSIONS

A new biologically inspired biped robot was developed to investigate control concepts, extracted from simulations, human gaits studies and previous robot experiments. In addition to improving the robot hardware design using high quality sensors, motors and well suited feet, some modifications in actuation structure were considered.

The SEA design applied now to biarticular muscles enabled these actuators to work as passive springs with adjustable rest length (e.g., for swing leg control and improved energy management) or active compliant actuators for injecting energy (e.g., for postural control in the stance phase). Enhancement in leg control quality using biarticular actuators was demonstrated by simulations and experiments of BioBiped3 robot. The multi-functionality of active biarticular structures can be exploited to facilitate control of locomotion sub-functions. Simplicity in control means simple controller rules (like PD or bang-bang control) and the minimum requirement of sensory information which are gained by aid of more complexity in mechanical design. For example, with the similar properties of SEA at hip monoarticular and thigh biarticular muscles, GRF control by monoarticular muscle is worse (larger errors and more oscillations) than that by biarticular muscle. To achieve similar performance, higher control effort and larger sensor and actuator bandwidth are required. These items can be used to assess simplification of control (e.g., with information-entropy-based approach presented in (Haeufle et al., 2014)) achieved by biarticular muscles.

Having biarticular actuators besides common monoarticular ones, provides several advantages which cannot be achieved by just two adjacent monoarticular actuators. Four of them which are demonstrated with experiments and simulations in this paper are: 1) direct access to perpendicular leg function with one actuator, 2) synchronizing adjacent joints without need for sensory feedback and high bandwidth actuator 3) passive energy transfer between adjacent joints 4) using motor redundancy (multiple actuators acting on one joint) to simplify control. In the following we discuss how these properties are achieved and how they can help improve locomotion control performance.

9.5.1 Posture control

The larger and the more consistent contribution (activation variations) of biarticular muscles (e.g., HAM) compared to monoarticular ones (e.g., GL) in perturbed standing experiments supports the idea of employing biarticular muscles for control of the perpendicular component of the GRF (Sec. 9.4.1). Therefore, providing access to balance control with small effects on axial leg function during the stance phase may help benefit from distribution of GRF control to different mono- or biarticular muscles. As a result,

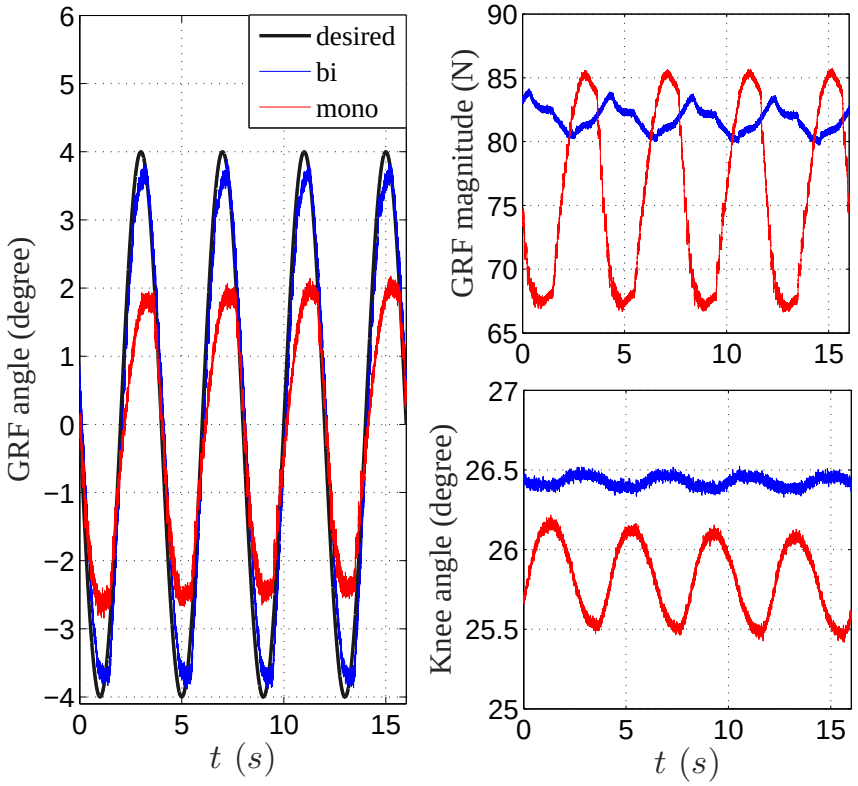

Figure 8: Ground reaction force (GRF) direction control using monoarticular (mono) hip or biarticular (bi) thigh actuators in static (standing) condition with the desired GRF angle (desired). GRF angle and magnitude and the knee angle are shown.

a simpler posture control strategy may be provided employing an appropriate mechanical design even with redundancy in actuators.

In order to validate this idea on our robotic setup (BioBiped3), GRF direction control experiments were performed in static and dynamic conditions (Sec. 9.4.3). These experiments demonstrate that the cross-talk between control of GRF direction and axial leg function is lower in biarticular compared to monoarticular muscles. The larger influences of hip torque produced by monoarticular muscle on force in the axial direction (compared to biarticular muscle) behave like disturbances for knee motor position control and result in larger oscillations in GRF magnitude. In spite of some unmodeled dynamics in the real robot such as friction and inertia, the biarticular actuator can still decouple perpendicular from axial leg force. In both cases, static and dynamic, biarticular actuators perform better than monoarticular hip actuators in terms of GRF direction control. Especially in the dynamic case, GRF direction oscillates a lot when it is controlled with monoarticular hip actuators. This indicates that we can use biarticular actuators to facilitate balance control. Roughly speaking, the ability to focus the leg force in a desired direction allows for simple control strategies like VPP (Maus et al., 2010).

Compared to upright standing, during locomotion the joint torques might rely more on system and muscle dynamics (e.g. exploiting the intrinsic compliance of muscles) rather than on precise control of joint torques. Sudden perturbations could then be compensated by the action of biarticular muscles, which can instantaneously change perpendicular leg force as described above. Human walking experiments support the suggested role of these muscles in tripping recovery (Pijnappels et al., 2005).

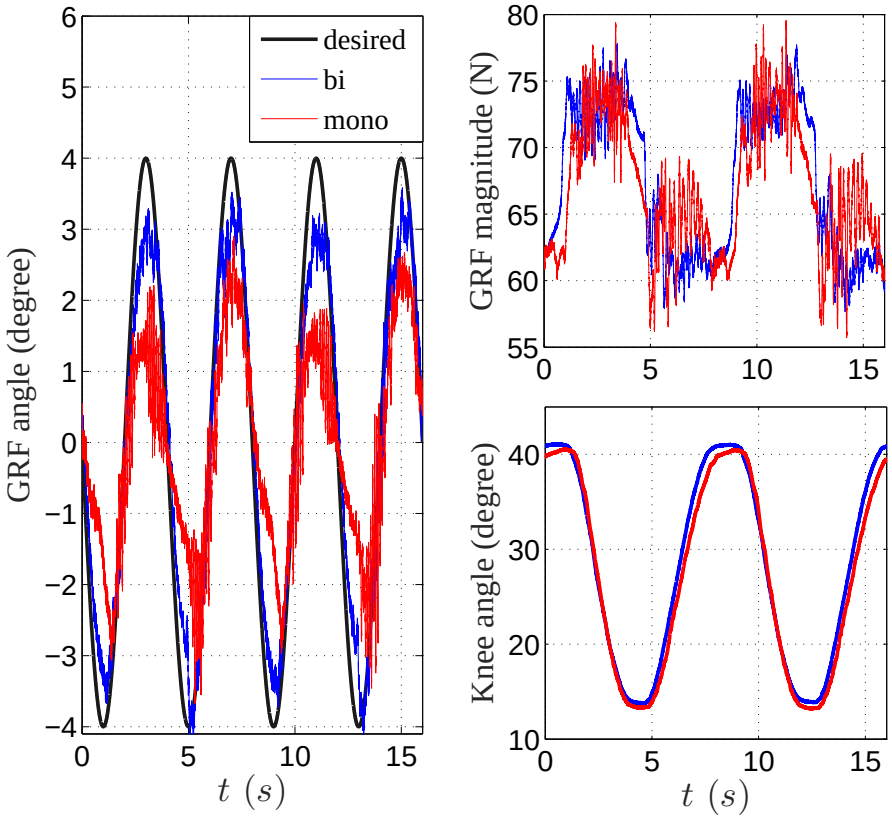

Figure 9: Ground reaction force control using monoarticular (mono) hip or biarticular (bi) thigh actuators for dynamic (squatting) motion with the desired GRF angle (desired). GRF angle and magnitude and the knee angle are shown.

9.5.2 Swing leg control

During the swing phase, biarticular actuators can support swing leg rotational movement control while monoarticular actuators (e.g., knee or ankle joints) can provide (axial) leg shortening and lengthening required for ground clearance. Such a task distribution can simplify control to setting spring rest lengths to a specific value for each gait condition (Sec. 9.4.2). This simple control strategy which is able to produce human-like force and kinematic behavior in walking, was also implemented on BioBiped model for forward hopping. Setting the biarticular springs rest angles to new values for changing the motion speed provides the simplest swing leg control approach without needing sensory information of the joints (e.g., angles or angular velocities). Designing non-backdrivable actuators enables setting the springs' rest lengths to desired values and switching off the motors (no actuation) to have maximum efficiency during different phases of locomotion (e.g., swing phase).

In (Zhao and Seyfarth, 2015), the stance and swing leg movement contributions in human walking dynamics are analyzed. It is shown that their effects on the GRF are in-phase in the vertical direction, increasing the axial loading of the leg; in the horizontal direction, their effects nearly cancel. With the proposed DPS model with biarticular passive springs, similar contributions of swing leg in GRF can be obtained (Fig. 6). This further supports the idea of a far-reaching mechanical decoupling of an axial and a non-axial leg function. Therefore, using biarticular thigh springs not only results in stable and human-like swing leg movement, but also supports GRF control and balancing.

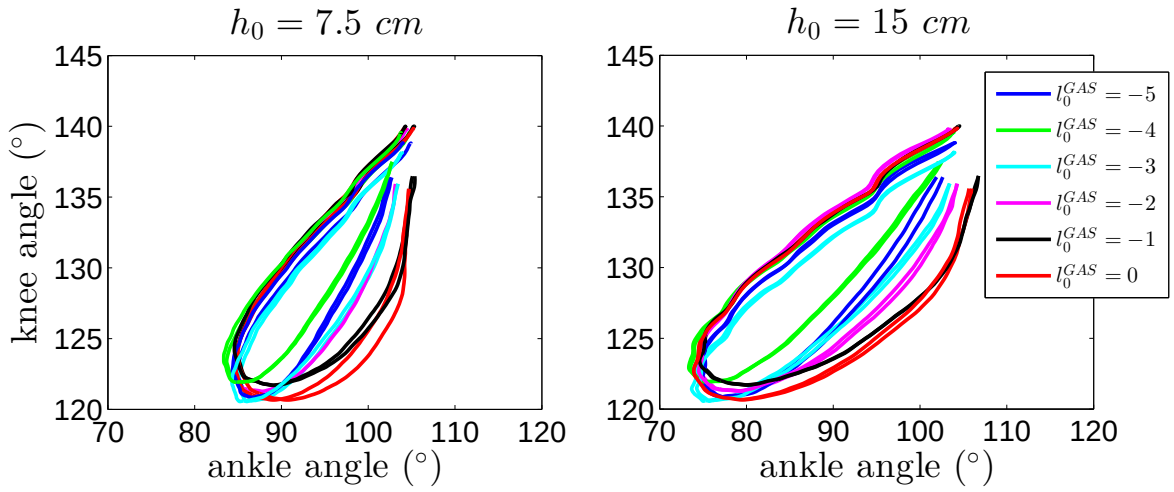

Figure 10: Synchronization of knee and ankle joints via the biarticular GAS muscle. Relative GAS length is given in cm. Two trials for each dropping height (h_0) with a specific GAS rest length (l_0^{GAS}) are shown with the same color.

9.5.3 Energy management in stance

In addition to reducing energy consumption with the aid of biarticular muscles during the swing phase, such intelligent structures can support energy recoiling from one joint to another in the stance phase. If not perfectly tuned during stance phase of a bouncy task like jumping, adjacent joints (e.g., knee and ankle) act against each other or work out of phase. This results in inter-joint losses or asynchronous movements of joints which can be reduced using biarticular muscles (Babič et al., 2009; Bobbert et al., 1987; Bobbert and van Ingen Schenau, 1988). With our passive rebound experiment (Sec. 9.4.4), we could confirm that a passive biarticular muscle (GAS) with appropriate resting length can transfer energy from one joint to the other and improve jumping height instead of losing that energy by opposing actuations in adjacent joints. As shown in Fig. 10, for a specific motion condition, one rest angle for GAS muscle results in the most synchronized joints' movement and the highest energy recoiling. Therefore, an adjustable GAS in BioBiped3 enables us to select the optimal value for each gait. As a result, we can benefit from geometry and physics instead of synchronization between two monoarticular actuators which needs precise measurements, actuators with large control effort, high bandwidth and detailed system knowledge.

Concluding, humanoid robots with bio-inspired design and control principles can demonstrate and evaluate biomechanical motion concepts and theories on legged locomotion. The versatile biarticular thigh muscles have the potential to simplify balance control in BioBiped3 during upright standing and locomotion. In addition, the Gastrocnemius can be applied to improve the axial leg function in bouncing tasks (Sec. 9.4.4) and was predicted to contribute to the catapult mechanism (Lipfert et al., 2014) in walking. In future, the novel anthropomorphic BioBiped3 robot can be used to demonstrate the enhanced motion capability regarding the locomotion sub-functions (repulsion, balance and swing leg motion) and in combining these features for achieving different gait patterns and gait conditions (e.g. speed and step length).

9.6 ACKNOWLEDGMENT

This research has been supported in part by the German Research Foundation (DFG) under grants no. SE 1042/6-2 and STR 533/7-2 and in part by the EU project BALANCE under Grant Agreement No. 601003.

9.7 AUTHOR CONTRIBUTIONS

Maziar A. Sharbafi is the main and corresponding author of the article. He was responsible for the conception and design of simulations and experiments, analysis and interpretation of data and writing of the manuscript. Christian Rode provided the modeling of biarticular muscles, simulation studies on ground reaction force control through biarticular muscles and human perturbed standing experiment. He has also a large contribution in writing and revising the paper and discussions. Stefan Kurowski provided the materials for BioBiped Robot section specially the hardware structure in addition to pictures of the robot. Dorian Scholz developed the software architecture and was one of the key developers of the BioBiped robots' hardware and basic control software. He also was the main person who handled maintenance of the robot and designed experiments with different series of BioBiped robot during different years. In addition, he contributed in writing parts of the article in Sec. 9.2, about the software architecture. Rico Möckel has been leading the group of researchers and students responsible for the design and implementation of the BiBiped3 hardware. He has also supported the paper writing process by contributing text and comments. Katayon Radkhah also contributed to the design of the BioBiped3 robot. Furthermore, she developed a detailed multi-body simulation model of the robot on actuation level which was used for forward hopping control. Guoping Zhao was the main person who implemented the experiments on BioBiped3 robot, collected data and provide descriptions in Sec. 9.4.3 and 9.4.4. Aida Mohammadinejad Rashty built the simulation model of DPS for swing leg control and mimicked human muscle actuations with this model. She provided the descriptions of Sec. 9.3.2. Oskar von Stryk and Andre Seyfarth were the supervisors of the project from the two groups involved in this project. They provided fundamental ideas to the BioBiped project and its successful funding by the German Research Foundation DFG and assisted for the revision of the article.

9.8 REFERENCES

Ahmadi, M. and Buehler, M. (2006). Controlled passive dynamic running experiments with the arl-monopod ii. *Robotics, IEEE Transactions on*, 22(5):974–986.

Alexander, R. M. (1990). Three uses for springs in legged locomotion. *The International Journal of Robotics Research*, 9(2):53–61.

Alexander, R. M. (2002). Tendon elasticity and muscle function. *Comparative Biochemistry and Physiology Part A: Molecular & Integrative Physiology*, 133(4):1001–1011.

Altendorfer, R., Moore, N., Komsuoglu, H., Buehler, M., Brown Jr, H. B., McMordie, D., Saranli, U., Full, R., and Koditschek, D. E. (2001). Rhex: a biologically inspired hexapod runner. *Autonomous Robots*, 11(3):207–213.

Babič, J., Lim, B., Omrčen, D., Lenarčič, J., and Park, F. (2009). A biarticulated robotic leg for jumping movements: theory and experiments. *Journal of mechanisms and robotics*, 1(1):011013.

Blickhan, R. (1989). The spring-mass model for running and hopping. *Journal of Biomechanics*, 22(11):1217–1227.

Bobbert, M. F., Hoek, E., van Ingen Schenau, G. J., Sargeant, A. J., and Schreurs, A. W. (1987). A model to demonstrate the power transporting role of bi-articular muscles. *Journal of Physiology*, 387(3):24.

Bobbert, M. F. and van Ingen Schenau, G. J. (1988). Coordination in vertical jumping. *Journal of biomechanics*, 21(3):249–262.

Bobbert, M. F. and van Soest, A. J. (2000). Two-joint muscles offer the solution, but what was the problem? *MOTOR CONTROL-CHAMPAIGN-*, 4(1):48–52.

Brown, B. and Zeglin, G. (1998). The bow leg hopping robot. In *IEEE International Conference on Robotics and Automation (ICRA98)*, pages 781–786.

Cleland, J. (1867). On the actions of muscles passing over more than one joint. *Journal of anatomy and physiology*, 1(1):85.

Dean, J. C. and Kuo, A. D. (2008). Elastic coupling of limb joints enables faster bipedal walking. *Journal of The Royal Society Interface*, 6(35):561–573.

Full, R. J. and Koditschek, D. (1999). Templates and anchors: Neuromechanical hypotheses of legged locomotion on land. *Journal of Experimental Biology*, 22:3325–3332.

Geyer, H., A, A. S., and Blickhan, R. (2006). Compliant leg behaviour explains basic dynamics of walking and running. *Proceedings of the Royal Society B: Biological Sciences*, 273:2861–2867.

Grizzle, J. W., Hurst, J., Morris, B., Park, H.-W., and Sreenath, K. (2009). Mabel, a new robotic bipedal walker and runner. In *In Proc. of American Control Conference*, pages 2030–2036.

Haeufle, D., Günther, M., Wunner, G., and Schmitt, S. (2014). Quantifying control effort of biological and technical movements: An information-entropy-based approach. *Physical Review E*, 89(1):012716.

Hof, A. (2001). The force resulting from the action of mono-and biarticular muscles in a limb. *Journal of biomechanics*, 34(8):1085–1089.

Hosoda, K., Sakaguchi, Y., Takayama, H., and Takuma, T. (2010). Pneumatic-driven jumping robot with anthropomorphic muscular skeleton structure. *Autonomous Robots*, 28(3):307–316.

Hutter, M., Remy, C. D., Hopflinger, M., and Siegwart, R. (2010). Slip running with an articulated robotic leg. In *IEEE/RSJ International Conference on Intelligent Robots and Systems (IROS)*, pages 4934–4939. IEEE.

Klein, T. J. and Lewis, M. A. (2009). A robot leg based on mammalian muscle architecture. In *Robotics and Biomimetics (ROBIO), 2009 IEEE International Conference on*, pages 2521–2526. IEEE.

Kubow, T. and Full, R. (1999). The role of the mechanical system in control: a hypothesis of self–stabilization in hexapedal runners. *Philosophical Transactions of the Royal Society B: Biological Sciences*, 354(1385):849–861.

Lakatos, D., Rode, C., Seyfarth, A., and Albu-Schaffer, A. (2014). Design and control of compliantly actuated bipedal running robots: Concepts to exploit natural system dynamics. In *IEEE/RAS International Conference on Humanoid Robots (Humanoids)*, pages 930–937. International Society for Optics and Photonics.

Lewis, M. A. and Klein, T. J. (2008). A robotic biarticulate leg model. In *2008 IEEE Biomedical Circuits and Systems Conference*.

Lipfert, S. W., Günther, M., Renjewski, D., and Seyfarth, A. (2014). Impulsive ankle push-off powers leg swing in human walking. *Journal of Experimental Biology*, 217(8):1218–1228.

Liu, Y., Zang, X., Liu, X., and Wang, L. (2015). Design of a biped robot actuated by pneumatic artificial muscles. *Bio-Medical Materials and Engineering*, 26(s1):757–766.

Maus, H.-M., Lipfert, S., Gross, M., Rummel, J., and Seyfarth, A. (2010). Upright human gait did not provide a major mechanical challenge for our ancestors. *Nature Communications*, 1:70.

Sharbafi, M. A., Mohammadinejad, A., Rode, C., and Seyfarth, A. (2017). Reconstruction of human swing leg motion with passive bi-articular muscle models. *Human Movement Science*, 52: 96–107.

Pijnappels, M., Bobbert, M. F., and van Dieen, J. H. (2005). How early reactions in the support limb contribute to balance recovery after tripping. *Journal of Biomechanics*, 38:627âĂŞ–634.

Pratt, J. E. and Krupp, B. T. (2004). Series elastic actuators for legged robots. In *Defense and Security*, pages 135–144. International Society for Optics and Photonics.

Prilutsky, B. I., Gregor, R. J., and Ryan, M. M. (1998). Coordination of two-joint rectus femoris and hamstrings during the swing phase of human walking and running. *Experimental Brain Research*, 120(4):479–486.

Radkhah, K. (2013). *Advancing Musculoskeletal Robot Design for Dynamic and Energy-Efficient Bipedal Locomotion*. PhD thesis, TU Darmstadt, Department of Computer Science.

Radkhah, K., Maufroy, C., Maus, M., Scholz, D., Seyfarth, A., and von Stryk, O. (2011). Concept and design of the biobiped1 robot for human-like walking and running. *International Journal of Humanoid Robotics*, 8(3):439–458.

Raibert, M., Blankespoor, K., Nelson, G., Playter, R., et al. (2008). Bigdog, the rough-terrain quadruped robot. In *Proceedings of the 17th World Congress*, volume 17, pages 10822–10825.

Raibert, M. H. (1986). *Legged Robots that Balance*. MIT Press, Cambridge MA.

Schenau, G. J. V. I. (1989). From rotation to translation: constraints on multi-joint movements and the unique action of bi-articular muscles. *Human Movement Science*, 8(4):301–337.

Scholz, D. (2015). *On the Design and Development of Musculoskeletal Bipedal Robots*. PhD thesis, TU Darmstadt, Department of Computer Science.

Scholz, D., Maufroy, C., Kurowski, S., Radkhah, K., von Stryk, O., and Seyfarth, A. (2012). Simulation and experimental evaluation of the contribution of biarticular gastrocnemius structure to joint synchronization in human-inspired three-segmented elastic legs. In *3rd International Conference on Simulation, Modeling and Programming for Autonomous Robots (SIMPAR)*, pages 251–260.

Semini, C., Tsagarakis, N. G., Guglielmino, E., Focchi, M., Cannella, F., and Caldwell, D. G. (2011). Design of hyq–a hydraulically and electrically actuated quadruped robot. *Proceedings of the Institution of Mechanical Engineers, Part I: Journal of Systems and Control Engineering*, page 0959651811402275.

Seok, S., Wang, A., Chuah, M., Hyun, D. J., Lee, J., Otten, D. M., Lang, J. H., and Kim, S. (2014). Design principles for energy-efficient legged locomotion and implementation on the mit cheetah robot. *IEEE/ASME Transactions on Mechatronics*.

Seyfarth, A., Grimmer, S., Häufle, D. F., and Kalveram, K.-T. (2012). Can robots help to understand human locomotion? *at-Automatisierungstechnik Methoden und Anwendungen der Steuerungs-, Regelungs-und Informationstechnik*, 60(11):653–661.

Sharbafi, M. A., Maufroy, C., Seyfarth, A., Yazdanpanah, M. J., and Ahmadabadi, M. N. (2012). Controllers for robust hopping with upright trunk based on the virtual pendulum concept. In *IEEE/RSJ International Conference on Intelligent Robots and Systems (Iros 2012)*, pages 2222–2227.

Sharbafi, M. A., Radkhah, K., von Stryk, O., and Seyfarth, A. (2014). Hopping control for the musculoskeletal bipedal robot biobiped. In *IEEE/RSJ International Conference on Intelligent Robots and Systems (IROS)*, pages 4868–4875.

Spagna, J. C., Goldman, D. I., Lin, P.-C., Koditschek, D. E., and Full, R. J. (2007). Distributed mechanical feedback in arthropods and robots simplifies control of rapid running on challenging terrain. *Bioinspiration & biomimetics*, 2(1):9–18.

Tokur, D., Rode, C., Hoitz, F., and Seyfarth, A. (2015). Response of leg muscles (mono- vs. bi-articular) to horizontal perturbations in the sagittal plane. In *25th Congress of the International Society of Biomechanics (ISB2015)*, pages 923–925.

Vanderborght, B., Verrelst, B., Van Ham, R., Van Damme, M., Beyl, P., and Lefeber, D. (2008). Development of a compliance controller to reduce energy consumption for bipedal robots. *Autonomous Robots*, 24(4):419–434.

Zhao, G. and Seyfarth, A. (2015). Contributions of stance and swing leg movements to human walking dynamics. In *International Conference on Climbing and Walking Robots (CLAWAR)*, pages 4868–4875. IEEE.

10 Article IX: How locomotion subfunctions can control walking at different speeds?

Authors:

Maziar Ahmad Sharbafi and André Seyfarth

Technische Universität Darmstadt
64289 Darmstadt, Germany

Published as a paper in

Journal of Biomechanics, ELSEVIER 2017.

ABSTRACT

Inspired from template models explaining biological locomotory systems and Raibert's pioneering legged robots, locomotion can be realized by basic sub-functions: elastic axial leg function, leg swinging and balancing. Combinations of these three can generate different gaits with diverse properties. In this paper we investigate how locomotion sub-functions contribute to stabilize walking at different speeds. Based on this trilogy, we introduce a conceptual model to quantify human locomotion sub-functions in walking. This model can produce stable walking and also predict human locomotion sub-function control during swing phase of walking. Analyzing experimental data based on this modeling shows different control strategies which are employed to increase speed from slow to moderate and moderate to fast gaits.

KEYWORDS:

Bipedal walking, locomotion control, stance leg axial function, swing leg adjustment, posture control, conceptual models.

10.1 INTRODUCTION

Legged locomotion in biological systems is a complex and not fully understood problem. Employing template models (Full and Koditschek, 1999) can simplify understanding of locomotion dynamics and control. Furthermore, large variability of the gaits and also of a specific gait condition (e.g., speed) increase the complexity, especially in case of adapting to a different gait or condition. One adaptation strategy which is common in daily activities is changing the motion speed. Orlovski et al. showed that walking cycle duration decreases with increasing speed which is mainly achieved by shortening the stance phase (Orlovsky et al., 1999). They also claimed that the hip and knee flexion at different speeds are nearly constant (Orlovsky et al., 1999), which is not a precise statement (Lipfert., 2010). From one (microscopic) point of view, muscle actuation adaptation can be considered as a source of inspiration to learn about human control strategies for speed adjustment. In 2002, Hof et al. demonstrated a clear dependency of walking speed on EMG profile (Hof et al., 2002). By analyzing this dependency they could predict the EMG signals for each of 14 leg muscles by functions using 6 constants and 10 speed-dependent basic patterns. These functions can be interpreted as central pattern generators for human walking (Hof et al., 2002). In (Den Otter et al., 2004), the muscle activities from normal walking speed (about 1.4 m/s) to very slow walking (0.06 m/s) were investigated. It was shown that the amplitude of lower extremity muscle activity increases with speed, resulting in positive slope of EMG-speed curves (gain values). However, for very slow speeds, some negative gain values were detected (e.g., in peroneus longus (PL) and rectus femoris (RF)) indicating an increase in EMG amplitude with decreasing walking speed.

From another (macroscopic) point of view, dividing legged locomotion to different sub-functions can simplify understanding operation of such a complex system (Fig. 1a). Elastic axial leg function (stance), rotational swing leg function (leg swinging) and body alignment (balancing/posture control) can be considered as three basic sub-functions of locomotion (Seyfarth et al., 2013, 2012). Aforementioned changes in control strategy (e.g., various trends of activation signals at different speeds) may be attributed to different roles of locomotion sub-functions at different speeds. Accordingly, a specific muscle is activated differently at different gait speeds, because of changing in the role of the related sub-function. For example, posture control at very slow speeds is very different from regular speeds which is achieved by completely different muscle activities (Den Otter et al., 2004).

Neptune et al. analyzed the muscle contributions in speed adjustment and gait switching (Neptune and Sasaki, 2005; Neptune et al., 2008) and showed that even higher activation in a muscle (at higher speeds) may not result in larger forces. For example, from moderate to fast walking, activation of the plantar flexor muscles (gastrocnemius (GAS) and soleus (SOL)) increase with walking speed, while forces developed by these muscles reduce (Neptune and Sasaki, 2005). These decreases in force production are attributed to the intrinsic force-length-velocity properties of muscles. Therefore, analyzing muscle contributions in speed control helps understand human motor control. However, because of the complexity of neuro-muscular systems in humans, without having a conceptual model of locomotion such analyses hardly address motion control concepts. In that respect, template models are simple but useful tools that can point to some important features of legged locomotion (Geyer et al., 2006). Geyer et al. showed that the simple BSLIP (bipedal spring loaded inverted pendulum) model can generate stable walking with different combinations of leg stiffness and attack angle (Geyer et al., 2006). Extension of this model by adding a rigid trunk (called BTSLIP) to represent the upper body helps mimic more features (e.g., posture control) of human walking.

Using BTSLIP model, Maus et al. introduced the virtual pendulum (VP) concept, observed in human walking (Maus et al., 2010). It was shown that during human walking the ground reaction forces intersect in one point above the center of mass (CoM), called virtual pivot point (VPP). As a result, the inverted pendulum model of gait can be translated to a virtual pendulum model at CoM hanged from VPP (Maus et al., 2010). Furthermore, the new *FMCH* (force modulated compliant hip) model was developed in (Sharbafi and Seyfarth, 2015), which employs a feedback signal for tuning the property of the passive mechanical system (spring). This approach suggests a new application of the positive force feedback in the neuro-muscular gait model of Geyer (Geyer et al., 2003; Geyer and Her, 2010). With such conceptual models, stance leg control, swing leg adjustment and postural control using hip torque between the stance leg and the trunk and their contributions to achieve stable walking can be analyzed. However, it was shown that walking with speeds higher than regular walking speed (about 1.4 m/s) is not achievable with such a template model (Geyer et al., 2006). This means that energy management is the missing part in SLIP-based models which prohibits walking fast with such template models. The goal of this study is to realize how humans utilize locomotion sub-functions (Fig. 1a) for stabilizing walking at different speeds based on a neuromechanical template model like FMCH (Sharbafi and Seyfarth, 2015). Our analysis shows that balancing and leg swinging controllers mainly change when the walking speed varies from slow to moderate speeds, while the stance leg controller contributes to the whole range of speeds. In addition, injecting energy during stance (e.g., with push-off) is required for fast walking which cannot be addressed with traditionally conservative SLIP-based models.

10.2 METHODS

In this study we analyze human walking using a new gait model (Fig. 1b). This model is utilized to characterize the locomotion sub-functions (Seyfarth et al., 2013, 2012) with few indicating parameters. Here, the stance leg axial function (stance) and the upper body posture control (balancing) are described by a variable leg spring and a compliant element at hip, respectively, while the swing leg angle of attack and angular velocity characterize the swing leg movement (leg swinging). In this section, first we describe the model and locomotion sub-function controllers. Then, the details of human walking experiment is presented. Finally, we show how the model can help explain (predict) human walking at different speeds.

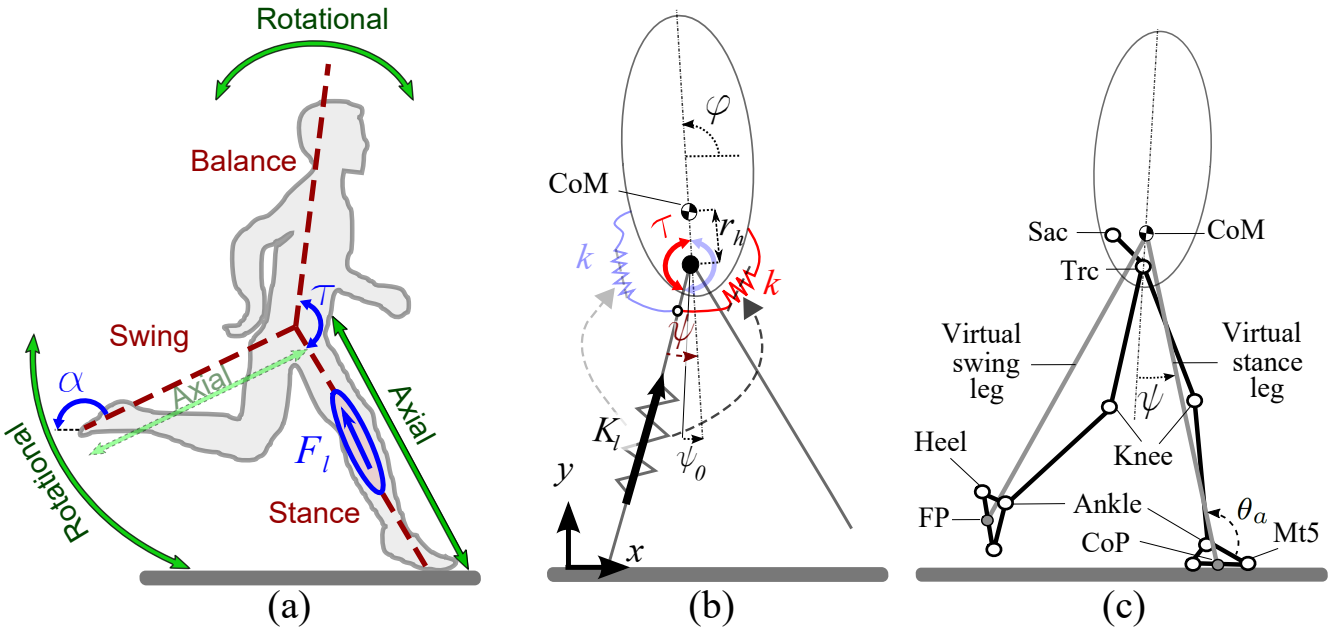

Figure 1: (a) Main locomotion sub-functions: stance (axial leg function), balancing and leg swinging and characterizing them with the leg spring (stiffness K_l), the swing leg angle (α) and the hip torque (τ). (b) FMCH for posture control in bipedal walking. The hip extending torque and counterclockwise angle are considered as positive directions. In current state, the red spring is producing (negative) rotational torque as a hip flexor muscles (Rectus femoris or Iliopsoas) while the blue hip extensor spring is slack. F_l, r_h, ψ, φ, k and ψ_0, are the leg force, distance from hip to CoM, hip angle (trunk to leg), trunk angle, the hip spring stiffness and rest angle, respectively. (c) Marker positions are recorded at the lower back (sacrum, Sac), the hip (greater trochanter, Trc), the knee (lateral knee joint gap), the toe (5th metatarsal joint, Mt5), the heel (calcaneus), and the ankle (lateral malleolus). The virtual stance leg is defined from center of mass (CoM) to center of pressure (CoP). The virtal swing leg is defined from CoM to foot point (FP) which is half way between Mt5 and Heel. The ankle angle θ_a and the hip angle ψ are shown. The figure is adopted from (Lipfert., 2010).

10.2.1 Model

The spring loaded inverted pendulum (SLIP) model is widely used as a template (Full and Koditschek, 1999) to describe locomotion (Seyfarth et al., 2002; Blickhan, 1989; Geyer et al., 2006), for inspiration of building legged robots (Grizzle et al., 2009; Altendorfer et al., 2001; Renjewski et al., 2015), and in legged locomotion control (Poulakakis and Grizzle, 2009; Liu et al., 2015; Sharbafi et al., 2014). We extend the model with a rigid trunk which is called BTSLIP (Bipedal+Trunk+SLIP) model (Sharbafi and Seyfarth, 2015; Rummel and Seyfarth, 2010) (see Fig. 1b). In the BTSLIP model, legs are represented by massless springs and the upper body is modeled by a rigid trunk with mass m and moment of inertia J.

Walking dynamics (gait cycle) has two phases: *single support (SS)* (one leg in contact with the ground) and *double support (DS)* (two legs in contact with the ground). SS starts at takeoff (TO) of a leg, when the leg leaves the ground and ends at touchdown (TD) of the same leg, when the distal end of the leg hits the ground. In SS, the leg contacted to the ground, is called stance leg and the swing leg moves virtually (no change in dynamics when the leg is massless) to finish the SS with hitting the ground at a desired

angle (angle of attack). Here, the leg force (F_l), the hip torque (τ) exerted between trunk and stance leg and the swing leg angle (α) are the control parameters. Using a linear spring, the stance leg axial function control can be represented by setting the spring stiffness K_l and the rest length l_0. Indicating the leg length by l, the leg force along the leg axis will be

$$F_l = K_l\ (l_0 - l) \tag{1}$$

The next controller is for swing leg adjustment. Although using a fixed angle of attack with respect to the ground can stabilize running (Seyfarth et al., 2002) and walking (Geyer et al., 2006), the region of attraction for the stable gait is quite small. The next level of swing leg adjustment approaches is adapting the leg angle during leg swinging using state feedback. In most of these control strategies, the foot landing position is adjusted based on the horizontal velocity (Poulakakis and Grizzle, 2009) (Sato, 2004). In our previous studies (Sharbafi and Seyfarth, 2015, 2013), we compared three different control strategies for swing leg adjustment: Raibert controller (Raibert, 1986), Peuker approach (Peuker et al., 2012) and VBLA (velocity based leg adjustment studies) (Sharbafi et al., 2012). It was shown that VBLA is the best in mimicking human leg adjustment in perturbed hopping (Sharbafi and Seyfarth, 2013), achieves the largest range of running velocities by a fixed controller (Sharbafi and Seyfarth, 2016) and provides a robust walking in simulation model with BTSLIP (Sharbafi and Seyfarth, 2015). For all these reasons, in this study, we utilize VBLA in our modeling. In this approach, the leg direction is given by a vector $\vec{O}$ as a weighted average of the CoM velocity vector $\vec{V}$ and the gravity vector $\vec{G} = [0, -g]^T$.

$$\vec{O} \;=\; (1-\mu)\vec{V} + \mu\vec{G} \tag{2}$$

where weighting constant μ accepts values between 0 and 1.

For balancing the upper body (posture control) as the third locomotion sub-function, hip torque (τ, the torque between trunk and stance leg) is utilized. In (Maus et al., 2010), it was shown that in human walking, the ground reaction forces go through one point above center of mass (CoM) which is called virtual pivot point (VPP). Therefore, the inverted pendulum model of balancing can be represented as a regular virtual pendulum (VP) with body mass centered at CoM hanging from VPP. Considering rotational springs between the upper body and the legs (like hip and thigh muscles) which can be modulated by the leg force as a reflex signal (Fig. 1b) results in a precise approximation of VPP for running (Sharbafi and Seyfarth, 2014) and walking (Sharbafi and Seyfarth, 2015). Here, we use this FMCH (force modulated compliant hip) model in our analysis. In this model, the hip torque τ is produced by the hip spring (with the variable stiffness k) which is modulated by the leg force F_l as follows

$$\tau = k(\psi_0 - \psi) = cF_l(\psi_0 - \psi) \tag{3}$$

in which, ψ, c and ψ_0 are the hip angle, the hip spring stiffness normalized to the leg force (hereafter, it is called normalized stiffness), and the rest angle, respectively (Fig. 1b). In DS phase, similar mechanism is considered for the second stance leg.

10.2.2 Walking experiment analysis

The data was collected in walking experiments on a treadmill (type ADAL-WR, Hef Tecmachine, Andrezieux Boutheon, France) at different speeds. Motion capture data (Qualisys, Gothenburg, Sweden) from 11 markers and ground reaction force data (12 piezo-electric force transducers within the treadmill) as shown in Fig. 1c. Twenty one subjects (11 female, 10 male) were asked to walk at different

percentages of their preferred transition speeds (PTS)[28]. The treadmill speed which equals the average velocity during strides was employed as the walking speed. The subjects were between 22 to 28 years old with $1.73 \pm 0.09m$ height and $70.9 \pm 11.7kg$ weight. For every subject and speed, between 21 and 72 walking cycles (5188 cycles in total) were averaged to give individual means (left and right side combined). The average of these data points are utilized to obtain an inter-individual grand mean (e.g., to find average speed of each phase in Fig. 2). Kinematic and kinetic data processing was described in (Lipfert., 2010),(Lipfert et al., 2012).

Based on these experiments (average values of different steps of 21 subjects), the gait cycle is comprised of 78% single support (SS) and 22% double support (DS) phases at normal walking speed. Contribution of SS increases to 84% and decreases to 65% for fast ($125\%PTS$) and slow walking speeds ($25\%PTS$), respectively. In addition, separating different legs' contributions in speed adjustment when two legs are in contact with the ground in DS is not straight forward. Therefore, in this paper, we focus on analyzing contribution of the locomotion sub-functions to walking speed, in the single support phase because (i) it constitutes the major part of the walking cycle (more than 65%), (ii) it includes all locomotion sub-functions (leg swinging is absent in DS), (iii) compared to DS the average speed in SS can better approximate the gait speed (Sec. 10.3-Fig. 2) and (iv) separating locomotion sub-functions is simpler.

Stance (axial leg function):

Since in SLIP based models, the leg is represented by massless spring, here the leg stiffness K_l and the rest length l_0 are considered to characterize the repulsive leg behavior with Eq.(1). We use the least square approach, suggested in (Lipfert., 2010) to find the stiffness and rest length from experimental data. As shown later in Sec.10.3-Fig. 4, the slope of the force-length curve changes sharply when the leg force gets its minimum value in the middle of the swing phase. As a result, to model leg repulsion, we consider a variable spring with two different sets of spring parameters which switch (from the first to the second set) in the middle of the single support. The relation between these two parameter sets and their evolution with speed increment are analyzed to describe stance leg axial function role in speed adjustment.

Leg swinging:

First, we investigate which of three control approaches (Raibert Raibert (1986), Peuker Peuker et al. (2012) and VBLA Sharbafi et al. (2012)) introduced in Sec. 10.2.1 can better describe human swing leg adjustment. For this, we calculate the control parameter (μ) for different control approaches and compared the parameter variations for different subjects at different speeds. For walking at a certain speed, the controller which has the smallest variance (for a range of subjects) can represent a unified approach for swing leg adjustment regardless the body parameters (e.g., weight and height). Based on these experimental data analyses, we select the VBLA for controlling the swing leg in simulations. However, in SLIP-based models the legs are massless and the swing leg movement during single support does not affect on motion dynamics except in determining touchdown moment which initiates the next double support phase. Therefore, the angle of attack α and the retraction speed ω can be considered as outcomes of the swing leg adjustment method which contribute to gait stability (Seyfarth et al., 2003) and gait condition (Poggensee et al., 2014).

[28] PTS is the preferred speed for transition between running and walking which is typically about $1.9 - 2.1\ m/s$ for humans (Lipfert., 2010) .

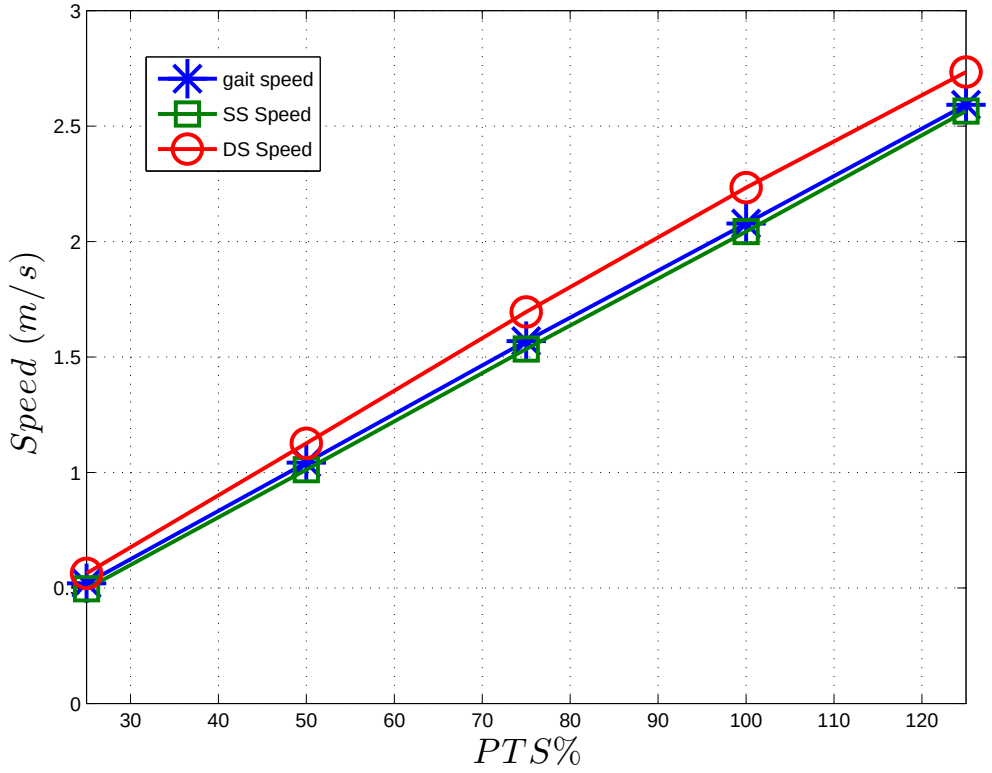

Figure 2: Relations between Single support (SS) and Double Support (DS) speeds with gait average speed. The data analysis is based on human walking experiments performed and explained in (Lipfert et al., 2012).

Balancing:

For posture control, first, we investigate the ability of FMCH in predicting human virtual hip torque in walking. The virtual hip torque is the torque between upper body and the virtual leg (defined by a line between the hip and the COP (center of pressure)). Based on Eq.(3), we compute the ratio between hip torque and leg force ($r_F^\tau = \frac{\tau_h}{F_S}$) and approximate the relation between r_F^τ and hip angle ψ (the angle between the stance leg and trunk orientation, shown in Fig. 1b) with a linear relationship. We use least square to find the line fitting best to experimental data. The precision of predicting human hip torque during swing cycle of walking with FMCH model is assessed by coefficient of determination (Steel and Torrie, 1960), denoted R^2. The FMCH model can be considered as a physical representation of the virtual pendulum (VP) concept observed in human/animal locomotion (Maus et al., 2010). Therefore, the balance control is characterized by the hip normalized stiffness (c) and rest angle (ψ_0) at different speeds as explained in (Sharbafi and Seyfarth, 2015). Variations of hip compliance and rest angle at different speeds show the contribution of posture control in speed adjustment.

10.3 Results and discussions

In this section, first, we illustrate correlation between walking average speed and single support (SS) and double support (DS) speeds (Fig. 2). Speed of each phase is the average speed of the Center of Mass (CoM) during that phase for 21 subjects over all collected steps. Then, the results of the proposed model to analyze relationship between locomotion sub-functions and walking speed are presented. All analyses

presented in this section are based on experimental data collected in (Lipfert., 2010) and explained in Sec. 10.2.2 (see (Lipfert et al., 2012) for more details).

We have found that the average speed during SS and DS are lower and higher than the gait speed, respectively (shown in Fig. 2). More importantly, SS speed is much closer than DS speed to the gait speed at different PTS values. The error between DS speed and gait speed is between 1.9 to 5.5 times the error between SS speed and gait speed. The difference between DS speed and SS speed grows as the walking speed increases. Therefore, it is fair to say the speed in single support is more dominant than that in double support in representing the gait speed. In the following, two main results are presented and discussed: i) the simulation results compared to human walking at regular speed (about $1.5m/s$) and ii) different locomotion sub-functions contribution to walking speed in the single support phase.

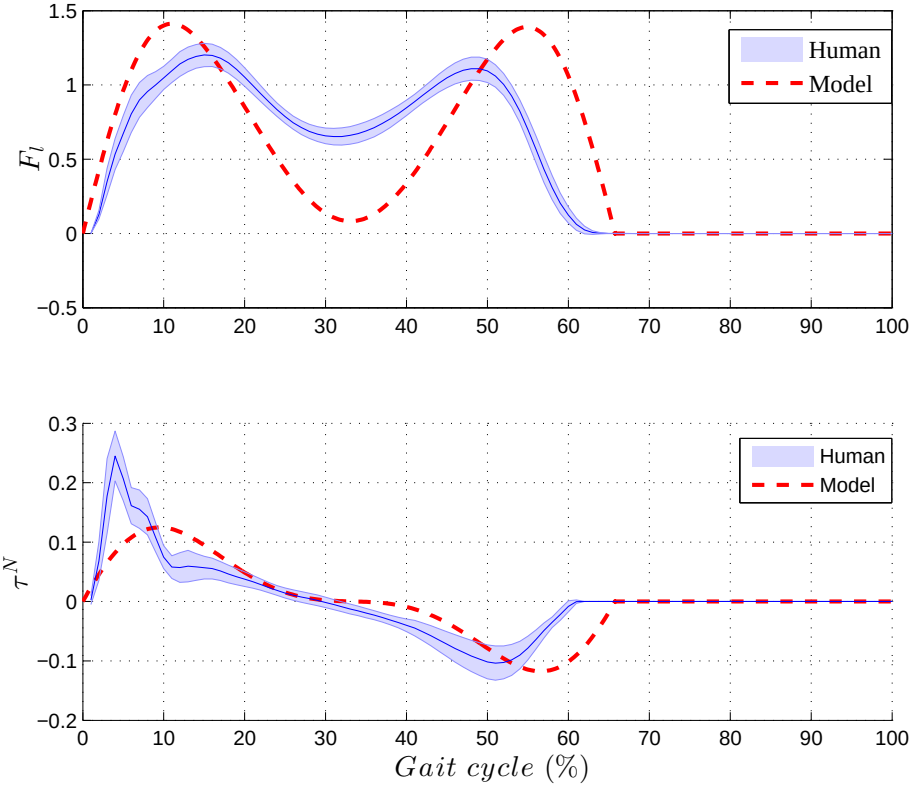

Figure 3: Comparison between human walking data at $75\%PTS$ and BTSLIP model simulation results at $1.4\ m/s$, The average (solid line) and variance (shaded region) of the normalized vertical leg force (top) and normalized hip torque (bottom) are shown for human subjects (N=21) at $75\%PTS$. Time is expressed relative to the gait cycle duration (in percent), while the average gait cycle of human walking at $75\%PTS$ is about $0.98\ s$. This value is the same for gait cycle of the simulations at $1.4\ m/s$ (data from (Lipfert., 2010)).

10.3.1 Verifying the model

In this section we demonstrate the similarities between force/torque in experiments and simulations. We use BTSLIP model with the FMCH and the VBLA as controllers for balancing and leg swinging. In Fig. 3, the average (solid line) and variance (shaded region) of the normalized leg force and normalized hip torque are shown for human subjects (N=21) at $75\%PTS$. Double hump force pattern can be observed in the simulation results (dashed lines) at $1.4\ m/s$ while the VBLA parameter is set to the value found in

human walking ($\mu = 72$). The model can also acceptedly mimic human hip torque patterns. This shows that the BTSLIP with the proposed controllers is able to reproduce human-like walking properties.

These results show that the simulation model can generate similar patterns as measured experimentally for approval of the model. The main focus of this paper is deriving the parameters of different sub-functions at different speeds and analyzing their evolution (as explained in Sec. 10.3.2) and not to extend the model to cover the whole speed range of experimental walking data. We could have selected a lower walking speed in our data (1 m/s) but we decided to select the preferred walking speed (1.5 m/s) despite the small speed different to the model because of the following reasons: i) With the human extracted body parameters (body mass and leg length) the BTSLIP model cannot predict faster walking solutions. To achieve this we need to extend the model, e.g. to change spring parameters during the gait which is not targeted in this paper. ii) The gait cycle time for 1.4 m/s in simulation is very close to that of human walking experiments at 75%PTS (both about 0.98 s). This similarity of gait cycle time supports the comparison between experimental data and model in Fig. 3. iii) This is the normal walking speed for humans.

10.3.2 Locomotion sub-functions analysis at different speeds

Here, we show how well the model equations can predict the experimental results at different speeds and the contribution of each locomotion sub-function in gait speed adjustment. Based on the proposed model, each locomotion sub-function is characterized by two parameters, as explained in Sec. 10.2.2.

Stance:

In order to investigate the axial function of the stance leg at different speeds, the leg force is drawn with respect to leg length in Fig. 4 (the blue solid line) for different motion speeds. A sharp breaking point is observed when the leg force gets its minimum value for all speeds. Considering the spring as a template for the axial leg function, this behavior can be approximated by a variable spring whose stiffness and rest length change in the middle of the swing cycle (red dashed lines in Fig. 4). Changes in spring properties at maximum knee flexion were also shown in running (Peter et al., 2009). In fast walking with 100%PTS and 125%PTS positive slopes appear in the second half of the swing cycle. This mean negative stiffness which is not physically interpretable by passive springs.

Our hypothesis for explaining such an active (not spring-like) behavior is the large push off starting from single support, required for fast walking. In order to assess this hypothesis, the leg force F_l and the ankle angle θ_a (shown in Fig. 1c) are depicted in Fig. 5. At all speeds the leg force starts to increase after passing the moment that the stance leg is vertical (VLO) [29]. When the ankle angle is at its minimum, heel off and simultaneously push off starts. It is observed that for slow walking (25%PTS and 50%PTS) no push off happens during SS. For walking at normal speed (75%PTS), push off happens shortly before the other leg touches the ground which is an efficient way to reduce losses at heel strike (Kuo, 2002). This control strategy may also justify why this speed is the normal speed.

Absence of negative stiffness in preferred walking speed (75%PTS) results from shortage of time between push off and the next touchdown to change the spring-like behavior of the stance leg. For fast walking (100%PTS and 125%PTS), push off occurs at about middle of SS where the minimums of the leg force and the ankle angle coincide. Conclusively, in order to walk fast, high energy injection through push off (increasing force and length at the same time) is required, which cannot be described by the physical spring template. This is in line with the inability of SLIP based models to generate fast walking (above 1.4 m/s) (Geyer et al., 2006). Furthermore, there is a high correlation between the ankle angle and

[29] VLO stands for "vertical leg orientation" (Rummel et al., 2010)

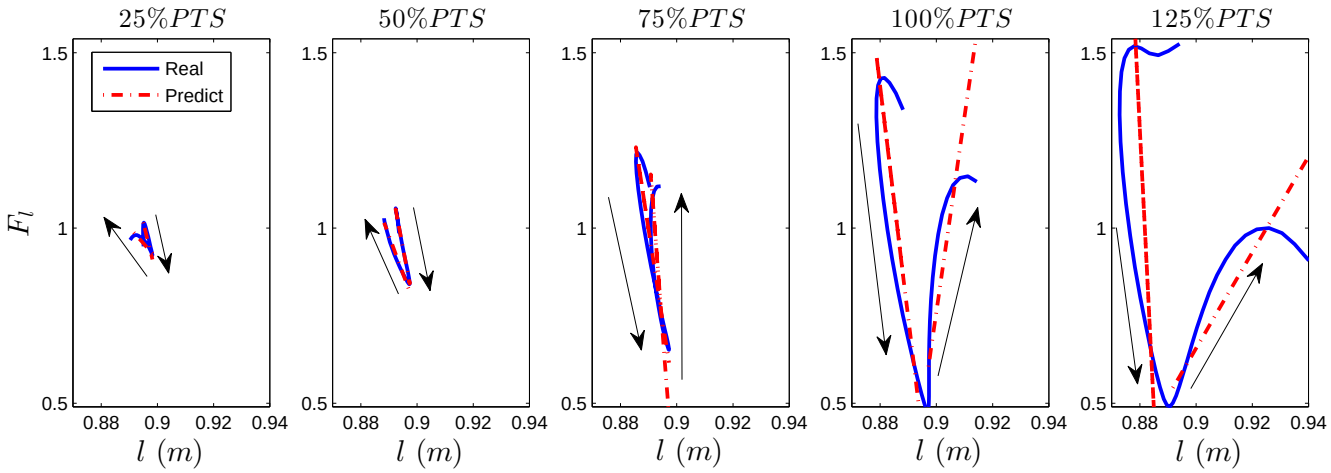

Figure 4: Leg force (F_l, normalized to body weight) vs. leg length (l) in swing phase of human walking experiment (Exp) and its prediction with springy leg (Predict) having two different stiffnesses.

Table 1: Swing leg adjustment control parameter mean ($\bar{\mu}$) and normalized standard deviation (σ_μ) for three different control approaches.

	Method	25%PTS	50%PTS	75%PTS	100%PTS	125%PTS
$\bar{\mu}$	Raibert	0.39	0.31	0.24	0.2	0.15
	Peuker	0.12	0.2	0.24	0.26	0.26
	VBLA	0.8	0.77	0.73	0.69	0.63
σ_μ	Raibert	0.17	0.11	0.07	0.08	0.09
	Peuker	0.19	0.11	0.09	0.09	0.01
	VBLA	0.04	0.03	0.02	0.03	0.04

the leg force in fast walking, because the ankle joint contributes to managing energy flow and controlling leg force more than the other joints (Malcolm, 2010).

Leg swinging:

In this section, we investigate different control approaches to explain human swing leg adjustment. For each approach, the control parameter is obtained by fitting the related equation (e.g., Eq. 2 for VBLA) to the experimental data at different speeds for all subjects. The parameter extraction was described for perturbed hopping in (Sharbafi and Seyfarth, 2013).

If one control approach can explain human swing leg adjustment better than others, the parameter of that approach calculated for different subjects at a specific speed should have the least deviation. Therefore, in order to find the most similar swing leg adjustment method to humans (regardless of the body parameters) the standard deviations (normalized to mean values) are compared in Table. 1. The VBLA has the lowest variance among different approaches. It means this approach is the most human-like leg adjustment approach. The average values ($\bar{\mu}$) show a monotonic trend in changing control parameter to increase the gait speed for all control approaches except from 100%PTS to 125%PTS in the Peuker approach.

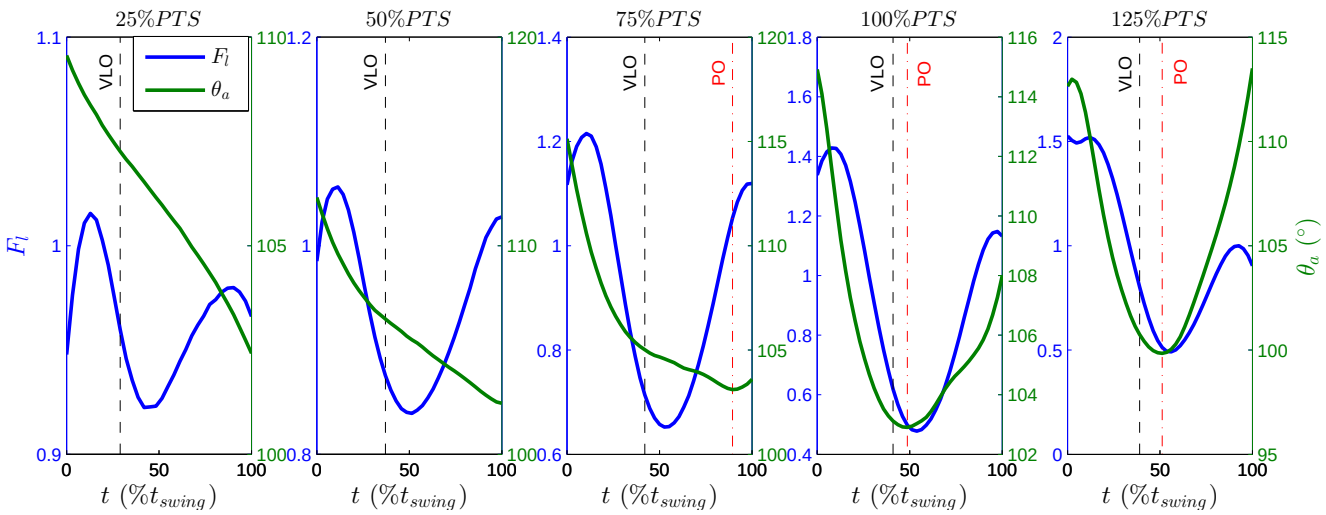

Figure 5: Leg force (F_l, normalized to body weight) and ankle angle (θ_a) during swing cycle (t_{swing}) at different speeds. Minimum of the ankle angle (where the angle increases afterward) shows the push off (PO) occurrence. The black vertical dashed line shows the instant of vertical leg orientation (VLO) (Rummel et al., 2010).

Balancing:

According to the FMCH model, the modulated spring stiffness and rest angles can be calculated as described in Sec. 10.2.2. Fig. 6 shows $r_F^\tau = \frac{\tau_h}{F_S}$ with respect to the hip angle (trunk to leg angle, shown by ψ in Fig. 1b). The experimental results are well approximated by a linear relationship with $R^2 > 97\%$. Hence, FMCH model can precisely predict the hip torque by applying the leg force as the reflex signal for tuning hip compliance (Fig. 7). This high precision prediction holds for all speeds except the first 10% and 20% of swing cycle at high speeds $100\%PTS$ and $125\%PTS$, respectively. These small deviations come from the high acceleration of the swing leg just after takeoff which can be considered as disturbance for posture control. In other words, the large energy injection in push off (of the other leg) behaves like a perturbation in fast walking. However, such perturbations are quickly rejected and the hip torque control using the leg force reflex results in postural balance.

10.3.3 Sub-function contributions to speed adjustment

The evolution of locomotion sub-functions' parameters with speed increment is shown Fig. 8. The variations of the rest length with respect to speed is monotonically decreasing in both halves of the single support. In addition, the leg stiffness in the first half of single support increases monotonically with speed. A similar increase is observed in leg stiffness in the second half of SS for slow to moderate speeds, whereas the stiffness gets negative values for fast walking.

The leg spring properties adaptation mechanisms during leg swinging from first to second half of the single support are as follows: (i) In slow walking ($25\%PTS$ and $50\%PTS$), the stiffness reduces while the rest length increases, as predicted by the variable leg spring (VLS) model (Riese and Seyfarth, 2012). (ii) In normal walking ($75\%PTS$), the rest length slightly decreases while the stiffness doubles in magnitude. However, since the leg length at switching point is close to rest length, change in energy is negligible. (iii) In fast walking ($100\%PTS$ and $125\%PTS$), injecting energy starts from middle of SS and continues until touchdown. This energy injection with push-off can be realized from negative stiffness as explained in Sec. 10.3.2. This is in line with the fact that SLIP-based gait models can not produce stable walking at fast speeds. Fig. 9 shows that for increasing speed the leg force-length lines rotate clockwise for both

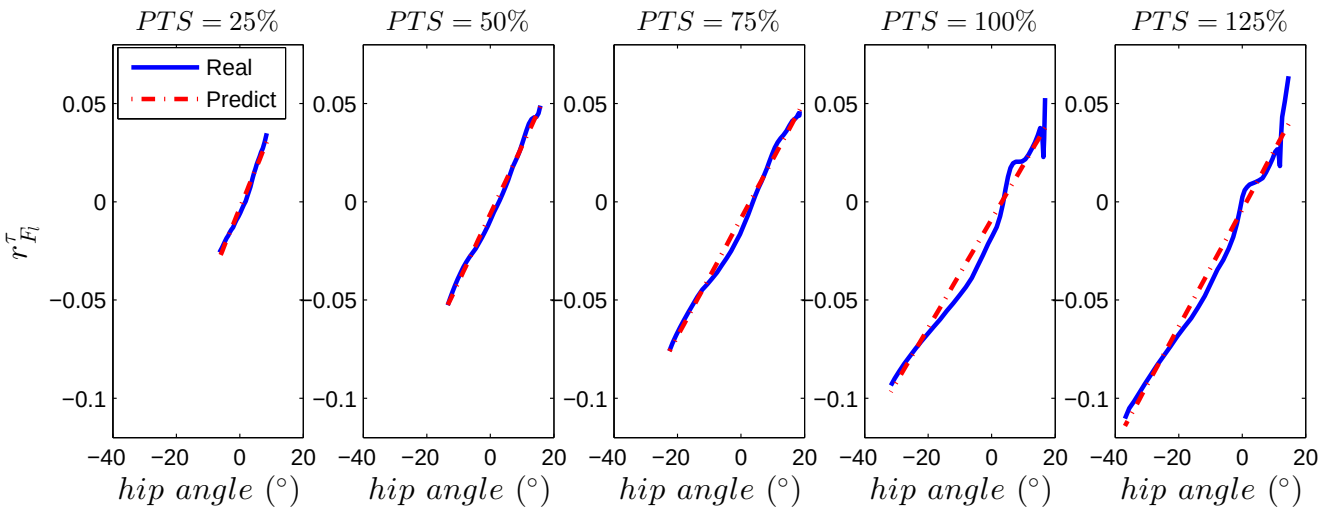

Figure 6: Hip torque τ to leg force F_l ratio ($r^{\tau}_{F_l}$) versus hip angle (ψ) for different speeds. Experimental results (Exp) and the fitted FMCH model (Predict).

halves of the swing phase. This rotation enters negative slopes in the second half of swing phase for fast walking. This figure presents a simple and smooth adaptation mechanism of axial leg function for increasing speed which is turning the force-length line (as a handle) in clockwise direction.

The swing leg angle of attack and retraction speed decreases and increases from 25% to 100%PTS, repectively. These trends are opposite for both at higher speeds. It means that larger steps with faster leg movement help speed up walking up-to 100%PTS. In this speed range, faster leg swinging with larger steps result in faster walking. However, this is not the strategy for increasing speed to more than the preferred transition speed to running. The reason may be that larger step length together with faster leg retraction is not desirable (easily achievable and efficient) in walking. Thus, for faster movement humans prefer to switch to running or use other locomotion sub-functions (e.g., stance leg axial function).

Similar to swing leg movement, for upper body postural control, from 25% to 100%PTS the changes are different from 100% to 125%PTS. From 25% to 100%PTS, the hip stiffness reduces with speed increment and the rest angle increases. It means that at higher speeds, the hip will become more compliant, allowing more oscillations in the upper body and it will be tilted more forward. Inverse of this trend for fast walking shows that if humans want to walk with speed in which running is preferred, they reduce the hip (to leg) elasticity (larger c) and walk with more upright posture (smaller ψ_0).

In summary, it can be concluded that the mechanism of increasing speed is not similar for different speed ranges. For walking faster than preferred transition speed to running the main locomotion sub-function which inject energy to the system is the stance axial leg function using large amounts of push off.

10.4 Conclusion

In this study, we analyzed the contribution of different locomotion sub-functions in speed adjustment using a new model. Accordingly, the human control strategies in relation to walking speed can be summarized as follows:

1. **from slow to moderate speeds:** Considering 75%PTS as normal (moderate) walking speed, monotonic behavior is observed in all sub-functions meaning the faster walking is achieved using (i)

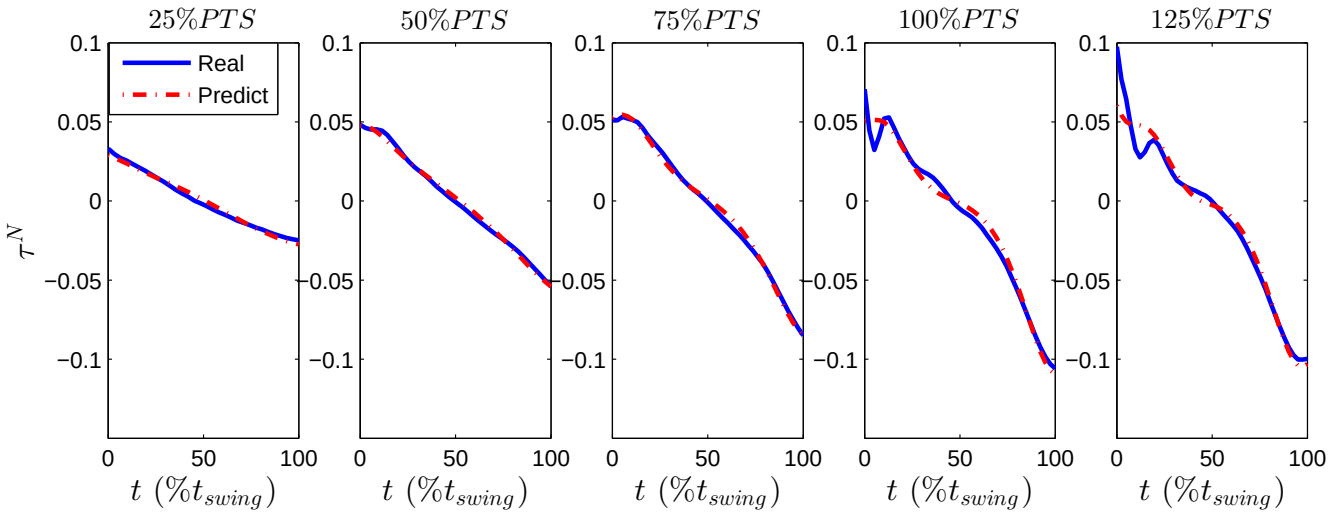

Figure 7: Hip torque normalized to body weight (τ^N) during the swing cycle (t_{swing}). Experimental results (Exp) and prediction of the FMCH model (Predict).

the stiffer legs with shorter rest lengths (ii) the larger steps with faster swing leg retraction and (iii) the more tilted upper body with more compliant hip.

2. **from moderate to fast speeds:** Speeding up requires to (iv) inject more energy which can be achieved by changing the stance leg properties (specially in the second half of single support phase) and having larger push offs, while the leg swinging and posture control strategies are similar to (i) and (ii) in previous speed range.

3. **from fast to very fast speeds:** To reach speeds faster than the preferred transition speed, similar to (iv) injecting more energy at push off is the main control strategy for stance while (v) the shorter steps (due to larger angle of attack) with slower swing leg retraction and (vi) the more upright upper body with less compliant hip are required.

In conclusion, upper body posture control and swing leg adjustment may be used to speed up walking from slow to preferred transition speed to running, but they do not significantly contribute to speed adjustment in faster movements. In walking at speeds in which running is preferred, these two locomotion sub-functions contribute mainly in stabilizing the gait and reducing losses. Energy management by stance control mechanism is the main speed adjustment approach at high speed walking. Injecting more energy at speeds above normal walking speed by negative stiffness in leg spring is consistent with findings in (Neptune and Sasaki, 2005) showing that plantar flexor muscle force production is greatly impaired near the preferred transition speed due to poor contractile conditions.

10.5 Acknowledgment

This research was supported in part by the EU project BALANCE under Grant Agreement No. 601003. We would like to thank Sasha Voloshina for her helpful feedback on this work.

Conflict of interest statement

We confirm that there are no known conflicts of interest associated with this publication and there has been no other significant financial support for this work that could have influenced its outcome.

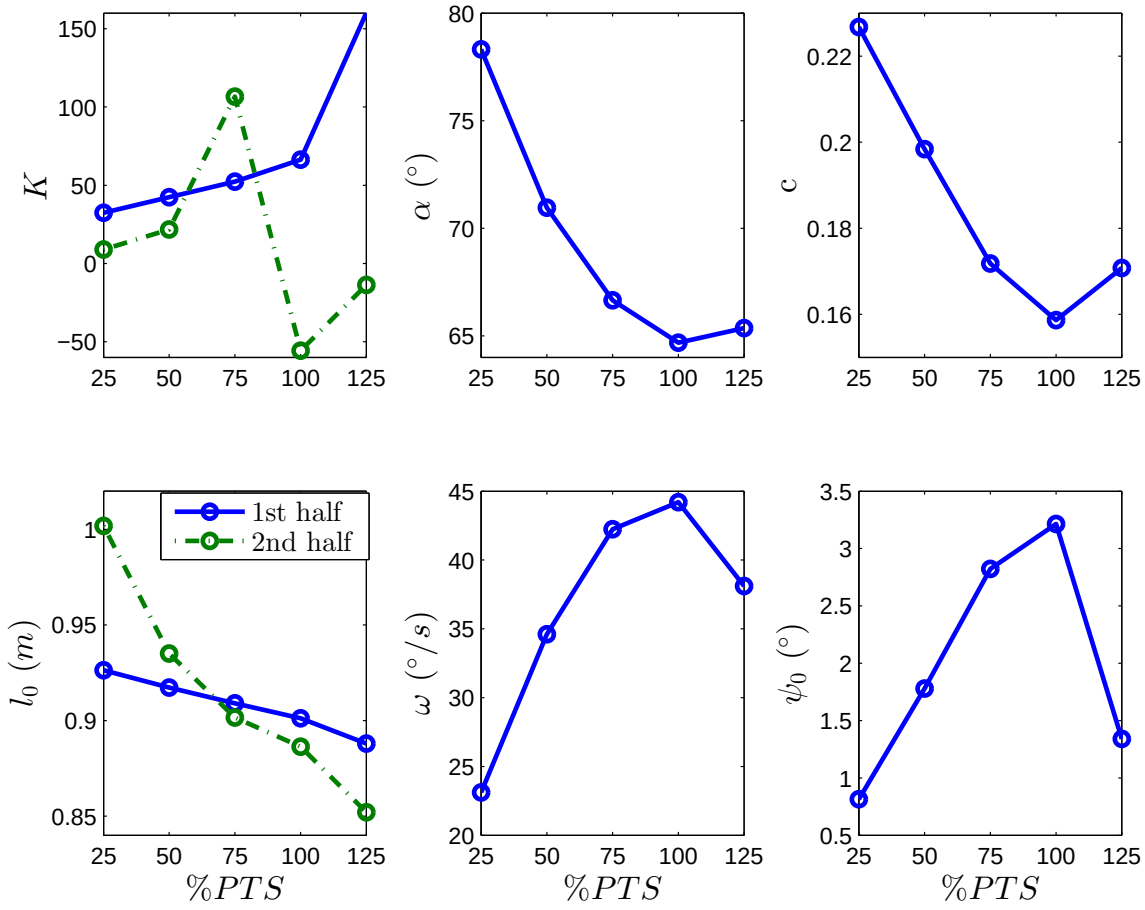

Figure 8: Locomotion sub-function variations with speed. K, l_0, α, ω c and ψ_0 are the leg stiffness, leg rest length, the swing leg angle, the angular speed at touchdown, normalized hip stiffness and the hip rest angle (in FMCH model), respectively. In the left figure, the blue line and green dashed line show the parameters for the first and second halves of the swing phase, respectively.

10.6 APPENDIX

Simulation model

The BTSLIP shown in Fig. 1, is presented here. Defining the states x, y and φ as the CoM horizontal and vertical positions and the trunk orientation, respectively; the hip point ($X_h = [x_h,\ y_h]$) which is positioned below CoM with distance r_h is obtained as follows

$$\begin{aligned} x_h &= x - r_h \cos\varphi \\ y_h &= y - r_h \sin\varphi \end{aligned} \tag{4}$$

The hip torque τ is determined by the controller (e.g., FMCH as given by 1) for stabilizing the posture of the trunk. The hip torque and the leg spring force produce the ground reaction force in interaction with the ground by

$$\begin{aligned} GRF_x &= F_s \frac{x_h}{l} + \frac{\tau y_h}{l^2} \\ GRF_y &= F_s \frac{y_h}{l} - \frac{\tau x_h}{l^2} \end{aligned} \tag{5}$$

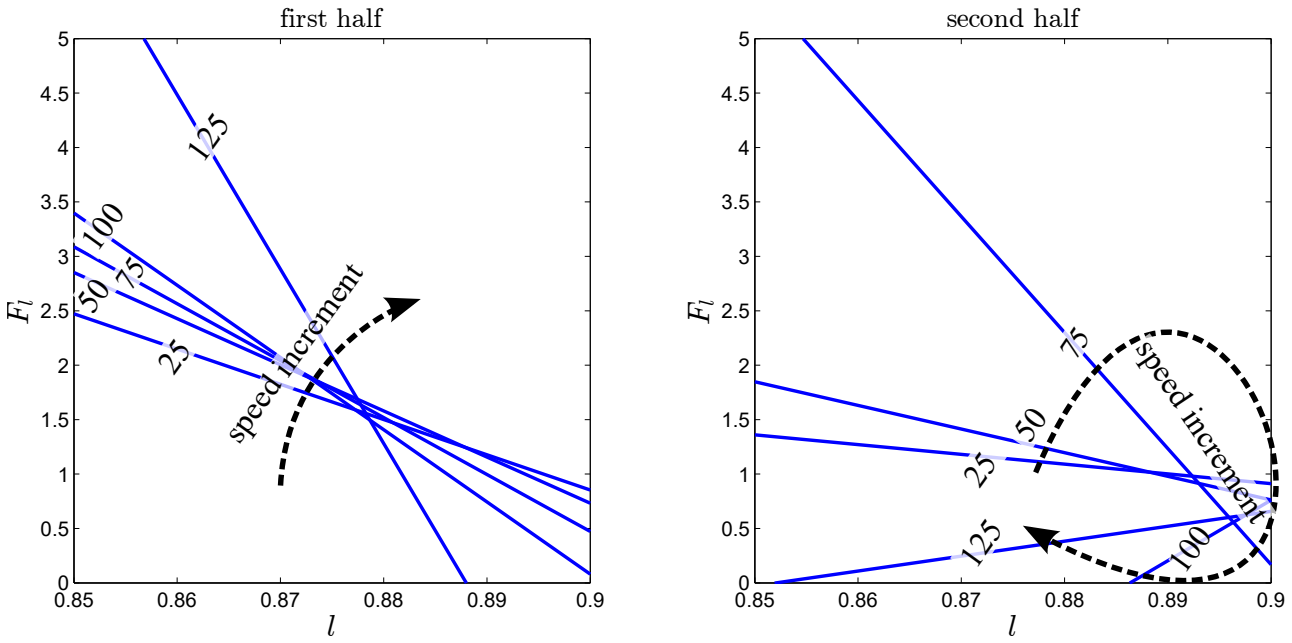

Figure 9: Leg force-length ($F_l - l$) characteristics (mean of 21 subjects) at different speeds (25%*PTS* to 125%*PTS*) in human walking. Clockwise rotation of lines with speed increment.

Considering g as the gravity acceleration, the motion dynamic in the single support (SS) is described by

$$\begin{cases} m\ddot{x} &= GRF_x \\ m\ddot{y} &= GRF_y - mg \\ J\ddot{\varphi} &= \tau + r_h(GRF_x \sin\varphi - GRF_y \cos\varphi) \end{cases} \tag{6}$$

When the swing leg in SS hits the ground the second stance leg appears and double support (DS) starts (hereafter we show the parameters related to this leg by subindex $_2$). DS ends with takeoff of the first stance leg (shown by $_1$). In this phase, the controller produces torques (τ_1 and τ_2) between legs and trunk to keep the system stable. Defining the position of the second stance leg by $[x_2,\ 0]$, the dynamic model of DS will be as follows:

$$\begin{cases} m\ddot{x} &= GRF_{x1} + GRF_{x2} \\ m\ddot{y} &= GRF_{y1} + GRF_{y1} - mg \\ J\ddot{\varphi} &= \tau_1 + \tau_2 + r_h(GRF_{x1} + GRF_{x2})\sin\varphi \\ & \quad -r_h(GRF_{y1} + GRF_{y2})\cos\varphi \end{cases} \tag{7}$$

where

$$\begin{cases} GRF_{x1} &= F_{s1}\frac{x_h}{l} + \frac{\tau_1 y_h}{l_1^2} \\ GRF_{y1} &= F_{s1}\frac{y_h}{l} - \frac{\tau_1 x_h}{l_1^2} \\ GRF_{x2} &= F_{s2}\frac{x_h - x_2}{l} + \frac{\tau_2 y_h}{l_2^2} \\ GRF_{y2} &= F_{s2}\frac{y_h}{l} - \frac{\tau_2 (x_h - x_2)}{l_2^2}. \end{cases} \tag{8}$$

10.7 AUTHOR CONTRIBUTIONS

Maziar A. Sharbafi is the main and corresponding author of this article responsible for the conception and design of modeling, analysis and interpretation of experimental data and writing of the manuscript. Andre Seyfarth was the supervisor of the project and contributed in discussions regarding interpretation of the results and writing the paper.

10.8 REFERENCES

Altendorfer, R., Moore, N., Komsuoglu, H., Buehler, M., Brown Jr, H.B., McMordie, D., Saranli, U., Full, R., Koditschek, D.E., 2001. Rhex: a biologically inspired hexapod runner. Autonomous Robots 11, 207–213.

Blickhan, R., 1989. The spring-mass model for running and hopping. Journal of Biomechanics 22, 1217–1227.

Den Otter, A.R., Geurts, A.C.H., Mulder, T., Duysens, J., 2004. Speed related changes in muscle activity from normal to very slow walking speeds. Gait & posture 19, 270–278.

Full, R.J., Koditschek, D., 1999. Templates and anchors: Neuromechanical hypotheses of legged locomotion on land. Journal of Experimental Biology 22, 3325–3332.

Geyer, H., Herr, H., 2010. A muscle-reflex model that encodes principles of legged mechanics produces human walking dynamics and muscle activities. IEEE Transaction on Neural Systems and Rehabilitation Engineering 18.

Geyer, H., Seyfarth, A., Blickhan, R., 2003. Positive force feedback in bouncing gaits? Proceedings of the Royal Society of London B: Biological Sciences 270, 2173–2183.

Geyer, H., Seyfarth, A., Blickhan, R., 2006. Compliant leg behaviour explains basic dynamics of walking and running. Proceedings of the Royal Society B: Biological Sciences 273, 2861–2867.

Grizzle, J.W., Hurst, J., Morris, B., Park, H.W., Sreenath, K., 2009. Mabel, a new robotic bipedal walker and runner, in: In Proc. of American Control Conference.

Hof, A., Elzinga, H., Grimmius, W., Halbertsma, J.P.K., 2002. Speed dependence of averaged emg profiles in walking. Gait & posture 16, 78–86.

Kuo, A., 2002. Energetics of actively powered locomotion using the simplest walking model. Journal of Biomechanical Engineering 124, 113–120.

Lipfert., S.W., 2010. Kinematic and dynamic similarities between walking and running. Verlag Dr. Kovaĉ,.

Lipfert, S. W., Günther, M., Renjewski, D., Grimmer, S., Seyfarth, A., 2012. A model-experiment comparison of system dynamics for human walking and running. Journal of Theoretical Biology 292, 11–17.

Liu, Y., Wensing, P.M., Orin, D.E., Zheng, Y.F., 2015. Trajectory generation for dynamic walking in a humanoid over uneven terrain using a 3d-actuated dual-slip model, in: IEEE/RSJ International Conference on Intelligent Robots and Systems (IROS).

Malcolm, P., 2010. Influence of intrinsic and extrinsic determinants on the transition from walking to running. Ph.D. thesis. Ghent University.

Maus, H.M., Lipfert, S., Gross, M., Rummel, J., Seyfarth, A., 2010. Upright human gait did not provide a major mechanical challenge for our ancestors. Nature Communications 1, 1–6.

Neptune, R.R., Sasaki, K., 2005. Ankle plantar flexor force production is an important determinant of the preferred walk-to-run transition speed 208, 799–808.

Neptune, R.R., Sasaki, K., Kautz, S.A., 2008. The effect of walking speed on muscle function and mechanical energetics. Gait & posture 28, 135–143.

Orlovsky, G.N., Grillner, S., Deliagina, T.G., 1999. Neuronal control of locomotion: from mollusc to man. Oxford University Press.

Peter, S., Grimmer, S., Lipfert, S.W., Seyfarth, A., 2009. Variable joint elasticities in running, in: Autonome Mobile Systeme 2009. Springer, pp. 129–136.

Peuker, F., Maufroy, C., Seyfarth, A., 2012. Leg adjustment strategies for stable running in three dimensions. Bioinspiration and Biomimetics 7.

Poggensee, K.L., Sharbafi, M.A., Seyfarth, A., 2014. Characterizing swing-leg retraction in human locomotion, in: International Conference on Climbing and Walking Robots (CLAWAR 2014).

Poulakakis, I., Grizzle, J.W., 2009. The spring loaded inverted pendulum as the hybrid zero dynamics of an asymmetric hopper. IEEE Transaction on Automatic Contro 54, 1779–1793.

Raibert, M.H., 1986. Legged Robots that Balance. MIT Press, Cambridge MA.

Renjewski, D., Sproewitz, A., Peekema, A., Jones, M., Hurst, J.W., 2015. Exciting engineered passive dynamics in a bipedal robot. IEEE Transactions on Robotics 13, 1244–1251.

Riese, S., Seyfarth, A., 2012. Stance leg control: variation of leg parameters supports stable hopping. Bioinspiration & biomimetics 7, 016006.

Rummel, J., Blum, Y., Maus, H.M., Rode, C., Seyfarth, A., 2010. Stable and robust walking with compliant legs, in: Robotics and Automation (ICRA), 2010 IEEE International Conference on, IEEE. pp. 5250–5255.

Rummel, J., Seyfarth, A., 2010. Passive stabilization of the trunk in walking, in: International Conference on Simulation, Modeling and Programming for Autonomous Robots, Darmstadt, Germany.

Sato, A., 2004. A planar hopping robot with one actuator: design, simulation, and experimental results, in: IEEE/RSJ International Conference on Intelligent Robots and Systems (IROS).

Seyfarth, A., Geyer, H., Günther, M., Blickhan, R., 2002. A movement criterion for running. Journal of biomechanics 35, 649–655.

Seyfarth, A., Geyer, H., Herr, H., 2003. Swing-leg retraction: a simple control model for stable running. The Journal of Experimental Biology 206, 2547–2555. doi:10.1242/jeb.00463.

Seyfarth, A., Grimmer, S., Häufle, D., Maus, H.M., Peuker, F., Kalveram, K.T., 2013. Computer models and robot validation. Routledge Handbook of Motor Control and Motor Learning , 90.

Seyfarth, A., Grimmer, S., Häufle, D.F., Kalveram, K.T., 2012. Can robots help to understand human locomotion? at-Automatisierungstechnik Methoden und Anwendungen der Steuerungs-, Regelungs- und Informationstechnik 60, 653–661.

Sharbafi, M.A., Maufroy, C., Seyfarth, A., Yazdanpanah, M.J., Ahmadabadi, M.N., 2012. Controllers for robust hopping with upright trunk based on the virtual pendulum concept, in: IEEE/RSJ International Conference on Intelligent Robots and Systems (IROS).

Sharbafi, M.A., Radkhah, K., von Stryk, O., Seyfarth, A., 2014. Hopping control for the musculoskeletal bipedal robot biobiped, in: IEEE/RSJ International Conference on Intelligent Robots and Systems (IROS), pp. 4868–4875.

Sharbafi, M.A., Seyfarth, A., 2013. Human leg adjustment in perturbed hopping, in: 6th International Symposium on Adaptive Motion of Animals and Machines (AMAM).

Sharbafi, M.A., Seyfarth, A., 2014. Stable running by leg force-modulated hip stiffness, in: IEEE International Conference on Biomedical Robotics and Biomechatronics (BioRob 2014).

Sharbafi, M.A., Seyfarth, A., 2015. FMCH: a new model to explain postural control in human walking, in: IEEE/RSJ International Conference on Intelligent Robots and Systems (IROS).

Sharbafi, M.A., Seyfarth, A., 2016. VBLA, a swing leg control approach for humans and robots, in: submitted to IEEE-RAS International Conference on Humanoid Robots.

Steel, R.G.D., Torrie, J.H., 1960. Principles and procedures of statistics: with special reference to the biological sciences .

11 Article X: Locomotion subfunctions for control of wearable robots

Authors:

Maziar Ahmad Sharbafi and André Seyfarth

Technische Universität Darmstadt
64289 Darmstadt, Germany

Accepted as a paper in

Frontiers in Neurorobotics (Special Issue on Forfront contrl of wearable robots), 2017.

ABSTRACT

A primary goal of comparative biomechanics is to understand the fundamental physics of locomotion within an evolutionary context. Such an understanding of legged locomotion results in a transition from copying nature to borrowing strategies for interacting with the physical world regarding design and control of bio-inspired legged robots or robotic assistive devices. Inspired from nature, legged locomotion can be composed of three locomotor sub-functions, which are intrinsically interrelated: **Stance**: redirecting the center of mass by exerting forces on the ground. **Swing**: cycling the legs between ground contacts. **Balance**: maintaining body posture. With these three sub-functions, one can understand, design and control legged locomotory systems with formulating them in simpler separated tasks. Coordination between locomotor sub-functions in a harmonized manner appears then as an additional problem when considering legged locomotion. However, biological locomotion shows that appropriate design and control of each sub-function simplifies coordination. It means that only limited exchange of sensory information between the different locomotor sub-function controllers is required enabling the envisioned modular architecture of the locomotion control system. In this paper, we present different studies on implementing different locomotor sub-function controllers on models, robots, and an exoskeleton in addition to demonstrating their abilities in explaining humans' control strategies.

KEYWORDS:

legged locomotion, locomotor sub-functions, stance leg control, swing leg adjustment, posture control, assistive devices, wearable robots.

11.1 INTRODUCTION

Unlike man-made vehicles, legged systems are the preferred biological technology for locomotion on ground. Research on legged locomotion, both in nature and robotics, helps us design and construct more agile and efficient moving systems. At the same time, it also supports understanding of human movement and control. In turn, this may help develop new approaches for locomotor rehabilitation and assistance. In this respect, findings in biology and robotics can greatly complement each other (Collins et al., 2015). Currently, the principles of animal and human locomotion and their applicability to artificial legged and assistive devices are not fully understood. Given the differences between biological and artificial body design and control, an important question is to what extent should we use biological design and control approaches for building artificial locomotor systems? Learning from nature does not require mimicking the biological locomotor system in detail. We can already greatly benefit of applying selected design and control principles, such as adding compliant structures to artificial systems or by arranging actuators analogous to bi-articular muscles in the human leg. In recent years, researchers from highly diverse disciplines such as biology, motion science, medicine and engineering have advanced research on legged locomotion by investigating underlying principles of body mechanics and related control design (Westervelt et al., 2007; Raibert, 1986; Alexander, 2003; Chevallereau et al., 2013; Duysens et al., 2002; Holmes et al., 2006; Winter, 2009). Considering nature as an ingenious teacher, bio-inspired approaches have become increasingly important in the study of legged locomotion (Ijspeert, 2008; Duysens et al., 2002; Koditschek et al., 2004). Legged locomotion can be composed of three locomotor sub-functions (Seyfarth et al., 2013): Stance (axial leg function), leg swinging and balancing, (Fig.1). Stance describes the elastic rebounding of the stance leg (ground contact) to counteract gravity (Blickhan, 1989). Leg swinging is mainly a rotational movement of the swing leg (Blum et al., 2010) combined with a minor axial leg movement for ground clearance. Since a major part of the body mass is located on the upper

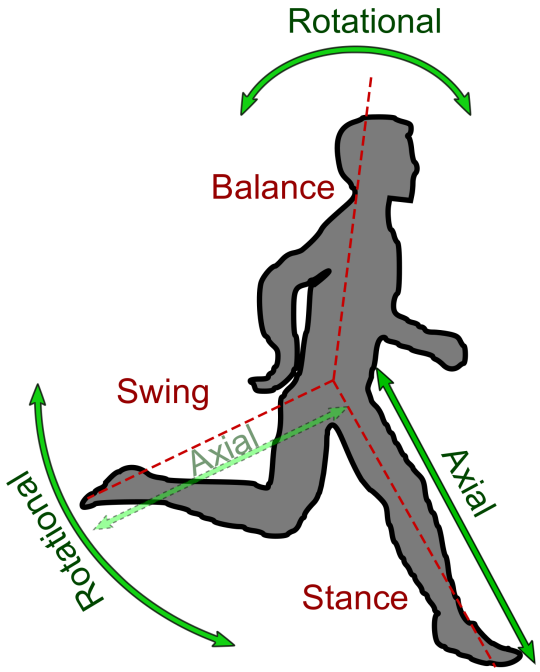

Figure 1: Main locomotion sub-functions; i) axial stance leg function, ii) rotational swing leg function and iii) balance for maintaining posture.

body, the human body is inherently unstable (Winter, 1995) and balancing (posture control (Massion, 1994)) is considered to be a third locomotor sub-function, as a key feature of human gaits.

In this paper we explain how understanding bipedal locomotion using the concept of three locomotor sub-functions can be employed to design and control assistive wearable robots. In that respect, first, we survey our previous studies on combinations of the control concepts of three locomotor sub-functions to achieve stable gaits (Sharbafi et al., 2014, 2013b, 2016), (Mohammadinejad et al., 2014),(Sharbafi et al., 2017; Sharbafi and Seyfarth, 2017),(Oehlke et al., 2016),(Zhao et al., 2017). Then, we show that considering such an architecture to control a wearable robot, an actuator can be designed with optimal performance for a range of motions required for different locomotor sub-functions. Therefore, a unifying actuation mechanism beside a bioinspired distributed control architecture can be employed to simplify interaction between different sub-functions and also between robot and human. It is noticeable that consistency between human and robot locomotion sub-function control not only facilitates interaction with humans, but also benefits from human movement control to orchestrate different sub-functions in the robot. For that, the controller for each sub-function needs to communicate with the related sub-function on human body through sensory feedback.

To implement the proposed distributed control architecture we employ the "Template & Anchor"concept (Full and Koditschek, 1999). Despite their high level of abstraction, template models are very useful tools to understand how these sub-functions are controlled and coordinated, both in nature (Blickhan, 1989) and legged robots (Raibert, 1986). In our studies we have applied mass-spring, physical and virtual pendulums as our template models for stance, swing and balance, respectively. Pendulum and mass-spring as two oscillators are very useful tools for explanation of legged locomotion as a rhythmic movement. Table. 1 presents an overview of locomotor sub-function concept including basic characteristics and samples of representative template models. In the following, first we describe this concept including relevant template models in Sec. 11.2. Then, Sec. 11.3 explains how these sub-functions help better understand human gaits. In Sec. 11.4, different instances of implementation on

Table 1: Overview of locomotion sub-functions with basic characteristics and their representation in template models

locomotion sub-function	**objective**	**leg force direction**	**biomechanical template models**
Stance	Interacting with ground	in leg axis	leg spring
Swing	adjust leg orientation during swing phase	perpendicular to and in leg axis	pendulum-like leg with adaptable length + hip spring
Balance	maintaining an upright body orientation	perpendicular to leg axis	hip spring, virtual pendulum

models, robots and exoskeletons are presented. Finally, Sec. 11.5 discusses how one can benefit from the proposed concept in design and control of wearable robots to facilitate interaction with humans and to provide a more harmonized control of different sub-functions through actuators.

11.2 LOCOMOTOR SUB-FUNCTION CONCEPT AND TEMPLATE MODELS

Legged locomotion is a complex task with integrated functional levels influencing all three locomotor sub-functions. Our separate treatment of these sub-functions allows integration of key functional features at each level of legged locomotion (mechanics, actuation, sensing and control).
For stable legged locomotion, a control architecture is required to employ the locomotion concepts. Template models (Full and Koditschek, 1999) which present reduced order systems of the locomotors, are our tools to understand how the sub-functions are controlled and coordinated. We need to know the corresponding control concepts and to learn from biology to simplify control. In addition, for interaction with humans, lower level force/torque control is beneficial in comparison to position control which might be harmful for humans (Haddadin et al., 2008). We show that such template-based control approaches are founded on impedance (e.g., stiffness) control which consider this latter concern.

In order to benefit from bioinspired locomotion concepts that can be used for implementation on robots or assistive devices, key characteristics of legged mechanisms need to be identified. Based on realizing legged locomotion with the aforementioned trilogy, we have investigated different bioinspired control approaches on human experimental data, conceptual models and finally robots and exoskeletons, presented in the next two sections. Here, we describe locomotor sub-functions and their related template models.

The proposed models which are based on the concept of locomotor sub-functions are inspired from human locomotion. This concept is used for gait modeling that can be further extended for design and control of robots. Here, we propose to implement this technique to control exoskeletons (as wearable robots) which have interactions with humans. The key idea is using the bioinspired control techniques based on locomotor sub-function theory to make the control of the wearable robots (lower-body exoskeletons) compatible with human movement.

11.2.1 Relevant template models

SLIP for stance

Stance function describes the repulsive function of the stance leg (in contact with the ground) to counteract gravity (Seyfarth et al., 2013). A spring-loaded inverted pendulum (SLIP) model (Blickhan, 1989) is a simple template model describing human-like axial leg function in walking and running (Geyer et al., 2006). In this model the force-length relationship of the leg in axial direction is approximated by a

spring which is linear in running and hopping and nonlinear in walking. SLIP is popular for its ability in describing human gaits and modeling of legged robots. However, it can be also employed as a template for control e.g., (Poulakakis and Grizzle, 2009; Wensing and Orin, 2013). In such studies the linear force-length relationship of the virtual leg (a line between CoM and CoP) is utilized as a target for control. In this approach, stance leg control goal is developing joint torques to yield spring-like behavior of the virtual leg. In Sec. 11.4, we explain how this method is used in different applications: (1) Mimicking human-like leg elastic behavior with a robot (Oehlke et al., 2016; Sharbafi et al., 2014) e.g., implemented by VMC (Virual model control) (2) energy management through ankle torque and biarticular muscles (Sharbafi et al., 2014, 2016). There are also Extended SLIP models, like ESLIP (Ludwig et al., 2012) or the variable leg spring (VLS) model (Riese et al., 2013), describing leg spring adjustments (stiffness, rest length) during the stance phase. These models can be also implemented to achieve higher control performance. Since this approach is consistent with human stance leg control, it is expected to provide appropriate interaction between human and robot while applying this technique to control a wearable robot.

Pendulum for swing

Leg swinging is mainly a rotational movement combined with a complementing axial leg movement to avoid foot scuffing on the ground. Regarding swing leg control, we follow two approaches: The first approach is an improvement of the Raibert leg adjustment approach (Raibert, 1986) using the CoM velocity to find the desired leg angle. This VBLA (velocity based leg adjustment) method (Sharbafi and Seyfarth, 2016) provides a stabilizing control strategy for different gaits (Sharbafi et al., 2014, 2013b; Sharbafi and Seyfarth, 2015) and also nicely describes human perturbation recovery for hopping in place (Sharbafi and Seyfarth, 2013). Although this can be employed to control the swing leg as one of the locomotor sub-functions, it is not at the focus of this paper because of lack of template model describing the control concept.

Instead of Velocity based leg adjustment, a second approach which can be considered as a template based control method for leg swinging is to assume a passive pendulum-like movement of the swing leg (Knuesel et al., 2005; Mohammadinejad et al., 2014). Mochon & McMahon presented a model comprising a stiff stance leg and a segmented swing leg (Mochon and McMahon, 1980) which provides a better match of human walking dynamics, compared with the inverted pendulum model. Another improvement in modeling human gait dynamics (GRF and COM movement) was obtained by replacing stiff leg with massless spring in SLIP model (Geyer et al., 2006). However, swing leg movement is still a missing part in SLIP based models. In (Mohammadinejad et al., 2014), we presented a new model combining SLIP for stance leg with pendulum movement for the swing leg in running. In this model the pendulum length is adapted at each step to attenuate any perturbation or error from desired movement. Adding hip rotational springs to this pendulum instead of pendulum length adaptation (see Fig. 2a) result is SPS (Springy pendulum SLIP) model. In Sec. 11.3, we show that this model can precisely predict human swing leg adjustment.

In this model, we consider two decoupled dynamics for the stance and swing leg with Eq. (1). This model is precise if the CoM moves horizontally (keeping the height) with constant speed. However, simulations show that this decoupled model can well approximate human swing leg movement as shown in Sec. 11.3.

$$\begin{bmatrix} \ddot{l} \\ \ddot{\theta} \\ \ddot{\varphi} \end{bmatrix} = \begin{bmatrix} \frac{k}{M}(l_0 - l) - g\cos(\theta) + l\dot{\theta}^2 \\ \frac{g}{l}\sin(\theta) - 2\frac{\dot{l}\dot{\theta}}{l} \\ \frac{-g\sin(\varphi)}{l_p} + k_{REF}max(\varphi_0^{REF} - \varphi, 0) - k_{HAM}max(\varphi - \varphi_0^{HAM}, 0) \end{bmatrix} \quad (1)$$

in which k, l_0 the stiffness and the rest length of the stance leg. In this equation we considered rotational springs to model the biarticular thigh muscles. For this, we use k_{REF} and k_{HAM} are the normalized stiffness of the rectus femoris and hamstrings muscles, respectively and φ_0^{REF} and φ_0^{HAM} are the rest angles for the related muscles. The rest of parameters can be found in Fig. 2a. The *max* function guarantees that the muscles are unidirectional. The normalized stiffness is calculated by the following equations

$$\begin{cases} k_{REF} = \frac{k_{REF}^{rot}}{ml_p^2} \\ k_{HAM} = \frac{k_{HAM}^{rot}}{ml_p^2} \end{cases} \tag{2}$$

in which, m, k_{REF}^{rot} and k_{HAM}^{rot} are the pendulum (swing leg) mass, stiffness of rotational springs for REF and HAM muscles, respectively. Here, the relation between leg mass, the muscle stiffness and the pendulum length is ignored by normalizing the stiffness.
Touchdown happens when the swing leg hits the ground. The subsequent double support is described with the BSLIP model (Geyer et al., 2006). Here, we neglect the swing leg mass and therefore the impact effect at touchdown. Considering the same stiffness and rest angle for both hip muscles ($k_h = k_{REF} = k_{HAM}$ and $\varphi_0^h = \varphi_0^{REF} = \varphi_0^{HAM}$) results in the following swing dynamics.

$$\ddot{\varphi} = \frac{-g\sin(\varphi)}{l_p} + k_h(\varphi_0^h - \varphi) \tag{3}$$

In Sec. 11.3, we use Eq. (3) to predict human swing leg angle and angular velocity during walking at different speeds.

In (Sharbafi et al., 2017) this pendulum-based model is extended to a two segmented swing leg equipped with biarticular springs. This models is called BDPS standing for Biarticular muscle equipped Double Pendulum SLIP (Fig.2b). In the SPS model (Fig. 2a) described by Eq. (1) the first two rows explain the stance leg dynamics of the SLIP model and the last row describes the swing leg dynamics. In that respect the stance and swing leg dynamics are decoupled. In the BDPS model we consider coupling between stance and swing leg dynamics which may help better predict human motor control and produce more synchronized joint control in robots. There are many other extended models which can be used as templates for control of different locomotor sub-functions. For example OĆonnor introduced a new SLIP-based model with additional mass in both legs, curved feet and hip rotational spring (OĆonnor, 2009). However, here we focus on the simplest models that can represent the gait features required for control of the sub-functions.

Judging from human leg muscle activities in the swing leg movement, biarticular hip muscles; rectus femoris (REF) and hamstrings (HAM) seem to be the main contributors for swing leg control in walking (Nilsson et al., 1985). By modeling these two muscles with biarticular springs, better mechanical understanding of their activities in producing stable gait is obtained. In addition, such a passive mechanism may also replicate strong correlation observed between RF and HA in human swing leg movement (Prilutsky et al., 1998), as a consequence of body mechanics. The role of elastic biarticular thigh muscles (represented as springs) on swing leg dynamics can be further investigated, and the appropriate spring parameters and morphology can mimic human swing leg motion in walking. The muscle lever arm ratio, muscle stiffness and muscle rest lengths influence the CoM motion and the swing leg behavior. With passive elastic biarticular muscles, walking motion characteristics, like swing leg retraction and symmetric stance leg behavior around mid-stance are predicted (Sharbafi et al., 2017).

In this model, the double pendulum with biarticular springs for the swing leg can be combined with any model of stance leg (e.g., SLIP model). Here we describe BDP (Biarticular muscle equipped Double

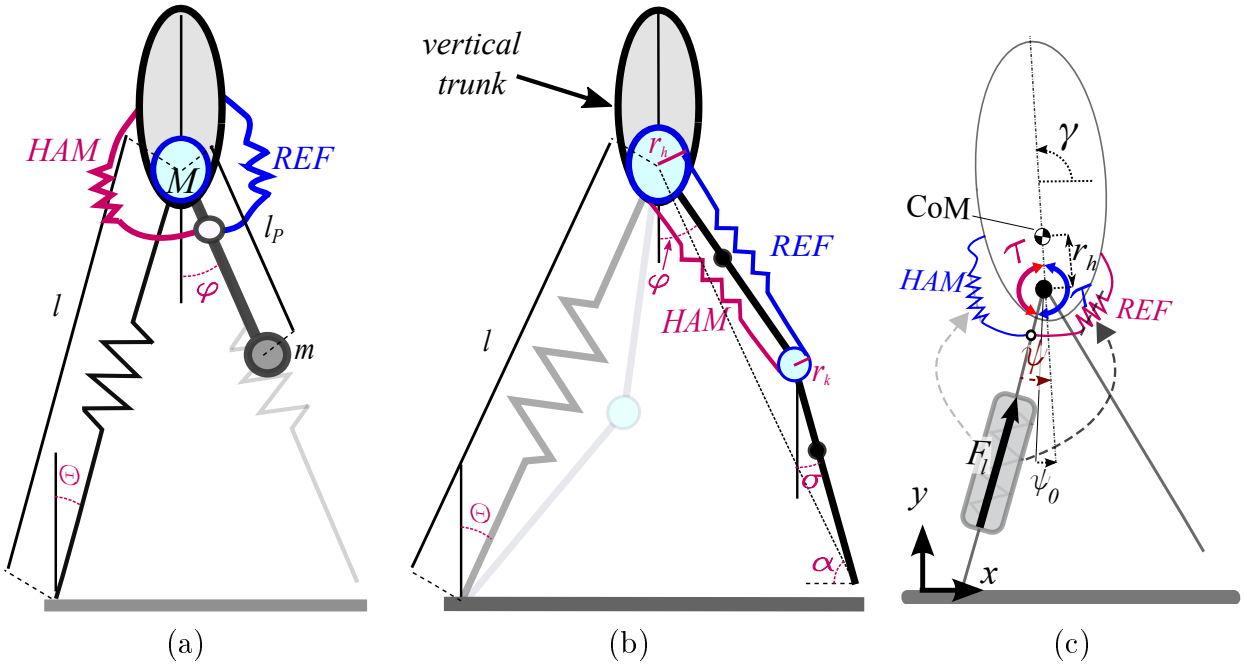

Figure 2: (a) SPS (Springy Pendulum SLIP) model of swing leg adjustment. (b) BDPS (Biarticular muscle equipped Double Pendulum SLIP) model for leg swinging. A virtual upright trunk is considered, from which the hip angle (φ) is computed in SPS and BDPS models. The spring of the stance leg can be replaced by any models mimicking SLIP like behavior (e.g., with segmented leg as shown by light colors). (c) FMCH for posture control in bipedal walking. In current state, the red spring is producing (negative) rotational torque as a hip flexor muscles (Rectus femoris or Iliopsoas) while the blue hip extensor spring (Biceps femoris or Gluteus Maximus) is slack.

Pendulum) formulation for swing leg modeling while representing BDPS as an example to have SLIP for the stance leg to complete the walking model. Depending on the stance leg model, switching mechanisms between two legs at touchdown and takeoff needs to be defined. Let q_s be the configuration variables of the stance leg (e.g., $q_s = [\theta\ l]^T$ for BDPS) and define $q = [q_s^T\ \varphi\ \sigma]^T$ as depicted in Fig. 2b (super index T shows transpose operator.). Then, the following dynamic equation of the model are obtained.

$$D(q)\ddot{q} + C(q,\dot{q})\dot{q} + G(q) = F \tag{4}$$

in which G, D and C are the gravity vector, the inertia and the Coriolis matrices, respectively. The last two rows of the force vector (F) are calculated from summation of the hip and knee torques generated by REF and HAM springs (see below). The hip torque is exerted between the thigh and a virtual upright trunk which approximates the normal upper body posture in human locomotion as described in Maus et al. (2010). For this, posture control as the third locomotor sub-function will be addressed in the next section. Suppose the lever arms at hip and knee are described by r_h and r_k, respectively. Then, the elongation of REF (from rest length) will be

$$\Delta l^{REF} = r_k\theta_k - r_h\varphi - l_0^{REF} \tag{5}$$

in which $\theta_k = \varphi - \sigma$ and l_0^{REF} are the knee angle and the REF spring rest length, respectively. The net torques generated by the REF acting at the thigh (τ_φ^{REF}) and the shank (τ_σ^{REF}) are computed as:

$$\begin{cases} \tau_\varphi^{REF} = k_{REF}(r_h - r_k)max(\Delta l^{REF}, 0) \\ \tau_\sigma^{REF} = k_{REF} r_k max(\Delta l^{REF}, 0) \end{cases} \tag{6}$$

where k_{REF} is the stiffness of the REF spring. By antagonistic arrangement the hip and knee torques provided by the HAM can be calculated in a similar manner. In the BDPS model that uses spring for stance leg generating leg force F_s, the force vector F will be calculated as follows.

$$F = \begin{bmatrix} 0 \\ F_s \\ \tau_\varphi^{REF} + \tau_\varphi^{HAM} \\ \tau_\sigma^{REF} + \tau_\sigma^{HAM} \end{bmatrix} \tag{7}$$

Such a simple bioinspired control approach can be easily implemented in robots (Sharbafi et al., 2016). During the swing phase, biarticular muscles can support swing leg rotational movement control while monoarticular muscles (e.g., knee or ankle joints) can provide (axial) leg shortening and lengthening (e.g. leg shortening is required for ground clearance). With such a muscle-specific task allocation, the target of control could be simply setting spring rest lengths to a specific value for each gait condition. Considering Variable Impedance actuators (VIA) as tunable compliant elements, such passive leg swinging methods can be mimicked by bi-articular VIAs. In section 11.4 the results of applying this model for control of leg swinging sub-function in BioBiped robot are presented.

Virtual pendulum for Balance

Humans and other bipeds unlike quadrupeds need to take care of their upper bodies to avoid falling. Since there is no upper body in SLIP model, it can not describe posture control. In other words, one of the shortcomings of the SLIP model is its inability in predicting ground reaction forces (GRF) direction while it is always intersecting CoM. In contrast, in the stance phase of (upright) human walking, the GRFs are intersecting in a virtual pivot point (VPP, (Maus et al., 2010)) or divergent point (DP, (Gruben and Boehm, 2012)) above the center of mass (CoM). Therefore, the SLIP model needs to be extended by a segment (e.g., rigid trunk) representing the upper body (e.g., TSLIP model for Trunk SLIP). Based on VPP concept, postural balance control can be understood as converting the upright inverted (body) pendulum into the regular pendulum model. In this model a virtual pendulum (VP) can be defined with a point mass at CoM hanging from the VPP. From a control point of view, this concept can be employed to derive balancing strategies.

From another point of view, having appropriate controllers for two other locomotor sub-functions, a stable gait is achievable by producing a hip torque to redirect the ground reaction forces to a predefined VPP (Sharbafi et al., 2012; Maus et al., 2010). In an extension of the model, the VPP is adjusted at each step (called virtual pendulum posture control, VPPC), which results in robust hopping (Sharbafi et al., 2013b). Surprisingly, the desired control performance can be partially achieved by an appropriate hip compliance design, as can be seen in (Rummel and Seyfarth, 2010; Sharbafi et al., 2013a). However, to achieve more human-like hip torque control and better matching to VPP concept, a reflex signal representing leg force is needed to adjust the hip compliance (Sharbafi and Seyfarth, 2014). As a result, a new model called FMCH (force modulated compliant hip) can physically implement the VPP concept with a neuro-muscular structure (Fig. 2c). In this model, the hip torque between the virtual leg and the

upper-body is generated by an adaptable spring. The virtual leg is defined from CoP to the hip. The hip torque τ is given by

$$\tau = k_{REF} max(\psi_0^{REF} - \psi, 0) - k_{HAM} max(\psi - \psi_0^{HAM}, 0). \quad (8)$$

in which, ψ, ψ_0 and k are the trunk to leg angle, rest angle and stiffness of the hip spring, respectively. The super-/sub-index REF and HAM indicate the corresponding muscle. First, we assume the same stiffness ($k_h = k_{REF} = k_{HAM}$) and rest angle ($\psi_0 = \psi_0^{HAM} = \psi_0^{HAM}$) for both hip springs. Then, the stiffness of this rotational spring (k_h) is adjusted using the leg force F_s feedback as follows:

$$\tau = k_h(\psi_0 - \psi) = cF_s(\psi_0 - \psi) \quad (9)$$

In this formulation, the hip stiffness k_h is given by leg force F_s multiplied by a constant value c. In addition to benefiting from motion dynamics to synchronize the locomotor sub-functions (like in the BDPS model), here a feedback from one sub-function (leg force from stance) to another (hip compliance controlling balance) improves coordination between locomotor sub-functions for generating a stable gait. This yields a clear VPP above CoM in the upper body coordinate system (Sharbafi and Seyfarth, 2014).

This approach results in stable walking (Sharbafi and Seyfarth, 2015) and running (Sharbafi and Seyfarth, 2014) as predicted by the model. FMCH model represented by Eq. (9) not only can describe human posture control (Sharbafi and Seyfarth, 2017), but also can be easily implemented on robots (Sharbafi et al., 2016) and exoskeletons (Zhao et al., 2017). The outcomes of such implementations are described in Sec. 11.4. Interestingly, it was found that the combination of locomotor sub-functions based on implicit coordination (with a limited exchange of sensory information) can produce stable gaits e.g., forward hopping (Sharbafi et al., 2014, 2016). This supports the idea of implementing separate sub-function controllers in wearable robots.

11.3 HUMAN GAIT

In (Sharbafi and Seyfarth, 2017), different sub-function models are utilized to predict human control strategies for walking at different speeds. The SLIP model with adaptable leg stiffness and rest length which are changing at middle of single support was used to predict the stance leg force. It was shown that the leg spring behavior is clearly changing at the middle of swing phase. The higher performance of SLIP model with a variable spring (compared to the fixed spring) in energy management and perturbation recovery were also depicted in (Ludwig et al., 2012) and Sharbafi et al. (2013b), respectively. Such a method can be implemented to control robots and assistive devices. In the next section we explain how to use this approach for control of (wearable) robots.

In the aforementioned study of different sub-functions' roles in speed adjustment, the angle of attack and the angular speed at touchdown moment were used to characterize the swing leg control (Sharbafi and Seyfarth, 2017). In addition, the VBLA controller was also compared to other methods regarding their abilities in explaining human leg adjustment. However, these are not the template model to be used for the second locomotor sub-function. Furthermore, none of the above methods can control the swing leg continuously during swing phase and they mostly aim at finding an appropriate angle of attack. Here, we utilize the two template models of swing leg control presented in previous section (see Fig.2a for SPS and Fig. 2b for BDPS).

Using the SPS model we predict the patterns of human leg angle and angular velocity changes in walking at different speeds as shown in Fig. 3. The blue curves show experimental data and the red dash-dotted curves demonstrate the prediction of the SPS model. In these graphs we use the initial leg angle

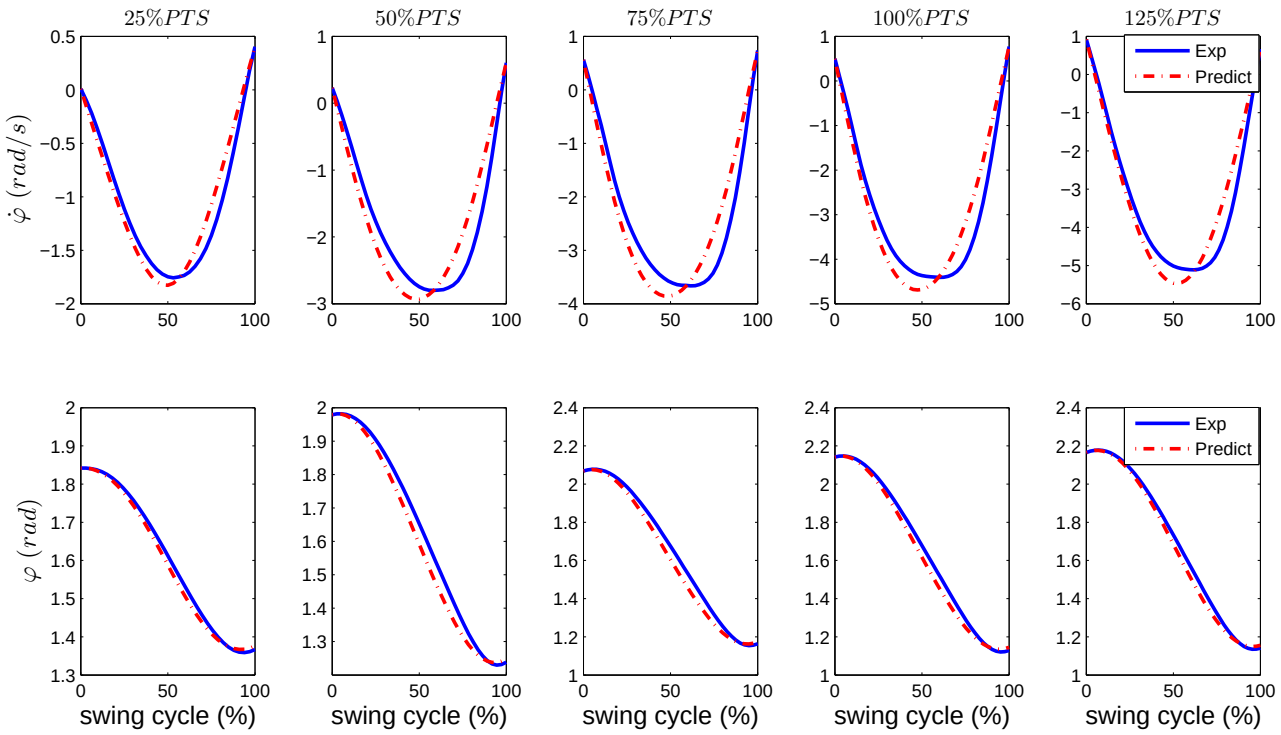

Figure 3: Swing leg angle and angular velocity in human walking experiment (Exp) are shown by blue solid line and predictions of these values by the SPS model (Predict) is shown by red dash-dotted lines.

($\varphi(0)$) and angular speed (($\dot{\varphi}(0)$) at takeoff and calculate the acceleration from experimental data and the swing trajectories ($[\varphi(t)\ \dot{\varphi}(t)]$) using Eq. (3). Implementation of this approach for control needs just the current leg angle for computing the required torque to generate the desired acceleration. The quality of prediction by the SPS model is shown in Table. 2 using R^2 index for correlation. It can be seen that the precision of predicting the leg angle during swing phase is 0.98 or 0.99 at different speeds.

Our another template for swing leg is the so called BDPS model in which the swing leg is modeled by a double pendulum equipped with biarticular springs. In (Sharbafi et al., 2017), it was shown that using this model stable walking can be achieved without energy consumption for leg swinging, while energy injection is performed by tuning the springs rest lengths just before takeoff. Using SLIP for modeling the stance leg, we have shown that appropriate tuning of the biarticular springs' rest lengths are sufficient for swing leg adjustment. Similarity between muscle force patterns of the BDPS model and human subjects were demonstrated in (Sharbafi et al., 2017). Therefore, if the posture control sub-function can perfectly keep the upper body upright, the leg swinging strategy beside spring-like behavior of the stance leg (with

Table 2: Precision of predicting human swing leg movement during single support of walking, with SPS model. Correlation between prediction and real values are shown by R^2 values.

Walking speed	**25%PTS**	**50%PTS**	**75%PTS**	**100%PTS**	**125%PTS**
Leg angle	0.99	0.98	0.98	0.99	0.99
Angular speed	0.94	0.87	0.89	0.91	0.93

appropriate stiffness and rest length) results in a stable gait.

For the third locomotor subfunction, the hip torques in the single support of human walking at different speeds were predicted by the FMCH model with sufficiently high precision. Hence, this model can be used as our template model for posture control. Considering the FMCH for posture control beside BDPS or SPS for swing leg and adjustable spring for stance leg can generate a stable model of locomotion which can explain human walking features precisely. In Sec. 11.4, we demonstrate how these models can be used for control of different sub-functions in isolation and in collaboration.

11.4 IMPLEMENTATION

Our template for stance leg control is the SLIP model, either with fixed stiffness for bouncy gaits, such as hopping and running or variable stiffness for walking. In a pilot research about control of knee actuator for lower limb exoskeleton, a segmented leg is developed that moves in vertical direction. This robot, called MARCO-Hopper-II, was the next generation of MARCO-Hopper developed 10 years ago (Seyfarth et al., 2007). In studies on MARCO-Hopper, the motor torque was simulating either a linear leg spring (based on SLIP model) or a muscle-reflex system. For stable hopping, significant energy supply was required after mid-stance, achieved by enhancing leg stiffness (Kalveram et al., 2012) or by continuously applying positive force feedback(Seyfarth et al., 2007). In (Oehlke et al., 2016), we have implemented the SLIP-based stance leg control on the MARCO-Hopper-II robot to mimic human hopping in place. The virtual model control (VMC) (Pratt et al., 2001) and energy-management (Kalveram et al., 2012) were two approaches to implement this control strategy on the robot. Stable hopping with similar features to human hopping was achieved using SLIP as the template for control. Similar to findings in human gaits, changing the stiffness of the virtual spring (between the hip and the foot) is required to control the robot for energy management. The hardware is to be extended with addition of spring in series with the electric motor as the next step of developing human-like motor control for assistive devices. Employing SEAs (series elastic actuators) for control of wearable robots is beneficial as can be seen in (Eslamy et al., 2012; Walsh et al., 2006).

In (Sharbafi et al., 2014), a similar approach for stance leg control was implemented on the detailed simulation model of BioBiped robot (Fig. 4a) for forward hopping. In Fig. 4a, the third version of this robot series, called Biobiped 3, is shown (see (Sharbafi et al., 2016) and `www.biobiped.de` for more information). In addition to apply VMC for SLIP-based control of the stance leg, we employed the VBLA (Sharbafi and Seyfarth, 2016) for swing leg adjustment. Stable forward hopping was achieved with this combination of two sub-functions while the upper body was balanced using mechanical constraints (Sharbafi et al., 2014).

Combination of different locomotor sub-functions (stance and swing) is tested on the detailed model of the robot using BDPS template model. Here, we use SLIP for control of the stance leg and the thigh biarticular actuators (muscles) for swing leg adjustment (see Sec. 11.2.1 for details). Stable forward hopping with adjustable horizontal speed is achieved using this technique. Fig. 4b shows the results of speed adjustment and the stable limit cycle in vertical direction. The simulation starts by dropping the robot from 1 m height. As shown in the bottom figure, the controller increases the robot speed to reach 1 m/s horizontal speed and hops with this speed for 3 seconds (from 5s to 8s). Then, by readjustment of the rest length of swing leg thigh springs and the stiffness of the virtual stance leg using the ankle joint, the speed increases to 1.75 m/s. The contributions of the stance and swing leg controllers are different for the first and the second commanded speeds. This demonstrates the ability of the proposed controller to consider different features in tracking a desired input. As a result, the small overshoot in reaching 1 m/s is not observed in the second acceleration phase to set the speed to 1.75 m/s, whereas

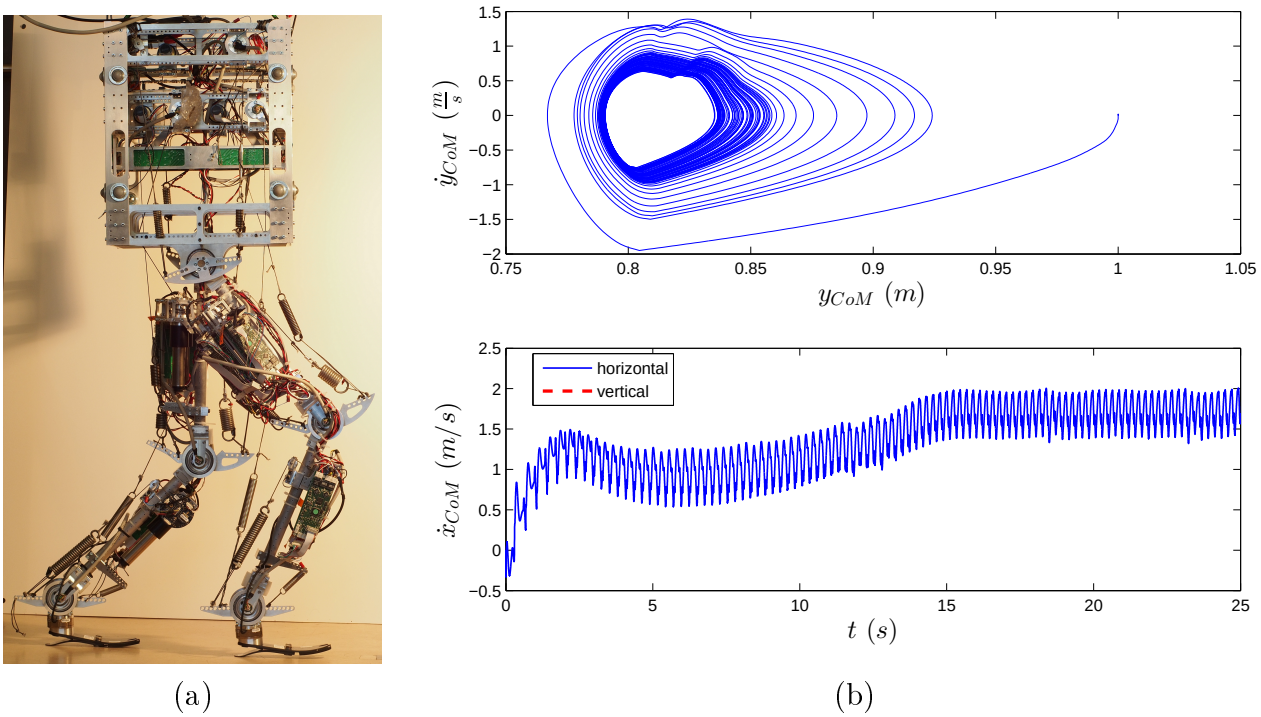

(a) (b)

Figure 4: (d) BioBiped 3 robot, (e) The results of forward hopping with BioBiped detailed model based on locomotor sub-function control concept. Top figure shows the limit cycle (y_{CoM} is the CoM height) and bottom figure illustrates the forward speed of the CoM ($\dot{x}_{CoM}$). The template model for control is the BDPS model. The speed is adjusted using the stiffness of stance leg spring through ankle joint control and the rest lengths of the biarticular thigh springs.

the settling time is smaller in response to the first commanded speed. Here, the role of the stance control (injecting a fixed amount of energy through SLIP-based controller using VMC) is more significant in the first phase (1 m/s) compared to second phase (1.75 m/s), while this is other way around for the swing leg control (adjusting the thigh biarticular muscles' rest lengths). This is implemented by larger relative changes (from first to the second phase) in swing leg control than stance control. Therefore, when the contribution of the stance leg control is higher, the response is faster including overshoot, whereas a higher contribution of swing leg control results in slower convergence without overshoot.

The top figure illustrates the phase plot in the space of CoM height y_{CoM} and vertical speed $\dot{x}_{CoM}$. It shows that after reaching a certain forward speed the phase trajectories converge to a stable limit cycles corresponding to hopping horizontal speed. In addition, with increasing the motion speed, the shape of the limit cycle is fixed, whereas the size shrinks. These results show that simple controller based on the locomotion sub-function concept can properly stabilize the robot motion. Note that the upper-body is playing the role of the coordinator between the two sub-functions. Here the posture control is exerted by enforcing physical constraints and there is no need for further exchange of sensory information. The same concept can be employed in control of exoskeletons while human posture control can be complemented by assistive swing and stance leg control from the robot.

Successful addition of posture control to aforementioned stance and swing leg controllers were shown with different combinations of sub-function controllers for different gaits (Sharbafi et al., 2013a,b; Shar-

bafi and Seyfarth, 2014). Recently, we have examined the idea of distributed control of sub-functions in two new directions: extending the template models to neuromuscular level and implementing the controllers on robots. In Fig. 5 we showed the required steps. In the first step, the rotational hip springs are replaced by muscle models as shown in Fig. 5a. With this model we could achieve stable walking with GRFs and hip torques similar to FMCH model (respectively to human gaits). Afterward, we substituted the leg spring with a two segmented leg including the knee extensor muscle (Fig. 5b) and could achieve stable walking. Although the patterns are not completely similar to previous models, the VPP exists which shows the consistency of the model with previous models and also to human posture control. The last step is using this model for human walking and emulate the exoskeleton via addition of actuators (e.g., SEAs) to assist human walking as shown in Fig. 5c. With this model using the FMCH-based controller, a method for control of the exoskeleton (e.g., wearable robot) is developed which is in line with the neuromuscular control of humans. The details of these simulation studies are out of scope of this paper and will be presented elsewhere. Here, we explain the results of our recent implementation of this method on a wearable robot. Based on the bioinspired VPP (virtual pivot point) concept, introduced in

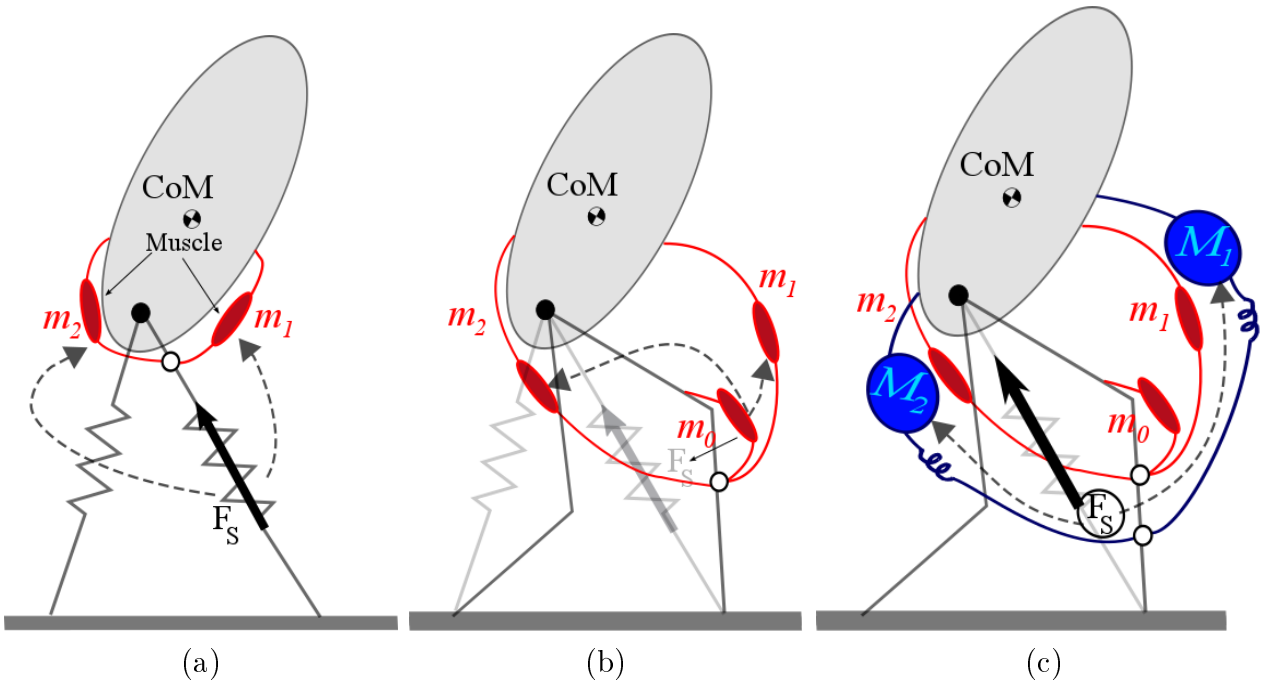

Figure 5: Steps of extending FMCH model to neuromuscular level and exoskeleton control. (f) replacement of hip spring with muscle model, (g) segmentation of the leg and replacement of the leg spring by knee extensor muscle, (h) implementation of assistive control in addition to muscle activation.

(Maus et al., 2010), we have developed the FMCH model, in which adaptable hip springs are considered for balancing while the spring stiffness is modulated by leg force. We have shown that this control approach results in a VPP using conceptual models (Sharbafi and Seyfarth, 2015).

In this experiment we have implemented an FMCH-based controller on a lower limb powered exoskeleton (LOPES II) and demonstrated that it can effectively assist humans during walking. The experiment is performed with four young healthy subjects (3 males, 1 female, age: $24-36$ *yrs*, height: $1.65-1.91$ *m*, weight: $70-77.7$ *kg*) wearing the exoskeleton, walking on a moving treadmill (see Fig. 6a). The walking speed is set to 0.6 m/s speed due to limitations in the robot. We recorded muscle activities (electromyo-

graphy (EMG) signals) of rectus femoris (REF), hamstring (HAM), medial gastrocnemius (GAS), and gluteus maximus (GLM). In addition, for the last two subjects, metabolics were measured (Oxycon Pro, Jaeger GmbH, Hoechberg, Germany) to assess how much energy expenditure can be reduced by the assistive controller. In this robot the knee and hip joints are active while the ankle is passive. The experiment protocol includes three phases: **i) Initiation:** to be familiarize with the exoskeleton, each subject had a test walking trial (about 3 to 5 min) wearing the exo. **ii) Warm-up:** It is 3 min walking with the robot in transparent mode for warming up (without data collection), **iii) data measurement:** 7 min assisted walking, 7 min transparent walking, and 3 min quiet standing for measuring the bias values. All trials are compared to the transparent mode in which the robot follows the human subject's movements and tries to vanish the interaction force between human and the robot. More details about the experiments can be found in (Zhao et al., 2017).

In this experiment the basic FMCH model is emulated by actuating the hip and knee actuators using the concept of biarticular muscles and the virtual leg. Since this controller is consistent with the VPP posture control concept (Sharbafi and Seyfarth, 2014, 2015) in human walking, the subjects feel comfortable with minimal opposing forces from the exoskeleton. This was quantitatively approved by measuring EMG signals and oxygen consumption. Figure 6b shows the reductions in muscle activation for different subjects. We compute the root mean square of the EMG signals for each trial subtracted by the EMG r.m.s. of the experiments performed in the transparent mode. It is observed that the average values for all muscles are positive meaning that this control technique can (in average) reduce the muscle activation of all four muscles. Concentration on different subjects' muscle activation also shows that the majority of the muscles are more relaxed (shown by positive numbers) in this assistive mode for every individual subject. For S2 (orange), all muscles have reduction in muscle activation. For S4 (green) HAM and GAS have significant reduction in EMG, while the two other muscle have small increase (not statistically significant) in muscle activation. For S3 (pink), all muscles are benefiting from assistance except HAM which shows increase in muscle activation. The results for the last subject is similar to S3, but with increase in REF instead of HAM. Thus, each subject benefits from assistance due to EMG reduction in majority of their muscles. The most assistance is observed in GAS muscle (positive for all subjects) and the least in REF muscle which might be related to their contributions in stance leg control. Furthermore, the results show that the robot and the subject interact with each other and the adaptation method varies between subjects. Using the ground reaction force (as a signal representing muscle reflexes) in adjusting the hip compliance makes the robot responsive to human reaction. This may also be a reason for different levels and patterns of assistance in different subjects.

Another measurable index for evaluating the performance of the controlled wearable robot is cost of transport. For this, we compare the oxygen consumption in two subjects (S3 and S4) with and without assistance (transparent mode). The results show 10.2% and 10.4% reduction in metabolic cost in the assistive mode compared to the transparent mode.

11.5 DISCUSSION

In this paper, we introduced different studies preformed based on the concept of dividing legged locomotion to three sub-functions. Modeling and control of legged locomotion are challenged by nonlinearity, hybrid dynamics, uncertainties, dynamic coupling, etc. Dividing this complex problem to underlying sub-problems, helps better understand, design and control of legged locomotion. We have supported this hypothesis by several studies resulting in (i) acceptable prediction of different features in human gaits, (ii) stability analysis of the developed models and (iii) successful implementation on hardware setups such as BioBiped, MARCO-Hopper-II and LOPES II. Therefore this new point of view in control can be a useful tool for managing the challenging legged locomotion problem.

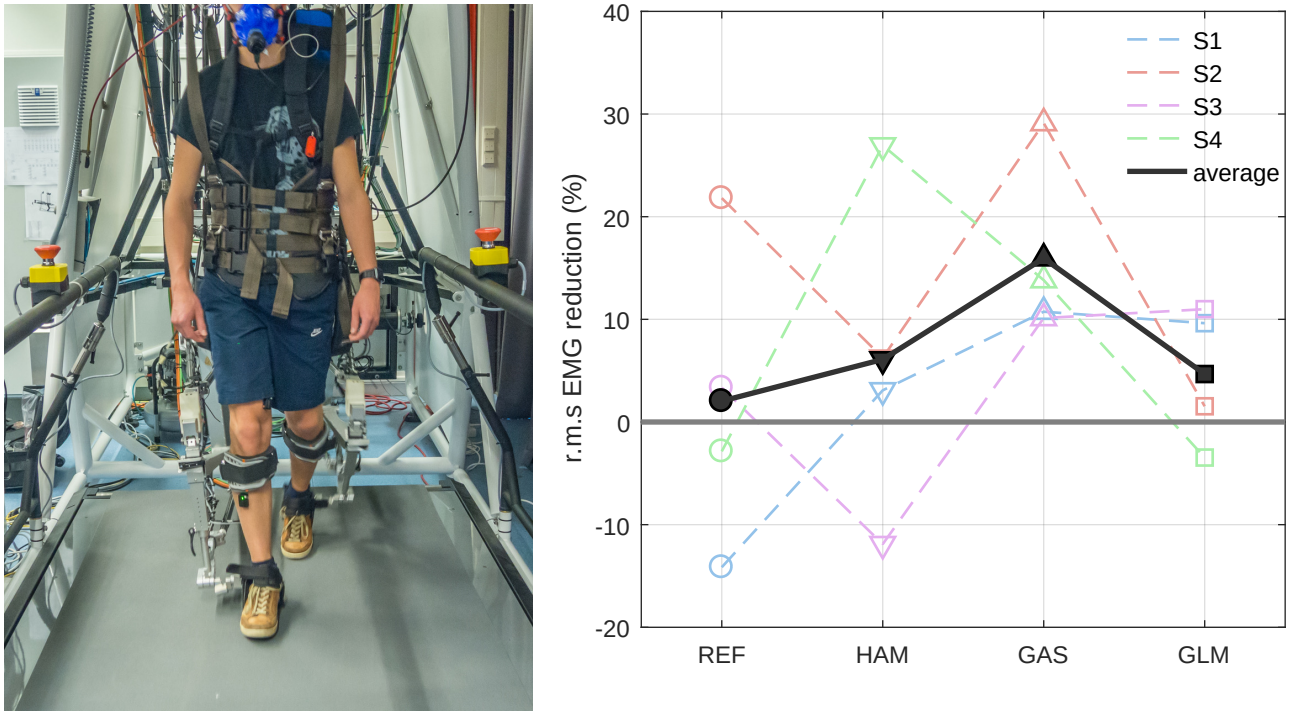

(a) (b)

Figure 6: (i) Experiment with LOPES II, (j) reduction in root mean square (r.m.s) of muscle activations for different subjects shown by different colors and dashed lines. The black solid line depicts the average of the EMG reduction for the four subjects. S1 to S4 indicate the subjects number.

In our studies, locomotor sub-function models are able to explain human gait in isolation and in interaction with each others both in conceptual models and detailed simulation model of robots. The stance and balance control approaches were also tested in experiments with MARCO II and LOPES II, respectively. In the studies on the BioBiped robot, we showed how stance and swing locomotor sub-functions can be synchronized if the posture is balanced. In this experiment the upper body was fixed by a frame as a physical constraint and in an exoskeleton, it can be performed by the a harness or another controller for balancing that assists (healthy or impaired) human subject. The proposed controller for swing leg is very simple, efficient and compatible with the FMCH based posture control when the leg switches from swing to stance. Therefore, the same mechanism (biarticular thigh muscles) and similar controller can be used between upper body and the leg for the swing and balance control.

In BioBiped experiments, motion speed adjustment by tuning the biarticular springs rest lengths provides a simple and efficient swing leg control approach with no need of sensory information from the leg configuration. In order to achieve high efficiency during different phases of the gait cycle (e.g., swing phase), non-backdrivable actuators are of advantage. They enable setting the springs' rest lengths to desired values, switching off the motors and operating with no (or little) resistance when no actuation is needed. Similar design and control can be employed to build an exoskeleton. The simple position control to set the biarticular springs' rest length via non-backdrivable motors can be implemented on soft exoskeletons (wearable robots) (Bartenbach et al., 2015).

The main idea of the proposed separate sub-function control in legged locomotion is the unifying control rule inspired from template models. Since the controllers use similar concepts of periodic movements through different oscillators, the sub-functions are harmonized by synchronizing the oscillators. Such an implicit coordination between different locomotor sub-functions is achieved via minimal sensory feedback. Roughly speaking, the spring in the SLIP model plays the role of a coordinator, the swing leg pendulum follows the CoM dynamics with fine tuning by hip springs and the force feedback used in FMCH synchronizes posture and stance control using the leg force which is generated by the leg spring. Hence, there is no need for extra higher level controller for synchronization of different sub-functions in steady state gait.

The built-in coordination with limited exchange of sensory information as the main advantage of distributed control using locomotor sub-functions, can be more visible in interaction with humans. In applications like control of wearable robots or prostheses, there is another high level supervisory controller from humans. Obviously, humans not only modify synchronization of different control level, by interacting with the robot, but also adapt to external torques and learn optimizing their efforts (as can be seen in the experiment with LOPES II). Indeed, reduction in energy consumption and muscle activation demonstrates that this adaptation improves support of human movement and the robot assists the human subject.

The next step of this research will be applying multiple (at least two) sub-functions controllers to the wearable robot (exoskeleton). For example, in LOPES II the BPDS and FMCH can be implemented for swing leg and balance control, respectively, through knee and hip actuation (the ankle which can be used for stance control is passive in this exoskeleton). In the recently developed wearable robot (called EMY) within the Balance project (`http://balance-fp7.eu/`), all three locomotor sub-functions can be controlled (with active hip, knee and ankle) and their interaction in assisting humans can be evaluated. In future, biomechanical gait templates should be extended to the sensor-motor level. Here, matching templates model could be identified taking actuator and sensor properties into account. With these models, additional design requirements for the different locomotor sub-functions both in biological and engineered systems can be derived.

CONFLICT OF INTEREST STATEMENT

The authors declare that the research was conducted in the absence of any commercial or financial relationships that could be construed as a potential conflict of interest.

11.6 ACKNOWLEDGMENT

This research was supported in part by the EU project BALANCE under Grant Agreement No. 601003. We would like to thank Guoping Zhao and Mark Vlutters for their support in experiments with LOPES II and Philipp Beckerle and Jonathan Oehlke for their contributions in experiments with MARCO II. We would also thank Aida Mohammadinejad and Christian Rode for their supports in modeling of SPS and BDPS and their helpful discussions.

11.7 AUTHORS CONTRIBUTIONS

MAS has the substantial contributions to the conception, drafting the work, final approval and is responsible for accuracy of the analysis and results. GZ has substantial contributions in design and performing experiments with LOPES II and analyzing the results. AS has also substantial contributions in design of the work, revising it critically for important intellectual content and final approval of the version to be published.

11.8 REFERENCES

Alexander, R. M. (2003). *Principles of animal locomotion* (Princeton University Press)

Bartenbach, V., Schmidt, K., Naef, M., Wyss, D., and Riener, R. (2015). Concept of a soft exosuit for the support of leg function in rehabilitation. In *Rehabilitation Robotics (ICORR), 2015 IEEE International Conference on* (IEEE), 125–130

Blickhan, R. (1989). The spring-mass model for running and hopping. *Journal of Biomechanics* 22, 1217–1227

Blum, Y., Lipfert, S., Rummel, J., and eyfarth, A. (2010). Swing leg control in human running. *Bioinspiration and Biomimetics* 5

Chevallereau, C., Bessonnet, G., Abba, G., and Aoustin, Y. (2013). *Bipedal robots: Modeling, design and walking synthesis* (John Wiley & Sons)

Collins, S. H., Wiggin, M. B., and Sawicki, G. S. (2015). Reducing the energy cost of human walking using an unpowered exoskeleton. *Nature* 522, 212–215

Duysens, J., Van de Crommert, H. W., Smits-Engelsman, B. C., and Van der Helm, F. C. (2002). A walking robot called human: lessons to be learned from neural control of locomotion. *Journal of biomechanics* 35, 447–453

Eslamy, M., Grimmer, M., and Seyfarth, A. (2012). Effects of unidirectional parallel springs on required peak power and energy in powered prosthetic ankles: Comparison between different active actuation concepts. In *Robotics and Biomimetics (ROBIO), 2012 IEEE International Conference on* (IEEE), 2406–2412

Full, R. J. and Koditschek, D. (1999). Templates and anchors: Neuromechanical hypotheses of legged locomotion on land. *Journal of Experimental Biology* 22, 3325–3332

Geyer, H., Seyfarth, A., and Blickhan, R. (2006). Compliant leg behaviour explains basic dynamics of walking and running. *Proceedings of the Royal Society B* 273, 2861–2867

Gruben, K. G. and Boehm, W. L. (2012). Force direction pattern stabilizes sagittal plane mechanics of human walking. *Human Movement Science* 31

Haddadin, S., Albu-Schaffer, A., De Luca, A., and Hirzinger, G. (2008). Collision detection and reaction: A contribution to safe physical human-robot interaction. In *Intelligent Robots and Systems, 2008. IROS 2008. IEEE/RSJ International Conference on* (IEEE), 3356–3363

Holmes, P., Full, R. J., Koditschek, D., and Guckenheimer, J. (2006). The dynamics of legged locomotion: Models, analyses, and challenges. *Siam Review* 48, 207–304

Ijspeert, A. J. (2008). Central pattern generators for locomotion control in animals and robots: a review. *Neural networks* 21, 642–653

Kalveram, K. T., Haeufle, D. F., Seyfarth, A., and Grimmer, S. (2012). Energy management that generates terrain following versus apex-preserving hopping in man and machine. *Biological cybernetics* 106, 1–13

Knuesel, H., Geyer, H., and Seyfarth, A. (2005). Influence of swing leg movement on running stability. *Human movement science* 24, 532–543

Koditschek, D. E., Full, R. J., and Buehler, M. (2004). Mechanical aspects of legged locomotion control. *Arthropod structure & development* 33, 251–272

Ludwig, C., Grimmer, S., Seyfarth, A., and Maus, H.-M. (2012). Multiple-step model-experiment matching allows precise definition of dynamical leg parameters in human running. *Journal of biomechanics* 45, 2472–2475

Massion, J. (1994). Postural control system. *Current opinion in neurobiology* 4, 877–887

Maus, H. M., Lipfert, A. W., , Gross, M., Rummel, J., and Seyfarth, A. (2010). Upright human gait did not provide a major mechanical challenge for our ancestors. *Nature Communications* 1, 1–6

Mochon, S. and McMahon, T. A. (1980). Ballistic walking. *Journal of biomechanics* 13, 49–57

Mohammadinejad, A., Sharbafi, M. A., and Seyfarth, A. (2014). Slip with swing leg augmentation as a model for running. In *Intelligent Robots and Systems, IEEE/RSJ International Conference on*. 2543–2549

Nilsson, J., Thorstensson, A., and HALBERTSMA, J. (1985). Changes in leg movements and muscle activity with speed of locomotion and mode of progression in humans. *Acta Physiologica Scandinavica* 123, 457–475

OĆonnor, S. M. (2009). *The Relative Roles of Dynamics and Control in Bipedal Locomotion*. Ph.D. thesis, University of Michigan

Oehlke, J., Sharbafi, M. A., Beckerle, P., and Seyfarth, A. (2016). Template-based hopping control of a bio-inspired segmented robotic leg. In *Biomedical Robotics and Biomechatronics, IEEE International Conference on*. 35–40

Poulakakis, I. and Grizzle, J. W. (2009). The spring loaded inverted pendulum as the hybrid zero dynamics of an asymmetric hopper. *IEEE Transaction on Automatic Control* 54, 1779–1793

Pratt, J., Chew, C.-M., Torres, A., Dilworth, P., and Pratt, G. (2001). Virtual model control: An intuitive approach for bipedal locomotion. *The International Journal of Robotics Research* 20, 129–143

Prilutsky, B., Gregor, R. J., and Ryan, M. M. (1998). Coordination of two-joint rectus femoris and hamstrings during the swing phase of human walking and running. *Experimental Brain Research* 120, 479–486

Raibert, M. H. (1986). *Legged Robots that Balance* (MIT Press, Cambridge MA)

Riese, S., Seyfarth, A., and Grimmer, S. (2013). Linear center-of-mass dynamics emerge from non-linear leg-spring properties in human hopping. *Journal of biomechanics* 46, 2207–2212

Rummel, J. and Seyfarth, A. (2010). Passive stabilization of the trunk in walking. In *International Conference on Simulation, Modeling and Programming for Autonomous Robots* (Darmstadt, Germany)

Seyfarth, A., Grimmer, S., Maus, M., Häufle, D., Peuker, F., and Kalveram, K.-T. (2013). Biomechanical and neuromechanical concepts for legged locomotion. *Routledge Handbook of Motor Control and Motor Learning* , 90–112

Seyfarth, A., Kalveram, K. T., and Geyer, H. (2007). Simulating muscle-reflex dynamics in a simple hopping robot. In *Autonome Mobile Systeme 2007* (Springer). 294–300

Sharbafi, M. A., , Radkhah, K., von Stryk, O., and Seyfarth, A. (2014). Hopping control for the musculoskeletal bipedal robot: Biobiped. In *Intelligent Robots and Systems, IEEE/RSJ International Conference on*. 4868–4875

Sharbafi, M. A., Ahmadabadi, M. N., Yazdanpanah, M. J., Nejad, A. M., and Seyfarth, A. (2013a). Compliant hip function simplifies control for hopping and running. In *Intelligent Robots and Systems (IROS), 2013 IEEE/RSJ International Conference on* (IEEE), 5127–5133

Sharbafi, M. A., Maufroy, C., Ahmadabadi, M. N., Yazdanpanah, M. J., and Seyfarth, A. (2013b). Robust hopping based on virtual pendulum posture control. *Bioinspiration & biomimetics* 8, 036002

Sharbafi, M. A., Maufroy, C., Seyfarth, A., Yazdanpanah, M. J., and Ahmadabadi, M. N. (2012). Controllers for robust hopping with upright trunk based on the virtual pendulum concept. In *IEEE/RSJ International Conference on Intelligent Robots and Systems (Iros 2012)*

Sharbafi, M. A., Mohammadinejad, A., Rode, C., and Seyfarth, A. (2017). Reconstruction of human swing leg motion with passive biarticular muscle models. *Human Movement Science* 52, 96–107

Sharbafi, M. A., Rode, C., Kurowski, S., Scholz, D., Möckel, R., Radkhah, K., et al. (2016). A new biarticular actuator design facilitates control of leg function in biobiped3. *Bioinspiration & Biomimetics* 11, 046003

Sharbafi, M. A. and Seyfarth, A. (2013). Human leg adjustment in perturbed hopping. In *AMAM*

Sharbafi, M. A. and Seyfarth, A. (2014). Stable running by leg force-modulated hip stiffness. In *Biomedical Robotics and Biomechatronics (2014 5th IEEE RAS & EMBS International Conference on* (IEEE), 204–210

Sharbafi, M. A. and Seyfarth, A. (2015). Fmch: A new model for human-like postural control in walking. In *Intelligent Robots and Systems, IEEE/RSJ International Conference on*. 5742–5747

Sharbafi, M. A. and Seyfarth, A. (2016). Vbla, a swing leg control approach for humans and robots. In *Humanoid Robots, 2016 IEEE-RAS 16th International Conference on*. 952–957

Sharbafi, M. A. and Seyfarth, A. (2017). How locomotion sub-functions can control walking at different speeds? *Journal of Biomechanics*

Walsh, C. J., Paluska, D., Pasch, K., Grand, W., Valiente, A., and Herr, H. (2006). Development of a lightweight, underactuated exoskeleton for load-carrying augmentation. In *Robotics and Automation, 2006. ICRA 2006. Proceedings 2006 IEEE International Conference on* (IEEE), 3485–3491

Wensing, P. M. and Orin, D. E. (2013). High-speed humanoid running through control with a 3d-slip model. In *Intelligent Robots and Systems (IROS), 2013 IEEE/RSJ International Conference on* (IEEE), 5134–5140

Westervelt, E. R., Grizzle, J. W., Chevallereau, C., Choi, J. H., and Morris, B. (2007). *Feedback Control of Dynamic Bipedal Robot Locomotion* (Taylor & Francis, CRC Press)

Winter, D. (1995). Human balance and posture control during standing and walking. *Gait & posture* 3, 193–214

Winter, D. A. (2009). *Biomechanics and motor control of human movement* (John Wiley & Sons)

Zhao, G., Sharbafi, M., Vlutters, M., van Asseldonk, E., and Seyfarth, A. (2017). Template model inspired leg force feedback based control can assist human walking. In *IEEE-RAS-EMBS International Conference on Rehabilitation Robotics*

12 Conclusion

Research on legged locomotion has different aspects. Historically, researchers from different disciplines (engineers to biologists) tried to understand this complex problem and to develop agile and efficient locomotor systems. For example, Aristotle was one of the first who realized the challenge of designing legged systems by questioning about different mechanisms of locomotion (e.g., legs and wings) and various leg designs (e.g., in humans and birds). These are still open questions today and finding the corresponding answers could benefit also from complementary research in robotics and biology.

Given the differences between biological and artificial locomotion, an important question is to what extent should we use biological design and control approaches for building legged systems? Further questions to be answered are selecting the right gait models with respect to human movement and, their extensibility regarding other gaits, gait transition or locomotion on rough terrains. In short, the translation of the biomechanical template models to the neuromuscular level is still a challenging problem and its validation is not straight forward. For this, we suggest to simplify the problem by splitting it to simpler sub-problems and using reduced abstract models which can explain the significant features of biological locomotor systems, required to be mimicked in machines.

In this thesis, bioinspiration refers to the insight obtained from biology that can be adapted to the needs and capabilities of engineered systems. A main challenge in using biology as an inspiration for designing legged locomotion is that the capabilities of engineered systems may be very different to their biological counterparts. For example, compared to artificial actuators (like electric motors), biological muscles consist of many small actuator units (contractile elements) with distributed properties (such as fast vs. slow twitch muscle fibers) (Koditschek et al., 2004). As a result, the biological motor system is capable of producing versatile movements, spanning tasks of highly different loading and speed conditions (Komi, 2008). In contrast, state-of-the-art artificial actuators are designed to work optimally for continuous operation at one specific working condition (Robinson et al., 1999; Vanderborght et al., 2013). In this thesis, we presented a new point of view for bio-inspired legged locomotion which includes three main steps: (i) introducing the concept of ***locomotor subfunctions*** to understand the underlying principles of human locomotion using ***template models***, (ii) applying this concept to the ***design and control*** of legged systems, (iii) verification of this approach by ***implementation on robots and exoskeletons***. This helps fill the gap between biology and robotics by introducing a simplified representation of biological legged locomotion, extending the concepts from abstract to detailed level for design and control, and finally implementation on hardware.

12.1 Locomotor subfunctions and template models

As the first step in our bioinspired template-based control approach, we have concentrated on the three locomotor subfunctions: **stance**, **swing** and **balance**. Similar to the template and anchor concept (Full and Koditschek, 1999), considering such a modular structure facilitates understanding legged locomotion. Stance was selected as the primary essential locomotor subfunction representing the interaction between legs and ground (e.g. in 1D hopping). Leg swinging is a locomotor subfunction required to extend the movement from 1D to 2D (and 3D). These two subfunctions are sufficient to model different gaits (e.g., running and walking, (Geyer et al., 2006; Maus and Seyfarth, 2014; Peuker et al., 2012; Seipel and Holmes, 2006). Finally, balancing is required for stabilizing the upper body. This defines the third locomotor subfunction.

We have selected a set of templates for a modular representation of legged locomotion. The SLIP model (Blickhan, 1989) and its extensions were used for stance leg function. Linear leg spring is appropriate to model bouncing gaits such as running and hopping. For walking, SLIP parameters are not constant (Lipfert, 2010). This can be described by adjusting spring stiffness and rest length during ground contact. Using this family of models, appropriate prediction of human stance leg function and generating human-like stable gaits in simulations were demonstrated in different chapters of this thesis. We have selected a pendulum as a template for swing subfunction. Based on this approach, the natural passive dynamics of the swing leg generates most of the required movement. This means that low torques and energy are required for leg swinging compared to stance. Extending this model to double pendulum equipped with adjustable biarticular springs is sufficient to predict human-like muscle forces, body kinematics and kinetics. For the last locomotor subfunction, we selected the virtual pendulum concept (Maus et al., 2010) as a base and we developed a new FMCH model. Similar to the previous two subfunctions, here, an adaptable oscillator (spring-mass or pendulum) was suggested as the template model. Therefore, all subfunctions stem from the same concept of mechanical oscillators with a minimal set of parameters.

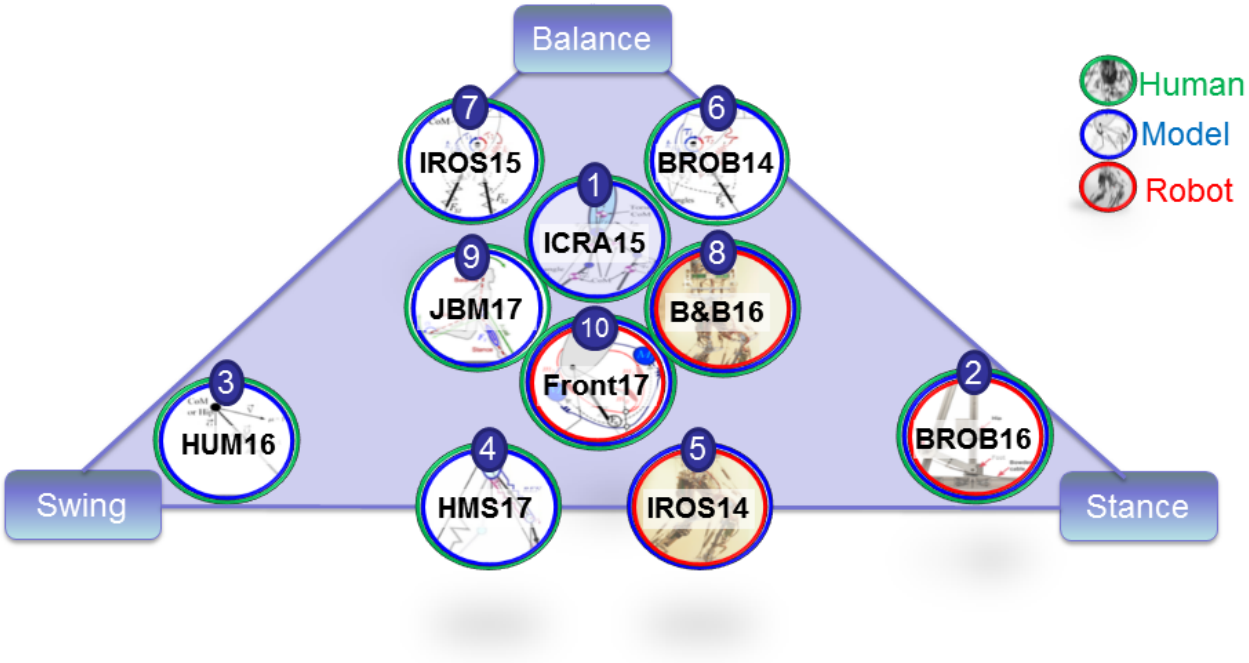

Figure 1: Organization of the papers (thesis chapters) in the context of locomotor subfunctions. The numbers show the order of presentation in this thesis. Circles with different colors show the analyzing methods of the related study, represented by Human, Model and Robot.

Fig. 1 represents legged locomotion as a composition of the three locomotor subfunctions. In this context, different gait models can be placed somewhere inside this triangle. The studies in this thesis are using models comprised of one or more of these subfuncitons and their positions in this triangle show the contribution of each subfunction. The first study comprises all three subfunctions, but without representing the individual subfunctions in the locomotor control. Then, the studies on the right and left

corners focus on just one specific subfunction. The next two studies investigate the combination of these stance and swing subfunctions which are placed on the bottom edge. Afterwards, two articles presented our approaches on balance control. Indeed these studies included two other stance and swing, but the focus was on balancing. Finally, with the last three studies we returned to the middle. In these studies, different aspects, from human experiments, modeling and implementation on robots are explored (shown with different colors in Fig. 1). Every study includes at least two of these three aspects which together provides the foundation for research in bioinspired legged locomotion.

12.2 Bioinspired design and control

Applying the modular concept of locomotor subfunctions for modeling and understanding human locomotion shows many advantages. This approach can be (and was already in this work) utilized for design and control of robots and exoskeletons. Inspired from nature, intelligent design of body morphology can optimize and simplify control by embedding part of the control in mechanics. In addition to develop new template models for locomotor subfunctions, our methods benefit from the biological design principle regarding mono- and biarticular actuation. For example, biarticular thigh muscles beside the monoarticular knee extensor muscle simplify GRF control by separating magnitude and direction of the force vector and assigning these components to different muscles. Such an approach can decouple the dynamics of a MIMO (multiple input multiple output) system to multiple SISO (single input single output) systems which are easier to be controlled.

After modifications in robot design (e.g., in BioBiped robot), we have employed the proposed modular template-based representation of legged locomotion for control of the robot. In order to benefit from this approach in control, we emulated physical elements (developed from template models) via controllers. For example human hopping was achieved in a robot (or its model) by emulating a virtual spring between hip and foot. In this method, the SLIP is introduced as the template using VMC (virtual model control) (Pratt et al., 2001) to represent the virtual spring behavior. The underlying template behavior is considered as target for control. Similar techniques were employed to implement different locomotor subfunctions (see below).

12.3 Implementation and verification in hardware systems

We have started with implementing the proposed approach on a hopping robot. Vertical hopping can be described by the first subfunction (stance). Implementing SLIP-based models on a hopping robot shows ability of the approach to explain human hopping within the design and control of the hopper robot.

For swing leg control (second subfunction), the double pendulum SLIP (DPS) model was successfully implemented on the BioBiped model. Fine tuning of muscle rest lengths in preparation for takeoff results in stable forward hopping. Combination of stance and swing leg control stabilizes the robot just by proper timing of transitions between stance and swing using state-machine control. No exchange of sensory information was required between the two subfunctions (stance and swing).

Successful implementation of the posture control method FMCH on LOPES II lower limb exoskeleton demonstrates the ability of our template-based controller to assist human walking (Zhao et al., 2017). Here, the different locomotor subfunctions were coordinated by human-robot interaction. In future we want to integrate the swing leg control together with stance and posture control in the same hardware system.

12.4 Outlook

People do the same motor task e.g., locomotion, differently, because of difference in their body, experiences (learning, emotional state), culture, phylogenesis and ontogenesis. Therefore, finding a predesigned control approach (e.g., using CPG or preflex control) that can cover all these diverse behaviors, resulting from numerous different roots is almost impossible. Instead, combination of motor control based on reactions (e.g., reflex control) with the feedforward approaches and smart design of mechanics could be one comprehensive solution. In addition, developing template models is an appropriate method in generalization of simple design and control concepts of locomotion. The templates do not provide specific design and control solutions. Instead, they illustrate the relationship between mechanics and control. The specific features of the system determine the possible (reachable) solutions within the space defined by templates. With this, the templates are independent of detailed specifications of the locomotor systems. As a result, a region of design and control solutions can be identified by templates if the motion task is defined. In addition, exploration of different locomotion solutions depending on environmental and gait conditions becomes possible. However, the templates do not appropriately represent adaptation mechanisms. Therefore, it is required to extend these models to incorporate such mechanisms, like in the FMCH model. This concerns the representation of the specific mechanical design and motor control including neuromuscular systems.

Based on the above argumentation, a new methodology in design and control of legged systems was developed in this thesis, based on the concept of locomotor subfunctions. We further developed this concept leading to a modular control approach with minimal exchange of sensory information. With the proposed method, we can improve our understanding of legged locomotion both in robots and biological legged systems.

By using template models we selected a bioinspired approach to develop human-like controllers for each subfunctions. This enables to create novel machines that closely interact with and assist humans such as prostheses or exoskeletons. These systems may support elderly or subjects with mobility impairments. They can enhance human performance in daily activities by targeting more efficient and robust assistive robots. This shows the wide spectrum of applications of the methodology proposed in this thesis. This research can be continued to resolve the following challenges.

First challenge could be in coordinating different locomotor subfunctions. We provided few solutions to support this coordination. Results showed that minimal sensory exchange can be sufficient to synchronize the subfunctions, e.g., stance and balance by leg force feedback. However, this study needs to be extended to different gaits considering other interactions between subfunctions and their responses to perturbations.

Further implementations of our approach on other assistive devices will demonstrate how humans interact with bioinspired hardware systems through the proposed approach. By now, we have started to investigate the advantages of this modular control approach in LOPES II exoskeletons by applying FMCH as a posture control method. Currently, we are extending the controller to include double-pendulum SLIP (DPS) model for swing leg control. Such bioinspired controllers can be directly used in soft exoskeletons (e.g., exosuits (Asbeck et al., 2013; Wehner et al., 2013)).

Another open question is about the ability of the proposed approach to facilitate gait transitions. In one of the presented studies (Article V), we have demonstrated how stance and swing leg control can collaborate to change the motion speed and switching from hopping in place to forward hopping and vice versa. In another study we showed roles of different subfunctions in human walking at different speeds. In future, these studies could be extended to switching between gaits, e.g., from walking to running. Such gait transitions could be achieved by adapting the template model properties (Martinez

and Carbajal, 2011). For example, in walking we need variable leg stiffness and rest length which is different from the original SLIP model for running with fixed spring parameters.

For implementation of the proposed method on more complex systems like humanoid robots, the anchoring mechanism needs to be further investigated. In this thesis, three different methods were utilized to apply the subfunction controllers on real systems. The first method was the direct implementation of the controller equations on the hardware systems and hardware models e.g., in FMCH on LOPES II exoskeleton or VBLA on BioBiped model. The second method was extending the template models to more complex ones using mechanical structures e.g., using biarticular muscles to control GRF in BioBiped3 robot. The third method was employing virtual model control to extend the template based control to a real testbed and hardware models e.g., in stance control of MARCO-Hopper-II and BioBiped model. With this approach we present a methodology to travel in the bioispired design and control loop, shown in Fig. 2. There is still a large need for novel anchoring techniques reflecting the complexity of a real system in selected motion tasks.

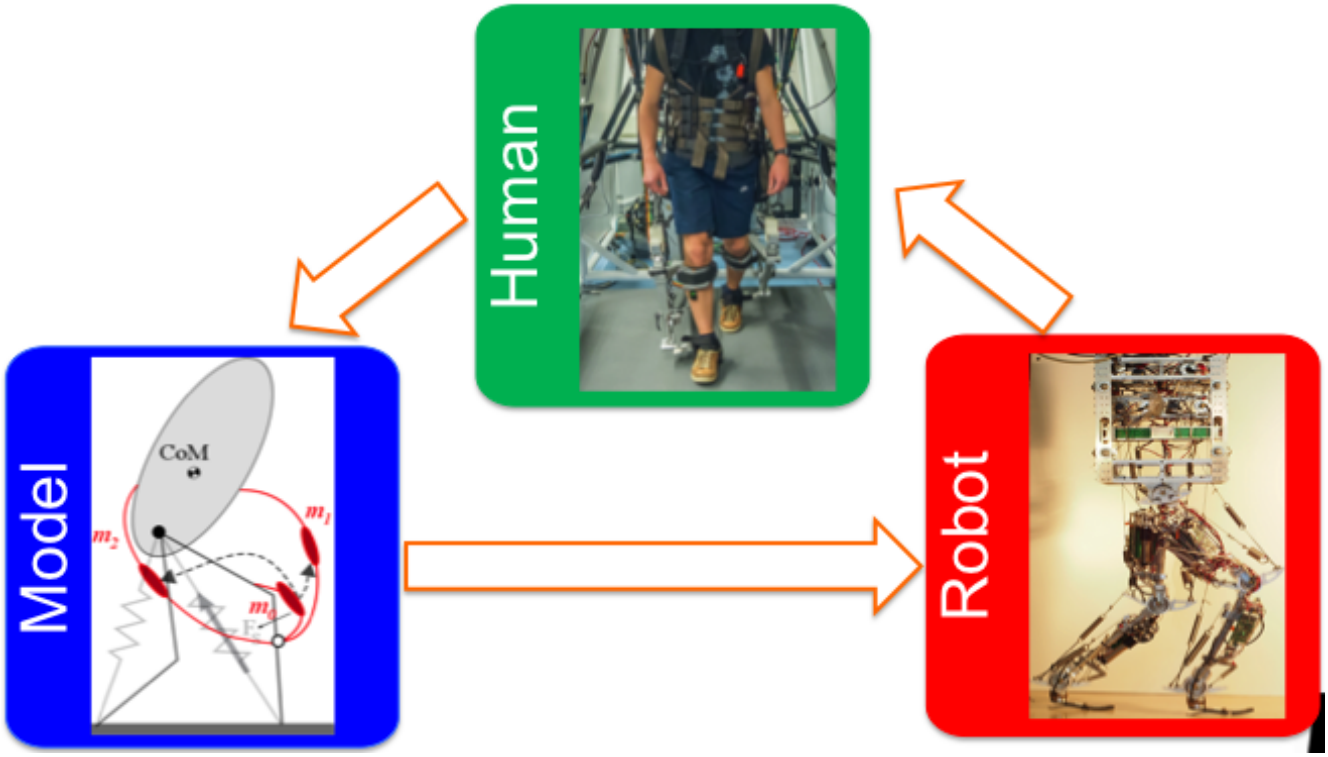

Figure 2: Bioinspired trilogy for design and control of legged system.

REFERENCES

Asbeck, A. T., Dyer, R. J., Larusson, A. F., and Walsh, C. J. (2013). Biologically-inspired soft exosuit. In *Rehabilitation robotics (ICORR), 2013 IEEE international conference on*, pages 1–8. IEEE.

Blickhan, R. (1989). The spring-mass model for running and hopping. *Journal of Biomechanics*, 22(11):1217–1227.

Full, R. J. and Koditschek, D. (1999). Templates and anchors: Neuromechanical hypotheses of legged locomotion on land. *Journal of Experimental Biology*, 22:3325–3332.

Geyer, H., Seyfarth, A., and Blickhan, R. (2006). Compliant leg behaviour explains basic dynamics of walking and running. *Proceedings of the Royal Society B*, 273(1603):2861–2867.

Koditschek, D. E., Full, R. J., and Buehler, M. (2004). Mechanical aspects of legged locomotion control. *Arthropod structure & development*, 33(3):251–272.

Komi, P. V. (2008). Stretch-shortening cycle. *Strength Power Sport. Oxford: Balckwell Science*, pages 184–201.

Lipfert, S. W. (2010). *Kinematic and dynamic similarities between walking and running*. Kovač.

Martinez, H. R. and Carbajal, J. P. (2011). From walking to running a natural transition in the slip model using the hopping gait. In *Robotics and Biomimetics (ROBIO), 2011 IEEE International Conference on*, pages 2163–2168. IEEE.

Maus, H. M., Lipfert, A. W., , Gross, M., Rummel, J., and Seyfarth, A. (2010). Upright human gait did not provide a major mechanical challenge for our ancestors. *Nature Communications*, 1(6):1–6.

Maus, H.-M. and Seyfarth, A. (2014). Walking in circles: a modelling approach. *Journal of The Royal Society Interface*, 11(99):20140594.

Peuker, F., Maufroy, C., and Seyfarth, A. (2012). Leg adjustment strategies for stable running in three dimensions. *Bioinspiration and Biomimetics*, 7(3).

Pratt, J., Chew, C.-M., Torres, A., Dilworth, P., and Pratt, G. (2001). Virtual model control: An intuitive approach for bipedal locomotion. *The International Journal of Robotics Research*, 20(2):129–143.

Robinson, D. W., Pratt, J. E., Paluska, D. J., and Pratt, G. A. (1999). Series elastic actuator development for a biomimetic walking robot. In *IEEE/ASME International Conference on Advanced Intelligent Mechatronics*.

Seipel, J. and Holmes, P. (2006). Three-dimensional translational dynamics and stability of multi-legged runners. *The International Journal of Robotics Research*, 25(9):889–902.

Vanderborght, B., Albu-Schäffer, A., Bicchi, A., Burdet, E., Caldwell, D. G., Carloni, R., Catalano, M., Eiberger, O., Friedl, W., Ganesh, G., et al. (2013). Variable impedance actuators: A review. *Robotics and autonomous systems*, 61(12):1601–1614.

Wehner, M., Quinlivan, B., Aubin, P. M., Martinez-Villalpando, E., Baumann, M., Stirling, L., Holt, K., Wood, R., and Walsh, C. (2013). A lightweight soft exosuit for gait assistance. In *Robotics and Automation (ICRA), 2013 IEEE International Conference on*, pages 3362–3369. IEEE.

Zhao, G., Sharbafi, M., Vlutters, M., van Asseldonk, E., and Seyfarth, A. (2017). Template model inspired leg force feedback based control can assist human walking. In *IEEE-RAS-EMBS International Conference on Rehabilitation Robotics*.

Maziar Ahmad Sharbafi

Curriculum Vitae

Education

08/2017	Phd, Dr. rer. nat. at Technische Universität Darmstadt, Germany Grade: summa cum laude - excellent
Dissertation:	Bioinspired template-based control of legged locomotion
09/2013	Phd, Dr. Ing., (Control Engineering) at University of Tehran, Iran Grade: summa cum laude - excellent
Dissertation:	Analytical approach to the conceptual design and motion control of bipedal robots using semi-passive elements
02/2006	MS. in Electrical (control) Engineering at University of Tehran, Iran Grade: 19.25/20
Thesis:	Using reinforcement-emotional learning in multidimensional and time critical environment (like rescue environment)
09/2003	BS. in Electrical (control) Engineering at Sharif University of Technology, Tehran, Iran Grade: 19/20
Thesis:	Designing fuzzy controller (rules and membership function) with Genetic algorithm

Experience

08/2017 - 08/2020	principal Investigator in Electric-Pneumatic Actuator (EPA) DFG granted project, Technische Universität Darmstadt, Germany
01/2012 - 08/2017	Researcher at Lauflabor Locomotion Laboratory, Human Science, Technische Universität Darmstadt, Germany
08/2011 - 12/2011	Researcher Internship at Lauflabor Locomotion Laboratory, Institute of Sports Science, Friedrich Schiller Universität Jena, Germany
10/2004 - 08/2011	Researcher at Mechatronics research Lab (MRL) and Lecturer at Azad University of Qazwin, Iran